

Energy Performance Impacts from Competing Low-slope Roofing Choices and Photovoltaic Technologies

Submitted in partial fulfillment of the requirements for

the degree of

Doctor of Philosophy

in

Civil and Environmental Engineering

Amy L. Nagengast

B.S., Civil Engineering, University of Wisconsin-Madison

M.S., Civil and Environmental Engineering, Carnegie Mellon University

Carnegie Mellon University
Pittsburgh, PA

December, 2012

For my grandparents: Jim and Myrna Rauch, Joe and Donna Nagengast

Acknowledgements

My sincere gratitude is extended to the following individuals and groups who have made a significant contribution to this research as well as have been integral to my Ph.D. experience. I need to also emphasize that many more individuals not specifically listed below have influenced the way I think, act, and react which I am forever grateful and forever changed.

First, a special thanks to my Ph.D. committee. Chris Hendrickson (co-chair) has been instrumental in helping me improve my scientific method and approach. He has been quick and timely with responses, approachable, and a beacon of time-management and organization. Scott Matthews (co-chair) asked insightful and perceptive questions which drove deeper understanding into a wide array of topics. Scott also fostered a friendly, open-minded and supportive learning environment. Don Coffelt brought invaluable practical advice as a fellow roof researcher and as a facilities decision maker. Vivian Loftness helped me bridge my research between engineering and architecture. Her understanding of and passion for the interaction between buildings and the environment has had a profound, long-lasting effect of me. While not on my Ph.D. committee, Professor Dave Sailor from Portland State University was an excellent knowledge source and a great help on green roofs and photovoltaics.

I owe enormous appreciation to those individuals who have been closely involved with Scalo Solar's Sunscape project. TJ Willetts has been a champion. He has been resourceful and willing to help even with the smallest of requests. Mike Carnahan has been the solar guru. He helped me maneuver the solar playing field, and I will never forget our times installing sensors on the rooftop during the hottest day in July. John Buck is passionate, dedicated, and intellectually curious about green roofs. Clayton Rugh first connected me to Sunscape. He has such a priceless repository of green roof knowledge that is founded in both academics and industry. I have cherished working with all of these individuals.

Equally important are those people who have been my endless advocates, my sounding boards, basically my backbone the last four years. My Porter Hall 115 officemates (Aranya Venkatesh, Catherine Izard, Rachael Nealer, Yeganeh Mashayekh, Mahbub Choudhury, Ranjani

Theregowda, and Adrian Ocneanu), who now are scattered across the world, offered me a rare community rooted in deep bonded friendship that I cherish greatly. They were there to celebrate the good times (often with excellent food) and picked you up from the low valleys with laughter, kindness and sincere hugs. They all had a unique mix of intellectual vigor paired with selflessness. This blend translated into a group dynamic where sharing inspiring ideas and technical skills occurred routinely. While not physically assigned to the office, all the comments above are absolutely applicable to Kim Mullins and Shira Horowitz who were honoree officemates. I honestly could not have done this Ph.D. without any one of them.

Special recognition needs to be extended to my green design institute research group. I have appreciated your feedback within the Green Design Reading Group (particularly Mike Blackhurst and Elizabeth Traut) and the outreach efforts within the Green Design Apprenticeship Program. Also, a big thanks to the other Civil and Environmental Engineering (CEE) as well as the Engineering and Public Policy (EPP) doctoral and master students that have been my good friends in and out of the academic setting. I would be remiss to not mention the sustained support from other CEE and EPP faculty and staff, especially Maxine Leffard, which I found extremely valuable.

To my long-time roommate Chase H. Butler, “I miss my Chaaaase” basically sums up many memories and emotions. We have been sidekicks and confidants through thick and thin. I am still amazed that a short visit at Silky’s and faith in a stranger five years ago turned into one of my most cherished friendships that always refreshes and revives me. To Kevin Lipkin, your humor is unprecedented and has been a source of merriment and many smiles. I enjoy our intellectual wit and banter. Thank you for helping me regulate my sanity and strive towards balance in my life. En Avant! Hakuchu! Lastly to my parents, John and Diane Nagengast, and my brother, Dan Nagengast, I greatly appreciate the unwavering support and love throughout my life. As a family, I have cherished our foundations in maintaining a hard work ethic and being genuinely interested about everybody and intellectually curious about everything.

I would also like to extend my appreciation to the funding sources that supported this thesis research: Carnegie Institute of Technology - Deans Fellowship, Phi Kappa Phi Love of Learning Award and the National Science Foundation (Grant No. CBET 1032722).

Abstract

With such a vast quantity of space, commercial low-slope roofs offer significant potential for sustainable roofing technology deployment. Specifically, building energy performance can be improved by installing rooftop energy technologies such as photovoltaic (PV) panels, and/or including designs such as white or green roofs instead of traditional black. This research aims to inform and support roof decisions through quantified energy performance impacts across roof choices and photovoltaic technologies. The primary dataset for this research was measured over a 16 month period (May 24, 2011 to October 13, 2012) from a large field experiment in Pittsburgh, Pennsylvania on top of a commercial warehouse with white, black and green roof sections, each with portions covered by polycrystalline photovoltaic panels. Results from the Pittsburgh experiment were extended to three different cities (San Diego, CA; Huntsville, AL; and Phoenix, AZ) chosen to represent a wide range of irradiance and temperature values.

First, this research evaluated the difference in electricity production from a green-moss roof and black roof underneath photovoltaic panels to determine if the green roof's cooler air increases the panel efficiency. Second, separate studies examine 1) average hourly heat flux by month for unobstructed and shaded roof membranes 2) heat flux peak time delay, and 3) air temperature across roof types.

Results of this research show green roofs slightly increased (0.8-1.5%) PV panel efficiency in temperatures approximately at or above 25° C (77°F) compared to black roofs. However in cool climates, like Pittsburgh, the roof type under the PV panels had little overall impact on PV performance when considering year round temperatures. Instead, roof decisions should place a stronger emphasis on heat flux impacts. The green roof outperformed both black and white roofs at minimizing total conductive heat flux. These heat flow values were used to develop a new, straight-forward methodology to roughly estimate heat flux impacts of different roof types in other climates using ambient temperature and solar irradiance. While managing heat flow is important for building energy performance, roof choices need to include a systems level analysis encompassing a year for the specific region to best quantify the overall energy impacts.

Table of Contents

Acknowledgements	i
Abstract.....	v
List of Tables	x
List of Figures.....	xiii
List of Acronyms	xvi
Chapter 1: Introduction and background	1
1.1 Motivation	1
1.2 Overview of typical roof types	4
1.2.1 Conventional black roofs	5
1.2.2 White roofs	5
1.2.3 Green roofs	8
1.3 Photovoltaic technologies	12
1.4 Roof energy balance with and without photovoltaics	14
1.5 Urban Heat Island effect	16
1.6 Relevant literature review	17
1.7 Hypotheses and supporting research questions	22
Chapter 2: Description of experimental site and study period weather conditions	25
2.1 Introduction	25
2.2 Project history and layout.....	25
2.3 Sunscape's roof surfaces and skylights.....	29
2.4 Types of photovoltaic arrays	34
2.5 Sensor installation and monitoring.....	39
2.6 Data collection.....	44
2.7 Pittsburgh weather conditions during study period (July 1, 2011- June 30, 2012).....	47
2.8 Weather parameter significance on photovoltaic power output on Sunscape.....	53
2.9 System configuration limitations and improvements for future studies	56
Chapter 3: Examining climate parameter impact on photovoltaic power output through a regression analysis	58
3.1 Introduction	58
3.2 Data	59
3.3 Methods	61
3.4 Linear and non-linear regression results	64
3.5 Linear regression results with wind direction and wind speed	68

3.6	Conclusions	72
Chapter 4: Quantifying the relationship between green roof temperature and Photovoltaic power performance on low-slope roofs..... 74		
4.1	Introduction	74
4.2	Data	76
4.3	Methods	77
4.4	Results from Pittsburgh case study	78
4.4.1	Base-case results.....	79
4.4.2	High temperature scenario	83
4.5	Characteristics of other case study cities.....	84
4.6	Method 1-Estimated results for other cities	85
4.7	Method 2-Estimated results for other cities	88
4.8	Conclusions	89
Chapter 5: Roof temperatures and heat flow analysis for different roof types 92		
5.1	Introduction	92
5.2	Methods	95
5.2.1	Study One and Two: Membrane temperature, ceiling temperature and heat flux	96
5.2.2	Study Three: Comparison of black, white and green roof air temperatures ..	101
5.3	Data	102
5.4	Pittsburgh heat flux results.....	104
5.4.1	Study One: Impact of ambient temperature on surface and ceiling temperature across black, white, moss and sedum roofs	104
5.4.2	Study Two: Impact of ambient temperature on surface and ceiling temperature across black and white shaded and unshaded roofs	108
5.4.3	Study One: Average hourly monthly surface and ceiling temperature profiles for black, white, moss and sedum roofs	110
5.4.4	Study Two: Average hourly monthly surface and ceiling temperature profiles for black and white shaded and unshaded roofs	113
5.4.5	Effects of seasonal sky conditions on membrane surface temperatures.....	116
5.4.6	Study One: Monthly heat flux results	119
5.4.7	Study Two: Monthly heat flux results	124
5.5	Heat flux separated by ambient temperature and solar irradiance	128
5.6	Heat flux results for other case study cities.....	140
5.7	Study Three: Black, white and green roof air temperature comparison.....	145
5.8	Conclusions	149

Chapter 6: Research conclusions and future work.....	152
6.1 Discussion	152
6.2 Research questions revisited	155
6.3 Future work	161
References	193
Appendix A: Complete list of data collected at Sunscape	193
Appendix B: Wind speed and wind direction statistical results	214
Appendix C: National Weather Service summary of sky conditions at the Pittsburgh International Airport.....	188
Appendix D: Total heat flux quantities for black, white and green-moss roofs	221

List of Tables

Table 1-1: Factors affecting a building owner's roof decision	3
Table 1-2: Conventional roof covering materials (Coffelt 2012; Levinson, Akbari, Konopacki, & Bretz 2005).....	5
Table 1-3: Examples of private and public benefits of white roofs	8
Table 1-4: Examples of private and public benefits of green roofs	11
Table 2-1: Surface properties of black, white and green roofs	30
Table 2-2: Photovoltaic array information installed at Sunscape	36
Table 2-3: PV racking configurations for polycrystalline panels on Sunscape	38
Table 2-4: Summary of manufacturer specifications for primary hardware devices on Sunscape	42
Table 2-5: Type and start date of data collected on Sunscape separated by roof technology	44
Table 2-6: Comparison of Sunscape (July 1, 2011-June 30, 2012) and TMY ambient temperatures	48
Table 2-7: Average power output of 60 Black roof- PV panels tilted at 15° on Sunscape from July 1, 2011- June 30, 2012	55
Table 2-8: Average power output of 60 Green roof-PV panels tilted at 15° on Sunscape from July 1, 2011- June 30, 2012	55
Table 3-1: List of measurements removed from July 1, 2011- June 30, 2012 Sunscape dataset .	60
Table 3-2: Correlation values for parameters used in regression equation 1 and equation 3 (July 1, 2011-June 30, 2012).....	65
Table 3-3: Linear regression values (Eq. 1) for Black and Green Roof back-surface panel temperature (July 1, 2011- June 30, 2012)	65
Table 3-4: Linear regression values (Eq. 3) for Black and Green-PV power generation temperature (July 1, 2011- June 30, 2012)	66
Table 3-5: Non-linear regression values (Eq. 4) for Black and Green Roof back-surface panel temperature (July 1, 2011- June 30, 2012)	67
Table 3-6: Non-linear regression values (Eq. 5) for Black and Green-PV power generation (July 1, 2011- June 30, 2012).....	68
Table 4-1: Average monthly difference (Green roof-PV minus Black roof-PV) in power output (kW) for panels above green and black roofs on Sunscape. (July 1, 2011- June 30, 2012)	81
Table 4-2: Average difference (Green roof-PV minus Black roof-PV) in power output (kW) for panels above green and black roofs partitioned by temperature and solar irradiance.	82
Table 4-3: Base-case and high temperature scenario summary results for all case study locations	87

Table 4-4: Comparison of Method 1 and 2 for net kilowatt hours produced from green roof-PV minus black roof-PV for three case studies.	89
Table 5-1: Summary of surface temperature, air temperature and heat flux studies.	102
Table 5-2: Linear regression coefficients from Eq. 8 for Black membrane temperature (May 24, 2011 - February 10, 2012)	105
Table 5-3: Monthly surface temperature diurnal fluctuation ($^{\circ}\text{C}$) (maximum-minimum hourly surface temperature value) and corresponding percent reduction from Black 2011 and Black 2012 roofs for July through October 2011 and 2012.....	114
Table 5-4: Total and percent difference of heat gain and loss by month, season and year for black, white and green-moss roofs (May 24, 2011-May 24, 2012).....	123
Table 5-5: Time delay of maximum heat flux from the monthly hourly profiles in Figure 5-14 (May 24, 2011- May 24, 2012).....	124
Table 5-6 : Total heat gain and loss by month, season for black and white shaded and unshaded roofs (July 5, 2012 –October 13, 2012)	127
Table 5-7: Percent difference of heat gain and loss by month and season from Table 5-6 for white, black shaded and white shaded roofs compared to black and white roofs (July 5, 2012 – October 13, 2012)	127
Table 5-8: Time delay of maximum heat flux from the monthly hourly profiles in Figure 5-15 (July 5, 2012- October 13, 2012)	128
Table 5-9: Measured BLACK roof instantaneous heat flux values (W/m^2) in Pittsburgh separated by solar irradiance and ambient temperature bins (May 24, 2011-May 24, 2012).....	130
Table 5-10: Measured WHITE roof instantaneous heat flux values (W/m^2) in Pittsburgh separated by solar irradiance and ambient temperature bins (May 24, 2011-May 24, 2012).....	130
Table 5-11: Measured GREEN-MOSS roof instantaneous heat flux values (W/m^2) in Pittsburgh separated by solar irradiance and ambient temperature bins (May 24, 2011-May 24, 2012).....	130
Table 5-12: Number of fifteen minute measurements itemized by direction of heat flow and roof type during May 24, 2011- May 24, 2011	131
Table 5-13: Measured BLACK roof instantaneous heat flux values (W/m^2) for assumed UNCONTROLLED condition in Pittsburgh separated by solar irradiance and ambient temperature bins (May 24, 2011-October 31, 2011 and April 1, 2012-May 24, 2012).....	132
Table 5-14: Measured WHITE roof instantaneous heat flux values (W/m^2) for assumed UNCONTROLLED condition in Pittsburgh separated by solar irradiance and ambient temperature bins (May 24, 2011-October 31, 2011 and April 1, 2012-May 24, 2012).....	132
Table 5-15: Measured MOSS-GREEN roof instantaneous heat flux values (W/m^2) for assumed UNCONTROLLED condition in Pittsburgh separated by solar irradiance and ambient temperature bins (May 24, 2011-October 31, 2011 and April 1, 2012-May 24, 2012).	133
Table 5-16: Measured BLACK roof instantaneous heat flux values (W/m^2) for assumed HEATING condition in Pittsburgh separated by solar irradiance and ambient temperature bins (November 1, 2011- March 31, 2012).	134

Table 5-17: Measured WHITE roof instantaneous heat flux values (W/m^2) for assumed HEATING condition in Pittsburgh separated by solar irradiance and ambient temperature bins (November 1, 2011- March 31, 2012).	134
Table 5-18: Measured MOSS-GREEN roof instantaneous heat flux values (W/m^2) for assumed HEATING condition in Pittsburgh separated by solar irradiance and ambient temperature bins (November 1, 2011- March 31, 2012).	135
Table 5-19: Number of hours from May 24, 2011 to May 24, 2012 corresponding to ambient temperature and solar irradiance ranges measured on Sunscape.	136
Table 5-20: Annual heat transfer (Wh/m^2) for the BLACK roof.....	137
Table 5-21: Annual heat transfer (Wh/m^2) for the WHITE roof	137
Table 5-22: Annual heat transfer (Wh/m^2) for the MOSS-GREEN	137
Table 5-23: Heat gained or lost under heating (outside air temp $<15^\circ\text{C}$) or cooling (outside air temp $>25^\circ\text{C}$) scenarios for black, white and green roofs in Pittsburgh	140
Table 5-24: The percent difference between white and green roofs compared with black roofs for heat loss under in the heating scenario and heat gained in the cooling scenario	141
Table 5-25: 2010 Commercial electricity and natural gas price for Pittsburgh, San Diego, Phoenix and Huntsville	144
Table 5-26: Differences in average air temperature measured 15cm (6in) above white and moss roofs compared with a black roof across a range of ambient temperatures (July 5, 2012-October 13, 2012)	147
Table 5-27: Roof types on Sunscape ranked from best to worst at reducing temperature swings, heat gain and heat loss.	150

List of Figures

Figure 1-1: Comparison of PV cost and performance in 2008. Graphic from (International Energy Agency, 2010)	13
Figure 1-2: Energy balance components with (left) and without (right) a PV panel (Scherba 2011; Gaffin 2010; Feng 2010).....	15
Figure 2-1: Location of Sunscape roof project (GoogleMaps, 2012).....	26
Figure 2-2: Sunscape construction and installation timeline	27
Figure 2-3: Roof types and PV and skylight technologies installed on Sunscape (picture courtesy of Scalo Solar).....	28
Figure 2-4: Roof of Scalo Solar before roof replacement.....	29
Figure 2-5: Profiles of four types of roof sections on Sunscape.....	30
Figure 2-6: Moss green roof before (left) and after (right) retrofit of sedum mats occurred on April 10, 2012	32
Figure 2-7: Images of small extensive green roofs: build up (left), modular (center), hilly (right)	33
Figure 2-8: Images of skylights installed at Sunscape-Carlisle SynTec Drylights (left), Ciralight smart skylight (center), Carlisle SynTec Tubular skylight (right).....	33
Figure 2-9: PV Panels types- ET Solar polycrystalline (left), Solyndra solar tubes (center), Unisolar thin film (right).....	34
Figure 2-10: Racking type and height differences for Green Roof- ^o 15 PV and Black roof - ^o 15 PV	37
Figure 2-11: The wiring diagram for 30 ^o tilt panels across black and white roof.....	39
Figure 2-12: General schematic of sensor type and location across roof types.....	40
Figure 2-13: Measurement location of for various data collected on Sunscape	41
Figure 2-14: New air sensors over moss-green roof.....	46
Figure 2-15: Monthly average hourly solar radiation values measured on Sunscape compared with TMY.....	49
Figure 2-16: Solar irradiance and air temperature comparisons of Sunscape (above) versus Pittsburgh's TMY (below) datasets	50
Figure 2-17: Wind speed and source wind direction histogram of NWS (above) and TMY (below) datasets	52
Figure 2-18: Monthly photovoltaic power output for 60 black roof PV panels tilted at 15 ^o	54
Figure 3-1: Schematic of method to predict PV power output from Sunscape data.....	62
Figure 3-2: Comparison of linear (Eq. 1) and non-linear (Eq. 4) equations for black back surface panel temperature.....	67

Figure 3-3: NWS (left) and Sunscape (right) histograms for daytime wind direction values between January 1, 2012- June 30, 2012.	69
Figure 3-4: Resulting R^2 values for the addition of wind speed and wind direction in Eq. 6 using Sunscape data from January 1, 2012 to June 30, 2012	72
Figure 4-1: Relationship between PV power output and cell temperature with varying solar irradiance values. Black Roof-PV are seen on the left and green roof-PV on the right. (July 1, 2011-June 30, 2012).....	79
Figure 4-2: Average back-surface panel temperatures for PV panels above the black or green roofs measured on Sunscape separated by ambient temperature (July 1, 2011- June 30, 2012)..	80
Figure 4-3: Measured hourly values from July 1, 2011 –June 30, 2012 at Sunscape	82
Figure 4-4: Comparison of climate parameters for case study locations.....	84
Figure 4-5: Typical Meteorological Year (TMY) daylight profiles based on solar radiation and ambient temperature.....	85
Figure 4-6: Case study ranges for annual net electricity revenue resulting from 60 PV panels over a green roof minus expected revenue over a black roof	88
Figure 5-1: Method schematic to calculate heating and cooling costs for each roof type.....	97
Figure 5-2: Heat flux (Equation 8) sign convention illustration with example temperatures	99
Figure 5-3: Location of temperature sensors installed at Sunscape used for Studies 1-3 in Table 5-1.	103
Figure 5-4: Average membrane surface temperatures compared with ambient temperature (May 24, 2011-May 24-2012)	107
Figure 5-5: Average ceiling temperature under different roof type compared with ambient temperature (May 24, 2011-May 24-2012)	107
Figure 5-6: Black and white shaded and unshaded average membrane surface temperatures compared with ambient temperature (July 5, 2012-October 13, 2012	109
Figure 5-7: Average hourly membrane temperature profiles for each month across black, white, moss and sedum roof types (May 24, 2011-May 24-2012).....	112
Figure 5-8: Average hourly ceiling temperatures profiles for each month across black, white and moss roof types (May 24, 2011-May 24-2012)	112
Figure 5-9: Average hourly membrane temperature profiles for each month across black and white shaded and unshaded roof sections (July 5, 2012-October 13, 2012).....	115
Figure 5-10: Average hourly ceiling temperature profiles for each month across white and black shaded and unshaded roofs (July 5, 2012-October 13, 2012).....	115
Figure 5-11: Fall and Winter average hourly profiles of membrane temperature across roof surfaces (October 2011 to March 2012)	118
Figure 5-12: Spring and Summer average hourly profiles of membrane temperature across roof surfaces (April 2012- June 2012; July 2011-September 2011)	118

Figure 5-13: Summer average hourly profile for membrane temperature across roof surfaces (July 5, 2012-September 30, 2012).....	119
Figure 5-14: Average hourly heat flux profiles for each month for black, white and moss roofs (May 24, 2011 to May 24, 2012)	122
Figure 5-15: Average hourly heat flux profiles for each month for black and white shaded and unshaded roofs (July 5, 2012-October 13, 2012).....	125
Figure 5-16: Heating and cooling scenario example for the black roof based on 15 ⁰ C (60 ⁰ F) and 25 ⁰ C (77 ⁰ F) thermal comfort set points (May 24, 2011-May 24, 2012).....	139
Figure 5-17: Annual net heat gained and loss through black, white and green roof under a heating or cooling scenario.....	142
Figure 5-18: Site and source energy required to offset the net heat gain or loss for white and green roofs in Figure 5-17 normalized to the black roof for all cities.	143
Figure 5-19: Additional net energy savings or costs for the white and green-moss roofs from the heating or cooling scenarios normalized to the black roof for all four cities.	145
Figure 5-20: Average air temperature 15cm (6in) above surface of black, white and green roofs separated by ambient temperature (July 5, 2012-October 13, 2012).....	148
Figure 5-21: Average hourly air temperature 15cm (6in) above surface of black, white and green roofs separated by month (July 5, 2012-October 13, 2012)	148

List of Acronyms

ASHRAE	American Society of Heating, Refrigerating and Air Conditioning Engineers
CIGS	Copper Indium Gallium Diselenide
EPA	Environmental Protection Agency
EPDM	Ethylene Propylene Diene Monomer
HVAC	Heating, Ventilating and Air-Conditioning
kW	kilowatt
kWh	kilowatt hour
LEED	Leadership in Energy and Environmental Design
LBNL	Lawrence Berkeley National Laboratory
MMBTU	Million British Thermal Units
NSRDB	National Solar Radiation Data Base
NREL	National Renewable Energy Laboratory
NWS	National Weather Service
PV	Photovoltaic
RH	Relative Humidity
SRI	Solar Reflectivity Index
TMY	Typical Meteorological Year
TPO	Thermoplastic polyolefin
UHI	Urban Heat Island

Chapter 1: Introduction and background

1.1 Motivation

With urban space at a premium, roofs are being targeted as an opportunity to deploy sustainable energy technologies for buildings. Most building efficiency and conservation efforts have focused on building interiors, neglecting substantial opportunities available from roofs. Huang and Franconi (1999) found that thirteen percent of heat lost or gained in a building can be attributed to roofs. Given the tremendous amount of roofing stock in the U.S., more sustainable roofing systems can reduce energy consumption, combat the Urban Heat Island (UHI) effect, mitigate stormwater runoff and generate renewable electricity via installed equipment.

Roofs have historically been designed primarily for protection from the outdoor elements (Konopacki, Garland, Akbari, & Rainer 1998). However, growing interest in sustainability and new technologies have challenged these traditional perspectives. For example, roofs can be designed to mitigate diurnal temperature swings resulting from solar radiation which can lead to higher efficiency in a building's energy management system and reduction in overall energy consumption. This shift in design decisions allows the use of roof space to blossom beyond traditional technologies and functions.

Roofs occupy a significant fraction of the built environment. Coffelt and Hendrickson (2012) estimated that roofs occupy $\geq 25\%$ of the total managed building area. Akbari, Rose, and Taha (2003) found that roofs occupy 20-25% of urban landscape in four U.S. cities. On a national scale, estimates for commercial building roofs for 2010 were approximately 2.6-8.2 billion square meters (28-88 billion square feet) of land area (Levinson & Akbari 2010; CEIR 2012; Chaudhari 2004). The majority of this commercial roof space is classified as low-slope with a grade less than 3:12 (less than 25° from horizontal) (Smith, 2009). With such a vast quantity of space, commercial low-slope roofs offer significant potential for sustainable roofing technology deployment.

Conventional roofs occupy the majority of low-roof space. The three most prominent conventional roofing types are built-up roofs, modified bitumen, and single-ply comprising

almost 90% the national roof space (Levinson & Akbari, 2010; Greenroofs.com, 2011; Gartland, 2008). These roofs are typically darker in color and the least expensive to install. White and green (or vegetated) roofs compete for the same roof space as black roofs, but have significantly less market share with 10% and less than 1% respectively (Levinson & Akbari, 2010; Greenroofs.com, 2011; Gartland, 2008). White roofs consist of coatings or paint that can be easily retrofitted over conventional roofs with minimal upcharge. One benefit to white roofs is the high albedo which reflects solar irradiance in turn reducing air conditioning costs. Most green roof installations in new and retrofit applications require a structural analysis to assess the building's ability to withstand the additional weight from plants, soil and water. Resulting from increased professional design services and materials for green roofs, they have a higher upfront cost than black and white roofs. However, green roofs are often installed for the energy benefits to the building (e.g. heat flux reduction) and environmental benefits such as storm water retention and urban heat island mitigation (Banting et al. 2005; Bass, Krayenhoff, Martilli, & Stull 2002; Susca, Gaffin, & Dell'Oso 2011; Vanwoert et al., 2005).

In urban areas, solar technologies have become more common on roofs often competing with black, white, green roofs (Denholm & Margolis, 2008). Areas that are large in size, contiguous, and without shade are ideal for solar (Dura-last Roofing 2011; Liu, 2006). Therefore, roofs are prime space for photovoltaics (PV) since roofs typically are unused except for heating, ventilation and air conditioning equipment (Kirby 2011, CEIR 2012).

While previous research often evaluates the impacts of roof technologies developed in isolation, there is scant research on the potential co-benefits associated with combining roof technologies. This gap partly exists from limited collaboration between green roof, white roof and solar industries fueled in part from the competition for the same roof budget. Synergies and trade-offs across roofing technology portfolios are unclear, but may be significant. For example, green and white roofs mitigate daily diurnal temperature variation, potentially enhancing PV performance by reducing peak operating temperatures (Meneses-Rodrigues, Horley, Gonzalez-Hernandez, Vorobiev, & Gorley 2005). In turn, PV panels placed above green roofs may enhance their performance by reducing evapotranspiration losses (Köhler, Wiartalla & Feige, 2007). Similarly,

alternative surface technologies can make renewable solar technologies more feasible by reducing heating and cooling loads.

Constraints to adopting alternate roofing technologies are studied qualitatively for individual roof types. Common reservations from a building owner's perspective preventing them from embracing and installing alternative roofing options for low-slope commercial buildings include: increased capital costs (compared with conventional roofs), structural capacity (for the green roof), and incomplete knowledge of alternative roof technology performance among building owners. (Weiler & Scholz-Barth, 2009; Peck, Callaghan, Kuhn & Bass 1999; Konopacki, Garland, Akbari & Rainer 1998)

Despite significant advances in technology performance and availability, the technical and economic potential of sustainable roofing technology is uncertain. Such uncertainties lead to inadequate decision support, leading to potentially inconsistent and potentially ineffective incentive programs. Some factors that do and potentially could (in the future) influence building owner's roof decisions are listed in Table 1-1. While the list in Table 1-1 is not rank ordered, in practice, some factors do influence the final roof decision more than others.

Table 1-1: Factors affecting a building owner's roof decision

Decision Factors	Description/Examples
1 Cost	first cost, maintenance cost, life-cycle cost, budget cycle
2 Institutional knowledge and inertia	familiar with roof installation, specifications, longevity and maintenance
3 Roof configuration	roof use (e.g. HVAC equipment only, foot traffic, food production), roof size, new or retrofit project, structural capacity, roof service life and durability
4 Energy	heat flux mitigation, energy costs reduction, urban heat island effect, renewable energy, HVAC capacity limits
5 Environmental Impacts	greenhouse gas emissions, stormwater quality and quantity, air quality, biodiversity
6 Innovative leader	market differentiator (e.g. Leadership in Energy and Environmental Design), increased property values
7 Governing authority	Environmental Protection Agency consent decree, campus master plan, insurance agency, codes and standards
8 Occupants	Aesthetics, occupant productivity, noise reduction, recreation

Roof decisions made or influenced by other stakeholders (e.g. government, designers, trade associations, occupants) may have a similar list of decision factors presented in Table 1-1, but will likely have different priorities than the building owner. For example, a city government may be more interested in reducing greenhouse gas emissions or urban heat island effect than minimizing cost. While the focus of the research is aimed at the building owner, the results are applicable to other roof stakeholders as well.

This research informs the building owner's roof decision by providing empirical data and results surrounding the energy decision factor listed in Table 1-1. The remaining sections in Chapter 1 give background information on the important roof technologies and energy concepts mentioned and used in the subsequent chapters. Chapter 2 outlines the experimental roof configuration located in Pittsburgh, PA which was constructed in 2010 and is the core dataset for this thesis. Chapter 3 uses the empirical data to derive regression functions to ultimately predict photovoltaic output between two black and green roofs under PV panels. Chapter 4 quantifies the difference in power output from PV panels over a black roof and green roof separately across a range of temperature and solar irradiance values. The regression equations from Chapter 3 are used in Chapter 4 to extend the results to other cities in dissimilar United States climates. Chapter 5 quantifies the heat flux, surface temperature and air temperature differences across roof types. Chapter 6 summarizes the thesis research and revisits the research questions posed in Section 1.7 and at the beginning of each chapter.

1.2 Overview of typical roof types

This section aims to provide context to describe the current state of low-slope roofs and their relationship to buildings in order to build a foundation to better understand the analysis in the subsequent thesis chapters. First, conventional or traditional roofing assemblies are introduced to provide a baseline for the conventional roof. Second, benefits and installation costs are briefly outlined for white roofs and green (or vegetated) roofs. Third, background information is provided on photovoltaics and the Urban Heat Island effect. Finally, a more focused literature

review is provided that form the current state of knowledge for the various studies. The chapter concludes with hypotheses and supporting research questions that will be evaluated in subsequent chapters.

1.2.1 Conventional black roofs

The top three most common roof coverings are built-up roofs, modified bitumen, and single-ply membranes with 20%, 18% and 46% of the reroofing market share by sales in 2004 (Gartland 2008; Good, 2005). Comparable ratios were found for new construction. Within single-ply membranes, Ethylene Propylene Diene Monomer (EPDM) is responsible for the 27% of the market (Gartland 2008; Good, 2005). The design service life of each of these conventional roof coverings is between 10-25 years. Descriptions of the common conventional systems and corresponding lifespan estimates can be found in Table 1-2. The average cost of material and installation for black roof is \$1-2/sq. ft or \$11-22/sq. m (Urban, 2010; Levinson, Akbari, Konopacki, and Bretz 2005).

Table 1-2: Conventional roof covering materials (Coffelt 2012; Levinson, Akbari, Konopacki, & Bretz 2005)

Roof System	Description	Service life (years)
Single Ply-EPDM	Synthetic rubber sheet adhered with ballast, fasteners or adhesives	15
Single Ply-PVC, TPO	Single membrane with welded seam systems including Polyvinyl chloride (PVC), thermoplastic polyolefin (TPO). Held in place using adhesives or fasteners	10-20
Modified Bitumen	Pre-fabricated polymer-modified asphalt layers often reinforced with mats, films, foils and mineral granules.	20-25
Built-Up Roofs	Alternating layers of bitumen and felts typically covered with aggregate or a cap sheet.	15-20

1.2.2 White roofs

White roofs differ from conventional roofing through the application of white coatings and single-ply membranes (US EPA, 2008a). The white coatings and single-ply membranes are highly reflective leading to a 50-60°F (28-33°C) reduction in surface temperature compared with conventional roofs (US EPA, 2008a; Konopacki et al., 1998; Urban & Roth, 2010). White roofs

are commonly referred to as “cool roofs¹.” As of 2008, white roofs were installed on less than 10% of roofs in the United States (Gartland, 2008).

Limiting our discussion to low-slope roofs, there are two ways to classify a white roof. First, a program can give specifics for solar reflectance or thermal emittance. One example is in California under Title 24, cool roofs material require 70% solar reflectance and 75% thermal emittance (US EPA, 2008a; Akbari & Levinson, 2008). Similarly, the White Roof Amendment in Georgia requires material to meet a minimum of 75% albedo and emissivity of 75% within ASTM guidelines (Young, 1998). Lastly, the EPA Star program requires a slightly lower value for initial reflectance (65%), but with a three-year aged reflectance of 50% (US EPA, 2008a).

The second option to classify a cool roof is through Solar Reflective Index (SRI) which is a composite index comprised of solar reflection and thermal emittance percentages. The range of SRI is 0 (standard black roof with a reflectance of 0.05 and emittance of 0.90) to 100 (standard white roof with reflectance of 0.80 and emittance of 0.90) where 100 is the most reflective surfaces (Akbari & Levinson, 2008). SRI is calculated using ASTM E1980 “Standard Practice for Calculating Solar Reflectance Index of Horizontal and Low-Sloped Opaque Surfaces.” The composite index allows flexibility in material reflection and emittance values. For example, the LEED Sustainable Sites Credit 7.2 (heat island effect—roof) requires an SRI of 78 which can be achieved by using materials with:

1. reflectance of 0.77 and thermal emittance of 0.2;
2. reflectance of 0.64 and emittance of 0.90; or
3. reflectance of 0.28 and emittance of 0.90 (Urban & Roth, 2010).

White roofs have a high initial solar reflectance of 0.70-0.80 (Akbari, Levinson, & Rainer 2005). Ultraviolet radiation, microscopic growths, dust, air pollutant depositions and acid rain cause the albedo of white roofs to degrade (Eilert, 2000; Miller, Cheng, Pfiffner, Byars 2002). Akbari et al. (2005) tested 13 roof samples five to eight years old and found that the white roof’s albedo declined 40-50% from the unweathered condition. Field tests of white single-ply membranes across seven sites in the U.S. found white thermoplastic roofs lost 30-50% of the initial installed

¹ It is becoming more common to group green roofs into the category of cool roofs as well.

reflectance after 3 years. However with cleaning, at least 70% to 100% of the unweathered reflectivity was restored with power washers or professional grade cleaners (Akbari et al. 2005; Miller et al., 2002). Cleaning is recommended every other year or every third year (Miller et al., 2002)

The benefits for white roofs can be broken down into private and public benefits from the decision factors discussed in Table 1-1. Direct benefits can be translated into quantifiable savings received by the building owner or occupants and can be easily incorporated into a return on investment analysis. Public benefits (or social benefits) are impacts to society as a whole and thus indirectly benefit the building owner. Typically to achieve measurable public benefits, projects must be large in quantity and/or size (e.g. city scale). (Foster, Lowe & Winkelman 2011; Carter & Keeler 2008; Center for Neighborhood Technology & American Rivers 2010; Rosenzweig, Gaffin, & Parshall, 2003).

Private and public benefits of cool roofs primarily reside in the energy and environment domain. On a building level, white roofs reduce the heat flux into the building by having a high albedo. The high white roof reflectivity mitigates heat flux in the summer which reduces cooling needs. White roofs save energy more in warmer climates with high solar radiation (Hoff, 2005). Many studies have found white roofs reduce summertime cooling energy by 10-50% compared with a traditional black roof (Konopacki & Akbari 2001; Akbari 2005; Konopacki, Gartland, Akbari & Rainer 1998). Additional private benefits, but not an exhaustive list, are itemized in Table 1-3. On a city scale, white roofs provide public benefits in the form of peak energy demand reduction and mitigation of the urban heat island effect. Akbari et al. (2001) found that the “peak urban electric demand rises by 2-4% for each 1 °C in daily maximum temperature above a threshold of 15 to 20°C.” Additional public benefits can be seen in the Table 1-3. The costs for a white membrane are similar to a black roof \$11-22/sq. m. (Levinson, Akbari, Konopacki, and Bretz 2005).

Table 1-3: Examples of private and public benefits of white roofs

Decision Factors (Table 1.1)	Private (building level)	Public (city level)
Energy and Environment	<ul style="list-style-type: none"> • Reduction in heat flux through the building saving energy cooling costs and lifespan of air conditioning system • Downsize cooling equipment (Levinson et al. 2005) 	<ul style="list-style-type: none"> • Reduction in peak load required which decreases the need for additional power plants (Banting et al., 2005) • Reduction in metropolitan temperatures (Urban Heat Island effect) • Reduction in greenhouse gas emissions (GHG) from electricity generation • Reduce ozone concentrations
Innovative Leader	<ul style="list-style-type: none"> • Use of recycled materials (Banting et al., 2005) • LEED credits 	<ul style="list-style-type: none"> • New employment opportunities for design and engineering professionals, tradesman, manufacturers, suppliers
Roof Configuration	<ul style="list-style-type: none"> • Reduction in diurnal temperature swings of the membrane which extends its lifespan 	

1.2.3 Green roofs

Green roofs are not a new technology, but their adoption in the U.S. is increasing. Peck (2011) with the organization *Green Roofs for Healthy Cities* surveyed their corporate members to find the green roof industry growth rate to be 28.5% in 2010 which is 12% higher than 2009.

Commercial and institutional buildings were the largest categories of green roof installations. However, even with these growth rates, the green roof installations in the U.S. are small compared to green roof pioneering countries like Germany. Earth Pledge (2004) listed that 14% of Germany's flat roofs are covered with vegetation. To date in the U.S., green roofs occupy approximately 26 million square feet of commercial buildings (Greenroofs.com, 2011).

Assuming Levinson and Akbari (2010) commercial roof space estimate of 28 billion square feet, green roofs occupy less than 1% in the United States. Therefore, the opportunity for growth is significant.

Germany is often cited for classifying green roofs based off their maintenance requirements (Dunnett & Kingsbury, 2008). The two main types of green roofs are extensive and intensive. Extensive green roofs (least maintenance) generally have a shallow growing medium, lower capital costs and limited plant diversity compared to intensive green roofs. Extensive green roofs material and installation costs range from \$10 - \$12/sq. ft (\$110-\$130/sq. m) (Clayton Rugh, Xero Flor Personal Communication March 2012; US EPA, 2008b) Intensive roofs (higher maintenance) require deeper soil, irrigation systems and have higher capital costs. Intensive green roof material and installation costs range from \$20-\$40/sq. ft (\$215-\$430/sq. m) and higher depending on the depth of the soil. (US EPA, 2008b).

As a result from the plants and soil medium properties, green roofs cool the surface temperature directly above the green roof. Many studies have documented lower green roof surface temperatures by 10-40⁰C through evapotranspirative cooling compared to black conventional roofing (Gaffin et al. 2005, DeNardo, Jarrett, Manbeck, Beattie, & Berghage 2005; Castleton, Stovin, Beck, & Davison 2010; Wong & Tan 2007; Simmons, Gardiner, Windhager, & Tinsley 2008). Another advantage of green roofs over black roofs is lower energy consumption by managing heat flow to internal building spaces (Niachou, Papakonstantinou, Sanamouris, Tsangrassoulis & Mihalakakou 2001; Dunnett & Kingsbury 2008). The thermal mass of a green roof decreases diurnal temperature swings at the site into a more moderate temperature band which can lengthen the membrane life (Oberndorfer et al., 2007; Köhler, Schmidt, Laar, Wachsmann, & Krauter 2002). By minimizing peak temperatures, the heating, ventilating and air-conditioning system works less to keep the internal building spaces at a comfortable temperature.

The benefits of green roofs also cross private and public boundaries and thus complicate quantifying the effectiveness of green roofs. Often these public impacts are not factored into private investment decisions (Rosenzweig et al., 2003; Banting et al. 2005). Roofs can generate public benefits in various ways. For example, the health benefits from reducing Combined Sewer Overflows, which decrease the pollutants in public waters, are not factored into the final roof cost-benefit analysis. Ignoring public benefits could entirely change a roof decision; Blackhurst,

Hendrickson & Matthews (2010) found that public benefits can be greater in magnitude than private benefits. Table 1-4 identifies examples of private and public benefits related to green roofs generally. This list is not exhaustive or specific to one type of green roof.

Table 1-4: Examples of private and public benefits of green roofs

Factors (Table 1-1)	Private (building level)	Public (city level)
Energy	<ul style="list-style-type: none"> • Reduces heat flux saving energy cooling costs • Additional heat storage in the winter requiring less energy for heating (Peck & Kuhn, 2003) • Increased efficiency of air cooling and ventilation systems (Castleton et al., 2010) • Downsize cooling equipment 	<ul style="list-style-type: none"> • Reduction in peak load required which decreases the need for additional power plants (Banting et al., 2005) • Reduction in metropolitan temperatures (Urban Heat Island effect) • Reduction in greenhouse gas emissions (GHG) from electricity generation
Environment	<ul style="list-style-type: none"> • Local sewage conveyance credit • Local green roof policy credit • Rainwater capture for irrigation • Reduces potable water consumption 	<ul style="list-style-type: none"> • Prevents Combined Sewer Overflows (CSO) • Retains and evaporates rainwater which reduces the stormwater runoff • Detains rainwater which slows peak stormwater runoff • Reduces strain or load on sanitary system (offsets stormwater management infrastructure) • Prevents flooding • Improves water quality by filtering or degrading contaminants • Provides wildlife habitat (Teemusk, 2007) • Absorption of air pollutants, gases, smog and dust (Teemusk, 2007; Theodosiou, 2009; Peck, 2003)
Innovative Leader	<ul style="list-style-type: none"> • Provides space available for food production (urban agriculture) • Increases sound insulation to interior spaces (Rosenzweig, 2003) • Increases property values (Banting, 2005) • Additional building marketability or differentiator (Peck, 2003) • Faster planning approval for projects from local building officials • Use of recycled materials (Banting, 2005) • LEED credits 	<ul style="list-style-type: none"> • New employment opportunities for various design and engineering professionals, tradesman, manufacturers, suppliers • CO2 sequestration capability (US DOE, 2004) • Improved public health (Rosenzweig, 2003)
Roof Configuration	<ul style="list-style-type: none"> • Reduces diurnal temperature swings of the membrane which extends its lifespan • Decreases spread of fire to the interior of buildings and to adjacent buildings 	
Occupants	<ul style="list-style-type: none"> • Visually pleasing (Rosenzweig, 2003) 	<ul style="list-style-type: none"> • Aesthetic value (Rosenzweig, 2003) • Reduction in urban noise (Theodosiou, 2009) • Provide green space and green space networks for recreation (Grant, 2006) • Social and psychological benefits to users (Theodosiou, 2009; Banting, 2005)

1.3 Photovoltaic technologies

Photovoltaic technology is growing in popularity in the U.S.. Photovoltaic (PV) panels (also known as solar electric systems) convert solar radiation into electrical energy (US DOE-EERE, 2011b). From 2009 to 2010, installed PV capacity increased 54% in the U.S. (US DOE-EERE, 2011a). However, even with installations on the rise, solar provides less than 1% of electricity in the US (US EIA, 2011).

For photovoltaic technologies, there are a considerable range of cost and panel efficiencies. Two primary types of Photovoltaics (PV) modules are crystalline silicon and thin film. Crystalline silicon (comprising Mono, Poly, and Ribbon) has the longest track record in the solar market and occupies roughly 70-90% of the PV market share (SEIA 2011; Solar Buzz, 2011). Crystalline silicon also has some of the highest PV conversion efficiencies at 15-20% (Solar Buzz, 2011; Ehrlich, 2011; Curtright, Morgan, & Keith 2008). The downsides to crystal silicon technology are its high production cost and weight. Thin film technology captures the majority of the remaining PV market share. While thin film solar is produced more quickly and cheaply than crystalline silicon, efficiency is lower at 6-13% (Curtright et al. 2008; US EIA, 2010a). Figure 1-1 illustrates the relationship between cost and performance between crystalline silicon and thin film as well as two less common PV types.

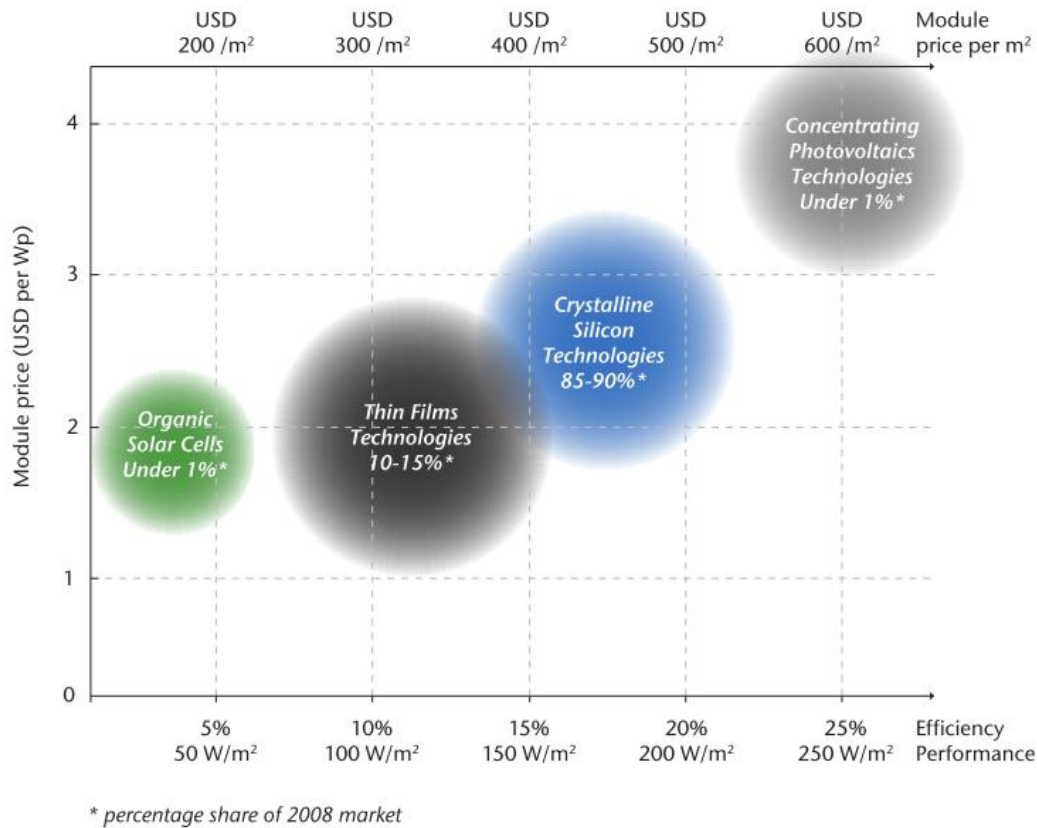


Figure 1-1: Comparison of PV cost and performance in 2008. Graphic from International Energy Agency (2010)

Conversion of sunlight to electricity across technologies can be decreased by dust, hot air temperatures, and shade among other factors (Meral & Dincer 2011; Sulaiman et al. 2011; Thakkar et al. 2010). Since Chapter 4 discusses panel efficiency in relation to temperature, a brief discussion is presented here for background. It is common knowledge that temperature and PV performance are inversely related. In other words, the lower the temperature, the higher the PV output (Köhler, 2007; Meneses-Rodrigues et al., 2005). PV manufacturers publish temperature coefficients relating losses in efficiency for each degree the temperature fluctuates from 25°C. Typically, these relationships are linear. Nordman and Clavadetscher. (2003) found with an 8°C temperature increase over 20°C, PV panels had a 1.7 to 5% decrease in power output. The reason for the decline in power output is the temperature sensitivity of the semiconductor material (e.g. silicon, copper indium diselenide (CIS)). At high temperatures, the solar cell p-n junction gap shrinks and the voltage decreases. The reduction in voltage leads to a reduction in power (Meral & Dincer 2011; Hui & Chan 2011).

1.4 Roof energy balance with and without photovoltaics

An energy balance accounts for energy transferred into and away from the earth surface or for this thesis a rooftop.. The energy balance equation is based on the first law of thermodynamics where energy is constant. There are five major components to the energy balance equation and seen in Figure 1-2:

1. Shortwave radiation
2. Longwave radiation
3. Sensible heat (i.e.. convection)
4. Latent heat (e.g. evapotranspiration rate for green roofs)
5. Heat conduction (Gaffin et al., 2005)

Shortwave radiation is comprised of both direct and diffuse solar radiation from the sun. The amount of shortwave radiation that reaches the earth surface depends on the quantity that is reflected by clouds, aerosols, and atmospheric gases and absorbed by the atmosphere (Gartland, 2008). The shortwave radiation that reaches the roofs is also reflected by roofing materials. Reflectance (also known as albedo) refers to the ability of a material to reflect solar radiation. Solar reflectance is measured on a scale of 0 to 1 where the higher the value the more solar reflectance. For example, a material with a solar reflectance of 0.70 reflects 70% of incoming solar irradiance (Urban 2010).

Long-wave radiation (or infrared radiation) is partially controlled by emissivity and temperature of the material and atmosphere (United States Environmental Protection Agency, 2008b). Emissivity is the relative ability of a material to emit heat away from itself by radiation. Emissivity is also given on a scale of 0 to 1. The higher emissivity the more absorbed heat is released by radiation. Sensible heat refers to heat transferred by convection through air flow (Ayata 2011). Green roofs have the added surface property of evapotranspiration where latent heat loss occurs through plants. Other roofs have latent heat loss if standing water is present (Rosenzweig et al., 2003)

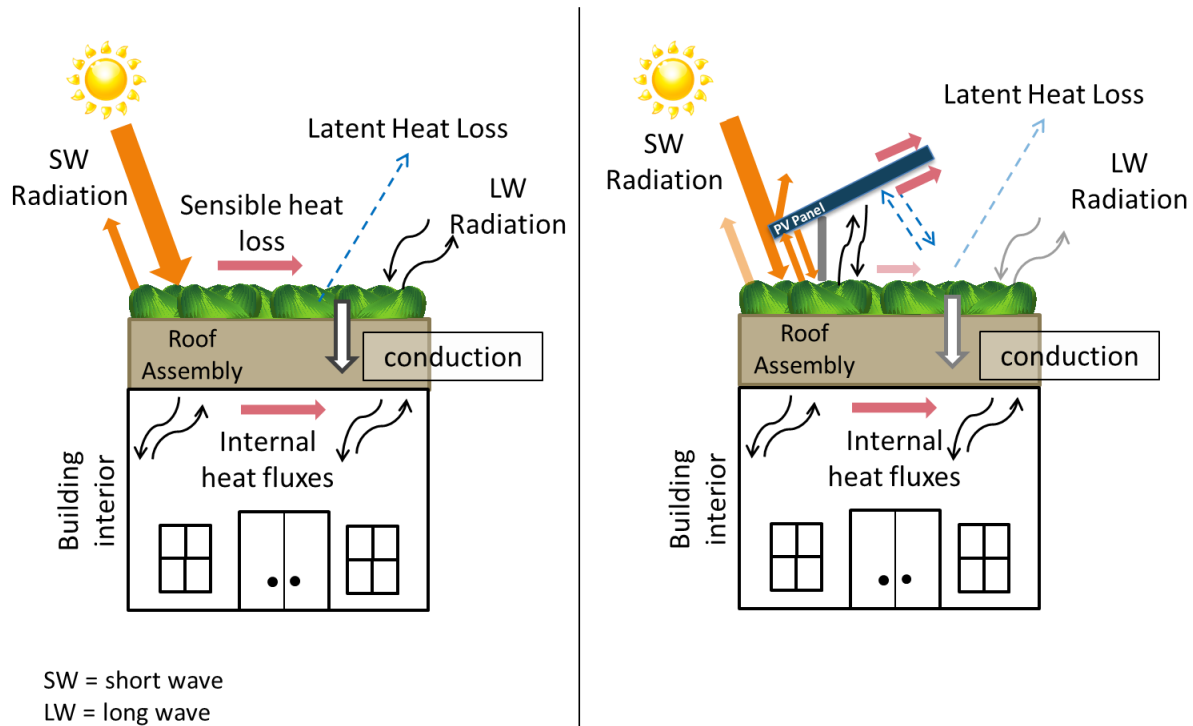


Figure 1-2: Energy balance components with (left) and without (right) a PV panel (Scherba 2011; Gaffin 2010; Feng 2010)

Black, white and green roofs have different rates of heat transfer into and out of a building throughout the year because of thermal characteristics of the roof assembly and material properties of the roof surface. Two material properties govern the conductive heat flow through an assembly: thermal conductivity and capacitance. Thermal conductivity is the rate of heat flow through a unit area induced by a temperature difference. Thermal capacitance (also known as heat capacity or thermal mass) is the ability of a material to hold thermal energy.

Figure 1-2 shows the energy balance with and without a PV panel. The two main differences with having a PV panel over a roof compared to a roof without PV are 1) less shortwave radiation reaches the rooftop surface, and 2) the reemitted heat from the rooftop outward is redirected by the PV panel back towards the rooftop surface impacting surface temperature. For this thesis research, only conductive heat flux was calculated in Chapter 5 with the use of surface temperatures.

1.5 Urban Heat Island effect

The Urban Heat Island (UHI) effect or phenomenon has been observed in many urban areas (Gartland, 2008). Generally, UHI is when urban cities are warmer than surrounding rural land. A study by Akbari (2005) found that air temperatures in a typical city are 2.5 °C higher than nearby rural areas. Using a mesoscale model, Taha et al. (1998) found ambient temperatures 0.5°C to 2°C warmer than nearby rural areas. “There is no single cause for the UHI” phenomenon (Gartland, 2008). Instead, the problem is created by a collection of factors. Some of the causes include:

- “dark colored, man-made materials: capture and store the solar radiation;
- impermeable surfaces: prevent heat removal by evaporation;
- slower wind speeds: limit heat removal by convection;
- transportation, industrial and energy processes: generate heat in the city (anthropogenic sources);
- air pollution: particles absorb and emit heat down to the city” (Gartland, 2008);
- weather; and
- urban geography (United States Environmental Protection Agency, 2008c)

UHI is important to mitigate because it:

- increases energy consumption and corresponding greenhouse gas emissions produced by power plants;
- increases smog formation;
- compromises human health and comfort through respiratory difficulties, heat cramps, non-fatal heat strokes, and heat-related mortality; and
- increases temperature of water runoff compromising aquatic systems (US EPA, 2009).

Akbari et al. (1992) found city ambient temperatures have increased 0.1°C- 0.4°C (0.2°C- 0.8°C) per decade from the early to mid-1900s until 1990 for four U.S. cities (San Francisco, CA, Los Angeles, CA, Washington, DC and Fort Lauderdale, FL). Cumulatively, these temperature

increases over the decades can be significant. For example, Los Angeles had 2.8°C (5°F) warmer air temperatures in 1990 than 1940 Akbari et al. (1992).

Additional energy is needed by air conditioners to counteract rising outside temperatures. For cities with a population larger than 100,000 residents, peak utility loads are predicted to increase 1.5-2% for every 0.6°C (1°F) in temperature above 15-20°C (Akbari et al. 1992; Akbari, Pomerantz, & Taha 2001). Modeling ten U.S. cities, Taha et al. (1998) found a 1-2°C increase in urban temperatures compared to rural temperatures resulted in a 3-11% increase in peak electricity demand. In addition, Akbari & Konopacki. (2005) found “elevated city temperatures are responsible for 20% of population-weighted smog concentrations.”

Strategies to mitigate UHI include increasing surface reflectivity in the city as well as vegetation cover (Bass 2002). Roofs can be used to implement UHI migration strategies through either white roofs or green roofs. Simulation results by Taha et al. (1998) suggest that increasing the urban albedo and fraction of vegetated land could reduce local air temperature by 5°C. Akbari & Konopacki. (2005) found that “cool roofs can reduce summertime air temperature of their surroundings by 1-2 K.” Cumulatively across U.S., the net annual energy savings (cooling minus heating savings) by increasing roof albedo is estimated by Akbari, Menon and Rosenfeld. (2009) to be over \$1 billion.

1.6 Relevant literature review

The literature review presented in Sections 1.2-1.5 was intended for the reader to become familiar with broad background concepts to better understand the analysis in the subsequent thesis chapters. In this section, the literature review is more focused on prior published research relevant to specific studies conducted as a part of this thesis. The goal after reading this section is for the reader to understand the current body of knowledge surrounding a specific topic.

In urban areas, solar technologies have become more common on roofs in order to provide on-site, renewable electricity. Areas that are large in size, contiguous, and without shade are ideal for solar (Dura-last 2011; Liu, 2006). Therefore, roofs are prime space for solar technologies

since roofs typically are unused except for heating, ventilation and air conditioning equipment (Kirby 2011; CEIR 2012). Furthermore, electricity produced on the roof for consumption in the building avoids average losses of 7% from transmission and distribution lines when generated at a power plant (United States Energy Information Administration, 2012).

The demand for solar energy is increasing which promotes accurate estimation of PV output when designing a PV system. Many solar PV output prediction models are based on the characterization of outdoor current-voltage (I-V) curves (Rosell 2006; Villalva 2009; Xiao 2004) defined by three points (the short-circuit current, open-circuit voltage and the maximum power point) with some models using five points (King 2004). If I-V curves are unavailable, other prediction methods must be used. For example, when irradiances and PV cell temperatures are known, PV power prediction models use linear equations incorporating a range of parameters such as corrections for temperature and low solar irradiance (Marion 2008) and/or material and system-dependent properties (i.e. glazing-covert transmittance and plate absorptance) (Skoplaki 2009a).

In the absence of measured solar radiation values, relative humidity and sky conditions (e.g. cloudiness) are helpful weather parameters in estimating the magnitude of solar irradiance reaching the earth surface, and thus, useful in estimating PV productivity (Gwandu 1995; Cess 1995). When PV cell temperature is not readily available, the cell temperature is often estimated using regression functions (Skoplaki 2009b). These regression equations are mostly linear and cell temperature can be determined directly or indirectly (i.e. through iterations). Often these functions use varying climate parameters as explanatory variables (Skoplaki 2009b; Tamizhmani 2003; King 2004). The most common weather variables used in regression equations include ambient temperature and solar radiation and to a lesser extent wind speed and direction (Griffith 1981; Skoplaki 2009a; Skoplaki 2009b). Wind speed and direction can influence the PV panel operating temperature by convection (Skoplaki 2009b).

Green (or vegetated) roofs also compete for the same roof space as solar technologies. While green roof installations are growing, they have less than 1% market share by roof area in the United States (Levinson & Akbari, 2010; Greenroofs.com 2011). Green roofs are frequently

installed for the energy benefits to the building (e.g. heat flux reduction) and environmental benefits such as storm water retention and urban heat island mitigation.

Often green roofs and PV panels are installed separately on roofs, but they can exist together harnessing potential co-benefits. Specifically with hot air temperatures, PV panels placed over green roofs (referred to as green roof-PV for this research) can utilize the cooler air to maintain or possibly increase efficiency compared to panels placed over black roofs (referred to as black roof-PV) (Köhler 2002). Hui et al. (2011) conducted a one day field experiment comparing one PV panel over a black and green roof in Hong Kong on a sunny day. The green roof's surface temperature was 5-11⁰C cooler than the black roof's, and the green roof-PV system produced 4% more power. Köhler (2007) also carried out a field experiment in Germany by comparing the average PV performance of two green roof-PV assemblies to the average of five black roof- PV systems. During the year 2000, the monthly average of the green roof-PV systems out performed black roof-PV assemblies monthly by -4% to 3% with a yearly average of 1.5%. Limitations to Köhler's (2007) study include differences in PV panel type and inverters between green roof-PV and black roof-PV.

While roof choices can influence the efficiency of PV panels, they also help regulate heat transfer or heat flux into a building. Managing heat flow can save a building owner money by reducing the need for mechanical conditioning (i.e. heating, ventilation and air conditioning systems) of interior spaces. Prior studies have used experimental and/or computational methods to calculate heat flux through roof assemblies into internal spaces. The approaches used to calculate heat flux to date include 1) direct heat flux measurements through transducers (Liu, 2003; Akbari, Levinson & Rainer 2005), 2) equations that quantify conductive heat flux through a temperature gradient (Wong et al. 2003; Akbari, 2003), or 3) simulation models taking into account some or all types of heat flows in the roof energy balance (refer to section 1.4) (Akbari, Levinson & Rainer 2005; Akbari & Konopacki 2005; Rosenfeld, Akbari, Romm & Pomerantz 1998). Simulation models are often used to more accurately determine the energy balance through a green roof (Tabares-Velasco & Srebric 2011; Sailor 2008).

Several field studies have measured the same building pre and post retrofit of a white roof membrane to understand the summertime daily air-conditioning use differences compared to a black roof. Akbari, Levinson and Rainer (2005) monitored a retail store in Sacramento, CA before and after the white roof retrofit during two months in the summer of 2002. From the addition of a white roof, Akbari (2005) found a 33-36°C reduction in maximum surface temperature, a 50% reduction in daily average cooling energy savings (70 Wh/m²/day) and 50% reduction in peak demand savings from 12pm-5pm (10W/m²). During the summer of 2000, the application of white single-ply roofing in Nevada increased the roof reflectivity of two small (15 sq. m each) non-residential buildings by 46% corresponding to a drop of 19-22°C in daytime temperature from the previously installed black roof (Akbari 2003). Given an R-20 roof assembly, the heat flux was reduced on average 33kWh/day which translated into \$0.67-0.84/m²/yr of air-conditioning savings. Overall, the reduction of heat gain from the roof surmounted to only 1% of the total air-conditioning use (Akbari 2003). For a 9,300m² retail building in Austin, TX, a white roof was retrofitted which reduced the surface temperature by 24°C in the summer. An increase of 78% in roof reflectivity resulted in 39 Wh/m²/day (11%) daily energy reduction with an R-12 roof assembly (Konopacki & Akbari 2001). In addition, the white roof reduced peak demand from 1pm-4pm by 3.8W/m² (14%). Konopacki et al. (1998) measured two medical offices and one retail store in northern California. The white coating resulted in a 28-31°C (50-55°F) lower roof surface temperature. The summertime average daily electricity consumption due to air conditioning was reduced by 13- 18% (36-63 Wh/m²/day). The retail store had 2% (4Wh/m²/day) overall reduction in electricity use.

A 2008-2009 field experiment in New York City, New York combined white, black and green roof sections on the Con Edison Learning Center to quantify differences in stormwater and heat transfer (Gaffin 2010). In the summer, the white and green roofs peak membrane surface temperatures were 17°C (30°F) and 33°C (60°F) respectively lower than the black roof. In terms of heat loss in the winter, the white roof and green roof had a reduction of 3% and 37% from black roof. For the summer months, the heat gain mitigation of both white and green roofs were significantly larger (55% and 84% respectively) in comparison to the black roof (Gaffin 2010). Two important caveats of this research 1) two models were used to estimate interior temperatures

and thus heat flux for white and black roofs instead of empirical measurements 2) the white roof had a double membrane layer while the black had only one.

The benefits of white roofs are valued less in northern climates with a short cooling season and long heating seasons (Hoff, 2005). In colder U.S., white and green roofs often incur a heating energy penalty compared to black roofs because they limit external heat from entering a building (Akbari & Konopacki 2005; Gaffin, Rosenzweig, Eichenbaum-Pikser, Khanbilvardi & Susca 2010; Levinson & Akbari, 2010). The heating penalty is the increased use of mechanical heating energy by white or green roofs compared to the conventional black roof during daytime hours in the winter (Akbari, Konopacki, & Pomerantz 1998). Snyder (2005) found that the “heating energy penalty” offsets the air-conditioning energy savings from white roofs. In other words, the cooling electricity savings in the summer counteracts the heating costs in the winter.

Building energy simulation programs have been used to model energy impacts within the building and to the surrounding community from different roof choices. Rosenfeld et al., (1998) used DOE-2 to determine a 10% reduction in electricity for air-conditioning in a one story office building occurred with the addition of white roofs and shade trees in Los Angeles. Akbari et al. (1998) also used building energy simulation software to determine energy savings from increasing roof albedo of 11 prototype buildings in 11 U.S. metropolitan areas (3 colder climates, 8 warm climates). The cooling energy savings from commercial buildings on average was 3-9% in southern climates. In northern climates (Philadelphia and Chicago), the net energy savings was near zero. The effects of white roofs were mitigated by the level of insulation. In other words, the more insulation the smaller the savings from the white roof. Extrapolating results from 11 U.S. cities (Konopacki 1997; Akbari et al. 1998) nationally, Rosenfeld (1998) found buildings saved 3% in electricity (i.e. reduction in cooling) from the addition of cool roofs. Taha et al. (1998) used a mesoscale model of ten regions in the U.S. to estimate energy impacts from a 15% increase in albedo and the city's vegetation fraction. Under this scenario, the results suggest up to a 5°C decrease in ambient temperature locally after the implementation of high albedo roofs and vegetation. Lowering the temperature 1-2°C could save 3-11% in peak electricity demand (Taha 1998).

In addition, Oak Ridge National Laboratory (2012) developed an on-line tool to assess the energy differences from increased reflectivity of roofs across climates. The Cool Roof Calculator was developed from the whole-building energy simulation program, DOE 2.1, and roof specific thermal performance calculations from AtticSim (New et al. 2011). Hoff (2005) used the Department of Energy Cool Roof Calculator to determine the net energy savings across the year from replacing a black roof (0.05 reflectance) with a white roof (0.55 reflectance).

More recent white roof research has relied heavily on various building simulation models with climate models to assess community benefits (e.g. reduction in smog, greenhouse gas emissions, urban heat island) from cool roofing technologies (Jacobson 2012; Oleson 2010; Levinson 2010; Akbari 2009). Scherba et al. (2011) explored urban heat island mitigation strategies using building simulation tools to model the sensible heat flux impacts from black, white and green shaded and unshaded roofs on the six U.S. cities. Scherba et al. (2011) estimates that total sensible flux could be reduced by 50% if PV covered white or green replaced black membranes.

1.7 Hypotheses and supporting research questions

At the beginning of each thesis chapter, a hypothesis and supporting research questions are proposed that guide the analysis. They are motivated and summarized in this section and then revisited in Section 6.2.

The demand for solar energy is increasing which promotes accurate estimation of PV output when designing a PV system. Since PV panel efficiency decreases with hot air temperatures, technologies are being investigated to improve performance under such conditions (Köhler, 2007; Meneses-Rodrigues, 2005). Green roofs are one potential solution because they cool the surrounding surface and air through evapotranspiration (Gaffin 2005, DeNardo 2005; Castleton 2010; Wong 2007; Simmons, 2008). Therefore, installing a green roof under PV panels could possibly increase panel efficiency compared to panels placed over black roofs (Köhler 2002). Chapter 3 investigates separate models for a black roof and a green roof under PV in order to estimate the differences between the two assemblies (i.e. green roof-PV and black roof-PV).

Chapter 3 hypothesis: Back-surface panel temperature and PV power output from green or black roofs under PV panels can be sufficiently modeled using a linear function with climate parameters as explanatory variables.

Chapter 3 supporting research questions:

3a) How well do linear and non-linear regression equations fit the Sunscape dataset for back surface panel temperature and power output?

3b) How important are wind speed and direction as explanatory variables in predicting PV power output?

Using the Pittsburgh Sunscape field experiment, Chapter 4 quantifies the difference in power output from PV panels over a black roof and green roof separately across a range of temperature and solar irradiance values. The regression equations from Chapter 3 are used in Chapter 4 to extend the results to other cities in dissimilar U.S. climates.

Chapter 4 hypothesis: The combination of PV panels over a green roof will produce more electricity than PV panels over a black roof.

Chapter 4 supporting research questions:

4a) Under what climate parameters does cooler air above the green roof increase PV output compared to black roofs on Sunscape?

4b) What is the magnitude of the difference in PV output for Sunscape and for other cities? Given the base-case and high-temperature scenario, what are a range of cost savings from the green roof-PV combination?

In addition to the impact of roof choice on PV panel efficiency, the roof also manages heat flow into interior building spaces. Different roofing materials and assemblies (e.g. black, white and

green roofs) affect heat flux. Using the Sunscape field experiment in Pittsburgh, Chapter 5 focuses on quantifying the conductive heat flow differences between black, white and green roof assemblies over a year.

Chapter 5 hypothesis: Green roofs are better building insulators than white or black roofs throughout the year.

Chapter 5 supporting research questions:

5a) What is the reduction in surface temperature and monthly diurnal hourly swing for white, green-moss and green-sedum compared to black roofs on Sunscape?

5b) What quantity of heat gained and lost was measured across black, white and green on Sunscape? How do these values change seasonally?

5c) How does shading of the white or black roof affect the roof heat flux? In terms of reducing heat gain or loss, how do shaded black and white roofs compare with black, white and green unshaded roofs?

Chapter 2: Description of experimental site and study period weather conditions

2.1 Introduction

Roofs are one important intersection between the built environment and nature. Traditionally, the primary function of roofs was to protect interior spaces from external weather elements. More recently, advances in roofing technologies have had a growing impact on private benefits (e.g. building energy consumption) as well as public benefits (e.g. reducing stormwater runoff and urban heat islands) (Banting et al. 2005; Bass, Krayenhoff, Martilli, & Stull 2002; Susca, Gaffin, & Dell’Osso 2011; Vanwoert et al., 2005).

A field experiment was constructed by Scalo Solar Solutions, a third party, to better understand how roof surfaces can affect photovoltaic power generation and the flow of energy into and out of buildings. The test bed was the core experimental set-up and yielded the dataset for this thesis work. To understand the analysis that follows in subsequent chapters, this chapter describes the specifics of the field experiment configuration. More specifically, background information on the project history and selected technologies lays the foundation for the site design. Discussions on data collection and sensor placement describe the data available for research.. Weather observed during the study period is compared with historical averages for context. Measured photovoltaic output from the field experiment is mapped to solar irradiance and temperature to outline their relationship. The chapter concludes with suggested roof design improvements for future field experiments.

2.2 Project history and layout

In August 2010, Scalo Solar Solutions LLC (Scalo Solar) received a Pennsylvania Energy Development Authority (PEDA) grant to transform their roof into a laboratory for testing and demonstrating various types of roof and solar technologies. Scalo Solar designs, acquires and installs solar arrays for commercial clients (Scalo, 2012). Scalo Solar was founded from Burns and Scalo Roofing Company which is the largest roofer in Western, PA (Scalo, 2012). Both Scalo Solar and Burns and Scalo Roofing Company share an office and warehouse to store roofing and solar products. The motivation behind the roof project was to “demonstrate the

most advanced technologies for generating alternative energy and reducing costs” (St. John, 2011). The reroofing and photovoltaic project was named “Sunscape.” Sunscape is located in Pittsburgh, Pennsylvania (40 °N, 79° W) approximately 17 km (10.7mi) southeast of the Pittsburgh International Airport and 8km (5mi) west of downtown Pittsburgh; the location is shown in Figure 2-1.

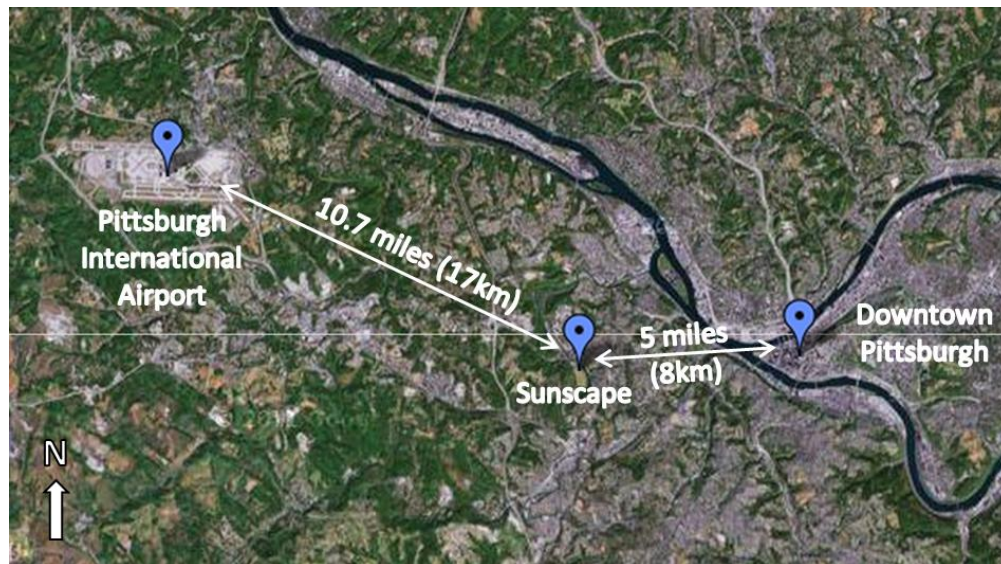


Figure 2-1: Location of Sunscape roof project (Google Maps, 2012)

Construction of Sunscape began in the fall of 2010 and was finished in the spring of 2011. Figure 2-2 outlines the major construction and installation milestones pertinent to Sunscape in chronological order. This research project connected with Sunscape beginning in January 2011.

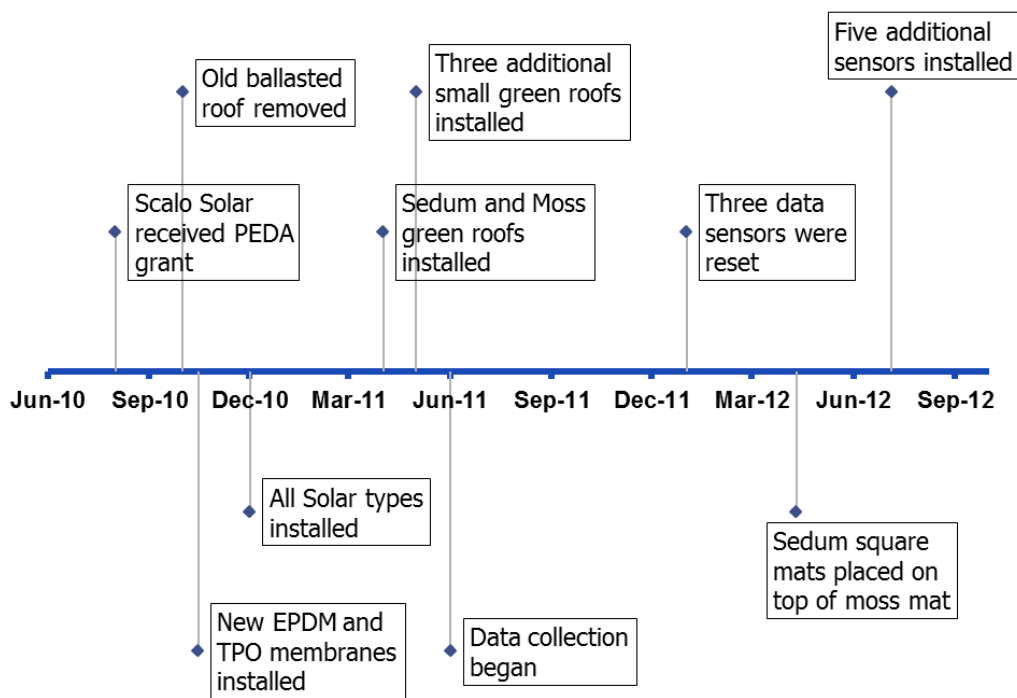


Figure 2-2: Sunscape construction and installation timeline

The final Sunscape project includes multiple types of solar energy and roof surfaces. Sunscape showcases three types of photovoltaic (PV) technologies, five types of green roofs, three types of skylights, a thermoplastic polyolefin (TPO) white roof and an ethylene propylene diene monomer (EPDM) black roof. Sunscape's 3,160sq.m (34,000sq. ft.) roof was separated into approximately:

- 1,580 sq. meters (17,000sq. ft.) of white TPO membrane
- 1,226 sq. meters (13,200sq. ft.) of black EPDM membrane
- 231 sq. meters (2,490 sq. ft.) of moss - green roof
- 123 sq. meters (1,320sq. ft.) of sedum - green roof
- 67 sq. meters (726 sq. ft.) total for three additional types sedum-green roof
- 49 sq. meters (527 sq. ft.) of skylights

On top of some of these roof surfaces, three PV types of were mounted:

- 150 ET Solar (PV brand) panels at 15° tilt across 600 sq. meters (6,445sq. ft.) of roof space,
- 30 ET Solar panels at 30° tilt across 150 sq. meters. (1,618sq. ft) of roof space,
- 272 Solyndra modules covering 530 sq. meters (5,711sq. ft) of roof space, and
- 30 UniSolar thin film modules covering 84 sq. meters (904 sq. ft) of roof space.

While each technology is described in greater depth in the following sections, an aerial view of each technology placement is depicted in Figure 2-3.

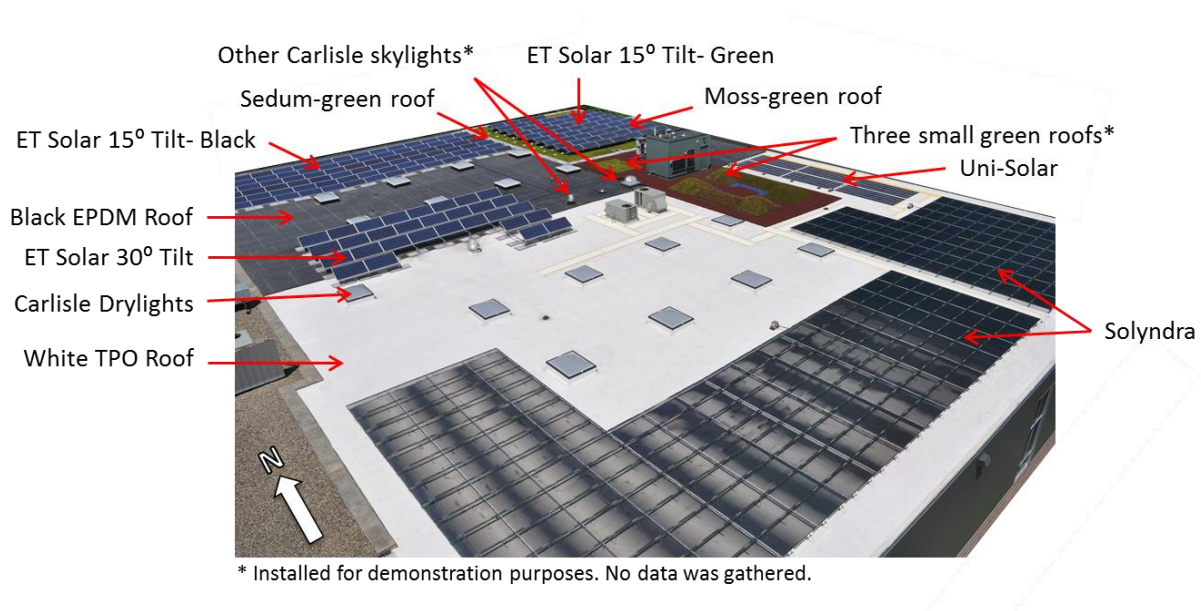


Figure 2-3: Roof types and PV and skylight technologies installed on Sunscape (picture courtesy of Scalo Solar)

The 9.1m (30ft) tall Scalo Solar’s building contains corporate offices and a warehouse for storing roofing materials. The Sunscape project is installed directly over the warehouse. The office portion of the building’s roof is unchanged. While the office space is temperature controlled on each floor, the warehouse has an open floor plan and has limited controls to moderate temperature. In the summer (April-October), a ventilation fan pushes hot air out of the warehouse; no efforts are made to maintain a specified temperature. In the winter (November-March), the warehouse is heated to 16°C (60°F).

2.3 Sunscape's roof surfaces and skylights

Scalo Solar removed the eight-year-old ballasted EPDM roof from the warehouse (Figure 2-4) in September 2010. However, the old insulation was left in place from the previous roof. On top of the insulation, Cuddy Roofing Co, Inc, a Scalo company, installed new secure rock cover board and placed white TPO or black EPDM membranes on different sections of the roof.



Figure 2-4: Roof of Scalo Solar before roof replacement

Figure 2-5 depicts the cross-section of the four roof types on Sunscape, the product name and manufacturer (if known) and the corresponding thickness of each roof layer. All roof types have the same steel deck, cover board, and insulation, (products 7-9 in Figure 2-5) below the membrane. This assembly has an R-value of $2.96 \text{ K}\cdot\text{m}^2/\text{W}$ ($16.8 \text{ h}\cdot\text{ft}^2\cdot^\circ\text{F}/\text{Btu}$) according to manufacturer specifications. The four roof surfaces differ in the surface membrane and the type of green roof installed (if any). Green roofs were only installed on the black EPDM membrane. The white roof has an initial solar reflectance of 0.79-0.87 depending on the test method used. After three years, the white TPO membrane's solar reflectance is expected to degrade 5-11% (Carlisle Syntec Systems 2012a). Similarly, the white membrane's initial thermal emittance value was 0.90 and then degrades by 4% after three years. The solar reflectance of the black EPDM membrane and the white TPO membrane is 9² and 110 respectively (Carlisle Syntec Systems, 2012b). No solar reflectance values were available for the green roof, but other published studies suggest the reflectance is 0.06-0.41 (Lazzarin, Castellotti, Busato 2005)

depending on the moisture content (Sailor, Hutchinson, & Bokovoy 2008). Higher soil moisture decreases the albedo.

Table 2-1: Surface properties of black, white and green roofs

Roof type	Solar Reflectance	Thermal Emittance	Solar Reflectance Index
Black EPDM Membrane	0.12	0.90	9 ²
White TPO Membrane	0.70-0.87	0.86-0.95	110
Typical green roofs (Sailor 2008; Lazzarin 2005)	0.06-0.41		

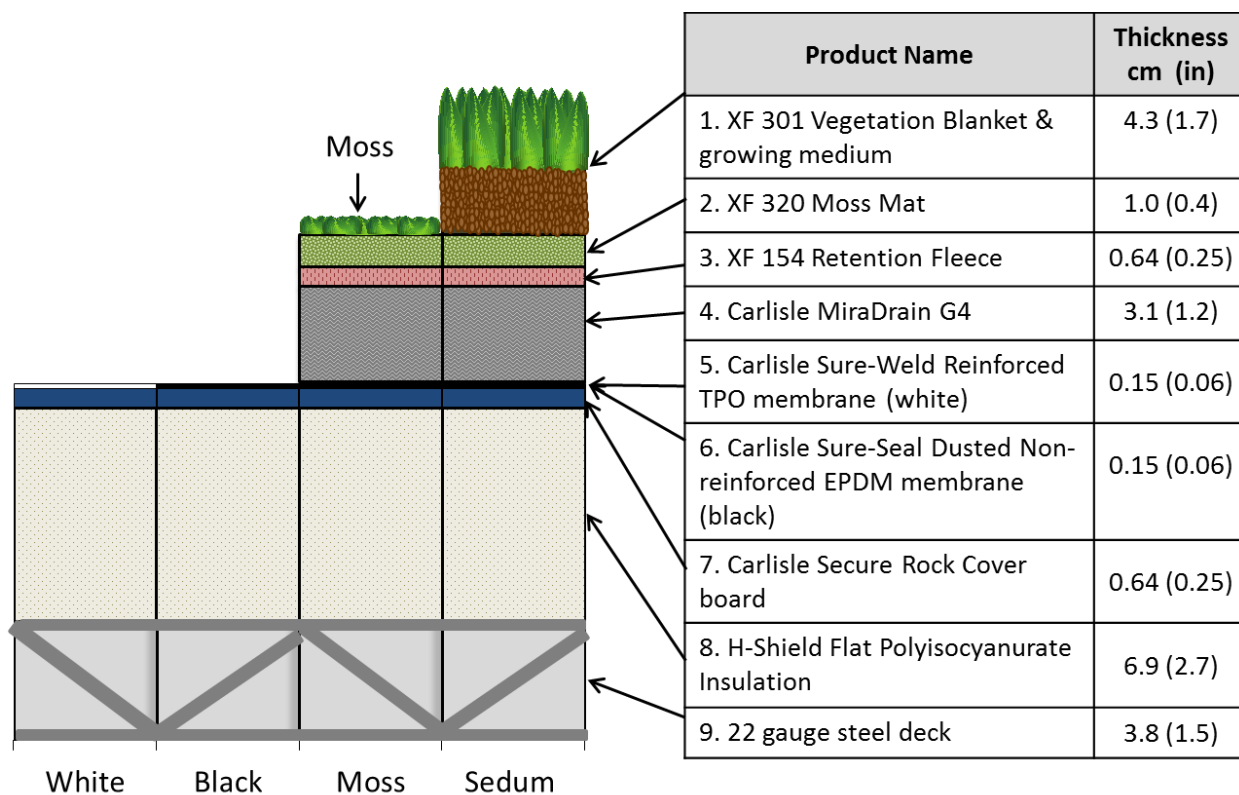


Figure 2-5: Profiles of four types of roof sections on Sunscape

Two main types of extensive green roofs are installed: sedum and moss. Both varieties were donated and installed by Xero Flor. The sedum-green roof for this installation is a vegetation blanket composed of “pre-cultivated drought-tolerant, low-profile vegetation (sedum) sown to a

² The black roof solar reflectance was calculated from Lawrence Berkeley National Lab Solar Reflectance Index (SRI) calculator which can be found at <http://coolcolors.lbl.gov/>

light weight fleece “and covered with XeroTerra growing medium (Xero Terra, 2012). The sedum plant species are a mixture of:

- *Hylotelephium spectabile*
- *Hylotelephium verticillatum*
- *Saxifraga granulata*
- *Sedum acre*
- *Sedum acre* var. *aureum*
- *Sedum album*
- *Sedum floriferum*
- *Sedum kamschaticum*
- *Sedum middendorffianum diffusum*
- *Sedum pulchellum*
- *Sedum reflexum* (rupestre)
- *Sedum sexangulare*
- *Sedum spurium* var. *coccineum*

The complete sedum green roof encompasses a vegetation blanket with sedum plants and growing medium, moss mat, retention fleece and drainage layer (products 1-4 in Figure 2-5) above the EPDM membrane. The moss-green roof consists of moss gathered from nature which was ground, filtered and then spread on top of the moss mat to grow (Clayton Rugh, personal communication, April 10, 2012). The moss and sedum green roofs only differ in cross-section above the moss mat. Installation of the moss and sedum roof sections can be visualized as a picture frame where the sedum frames the moss.

Both the moss and sedum roofs are irrigated. The moss has spray irrigation while the sedum has drip irrigation. The spray irrigation consists of poly vinyl chloride (PVC) tubing with spray nozzles every 2.7m (9ft). The tubing is supported by the PV racking system. The spray irrigation system often leaks because of improper line drainage resulting from insufficient PVC tube supports. The drip irrigation lays directly on the sedum roof vegetation blanket and does not have similar leakage problems. Both irrigation systems are designed to turn on when the moisture content falls below $0.15 \text{ m}^3/\text{m}^3$ or the surface temperature goes above 38°C (100°F)

(Eric French and John Buck, personal communication, April 2012). These systems turn off when these two thresholds are not exceeded.

Regardless of irrigation, the moss was not able to mature fully between the PV panels so sedum mats were retrofitted one year after the initial green roof installation. Because of too much sunlight between the PV panel rows, the moss did not grow well. However underneath the panels, the moss flourished (Figure 2-6). To provide uniform plant coverage across the moss-green roof, 1m x 1m sedum mats were retrofitted in between PV rows on April 10, 2012, approximately one year after the installation of the moss green roof. These sedum mats were identical to the XF301 vegetation blankets and growing media installed as part of the original sedum-green roof, but were smaller in size³.



March 8, 2012



May 30, 2012

Figure 2-6: Moss green roof before (left) and after (right) retrofit of sedum mats occurred on April 10, 2012

In addition to the sedum and moss Xero Flor green roofs, three small Carlisle SynTech ultra-extensive green roofs (87sq. m total area) were placed on Sunscape in May 2011 (Figure 2-7).

³ A t-test done at the end of the project showed no statistically significant difference ($p < 0.05$) between the green roof-PV power output before and after the sedum mat installation.

These green roofs are similar in cross-section to the sedum green roofs by Xero Flor (Figure 2-5). The purpose of these roofs are to demonstrate three different installation types to building owners: 1) build-up, 2) modular trays and 3) hilly. For the hilly installation, an extensive green roof is placed on top of expanded polystyrene foam blocks to create the look of mounds or small hills (St. John, 2011). Since no data was gathered for these roofs, they are excluded from any further analysis in this thesis.



Figure 2-7: Images of small extensive green roofs: build up (left), modular (center), hilly (right)

Three different types of skylights are also installed. Seventeen Carlisle SynTec Drylights are placed across both black-EPDM and white-TPO roofs. In addition, one Carlisle SynTec Tubular skylight and one Ciralight smart skylight, which follows the sunlight to increase daylight penetration, are installed to display other types of skylights. Photos of the skylights are depicted in Figure 2-8. In this thesis research, no analysis was conducted pertaining to the effects of the skylights.

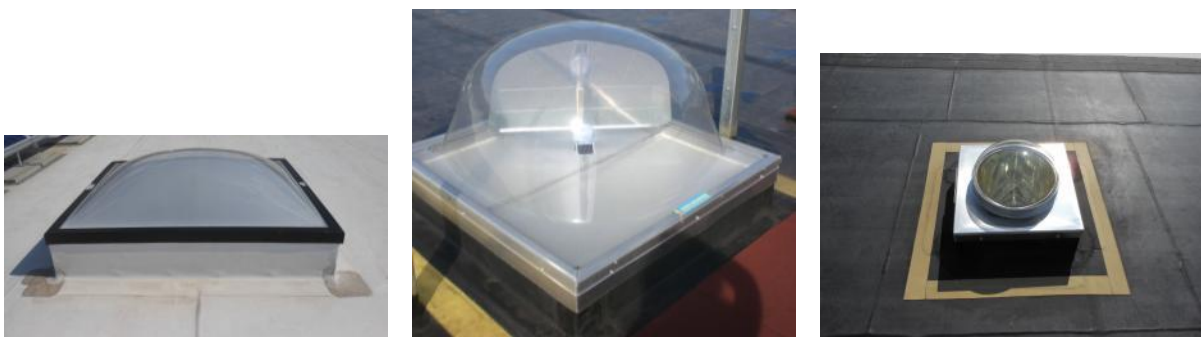


Figure 2-8: Images of skylights installed at Sunscape-Carlisle SynTec Drylights (left), Ciralight smart skylight (center), Carlisle SynTec Tubular skylight (right)

2.4 Types of photovoltaic arrays

Three types of photovoltaics (PV) technologies (polycrystalline, thin film, solar tubes) are mounted and connected at Sunscape to showcase the variety in PV technologies (Figure 2-9). One hundred and eighty ET Solar brand polycrystalline panels (49.7kW installed capacity) was selected for Sunscape to represent a mature PV technology that has been widely installed (US DOE-EERE 2011a). Each panel has dimensions of 1.96m by .99m (77 x 39.1 in). Unisolar's thin film laminate panels (4.7 kW capacity) uses a different technology that has become more common in the PV market. Each Unisolar thin film panel (30 total panels) has dimensions of 5486 x 394mm (216 x 15.5 inch). Lastly, 272 Solyndra's solar tubes were installed (51.4kW capacity) as an innovative, new technology with promise. These tubes are sized at 1820 by 1080 mm (71.7 x 42.5 inch). Although, both Unisolar and Solyndra filed for bankruptcy in 2012 and 2011 respectively, these PV panels are still being installed. Because the focus of this research compares data across roof types, power output from Unisolar thin film panels and Solyndra solar tubes were not examined in this thesis as they were only installed on the white roof.



Figure 2-9: PV Panels types- ET Solar polycrystalline (left), Solyndra solar tubes (center), Unisolar thin film (right)

In addition to variations in technology, these three types of PV have differences in panel tilt (0-30° from horizontal) and roof type (black-EPDM, white-TPO and green-moss) underneath the panels. All PV panels at Sunscape are installed with a set tilt and azimuth which does not move because the panels lack tracking systems. Solyndra solar tubes and Unisolar thin-film modules are installed with no tilt and placed directly on the white-TPO roof. The ET Solar polycrystalline panels have an angle of inclination of 15° or 30° from horizontal mounted with landscape orientation and facing south. All technologies are consistent with recommended installation specifications. Generally, the optimal panel tilt is close to the location's latitude $\pm 20^\circ$ to shorten

the distance between the sun and the panel and allow maximum direct solar radiation (Kern & Harris, 1975; Lewis, 1987; Rowlands et al. 2011). Therefore, in Pittsburgh at 40° N the optimal tilt range is 20-60°.

Since the angle of the sun is lower in the winter and higher in the summer, a fixed tilt PV panel will perform differently across the year (Lewis, 1987). A lower tilt PV panel should perform slightly better in the summer when the sun angle is high compared to the winter. In Pittsburgh at 40° N, the 30° tilt panels were expected to have more power output compared to the 15° tilt panels. However, higher panel tilts result in larger spacing between panel rows to prevent shading of adjacent panels in the winter when the sun angle is lower. Larger row spacing results in fewer panels on the roof. To maximize the installed PV capacity, Sunscape increased the number of panels by using a lower tilt angle of 15° even though panel efficiency decreased. A useful metric for panel tilt angle compares manufacturer specified peak panel watts to allocated roof space (including row spacing). For Sunscape, the 30° tilted panels result in 5.1W/sq. ft. of roof space while the 15° tilted panels correspond to 6.4 W/sq. ft of roof space. In other words, the 30° tilted panels required a larger footprint for installation. Table 2-2 summarizes the specific configurations for all three types of PV technologies.

The material and labor costs for the three different types of photovoltaics on Sunscape are summarized in Table 2-2. The 15° tilt polycrystalline panels over the black-EPDM roof had the lowest cost (\$3.65/Watt) while Solyndra was the most expensive (\$4.15/Watt) (Mike Carnahan, personal communication, March 2012). The cost difference between types of panels was because of market technology prices and effort required to install the panels. Within the polycrystalline panels, costs varied across tilts and with and without the green roof due to racking configurations summarized in Table 2-3. Another way to report the cost of PV is normalized the labor and material cost per watt (\$3.65-4.15/Watt) by area of roof space for each panel (5.1-9W/sq. ft. of roof space). The result of multiplying these two factors together for each PV type was installed costs of approximately \$20.40-\$37.35/sq. ft. of roof space Table 2-2.

Table 2-2: Photovoltaic array information installed at Sunscape

Manufacturer	PV Type	Roof Type	Panel Tilt	Panel tilt roof metric (Watt/sq. ft of roof space)	Number of modules	Panel Size	Power Capacity	Approx. PV materials and labor costs (\$/Watt)	Approx. PV installed costs (\$/sq. ft of roof space)
ET Solar P672275	Polycrystalline	Black-EPDM	15°	6.4	90	1956×992mm (77×39.1 inch)	24.8kW	\$3.65	\$20.40
		Green-moss	15°	6.4	60		16.6kW	\$3.85	\$24.64
		Black & White	30°	5.1	30		8.3kW	\$4	\$20.40
UniSolar PVL- 144	Thin-film	White-TPO	0°	5.2	30	5486 x 394mm (216 x 15.5 inch)	4.7kW	\$4	\$20.80
Solyndra 150-191	CIGS and thin-film	White-TPO	0°	9	272	1820x 1080 mm (71.7 x 42.5 inch)	51. 4kW	\$4.15	\$37.35

At Sunscape, the polycrystalline panels have two variations in racking types. The arrays use either ballasted or attached mount racking systems. The two arrays (15° and 30° tilt) over black roofs are both anchored using a ballast-weighted system of concrete squares (Figure 2-10). Ballast mounting systems have no roof penetrations. They rely on “weight of the PV modules, the mounting racks, and extra ballast to meet wind-loading design considerations” (Stafford, 2011). In contrast, the PV arrays over the moss-green roof are anchored with penetrations that went through the roof as shown in Figure 2-10. One reason why the different racking systems were chosen was to maximize the area of the green roof. Ballasted racking systems would have occupied significantly more surface area.

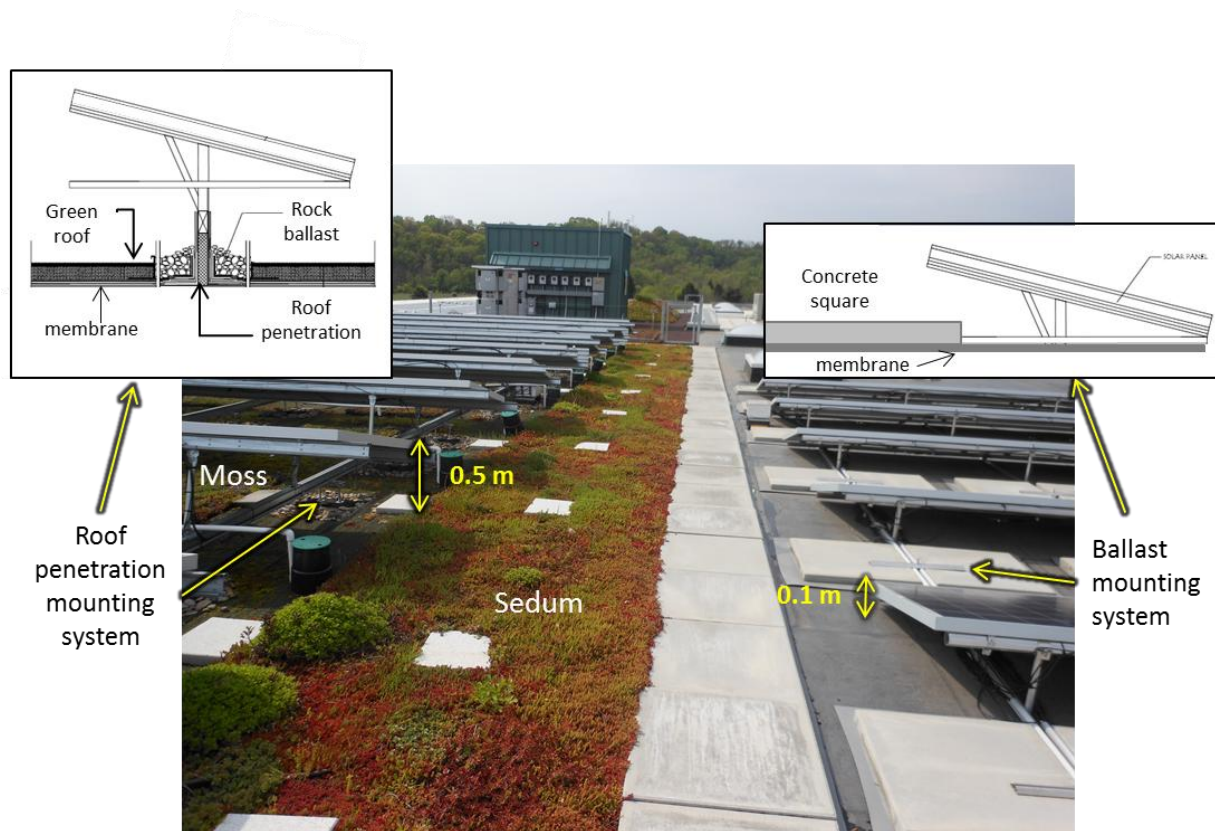


Figure 2-10: Racking type and height differences for Green Roof-°15 PV and Black roof-°15 PV

In addition to the differences in mounting systems, the polycrystalline panels varied in racking height and row spacing (Table 2-3). The shortest distance from the roof surface to the top edge of the PV panel is four times higher for the green roof compared to equivalent black roof system

(Figure 2-10). The higher racking configuration was chosen, in part, from the potential of vegetation growing high enough to shade the PV panels. The 30° panels are mounted slightly higher than the green roof- PV because of the variations in roof slope. The roof on top of Scalo is sloped to allow water drainage and avoid ponding. Some of the steepest parts of the roof are underneath the 30° panels which resulted in a taller racking system. The last variation is spacing between PV panel rows. Both 15° PV have the same row spacing, but the 30° tilt panels are slightly larger (Table 2-3).

Table 2-3: PV racking configurations for polycrystalline panels on Sunscape

PV Type	Racking type	Distance from front, top-edge surface to roof	Spacing between PV rows
ET Solar 15°-Green	Roof penetration	0.51 meters (20 in)	1.9m (73 in)
ET Solar 15°-Black	Ballasted	0.13 meters (5 in)	1.9m (73 in)
ET Solar 30°-Black/White	Ballasted	0.58 meters (23 in)	2.5 m (98 in)

For the polycrystalline PV system at Sunscape, the wiring design connects ten polycrystalline panels together in series to form a string. Three strings are further aggregated into one inverter where power output is measured. On Sunscape, 18 strings for the polycrystalline panels correspond to six inverters. For example, three strings (B-16, B-17 and B-18) each have ten panels for the 30° tilt panels shown in Figure 2-11. String B-16 consists of PV panels only on the black roof while B-17 and B-18 strings have PV panels on both white and black roofs (Figure 2-11). No micro-inverters are installed on individual panels to measure panel level power output. Therefore, as currently configured, power output cannot be disaggregated down to the string or panel level. Sub-metering on individual panels or strings would have been useful particularly for the 30° tilt panels, as modules are installed on both black and white membranes. If string level power output was available, comparisons across strings may have identified power differences resulting from black and white roofs. As a result, no black roof versus white roof analysis on PV power output was done in this dissertation.

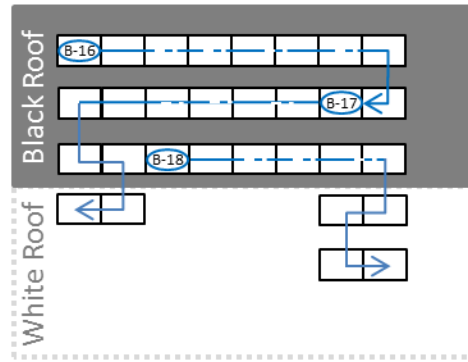


Figure 2-11: The wiring diagram for 30° tilt panels across black and white roof

2.5 Sensor installation and monitoring

Sunscape’s sensors record temperature, moisture, and electricity production across roof surfaces and PV technologies. A general schematic of sensor type and locations across the four main surface cross-sections is illustrated in Figure 2-12. Air and surface temperatures are collected below, on and above the various roof surfaces. For the polycrystalline panels, temperature sensors are also installed at the top of the panel and on the back surface of the PV panel to understand the effect of roof surface temperature. The air temperature sensors at the top of the PV panels vary in height because of the non-uniform racking system across polycrystalline panels above the black and green-moss roofs (Figure 2-10). Moisture sensors capture wetness in the green-moss and green-sedum roofs. Power output is measured for the different PV technologies at two main inverters on top of the roof. More details on sensor placement in proximity to the membrane and the data collected at each sensor are found in Section 2.6.

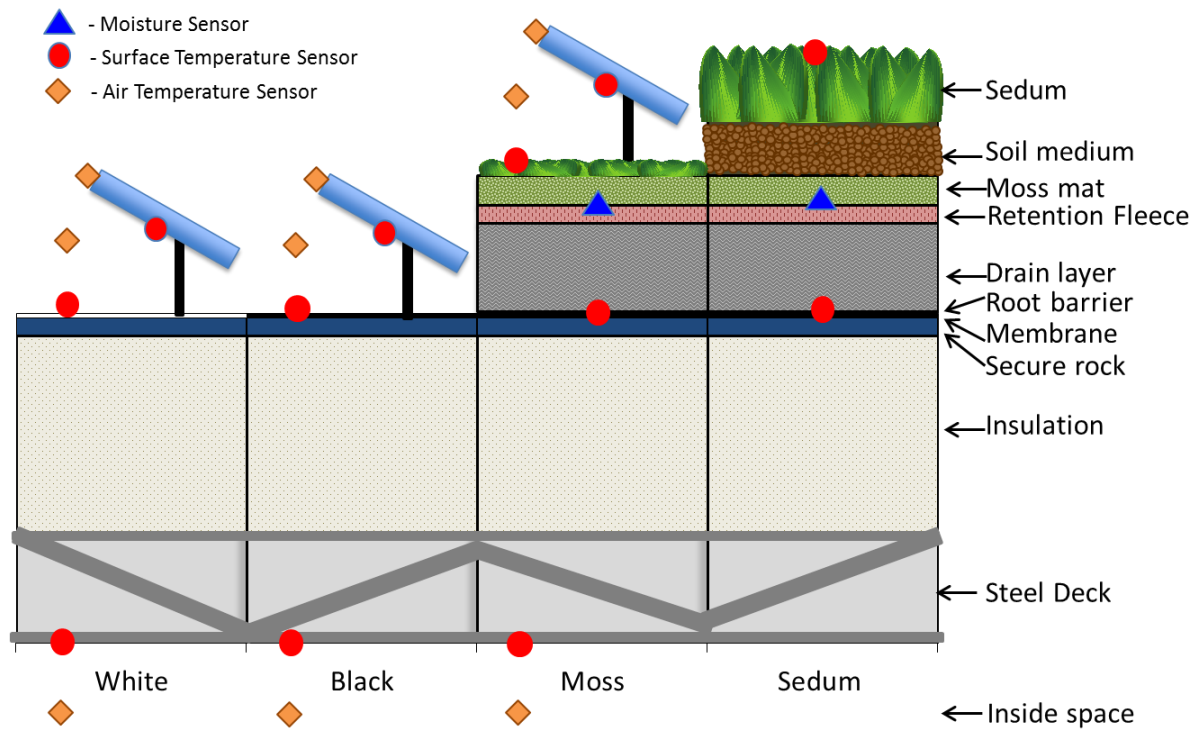


Figure 2-12: General schematic of sensor type and location across roof types (not drawn to scale)

Sunscape’s sensor design did not incorporate redundancy, i.e. only one sensor for each measurement. For example, the White-TPO surface temperature representing 1,580 sq. meters (17,000sq. ft.) of roof space is only collected in one place by one sensor not across many locations. With a finite budget for sensors, the sensor design was chosen to maximize the variety of data collected instead of having sensor redundancy. An alternative design would have fewer types of data collected but with redundant sensors.

In addition to instrumenting the roof surfaces and PV, a site-specific weather station, two pyranometers and a skylight collects temperature, wind and solar irradiance data. The Met One 34B weather station records data on wind speed and direction, solar radiation, rain, and ambient temperature on top of the penthouse (#9 in Figure 2-13). Relative humidity is not measured. Two additional Hukseflux LP02 pyranometers are installed at 15° and 30° from the horizontal to measure incoming solar radiation received on polycrystalline panels tilted to 15° and 30° . Lastly, surface temperatures above and below the acrylic skylight dome are measured on one Carlisle Drylight located on the black EPDM roof (#10 in Figure 2-13). While the Sunscape installation has over 45 sensors in total, measurements are collected in ten distinct

areas on Sunscape depicted in Figure 2-13. Table 2-5 provides additional information on specific data collected at locations 1-8 in Figure 2-13.

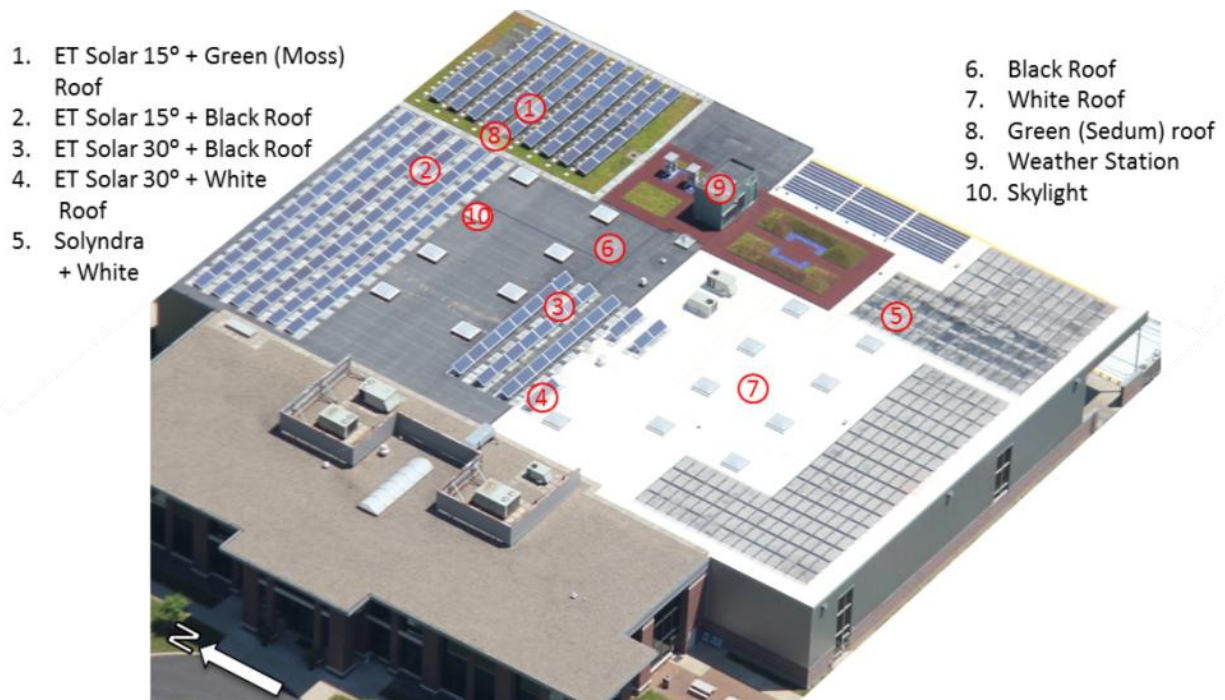


Figure 2-13: Measurement location of for various data collected on Sunscape (Photo courtesy of Scalo Solar)

Two separate data management systems are placed on Sunscape to manage the collected data. Both systems use an electronic data logger or base station to gather measurements from site instrumentation. Through an Ethernet connection, measurements are transmitted to two separate third-party hosted data storage servers off-site. Data is accessible via two website interfaces. These two overarching management systems are referred to as Draker and Hobo because of the parent service company agreements. A summary of the main hardware components of both systems including manufacturer tolerance ranges and operating temperatures is listed in Table 2-4. In the case of Draker, primary system hardware is from Campbell Scientific (CR1000 Base station) and Omega Engineering. Draker provides the online web management application and data storage under a five year service agreement until 2015. Onset Hobo provides all the hardware, software, data storage and web interface for a similar time duration.

Table 2-4: Summary of manufacturer specifications for primary hardware devices on Sunscape

Hardware Name	Model Number	Input Range	Accuracy	Operating Temperature
Campbell Scientific Data logger	CR1000	±5 V DC	±(0.06% of reading + offset), 0° to 40°C ±(0.12% of reading + offset), -25° to 50°C	-25° to +50°C (-13° to 122°F)
Omega Engineering Thermocouples	5TC-TT-J-24-36	See operating temperature	±1.5°C from -40 to 375°C	-40 to 750°C (-40°F to 1382°F)
Onset Hobo Data Logger	U30-WIF-000-S100-003	0-20 V DC but configurable	±0.25% accuracy from 50 mV to full scale	-20°C to 40°C (-4°F to 104°F)
Onset Hobo Thermocouples	S-TMB-M017	See operating temperature	< ±0.2°C from 0° to +50°C (< ±0.36°F from +32° to +122°F),	-40° to +100°C (-40° to +212°F)
Hukseflux pyranometers	LP02	0 to 2000 W/m ²	± ≤25 W/m ²	-40° to +80 °C (-40° to +176°F)
Met One Instruments Weather Station- wind speed	34B	0 - 167 mph (0 - 75 m/s)	Accuracy < 22.7 mph: .25 mph (0.1 m/s) Accuracy > 22.7 mph: ±1.1% of true	-30°C to +70°C (-22°F to +158°F)
Met One Instruments Weather Station- wind direction	34B	0-356°	±4°	-30°C to +70°C (-22°F to +158°F)

Draker is the primary data collection and monitoring system which uses Omega Engineering thermocouples (Model No. 5TC-TT-J-24-36). Thermocouples contain two separate, dissimilar metals which each generate a voltage. Temperature measurements are proportional to the voltage difference across metals. The Omega thermocouples were determined to be not appropriate for soil moisture measurements within green roofs. As a result, a second type of sensor (Onset Hobo S-TMB-M017 thermocouples) was selected for soil moisture measurements across the green-sedum and green-moss roofs. Since this Onset Hobo sensor was unfamiliar to Draker, Draker was unwilling to incorporate the soil moisture sensor into the overall Sunscape monitoring system. Consequently a second smaller monitoring system, Onset Hobo computer logger, is incorporated into the Susncape project. For consistency, Onset Hobo sensors are also used for all

temperature measurements relating to the green roofs and the black roof-PV 15° assembly. The Onset Hobo data logger has the additional functionality to manage the moisture and temperature thresholds to control the green roofs irrigation systems. Resulting from this history, the Onset Hobo computer logger monitors approximately one-third of the data while the Draker system records the rest. Appendix A lists the complete list of data collected for each system.

Both datasets are accessible via the internet. To access the data, a user needs a password for Draker Laboratories or a specific URL for Onset Hobo computer logger. Real-time data can be viewed through both internet interfaces. Limited real-time data can be accessed on-site through a hand-held keypad display for Draker and by manually downloading the data from Hobo's base station. From either website, the data are downloaded as a comma separated values (.csv) file. Data in this format were imported into Microsoft Excel and Matlab for further analysis. Within the Draker interface, datasets can be customized to incorporate the raw data of interest. For example, datasets including only weather station information can be created by selecting boxes corresponding to those sensors. Draker data downloads are limited by 1.5 million data points; as a result, increasing the number of data categories reduces the time period available for each download. In contrast to the filtering capabilities of Draker, all available data are included in all downloads within the Onset Hobo internet system called Hobolink. Due to the Onset Hobo data logger memory capacity, only 500,000 data points can be downloaded through Hobolink at one time. Therefore, multiple downloads were need to obtain a year's worth of data.

If the Ethernet connection is disconnected, both monitoring systems have on-site memory within the base station to avoid loss of data. The Campbell Scientific CR1000 Base station has 4 megabytes of memory equivalent to approximately 1000 days of storage based on the 15 minute sampling frequency and 18 total Draker-managed sensors on Sunscape. The Onset Hobo Data Logger has 512 kilobytes of memory which translates to about 178 days of storage before data from the fifteen sensors begin to overwrite. On Sunscape, one year of data from all 33 sensors would require 2.3 megabytes at a 15 minute sampling frequency.

2.6 Data collection

Data, on Sunscape, are collected across the eight roof type or roof type-PV combinations on Sunscape (Table 2-5). However, the quantity and type of data varies across each combination. The green roof-PV 15° (Table 2-5 - #1) and black roof-PV 15° (Table 2-5 - #2) systems have the most data locations while Solyndra solar tubes has the least. Table 2-5 summarizes the measurements listed by height from outside the building to inside categorized by each of the eight roof type or roof type-PV combinations. All data were recorded at 15 minute intervals.

Table 2-5: Type and start date of data collected on Sunscape separated by roof technology

Data available from:		January 26,2011	January 1, 2012	July 5, 2012	No data					
<div>Outside</div> <div><div></div></div> <div>Inside</div>	Height above roof cm (in.)	Measurement description	Roofs with PV					Roofs without PV		
			1. ET Solar 15° + Green (Moss) Roof	2. ET Solar 15° + Black Roof	3. ET Solar 30° + Black	4. ET Solar 30° + White	5. Solyndra + White	6. Black (EPDM)	7. White (TPO)	8. Green (Sedum)
	NA	PV Output								
	84 (33)	back-surface PV panel temp.								
	76 (30)	Air temp.								
	66 (26)	back-surface PV panel temp.								
	33 (13)	Air temp.								
	23 (9)	back-surface PV panel temp.								
	15 (6)	Air temp.								
	0	Green roof surface temp								
	0	membrane surface temp.								
	0	Underside metal deck surface temp.								
-15 (-6)	Air temp. below metal deck									
	Moisture									
	Irradiance									

Data collection began in phases during 2011 and 2012. January 26, 2011 was the first record for all PV output arrays as well as for the temperatures sensors in the following combinations mentioned in Table 2-5:

- ET Solar 30° +Black ((Table 2-5 - #3),
- Solyndra +White (Table 2-5 - #5)
- Black (EPDM) Roof (Table 2-5 - #6), and
- White (TPO) Roof (Table 2-5 - #7).

Furthermore, all skylight and climate parameters from the weather station, except wind were also available from January 26, 2011. Unfortunately, the wind speed, direction and maximum wind speed were unreliable before January 1, 2012 as sensors needed to be replaced or reset.

Two additional groups of data collection began after January 26, 2011. Reliable data highlighted by three green boxes⁴ in Table 2-5 began on January 1, 2012. Before that time, these three sensors were faulty because intermittent 0 values were recorded. The sensors for the moss-green roof-15° PV (Table 2-5 - #1), black roof-15° PV (Table 2-5 - #2) and sedum green roof (Table 2-5 - #8) started data collection on May 24, 2011 when the sensors were installed.

Thus, the main core dataset for this research began on January 26, 2011 and ended on October 13, 2012. The study period concluded in October 2012 due to research time limitations. Within this 21 month time frame, chapters in this thesis used different subsets of the data for analysis. The specific data subset and further measurement inconsistencies are described at the beginning of each chapter.

As a result of the initial Sunscape layout choices discussed above in Section 2.4, no comparisons could be made with the white roof and polycrystalline panels at 30° tilt. Therefore, three additional sensors (Table 2-5 shaded yellow in column “ET Solar 30° +White”) were added on July 5, 2012 for research purposes to enhance the comparisons available at Sunscape. These three sensors allowed analysis across black and white roofs containing the same polycrystalline 30° tilt panels. More specifically, one sensor measuring back-surface panel temperature was added to one 30° tilted polycrystalline panel over the white roof to evaluate differences across

⁴ The green boxes are for back surface panel temp at 84cm height under ET Solar 30° +Black (Table 2-5 - #3), 15cm (6in.) air temp under Solyndra + White (Table 2-5-#5), and 15cm (6in.) air temp under Black (Table 2-5 - #6).

the black and white roofs. In addition, panel-shaded surface temperatures were added above and below the white roof to measure heat flux. These two sensors allow heat flux calculations to be compared at points in pure sun to those in the shade. To make a useful comparison, the black roof-PV 30° surface temperature sensor was relocated from direct sun to the shade underneath the panels. Since the PV output cannot be disaggregated to a string or panel level, no analysis can be conducted on the difference in power output resulting from white or black roofs.

Furthermore, two additional air temperature sensors (Table 2-5 shaded yellow in column “ET Solar 15° +Green (Moss) Roof”) were added to enhance air temperature comparisons with other roofs. More specifically, the two air sensors at heights of 15cm (6in) and 33cm (13in) were installed over the green-moss roof (Figure 2-14) to match heights of sensors on other roof types. Originally, only white and black roofs had a 15cm (6in) air temperature sensor. To increase meaningful results from Sunscape, the green roof needed an equivalent measurement. Since the black roof-PV 15° assembly has a lower racking configuration than the green roof-PV 15°, matching air temperature sensors at 33cm (13in) were needed to assess the impact of roof type on air temperature. All six sensors (five new and 1 relocated) indicated by yellow shading in Table 2-5 had reliable data starting on July 5, 2012. Appendix A lists the complete list of data, the unit of measurement and beginning date of data collection.



Figure 2-14: New air sensors over moss-green roof

2.7 Pittsburgh weather conditions during study period (July 1, 2011- June 30, 2012)

Weather information collected on Sunscape was compared to historical averages for benchmarking purposes. Typical meteorological year (TMY) datasets were first created in 1978 by Sandia National Laboratories to determine one year of average hourly weather and solar information (Wilcox & Marion, 2008). The first TMY iteration used historical values from 1952-1975 for 248 sites. Since 1978, the National Renewable Energy Laboratory has updated the dataset twice (TMY2 and TMY3) with more current meteorological data from 1961-2005 and expanded to 1,400 sites across the United States (Wilcox & Marion, 2008). This research uses the most current TMY3 (referred to as TMY for this thesis) values which has uncertainly ranges of 9-13% for weather parameters (National Renewable Energy Laboratories, 2005). Since TMY values were collected hourly (recorded on the hour) and Sunscape values were measured in 15 minute intervals, TMY hourly values were repeated three times (fifteen, thirty and forty-five minutes past the hour) in order to map with Sunscape data. Using TMY data for comparisons helps place the measurement year into context.

Ambient air temperatures measured on Sunscape during July 1, 2011 to June 30, 2012 were compared to TMY values for Pittsburgh. Table 2-6 lists the range of monthly average air temperatures measured on Sunscape and compares the average to TMY data. For ten of the twelve months, Sunscape ambient temperatures were 1-5°C hotter than baseline TMY average values for Pittsburgh. For the other two months, October was similar to the TMY data and April was 2°C colder than historical averages. Overall, the temperatures were 2°C higher on average during July 1, 2011 to June 20, 2012 compared with TMY.

Table 2-6: Comparison of Sunscape (July 1, 2011-June 30, 2012) and TMY ambient temperatures

Month	Sunscape Temperature (°C)			TMY (°C)			Difference in Averages (°C)
	Min	Average	Max	Min	Average	Max	
January	-15	1	18	-17	-1	19	2
February	-10	3	19	-16	0	15	3
March	-7	11	31	-7	8	26	4
April	-1	11	30	-3	13	27	-2
May	3	20	35	0	15	33	5
June	8	22	39	8	19	29	3
July	13	25	39	13	22	29	4
August	10	23	36	9	21	30	2
September	4	19	39	8	18	30	1
October	-1	12	33	0	12	24	0
November	-3	8	22	-4	7	25	1
December	-8	3	17	-12	1	12	2

Similar to ambient temperature, solar irradiance was also higher over the study period compared with the TMY benchmark year. Figure 2-15 illustrates a typical hourly solar irradiance profile for an average 24 hour day in each month. From April to August, TMY solar irradiance values generally were higher earlier in the day but have lower peaks to Sunscape. In the winter months (Nov-Jan) the TMY and Sunscape average hourly profiles were similar. Another useful way to compare datasets was through solar radiation totals. The summation of solar irradiance over time is solar radiation. Below the months in Figure 2-15 is the percent difference in solar radiation between Sunscape and TMY for each month. For all months except February, March and October, the total monthly solar radiation was 2-38% higher than the typical meteorological year. For annual total solar radiation, the Sunscape dataset is 12% higher. Generally, higher temperatures correspond to higher solar radiation; the data in Table 2-6 and Figure 2-15 are consistent with this trend.

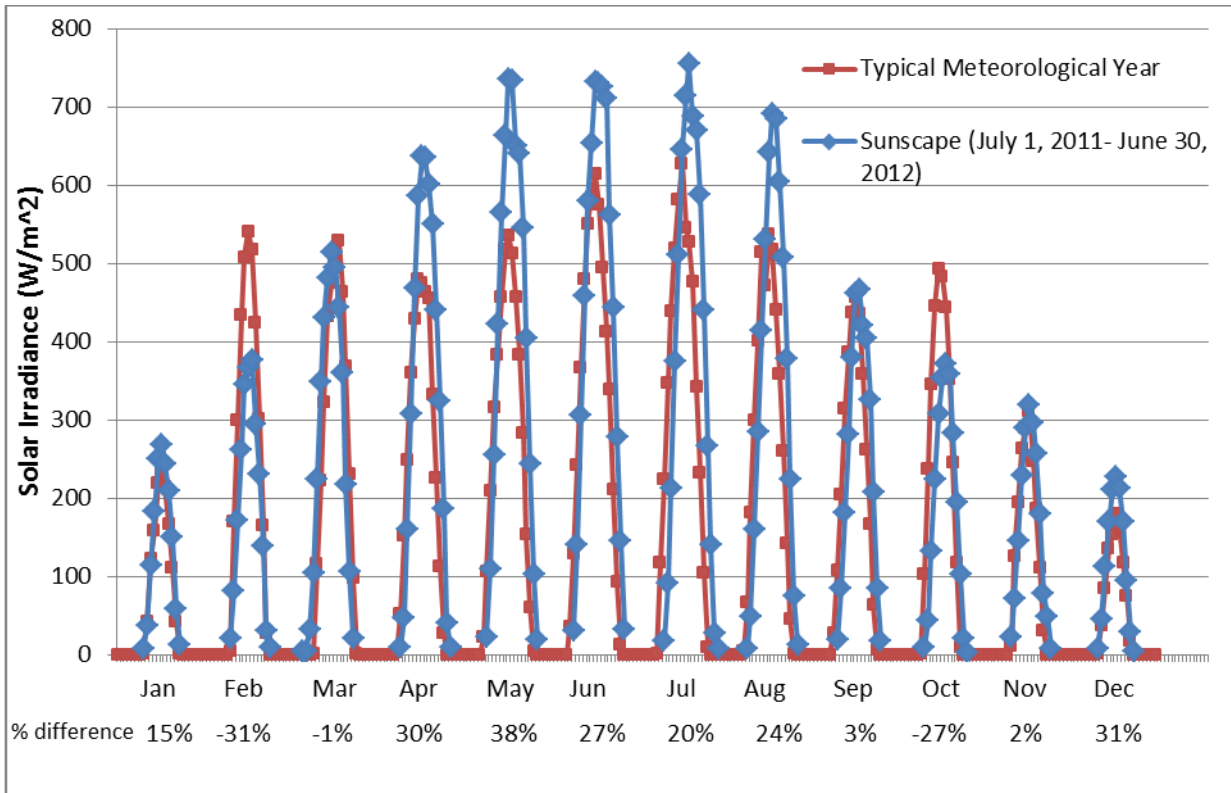


Figure 2-15: Monthly average hourly solar radiation values measured on Sunscape compared with TMY

Another useful way to compare datasets was to combine both the solar irradiance and air temperature daytime hourly values. Figure 2-16 illustrates the number of hours corresponding to a specified ambient temperature and solar irradiance range for measured values at Sunscape and TMY values for Pittsburgh. Places that are hot and have high solar radiation values (e.g. Phoenix, Arizona) have darker cells towards the lower right of Figure 2-16. While the Sunscape and TMY profiles generally have the same shape, the Sunscape measured values are slightly hotter and have higher solar irradiance values. Typically, Sunscape would not have different temperature and solar radiation values than TMY, but the study period was a particularly warm and sunny year as in Table 2-6 and Figure 2-15. In addition, both datasets have a similar quantity of daytime hours throughout the year. While days are longer in July and shorter in January, daylight hours were not adjusted on a monthly basis. Instead, daytime measurements were defined in this thesis as having solar irradiance values greater than 4 W/m^2 . This solar irradiance threshold is quite small compared to the average solar irradiance value of 335 W/m^2 or the maximum value of 1154 W/m^2 measured at Sunscape.

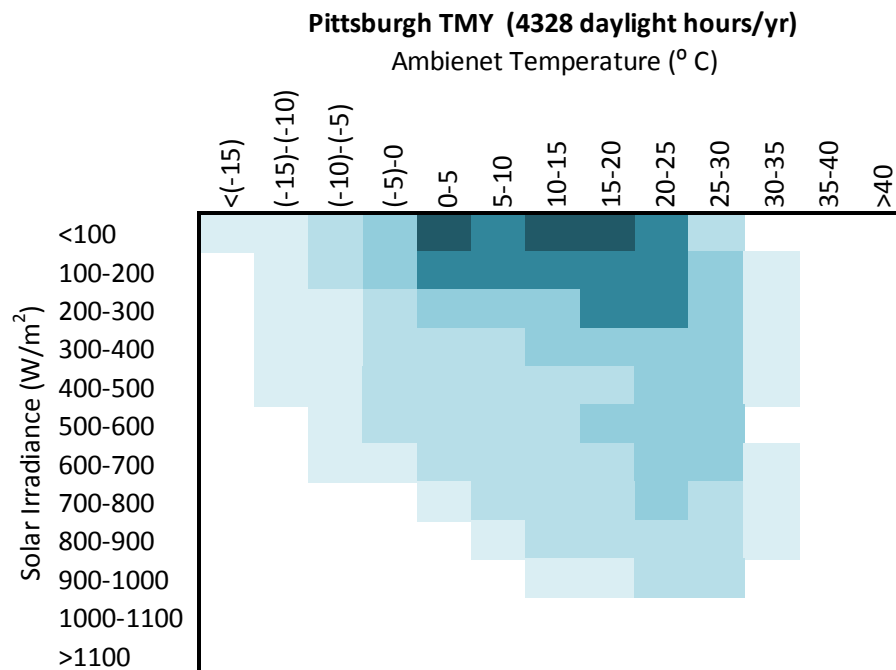
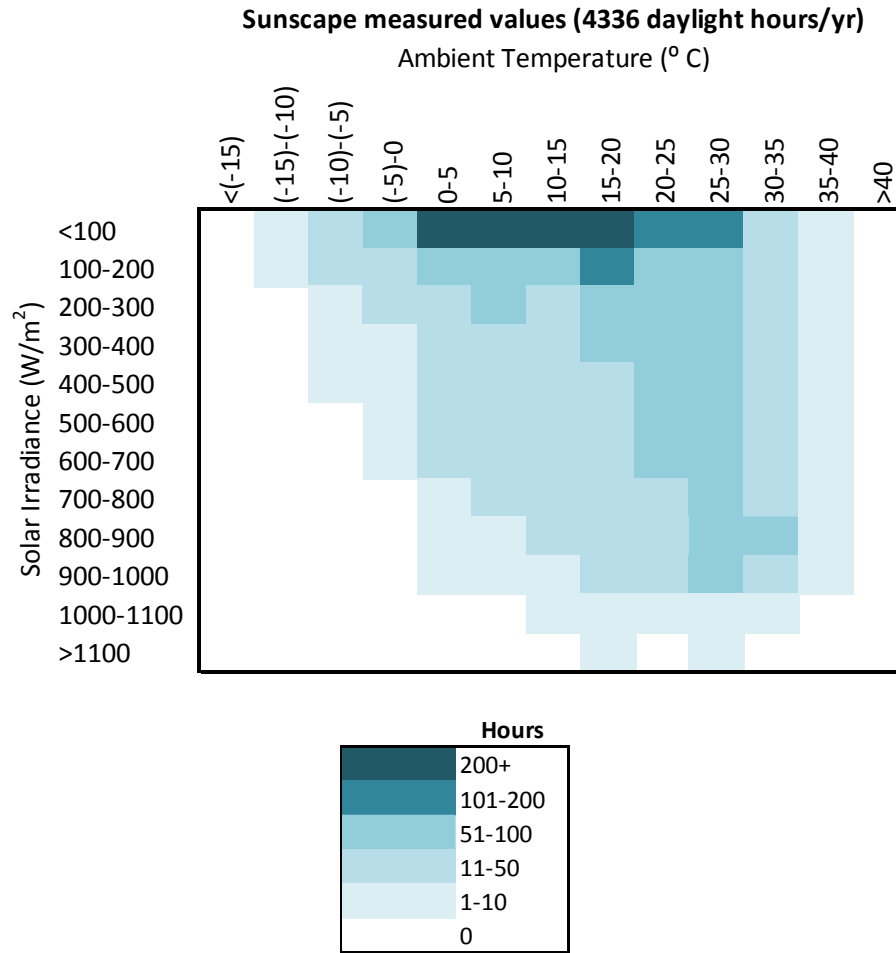


Figure 2-16: Solar irradiance and air temperature comparisons of Sunscape (above) versus Pittsburgh's TMY (below) datasets

Since wind speed and temperature recording at Sunscape began January 1, 2012, the wind data from National Weather Service (NWS) located at the Pittsburgh International Airport was used instead as a comparison with TMY data for the entire July 1, 2011- June 30, 2012 period (NOAA- National Climatic Data Center 2012). The NWS station is located 10.7 miles northwest of Sunscape (Figure 2-1). While the NWS data was used for comparison purposes, six months of site-specific wind data were used and are discussed in subsequent chapters. In order for the NWS to classify average wind speed, the wind must be constant for 2 minutes (NOAA-National Weather Service, 2012). If wind speed is 0m/s, the wind speed is considered calm. Similarly, wind direction must be constant for 2 minutes. If “(1) the wind direction fluctuates by 60° or more during the 2-minute evaluation period and the wind speed is greater than 6 knots; or (2) the direction is variable and the wind speed is less than 6 knots” the wind direction is considered variable (NOAA-National Weather Service, 2012). Over the study period, the NWS wind dataset shows 2% of the annual hourly data points as calm and 21% as variable.

The remaining 77% of NWS data for wind direction and speed are illustrated by the wind-rose histogram in Figure 2-17. The wind direction is reported by where the wind is coming from. In other words, wind blowing from east to west is an east wind. Approximately 38% of the wind is blowing from the south west (between 180-270 degrees). In terms of wind speed, Figure 2-17 shows the wind speed allocated to each wind direction histogram. Over the 2011-2012 study periods, the NWS Pittsburgh data from the airport weather station report 60% of the wind is less than 4m/s.

A similar wind rose histogram showing wind speed and direction for TMY data is also provided in Figure 2-17. Generally, the NWS data were in good agreement with the TMY data for wind direction and speed. Both datasets show the majority of wind coming from the southwest (38% in NWS versus 40% in TMY). Furthermore, the average wind speeds across the year were within 5% (3.8m/s in NWS versus 4m/s TMY). Notable differences between the datasets include the quantity of hours with calm wind (2% NWS vs. 5% TMY) and the lack of variable wind category within TMY data.

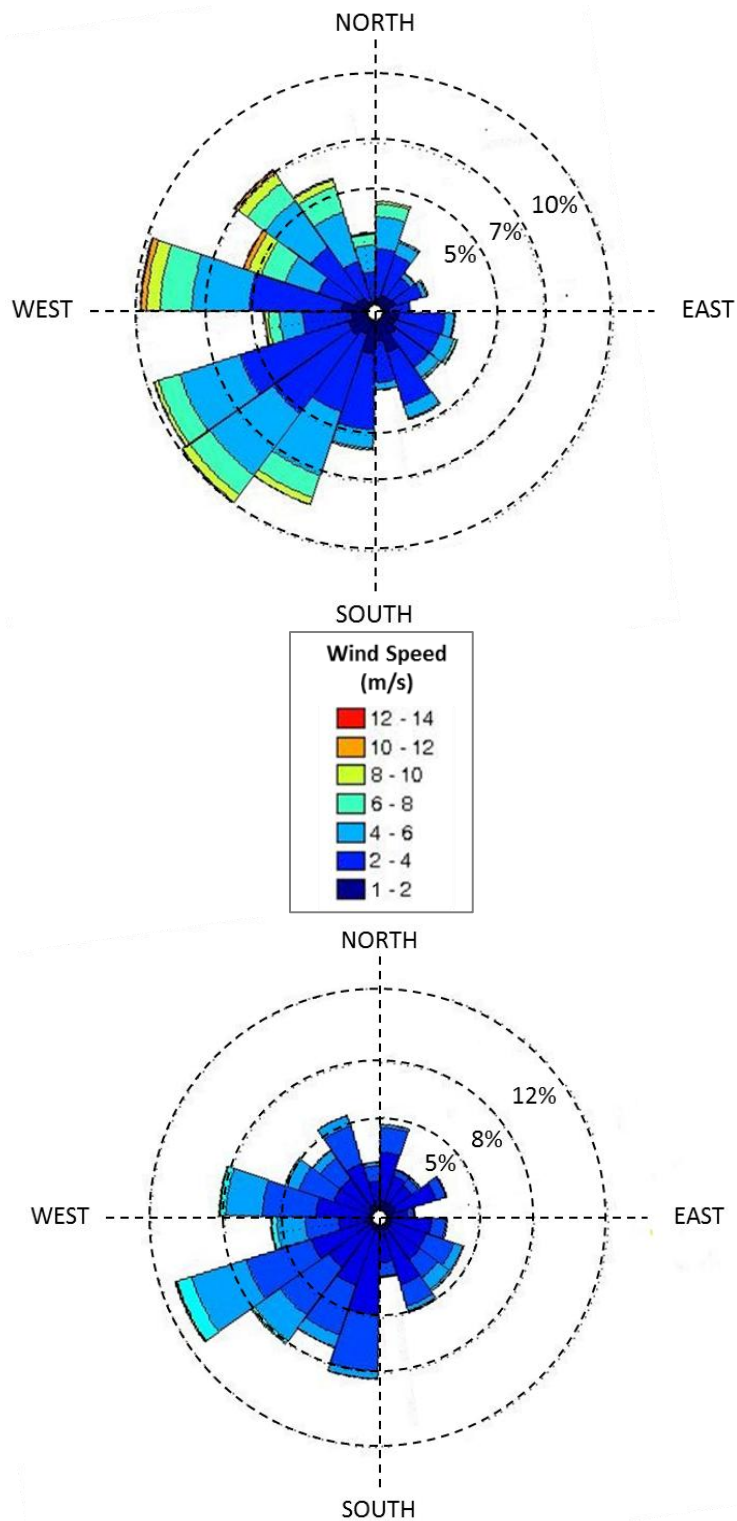


Figure 2-17: Wind speed and source wind direction histogram of NWS (above) and TMY (below) datasets⁵

⁵ The wind rose Matlab function which was used to make this figure can be found at mathworks.com (<http://www.mathworks.com/matlabcentral/fileexchange/17748-windrose>)

Last, relative humidity (RH) for the measurement year using the NWS dataset compared to the TMY year were 5% lower on average across the year (71% RH TMY vs. 66% RH NWS). On a monthly basis, the NWS dataset across the measurement year had 2-24% lower RH values except for February when the NWS was 13% higher. In September, both datasets had the same average RH. These results are consistent with the solar irradiance values presented in Figure 2-15; higher RH corresponds to lower solar irradiance values. Relative humidity is helpful in estimating the magnitude of solar irradiance reaching the earth surface, and thus, useful in estimating PV productivity (Gwandu 1995; Cess 1995). Since actual irradiance values were measured at Sunscape, relative humidity was only used as a reference. While RH was included in this section for completeness, RH was not used specifically in any analysis.

In summary, the measurement period from July 1, 2011 to June 30, 2012 contained slightly warmer temperatures and higher solar radiation values compared with the historical TMY. The lower relative humidity data from the measurement year were consistent with higher temperature and solar radiation values. The wind direction and speed were quite similar between the two datasets.

2.8 Weather parameter significance on photovoltaic power output on Sunscape

Typical power output varies by month due to deviations in daylight hours and weather parameters. For example, the 60 panels installed above the black roof had average monthly power output of 2.4kW (15% of peak installed capacity) in January to 5.7kW (35% of peak installed capacity) in May and June. Within each month, power output had a significant range (~14kW) from the minimum to the maximum power output depicted in Figure 2-18. Figure 2-18 also shows the percentage of total annual daylight hours for each month. Winter months have approximately 4% fewer daytime measurements compared to summer months. This observation is consistent with shorter winter daylight hours. Overall, more power was produced by PV in summer months compared to winter months as a result of more incoming solar radiation (Figure 2-15) and longer daylight periods (Figure 2-18).

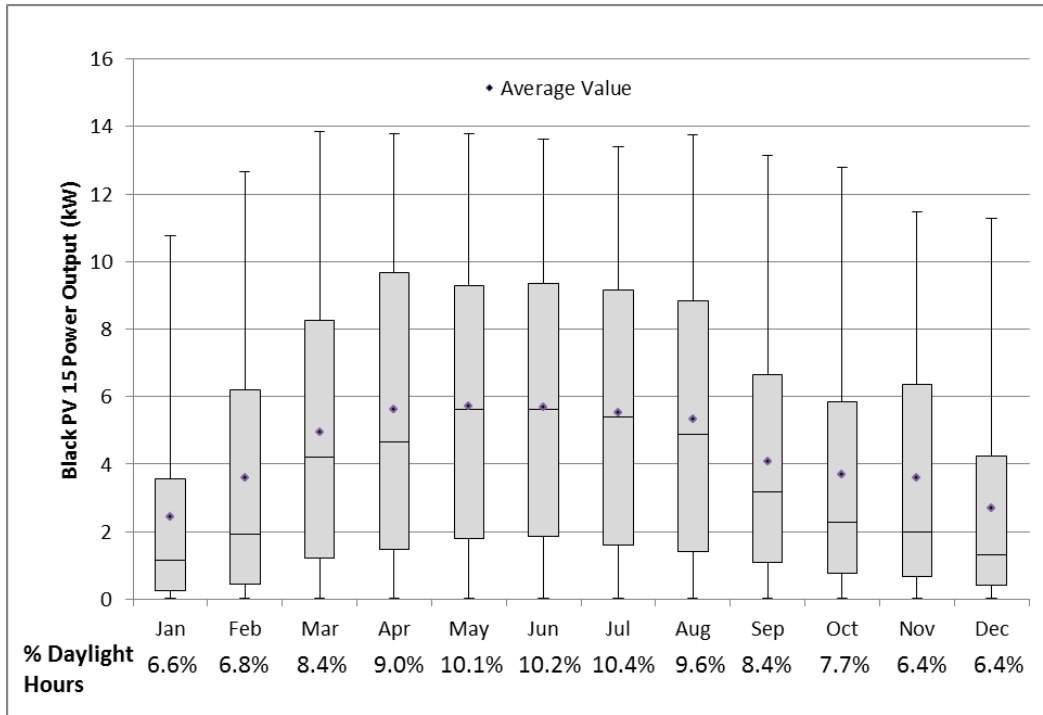


Figure 2-18: Monthly photovoltaic power output for 60 black roof PV panels tilted at 15°

As discussed in Chapter 1, photovoltaic power output can vary on account of incoming solar irradiance and ambient temperature. Generally, power output increases with solar irradiance and temperature. Table 2-7 shows increasing average power output as solar irradiance increases down any temperature column for 60 PV panels tilted at 15° over the black roof. Table 2-8 shows a similar result but for 60 PV panels tilted at 15° over the green roof on Sunscape. Power output also increases along rows in Table 2-7 and Table 2-8 until approximately 10-20°C in ambient temperature where power begins to decline for most rows (indicated by a dark line in Table 2-7 and Table 2-8). The decline in power output as a result of higher temperatures is typical among polycrystalline panels (Meral 2011). Therefore, optimal locations for power output have high solar radiation with moderate air temperatures (bottom middle of Table 2-7 & Table 2-8). Values shaded yellow in Table 2-7 and Table 2-8 only contain one or two data points so caution should be used in assessing their accuracy. In Pittsburgh, the average power output across the year was 4.60kW for the black roof-PV and 4.58kW for the green roof-PV assembly with averages of 335 W/m² in solar irradiance and 17° C (63°F) in daytime temperature.

Table 2-7: Average power output of 60 Black roof- PV panels tilted at 15° on Sunscape from July 1, 2011- June 30, 2012
(Cells highlighted yellow have 2 or less data points. The dark line above 10° C indicates a decline in power output)

		Ambient Temperature (° C)											Weighted Average (kW)
		<-10	-10 - -5	-5-0	0-5	5-10	10-15	15-20	20-25	25-30	30-35	>35	
Solar Irradiance (W/m ²)	<100	0.1	0.3	0.4	0.6	0.6	0.6	0.6	0.5	0.6	0.7	1.0	0.6
	100-200	0.5	0.8	1.4	2.1	2.2	2.1	2.2	2.1	2.0	1.9	1.9	2.0
	200-300		1.0	2.1	3.8	3.8	3.7	3.7	3.7	3.5	3.4	3.4	3.5
	300-400		0.3	4.4	5.0	5.3	5.3	5.2	5.1	4.9	4.8	4.7	5.1
	400-500		0.5	5.7	6.5	6.8	6.7	6.6	6.5	6.3	6.1	5.8	6.4
	500-600			7.2	7.5	8.3	8.2	7.9	7.8	7.5	7.4	7.3	7.8
	600-700			8.3	8.4	9.6	9.5	9.2	9.0	8.7	8.6	8.5	9.0
	700-800				10.5	10.9	10.7	10.5	10.2	10.0	9.7	9.4	10.2
	800-900				11.9	12.2	11.9	11.6	11.3	11.0	10.8	10.6	11.1
	900-1000				12.9	13.2	12.9	12.7	12.3	12.0	11.7	11.3	12.1
	1000-1100						13.4	13.3	13.1	12.9	12.4		13.0
	>1100							13.8		13.6			13.6
Weighted Average (kW)		0.13	0.56	1.40	2.84	3.40	3.82	4.09	4.98	6.60	7.59	8.18	4.60

Table 2-8: Average power output of 60 Green roof-PV panels tilted at 15° on Sunscape from July 1, 2011- June 30, 2012
(Cells highlighted yellow have 2 or less data points. The dark line above 10° C indicates a decline in power output)

		Ambient Temperature (° C)											Weighted Average (kW)
		<-10	-10 - -5	-5-0	0-5	5-10	10-15	15-20	20-25	25-30	30-35	>35	
Solar Irradiance (W/m ²)	<100	0.1	0.3	0.3	0.6	0.6	0.6	0.6	0.5	0.6	0.7	0.9	0.6
	100-200	0.5	0.7	1.4	2.0	2.2	2.0	2.1	2.1	2.1	2.0	2.0	2.0
	200-300		0.9	2.0	3.7	3.7	3.6	3.6	3.6	3.5	3.5	3.5	3.5
	300-400		0.3	4.3	4.9	5.2	5.2	5.1	5.0	4.9	4.8	4.8	5.0
	400-500		0.5	5.6	6.3	6.6	6.6	6.5	6.4	6.3	6.2	6.0	6.4
	500-600			7.0	7.3	8.2	8.0	7.9	7.7	7.6	7.5	7.4	7.7
	600-700			8.2	8.3	9.5	9.4	9.1	8.9	8.8	8.7	8.6	8.9
	700-800				10.3	10.8	10.6	10.4	10.1	10.0	9.80	9.59	10.2
	800-900				11.8	12.0	11.8	11.6	11.3	11.1	10.9	10.7	11.2
	900-1000				12.8	13.2	12.9	12.7	12.4	12.1	11.9	11.4	12.2
	1000-1100						13.4	13.4	13.2	13.0	12.6		13.1
	>1100							13.8		13.6			13.7
Weighted Average (kW)		0.12	0.50	1.33	2.78	3.35	3.75	4.04	4.95	6.64	7.70	8.32	4.58

2.9 System configuration limitations and improvements for future studies

Sunscape serves as a demonstration of current roof surface and solar technologies, a test bed for research, and a vision for future roofs. A mixture of project objectives coupled with a public and private joint venture led to the current Sunscape configuration. While many stakeholders with different interests had input into the final layout, design choices did constrain the research possibilities.

Unfortunately, the green-moss roof did not grow well in pure sun as was originally expected. Therefore, the moss surface temperature sensor placed in direct sun only measured the surface temperature of the moss mat material. Adding a sensor underneath the PV panels in the shade where the moss grew would have been helpful for comparison of surface temperatures and heat flux across other roof surfaces.

The placement and wiring of PV panels limited the analysis between roof surface and PV. Maintaining a uniform PV racking height would have ensured a more equivalent comparison between black roof-PV and green roof-PV tilted at 15°. In addition, a white roof-PV dataset would have created a more comprehensive analysis between roof type and PV. Installing micro-inverters on select 30° tilt panels or the ability to monitor string level power output would make the current Sunscape configuration more useful to investigate black roof-PV and white roof-PV relationships.

For data collection, sensor redundancy would improve the accuracy of the results. For example, averaging across multiple sensors would reduce the impact of partial sensor shading or uneven air or surface temperatures. More specifically in this experimental design, three sensors for each data point would have:

- provided more robust averages,
- supplemented additional data if one sensor became faulty or provided inconsistent measurements, and
- identified inconsistent data through comparison with the other two readings.

Furthermore, incorporating relative humidity as a part of the weather station would remove the need to use the National Weather Service data. Finally, adding additional sensors to direct sun

and full-shade locations would enable a more complete analysis of heat flux through all types of roof surfaces.

From this experimental configuration, some recommendations for future sensor design of field experiments include:

- Careful consideration of seasonal sun angles needs to be taken into account to avoid sensors receiving partial sun or shade.
- Horizontal and vertical spacing between sensors should be consistent across comparison test beds.
- Avoid placing reflective tape or other sensor marker indicators near sensors which could alter measurement readings. On Sunscape, yellow reflective tape was originally used to frame sensor locations in order to bring attention to their location. However, the yellow tape was removed as the temperature sensor was slightly altered due to the yellow reflective tape.
- Provide sensor redundancy (at least 3) for each main data point of interest. Additional sensors should be added for larger testbeds or for areas with projected large variation in measurements.
- At least twice a year, all sensors should be visually inspected to ensure no corroding or degradation has occurred. Also, the measurement consistency of the sensors should be verified periodically by downloading the data and conducting preliminary analyses. Some electronic monitoring and data collection systems have automatic warning systems alerting users if measurements were recorded outside a certain range which is a useful feature. Both physical inspection and data verification allow early detection of faulty or inconsistent data which can prompt quick remedial action.
- Place a waterproof label on each sensor with the corresponding name as it appears verbatim in the data collection and monitoring system.

Chapter 3: Examining climate parameter impact on photovoltaic power output through a regression analysis

3.1 Introduction

The demand for solar energy is increasing which promotes accurate estimation of PV output when designing a PV system. Many solar PV output prediction models are based on the characterization of outdoor current-voltage (I-V) curves (Rosell 2006; Villalva 2009; Xiao 2004) defined by three points (the short-circuit current, open-circuit voltage and the maximum power point) with some models using five points (King 2004). When irradiances and PV cell temperatures are known, other PV power prediction models use linear equations incorporating a range of parameters such as corrections for temperature and low solar irradiance (Marion 2008) and/or material and system-dependent properties (i.e. glazing-covert transmittance and plate absorptance) (Skoplaki 2009a).

In the absence of measured solar radiation values, relative humidity and sky conditions (e.g. cloudiness) are helpful weather parameters in estimating the magnitude of solar irradiance reaching the earth surface, and thus, useful in estimating PV productivity (Gwandu 1995; Cess 1995). When PV cell temperature is not readily available, the cell temperature is often estimated using regression functions (Skoplaki 2009b). These regression equations are mostly linear and cell temperature can be determined directly or indirectly (i.e. through iterations). Often these functions use varying climate parameters as explanatory variables (Skoplaki 2009b; Tamizhmani 2003; King 2004). The most common weather variables used in regression equations include ambient temperature and solar radiation and to a lesser extent wind speed and direction (Griffith 1981; Skoplaki 2009a; Skoplaki 2009b). Wind speed and direction can influence the PV panel operating temperature by convection (Skoplaki 2009b).

The Pittsburgh-Sunscape data was used to estimate two empirically derived regression equations to predict back-surface panel temperature and power output which were applied to three other United States cities (discussed in Chapter 4). Chapter 3 examines linear and non-linear regression equations based on sections of PV panels tilted at 15° over black roofs (referred to as black roof-PV) and green roofs (referred to as green roof-PV) on Sunscape. The initial analysis

uses ambient temperature and solar radiation as explanatory variables. A secondary analysis adds wind speed and direction as explanatory variables to understand if these factors improve the fit of the regression. Relative humidity and cloudiness were both considered as explanatory variables in the regression equations to predict PV power output, but then removed. This chapter aims to evaluate the following hypothesis and answer the supporting research questions:

Chapter 3 hypothesis: Back-surface panel temperature and PV power output from green or black roofs under PV panels can be sufficiently modeled using a linear function with climate parameters as explanatory variables.

Chapter 3 supporting research questions:

3a) How well do linear and non-linear regression equations fit the Sunscape dataset for back surface panel temperature and power output?

3b) How important are wind speed and direction as explanatory variables in predicting PV power output?

3.2 Data

For the research contained in this chapter, data from July 1, 2011 to June 30, 2012 were analyzed. While PV data were available from January 26, 2012 (described in Section 2.6), the green roof-PV and black roof-PV surface measurements did not begin until May 24, 2011. The dataset was further restricted by PV output measurement inconsistencies discussed more in depth below. Time and research constraints truncated the study period on June 30, 2012. During the one year assessment, data analyzed at Sunscape included:

- Back-surface PV panel temperature measured in the center of one panel for both green roof-PV and black roof-PV assemblies;
- Aggregate PV array output (kW). The cumulative output from 90 PV panels over the black roof were multiplied by two-thirds to match 60 panels above the green-moss roof; and

- Solar irradiance (W/m^2) measured parallel to the PV panel which is tilted at 15° from the horizontal (e.g. pyranometer tilted in the same plane of PV panel array).
- Ambient temperature
- Site wind speed and direction (January 1, 2012-June 30, 2012)⁶

The resulting core dataset consisted of 35,138 fifteen minute measurements (the study period was a leap year) from July 1, 2011 to June 30, 2012. The dataset began in July 2011 because PV output readings were 0 or the power difference between green and black roof-PV arrays was implausibly large. Typically, PV output readings, even at midnight, have a small non-zero value. In addition, 69 (0.4%) additional data points during the study period were removed because the difference in power output between green and black roof-PV arrays was five standard deviations away from the mean. These data points corresponded to eight days (Table 3-1). There were no known events or activities on the roof that would cause such extreme measurements (TJ Willets, Mike Carnahan personal communication, October 4, 2012). The most plausible explanation for the difference is sensor malfunction or disconnection.

Table 3-1: List of measurements removed from July 1, 2011- June 30, 2012 Sunscape dataset

Month	Time Ranges	No. of Data Points Removed
January 5, 2012	12:45-13:45	5
February 9, 2012	12:00, 12:15	2
February 12, 2012	14:00,14:30,15:00-15:45	6
February 13, 2012	8:45-11:30	12
February 26, 2012	10:00-11:00	5
November 24, 2011	14:15-16:00	8
November 25, 2011	9:00-16:00	29
March 5, 2012	14:15, 14:30	2

Last, only daytime measurements were included in the regression analysis that follows. Night measurements, when PV panels do not produce power, were excluded. While days are longer in July and shorter in January, daytime measurements were defined as having solar radiation values greater than 4 W/m^2 out of maximum 1154 W/m^2 measured at Sunscape. This daytime threshold of 4 W/m^2 was determined as the maximum measured value for solar radiation between the

⁶ The wind data used in this chapter was measured on site which is different than the National Weather Service wind speed and direction data used in Section 2.8.

hours of midnight to 1am throughout the year. With this threshold, 50% of the Sunscape dataset constituted daytime measurements.

3.3 Methods

The Sunscape data were used 1) to analyze differences in power output from panels over green and black roofs on Sunscape, and 2) to predict the power output of PV panels over black and green roofs in other climates as well as over the white roof on Sunscape. The results for all of these analyzes are discussed in Chapter 4.

This chapter discusses the method used for predicting PV power output. The Sunscape data were used to estimate two empirically derived regression equations. These equations were applied to data in Chapter 4. Two regression equations derived from Sunscape and a third equation from King et al. (2004) was used to convert back-surface panel temp to PV cell temperature. In other words, to predict the PV power output requires three equations which are illustrated in Figure 3-1. The first equation relates ambient temperature to back-surface panel temperature (Figure 3-1: Step 1). King et al. (2004) derives an equation which relates back-surface panel temperature to module cell temperature (Figure 3-1: Step 2). The third equation estimates power output based on module cell temperature and irradiance explanatory variables (Figure 3-1: Step 3). Sunscape's data were used to develop equations 1 and 3. Some PV power-temperature equations identified in Skoplaki et al. (2009b) relate ambient temperature directly to cell temperature in one equation while in this research cell temperature was calculated in two. Since back-surface panel temperature was measured at Sunscape, using it as an intermediate value to calculate cell temperature was one way to capture the differences in temperature from green and black roofs.

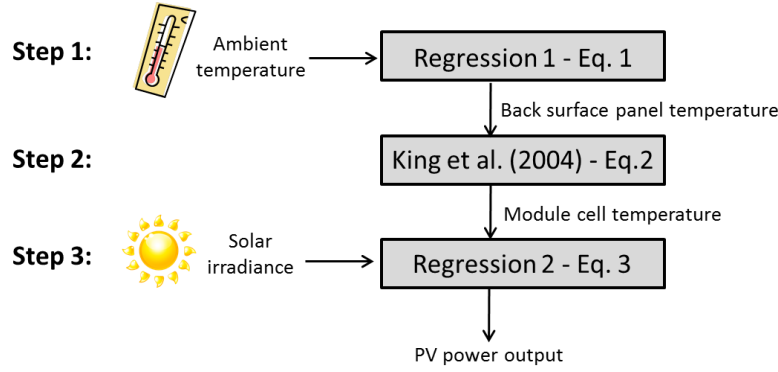


Figure 3-1: Schematic of method to predict PV power output from Sunscape data

Linear and non-linear regression equations were used to find the relationships between ambient temperature and PV back-surface panel temperature (Eq. 1 and 4) and PV output (Eq. 3 and 5) for both roof types. Between both sets of linear (Eq. 1 and 3) and non-linear (Eq. 4 and 5) regression equations, Equation 2 was used as an intermediate step. All four of the regression equations were applied to both green roof-PV and black roof-PV assemblies. Therefore, a total of eight regression equations were used to estimate PV output (i.e. the method outlined in Figure 3-1 was repeated four times). Equation 1 shows the regression equation for back-surface panel temperature as a linear function of ambient temperature derived from Sunscape data.

Linear Equations:

$$y_1 = \beta_0 + \beta_1 x_1 \quad (\text{Eq. 1})$$

Where:

y_1 = back-surface panel temperature ($^{\circ}\text{C}$)

β_0 = Y_1 -intercept

β_1 = ambient temperature coefficient

x_1 = ambient temperature ($^{\circ}\text{C}$)

King et al. (2004) derives equation (Eq. 2) which relates back-surface panel temperature to cell temperature. For this research, the regression-estimated back-surface panel temperatures were used to derive cell temperature of PV panels above green and black roofs. The predetermined temperature difference (ΔT) in Equation 2 was assumed to be 3°C (King 2004).

$$y_2 = y_1 + (x_2/x_0)\Delta T \quad (\text{Eq. 2})$$

Where:

y_2 = module cell temperature ($^{\circ}\text{C}$)

y_1 = back-surface panel temperature ($^{\circ}\text{C}$)

x_2 = solar irradiance on 15° tilt module (W/m^2)

x_0 = reference solar irradiance on module ($1000 \text{ W}/\text{m}^2$)

ΔT = temperature difference ($^{\circ}\text{C}$) between the cell and the module back at an irradiance of $1000 \text{ W}/\text{m}^2$.

Equation 3 shows the regression equation for PV output as a function of solar irradiance and cell temperature derived from Sunscape data. In Section 3.5, the regression model Equation 3 was expanded to consider additional explanatory variables (i.e. wind speed and direction) but their contributions were found to be negligible.

$$y_3 = \beta_2 + \beta_3 y_2 + \beta_4 x_2 \quad (\text{Eq. 3})$$

Where:

y_3 = PV output (kW)

β_2 = Y_3 -intercept

β_3 = module cell temperature coefficient

β_4 = irradiance coefficient

y_2 = cell temperature module ($^{\circ}\text{C}$)

x_2 = solar irradiance on 15° tilt module (W/m^2)

Equation 4 shows the regression equation for back-surface panel temperature as a non-linear function of ambient temperature derived from Sunscape data.

Non-Linear Equations:

$$y_4 = \beta_5 + \beta_6 x_1 + \beta_7 x_1^2 \quad (\text{Eq. 4})$$

Where:

y_4 = back-surface panel temperature ($^{\circ}\text{C}$)

β_5 = Y_4 -intercept

β_6 = ambient temperature coefficient

β_7 = ambient temperature squared coefficient

x_1 = ambient temperature ($^{\circ}\text{C}$)

Equation 5 shows the regression equation for PV output as a non-linear function of solar irradiance and cell temperature derived from Sunscape data.

$$y_6 = \beta_8 + \beta_9 y_5 + \beta_{10} y_5^2 + \beta_{11} x_2 + \beta_{12} x_2^2 \quad (\text{Eq. 5})$$

Where:

y_6 = PV output (kW)

β_8 = Y_5 -intercept

β_9 = module cell temperature coefficient

β_{10} = module cell temperature squared coefficient

β_{11} = irradiance coefficient

β_{12} = irradiance squared coefficient

y_5 = cell temperature module ($^{\circ}\text{C}$)

x_2 = solar irradiance on 15° tilt module (W/m^2)

3.4 Linear and non-linear regression results

For the Sunscape dataset, the correlation coefficients for solar irradiance, ambient temperature and PV output were positive. The positive correlation was not surprising, as ambient temperature increases so do back-surface panel temperatures over both green and black roofs. In addition as ambient temperature and solar irradiance values rise, the same result was seen with PV output. Solar irradiance (0.99) was more strongly correlated to PV output than cell temperature (0.41-

0.42). In other words, PV panels will decrease in power more with lower irradiance values compared with higher temperatures. All correlation coefficients for parameters used in linear regression equations (Eq. 1 and Eq. 3) are listed in Table 3-2.

Table 3-2: Correlation values for parameters used in regression equation 1 and equation 3 (July 1, 2011-June 30, 2012)

	Irradiance (W/m ²)	Black Roof- PV Power (kW)	Green Roof- PV Power (kW)	Ambient Temperature (°C)	PV cell Temp green (°C)	PV cell Temp black (°C)	PV Panel Temp - Green Roof- PV (°C)	PV Panel Temp - Black Roof- PV (°C)
Irradiance (W/m ²)	1.0							
Black Roof-PV Power (kW)	0.99	1.0						
Green Roof-PV Power (kW)	0.99	1.0	1.0					
Ambient Temperature (°C)	0.43	0.41	0.42	1.0				
PV cell Temp green (°C)	0.78	0.76	0.77	0.88	1.0			
PV cell Temp black (°C)	0.81	0.80	0.81	0.85	1.0	1.0		
back-surface panel Temp - Green Roof- PV (°C)	0.75	0.74	0.75	0.90	1.0	0.99	1.0	
back-surface panel Temp - Black Roof- PV (°C)	0.80	0.78	0.79	0.87	1.0	1.00	0.99	1.0

The linear regression results from Equation 1 related ambient temperature to back-surface panel temperature relatively well with coefficients of determination $R^2=0.75$ for black roof-PV and $R^2=0.80$ for green roof-PV assemblies (Table 3-3). For an average 1⁰C change in ambient temperature, the ambient temperature coefficients (Table 3-3) estimate the back of a black roof-PV panel to increase in temperature by approximately 15% more than the comparable green roof. This relationship was not too surprising given the 10-40 ⁰C cooler surface temperatures from a green roof reported from previous studies referenced in Section 1.2.3.

Table 3-3: Linear regression values (Eq. 1) for black and green roof back-surface panel temperature (July 1, 2011- June 30, 2012)

	Black back-surface panel temperature			Green back-surface panel temperature		
	Coefficient	t-statistic	P-Value	Coefficient	t-statistic	P-Value
Intercept	1.2	9	3.7E-21	1.3	14	2.0E-41
Ambient Temperature (°C)	1.5	229	0	1.3	266	0
R-Squared	0.75			0.8		
No. of Observations	17343			17343		

In the second linear regression equation derived from Sunscape (Eq. 3), irradiance and PV cell temperature (response variable from Eq. 2) account for 98% ($R^2 = 0.98$) of the variation in the estimation of power output. Coefficients were statistically significant at the 95% confidence interval ($p < 0.05$) for all values except the PV cell temperature for green roofs (Table 3-4). Since the green roof- PV cell temperature coefficient was not statistically significant, the near zero slope was more important than the positive value when compared with the cell temperature coefficient of the black roof-PV.

Table 3-4: Linear regression values (Eq. 3) for black and green-PV power generation temperature (July 1, 2011- June 30, 2012)

	Black roof-PV Power Output		
	Coefficient	t-statistic	P-Value
Intercept	0.17	21	9.5E-96
PV cell Temp black (°C)	-2.4E-03	-5.6	2.2E-08
Irradiance (W/m ²)	0.013	503	0
Adjusted R-Squared	0.98		
No. of Observations	17343		

	Green roof-PV Power Output		
	Coefficient	t-statistic	P-Value
Intercept	0.10	13	2.8E-37
PV cell Temp green (°C)	5.6E-04	1.3	0.21
Irradiance (W/m ²)	0.013	573	0
Adjusted R-Squared	0.98		
No. of Observations	17343		

The non-linear regression to predict back-surface panel temperature had slightly higher R^2 values for both black ($R^2 = 0.78$ non-linear vs. 0.75 linear) and green ($R^2 = 0.82$ non-linear vs. 0.80 linear) roof PV assemblies. Table 3-5 lists the resulting coefficients and supporting statistical parameters for the non-linear back surface panel temperature equation (Eq. 4). All explanatory variables were statistically significant ($p < 0.05$).

Table 3-5: Non-linear regression values (Eq. 4) for black and green roof back-surface panel temperature (July 1, 2011-June 30, 2012)

	Black back-surface panel temperature			Green back-surface panel temperature		
	Coefficient	t-statistic	P-Value	Coefficient	t-statistic	P-Value
Intercept	0.16	0.66	0.03	0.39	2.1	0.51
Ambient Temperature(°C)	1.0	36	0	0.99	45	6.4E-262
Ambient Temperature^2 (°C)	0.02	20	2.2E-70	0.01	18	4.7E-87
Adjusted R-Squared	0.78			0.82		
No. of Observations	17343			17343		

Figure 3-2 illustrates the accuracy between measured values on Sunscape compared with the linear and non-linear regression estimates for the black roof-PV system.

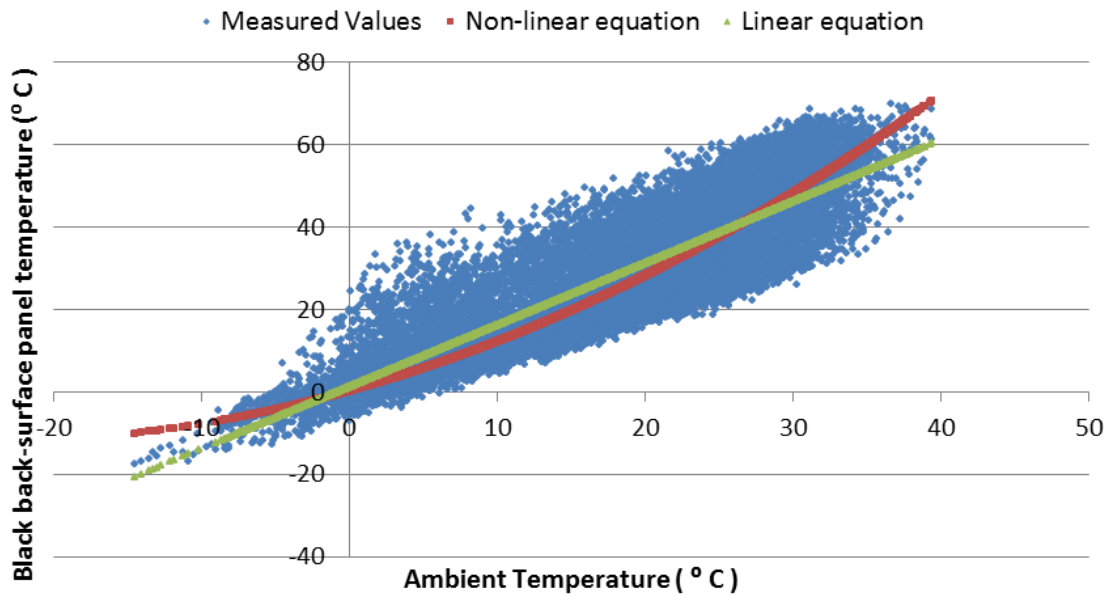


Figure 3-2: Comparison of linear (Eq. 1) and non-linear (Eq. 4) equations for black back surface panel temperature

The second non-linear regression equation for PV output (Eq. 5, Table 3-6) did not improve upon the coefficient of determination when rounded to two significant figures compared to the linear regression equation in Table 3-4. However, all explanatory variables were statistically significant at a 95% confidence interval ($p < 0.05$). Table 3-6 lists the resulting coefficients and supporting statistical parameters for the non-linear PV power output equation (Eq. 5) for both groupings of panels over the black and green roof.

Table 3-6: Non-linear regression values (Eq. 5) for black and green-PV power generation (July 1, 2011- June 30, 2012)

	Black roof-PV Power Output		
	Coefficient	t-statistic	P-Value
Intercept	-0.38	-40	0
PV cell Temp black (°C)	0.041	52	0
PV cell temp black^2 (°C)	-8.4E-04	-64	0
Irradiance (W/m ²)	0.015	277	0
Irradiance ^2 (W/m ²)	-1.2E-06	-20	1.3E-91
Adjusted R-Squared	0.98		
No. of Observations	17343		

	Green roof-PV Power Output		
	Coefficient	t-statistic	P-Value
Intercept	-0.39	-40	0
PV cell temp green (°C)	0.041	47	0
PV cell temp green ^2 (°C)	-9.1E-04	-53	0
Irradiance (W/m ²)	0.015	289	0
Irradiance ^2 (W/m ²)	-1.3E-06	-23	2.3E-119
Adjusted R-Squared	0.98		
No. of Observations	17343		

Since the non-linear functions do not greatly improve the goodness of fit to the data over linear equations, the linear regression equations were chosen because they would be easier for a decision maker to use and understand if the equations were included in a decision support tool. However, at the ambient temperature extremes (above 35° C or below -10°C in Figure 3-2), the linear equation would result in significantly different results compared with the non-linear equation. Both linear regression equations were used in the following analysis to assess the importance of wind direction and speed. Furthermore, the linear regression equations were also applied in Chapter 4.

3.5 Linear regression results with wind direction and wind speed

Since Sunscape had only six months of reliable wind speed and direction data, the timeframe used to assess the impact of wind speed and direction was January 1, 2011- June 30, 2011 (8.862

fifteen minute daytime measurements). The National Weather Service (NWS) station wind speed and direction data were used as a supplementary dataset (NOAA-National Climatic Data Center, 2012) for comparison purposes. As mentioned previously (Figure 2-1), the NWS weather station was located 10.7 miles Northwest of Sunscape at the Pittsburgh International Airport Weather station. In Section 2.7, the NWS dataset was used to compare July 1, 2011 to June 30, 2012 to a typical meteorological year for Pittsburgh. In this section, the NWS dataset was compared to wind speed and direction collected on-site over a shorter time period. Figure 3-3 shows a six month (January 1, 2012-June 30, 2012) histogram for the two wind direction datasets. The NWS wind direction histogram shows more wind coming from the west while on-site the winds came from the south and northwest. Therefore, in hilly regions, such as Pittsburgh, a site weather station which records wind direction was important.

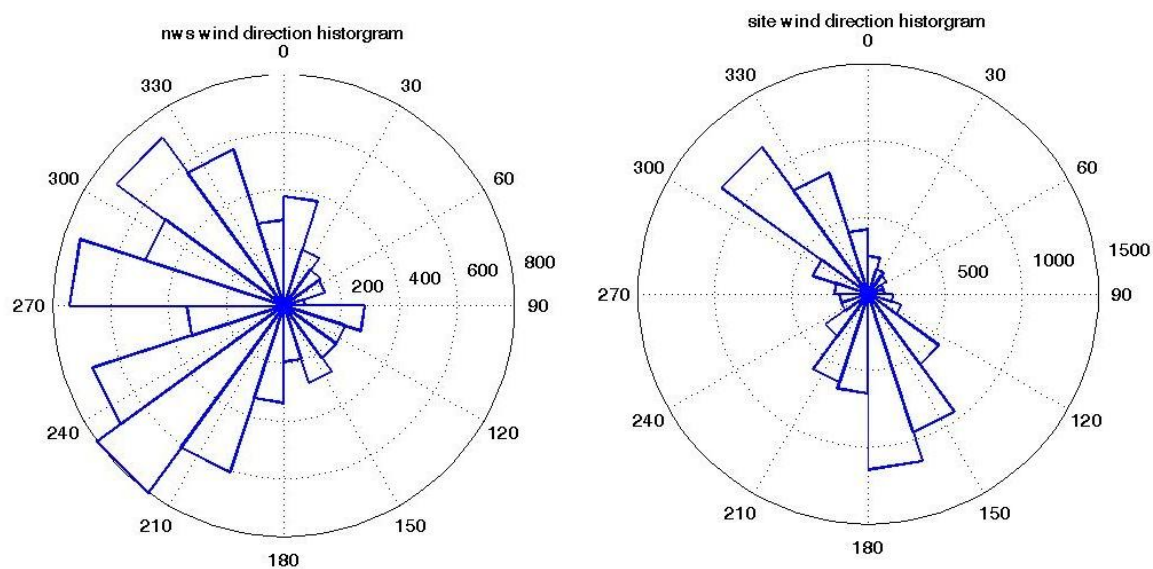


Figure 3-3: NWS (left) and Sunscape (right) histograms for daytime wind direction values between January 1, 2012- June 30, 2012. Wind direction corresponds to where the wind is coming from.

Wind direction and speed were incorporated as explanatory variables into the linear back-panel surface temperature regression (Eq. 1) described above for both black roof-PV and green roof-PV. Wind direction and speed could have been incorporated into the linear PV output regression equation (Eq. 3) as well. However, the back-panel surface temperature regression makes more physical sense as wind is more likely to affect back surface panel temperature through

convection and thus cell temperature than PV output (Skoplaki 2009a). Equation 1 was revised to incorporate wind direction and speed in Equation 6 below.

Wind direction could impact back surface panel direction if air from a certain direction is often warmer or cooler. In the case of Sunscape, one hypothesis could be that wind from the east during the day brings cooler air from the green roof over to the black roof decreasing the back surface panel temperature⁷. To understand the impact of wind direction on back surface panel temperature, the wind direction explanatory variables (x^4 - x^7) were binary. For example, to test wind direction coming from the North, measurements with 350-10° would receive a “1” all other wind direction measurements would receive a “0”. Wind direction groupings were created for each cardinal direction. Therefore, North winds were defined as 350°-10°, East winds were 80°-100°, South winds were 170°-190° and West winds were 260°-280°. These four directions were chosen to align with Sunscape’s physical configuration and orientation of the PV panels. The bin 20° bin size was chosen to account for some variation in the wind. Ambient temperature (AT), wind speed (WS) and wind direction (WD) were evaluated separately in Equation 6 and then together. Therefore a total of ten versions of Equation 6 were conducted for both Black roof-PV and green roof-PV.

⁷ This hypothesis was given as an example, but not tested.

$$y_7 = \beta_{13} + \beta_{14}x_1 + \beta_{15}x_3 + \beta_{16}x_4 + \beta_{17}x_5 + \beta_{18}x_6 + \beta_{19}x_7 \quad (\text{Eq. 6})$$

Where:

y_7 = back-surface panel temperature ($^{\circ}\text{C}$)

β_{13} = Y_1 -intercept

β_{14} = ambient temperature coefficient

β_{15} = wind speed (WS) coefficient

β_{16} = wind direction (WD)-North coefficient

β_{17} = wind direction-East coefficient

β_{18} = wind direction-South coefficient

β_{19} = wind direction-West coefficient

x_1 = ambient temperature ($^{\circ}\text{C}$)

x_3 = wind speed (m/s)

x_4 = wind direction-North (350° - 10°)

x_5 = wind direction-East (80° - 100°)

x_6 = wind direction-South (170° - 190°)

x_7 = wind direction-West (260° - 280°)

Adding wind speed and direction as explanatory variables did not significantly impact the coefficient of determination. The differences from wind speed (WS) and direction (WD) can be seen by comparing R^2 values to the base-case (e.g. ambient temperature (AT) only) ⁸. Figure 3-4 displays the corresponding R^2 values for ten iterations of Equation 6 using different explanatory variables for both green roof-PV and black roof-PV combinations. Wind speed increases the coefficient of determination of the regression model more than wind direction. In addition, the coefficients corresponding to wind coming from the south and west (in the WD only cases) were not statistically significant with a 95% confidence interval. Combining both wind direction and speed to ambient temperature as explanatory variables adds little. Across any iteration in Figure 3-4, R^2 values increase from the ambient temperature (AT) scenario by 0.4% for the green roof-PV and 0.6% for the black roof-PV combinations. Therefore, wind speed and direction were not

⁸ The R^2 value from Equation 1 (Section 3.4) differs from Equation 6 for the ambient temperature only explanatory variable because these regression equations were evaluated over different time periods.

included in the regression equations used in Chapter 3. Detailed statistical information on each iteration of Equation 6 for black roof-PV and green-roof PV can be found in Appendix B.

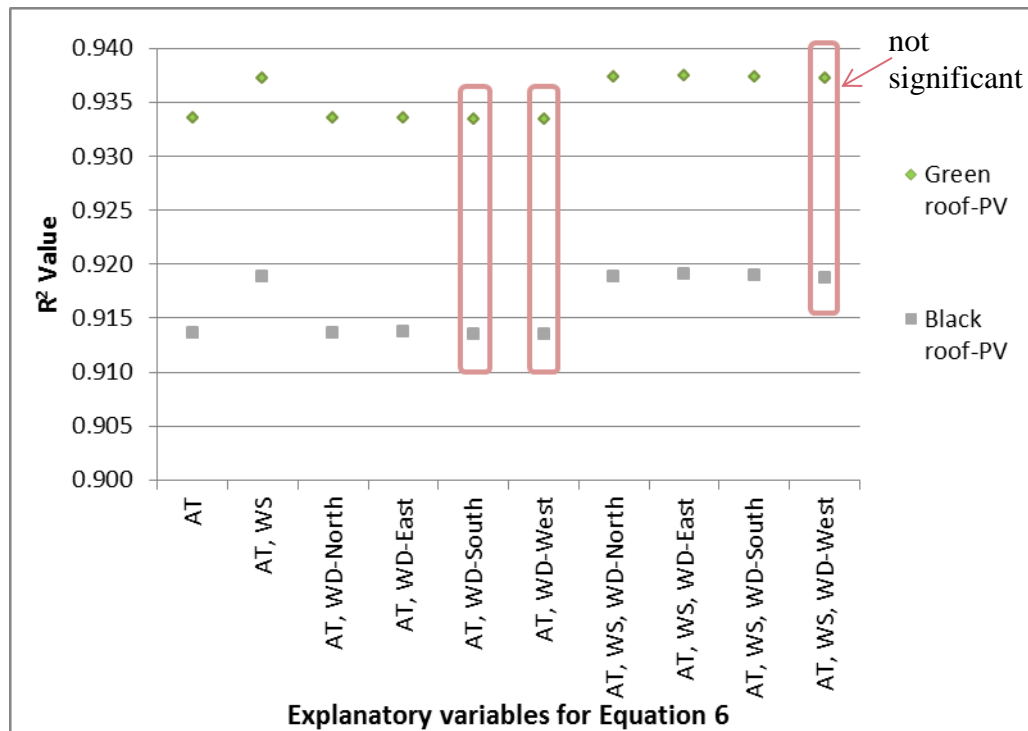


Figure 3-4: Resulting R^2 values for the addition of wind speed and wind direction in Eq. 6 using Sunscape data from January 1, 2012 to June 30, 2012 (AT = Ambient temperature, WD =wind direction, WS=wind speed)

3.6 Conclusions

Significant discussion was spent in this chapter comparing linear versus non-linear regression equations derived from Sunscape. Overall, the non-linear regression equations did not greatly improve the coefficient of determination (R^2) value compared to the linear equations. For simplicity and ease of use in a possible future decision support tool, the analysis conducted in Chapter 4 used the linear regression results presented in this chapter. The limitation to using linear regression was that towards the extremes of temperature, the linear equations were less accurate.

Wind speed and direction added little to increase the goodness of fit for the regression equations when included individually or together as explanatory variables. Wind speed had a larger impact on increasing the R^2 value than wind direction. Possibly choosing different wind directions or

increasing the size of bins (e.g. North (350°-10°) may change the outcome. Because these two parameters did not largely change the accuracy of the regression equations, they are not included in the linear regression equations used in Chapter 4.

Another important take away was the importance of site specific wind data. As seen in Figure 3-3, wind can vary considerably especially across a hilly region such as Pittsburgh. Therefore, using off-site wind data could misinform PV design or provide misleading wind impact results.

Chapter 4: Quantifying the relationship between green roof temperature and Photovoltaic power performance on low-slope roofs

4.1 Introduction

In urban areas, solar technologies have become more common on roofs in order to provide on-site, renewable electricity. Areas that are large in size, contiguous, and without shade are ideal for solar (Dura-last 2011; Liu, 2006). Therefore, roofs are prime space for solar technologies since roofs typically are unused except for heating, ventilation and air conditioning equipment (Kirby 2011; CEIR 2012). Furthermore, electricity produced on the roof for consumption in the building avoids average losses of 7% from transmission and distribution lines when generated at a power plant (United States Energy Information Administration, 2012).

Green (or vegetated) roofs also compete for the same roof space as solar technologies. While green roof installations are growing, they have less than 1% market share by roof area in the United States (Levinson & Akbari, 2010; Greenroofs.com 2011). Green roofs are often installed for the energy benefits to the building (e.g. heat flux reduction) and environmental benefits such as storm water retention and urban heat island mitigation.

Often green roofs and PV panels are installed separately on roofs, but they can exist together harnessing potential co-benefits. Specifically with hot air temperatures, PV panels placed over green roofs (referred to as green roof-PV for this research) can utilize the cooler air to maintain or possibly increase efficiency compared to panels placed over black roofs (referred to as black roof-PV) (Köhler 2002). Hui et al. (2011) conducted a one day field experiment comparing one PV panel over a black and green roof in Hong Kong on a sunny day. The green roof's surface temperature was 5-11⁰C cooler than the black roof's, and the green roof-PV system produced 4% more power. Köhler (2007) also carried out a field experiment in Germany by comparing the average PV performance of two green roof-PV assemblies to the average of five black roof- PV systems. During the year 2000, the monthly average of the green roof-PV systems out performed black roof-PV assemblies monthly by -4% to 3% with a yearly average of 1.5%. Limitations to

Köhler's (2007) study include differences in PV panel type and inverters between green roof-PV and black roof-PV.

This study improves on previous literature by quantifying the relationship between ambient temperature and PV output by comparing the performance of green roof-PV and black roof-PV systems over a one year field experiment with the same PV panel type, tilt and inverter. The test bed used in this research had a higher number of panels (60) and installed power which is helpful in understanding scaling impacts. In addition, this project has four times more installed power than Köhler's (2007) study.

For this research, two methods were used to apply Pittsburgh Sunscape data to other climates. The first method uses regression equations described in Chapter 3. These Pittsburgh-based regression equations were used to estimate the difference in PV power from green and black roofs if a combination system were located in three case study locations (Huntsville, AL; San Diego, CA; Phoenix, AZ) under a base-case and high temperature scenario. The second method was to use average differences in power output for specific solar irradiance and ambient temperature bins derived from Sunscape and apply them to the other cities. Only a base-case scenario was considered for this second method. The objectives of this research led to the following hypothesis and supporting research questions:

Chapter 4 hypothesis: The combination of PV panels over a green roof will produce more electricity than PV panels over a black roof.

Chapter 4 supporting research questions:

4a) Under what climate parameters does cooler air above the green roof increase PV output compared to black roofs on Sunscape?

4b) What is the magnitude of the difference in PV output for Sunscape and for other cities? Given the base-case and high-temperature scenarios, what are a range of cost savings from the green roof-PV combination?

The relationship between PV power output and temperature is given by a temperature coefficient. Generally, temperature coefficients are negative and change with different solar irradiance measurements and types of panel (Whitaker 1991). The panel manufacturers provide the temperature coefficient typically in the form $\pm\%P_{\max}/^{\circ}\text{C}$ (Meral 2011; ET Solar, 2012) where P_{\max} is the maximum rated power under standard test conditions ($1000\text{W}/\text{m}^2$, 1.5 air mass and a cell temperature of 25°C). For example, the PV panels used in this research on Sunscape have a $-0.46\%/^{\circ}\text{C}$ temperature coefficient which is representative for mono and polycrystalline panels (ET Solar, 2012; Alchemie Limited 2012). Therefore, operating under $1000\text{W}/\text{m}^2$ these panels are expected to decrease in maximum power by -0.46% for every 1°C increase in PV cell temperature above 25°C (ET Solar, 2012). Thin film panels typically have a slightly lower temperature coefficient around $-0.25\%/^{\circ}\text{C}$ (Shaari 2009; ET Solar, 2012; Alchemie Limited 2012). Often PV cell temperatures are recorded between $40\text{--}70^{\circ}\text{C}$ under clear sky conditions (Emery 1999) so the decline in performance could be significant. However, the usefulness of temperature coefficients is limited in the field because climate conditions vary significantly from the standard test conditions (King 1997).

4.2 Data

One year worth of Sunscape data (July 1, 2011 to June 30, 2012) were used to evaluate the difference in PV power output between PV panels overtop green and black roofs. Measurement values were removed from this dataset due to measurement inconsistencies and nighttime values described in Section 3.2. The resulting dataset used for the analysis in this chapter has 17,343 fifteen minute measurements.

For the three case studies beyond Pittsburgh, average hourly climate parameters were obtained through the National Solar Radiation Data Base (NSRDB) (National Renewable Energy Laboratory 2005). The National Renewable Energy Laboratory derived one year worth of average hourly solar radiation and meteorological values for 1,400 U.S. locations based on data collected from 1961-2005 and archived in the NSRDB as Typical Meteorological Year 3 (referred to as TMY in this analysis). Using the TMY data for the three case study locations ensures results were consistent with average climate values and not skewed by extreme

conditions. The same daytime restriction (solar radiation greater than 4W/m²) was imposed on three case studies for consistency.

4.3 Methods

This chapter used two different methods to extend the Pittsburgh findings to three other climates in the United States. Method one applied the results from the linear regression equations discussed in Chapter 3. Since wind speed and wind direction explanatory variables and non-linear regression equations did not greatly improve the regression equations goodness of fit to Sunscape data, linear regression equations (Eq. 1 & 3) were chosen for this analysis.

The second method (Equation 7) applied the average power difference between black roof– PV and green roof-PV measured from Sunscape to TMY hourly profiles for each city. The result determined the net kilowatt hours between the two assemblies .

$$\sum_1^j \sum_1^i \left(\left(\frac{\sum_1^N G-B}{N} \right)_{ij} \times H_{ijc} \right) = \frac{kWh_c}{yr} \quad (\text{Eq. 7})$$

Equation 7 requires two solar irradiance (i) by ambient temperature (j) matrices to determine the net kilowatt hours. The first matrix calculates the average difference in power output by subtracting the difference in kW power output from green roof-PV (*G*) and black roof-PV (*B*) measured at Sunscape divided by the number of measurements (*N*) pertaining to a cell_{ij}. The second matrix contains the number of hours (*H*) within each solar irradiance and ambient temperature cell. The cells of these two matrices are multiplied element by element to obtain the net kilowatt hours (kWh) within each cell for each case study city (*c*). The net kWh are summed down solar irradiance rows and across ambient temperature columns to determine the total net kWh produced by either green roof-PV or black roof –PV system annually.

From the Sunscape and TMY datasets, the matrix size was as 13 x 12. The overall matrix size was determined by choosing the largest range that would encompass the maximum and minimum temperature and solar irradiance values for all four cities (Pittsburgh, San Diego, Huntsville and Phoenix). For each case study location, the same matrix was used. The ambient temperature columns were defined by a -20°C to 45 °C range in 5°C increments for ambient temperature and 4-1200 W/m² range in 100 W/m² increments for solar irradiance. The ambient temperature 5°C interval was roughly chosen 1) to have at least 30 fifteen minute measurements

in each column 2) to balance chart readability with high resolution bins. Daytime values were sectioned into 100 W/m^2 increments as these bins provided a natural breakpoint for comparison with the temperature coefficient measured at 1000 W/m^2 .

Sunscape did not have data for all cells in the 13×12 matrix especially corresponding to the extremes of the solar irradiance and temperature ranges. In these instances, the nearest row and/or column cells with data were averaged. On the edges of the matrices (e.g. $1100\text{-}1200 \text{ W/m}^2$, -15°C -20°C and 40°C -45°C), the nearest row or column cell value was used.

4.4 Results from Pittsburgh case study

Manufacturer-supplied temperature coefficients can be used to estimate power from a panel at various sites. Since generally these temperature coefficients for PV panels are tested at 1000 W/m^2 , the usefulness of the temperature coefficient at other irradiance levels is limited. Only 1% of the 17,343 measurements recorded at Sunscape were within 25 W/m^2 of 1000 W/m^2 . Furthermore, the average solar irradiance value for all daytime Pittsburgh data was 335 W/m^2 . Figure 4-1 shows calculated cell temperatures and measured power output for black roof-PV and green-roof PV panels installed at Sunscape across a variety of solar irradiance values. Four solar irradiance ranges were chosen to represent the spectrum of values measured at Sunscape. Generally, power output declines at a faster rate with increasing solar radiation values due to the strong correlation with ambient temperature (Refer to Section 3.4). Comparing black roof-PV and green roof-PV values in Figure 4-1 across irradiance values, the green roof-PV slopes are slightly more gradual and values have a smaller range of cell temperatures. Therefore, using the manufacturer-supplied temperature coefficient calibrated to 1000 W/m^2 to determine power reduction according to cell temperature would be an overestimate for places like Pittsburgh where often the solar irradiance is lower. Even for places like Phoenix with high levels of solar radiation, only 7% of TMY daytime hours have solar irradiance values near 1000 W/m^2 .

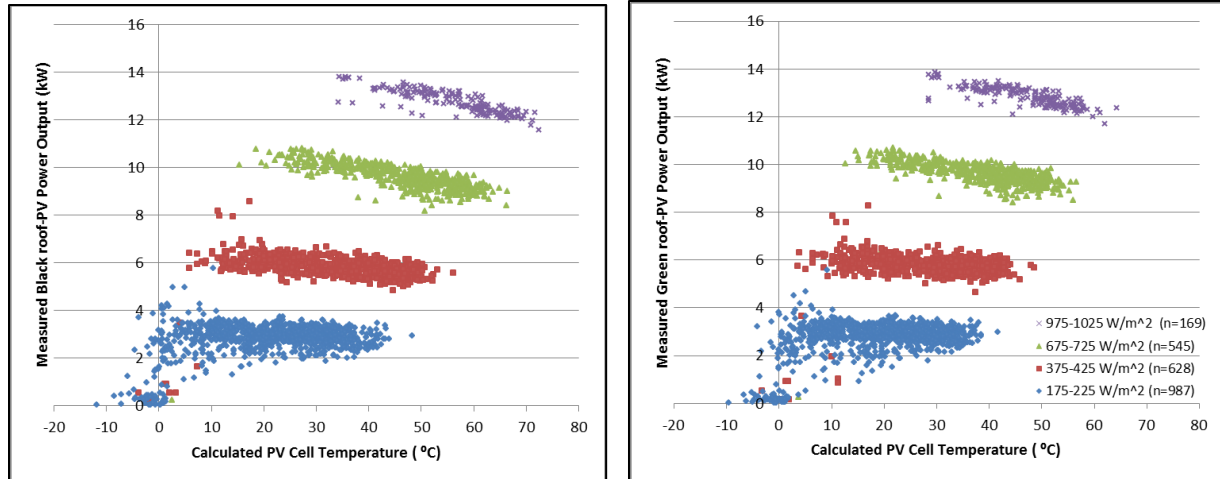


Figure 4-1: Relationship between PV power output and cell temperature with varying solar irradiance values. Black Roof-PV are seen on the left and green roof-PV on the right. Legend values in parentheses are number of measurements collected at Sunscape within the solar irradiance range (July 1, 2011-June 30, 2012)

4.4.1 Base-case results

The base-case results represent the average power difference between black roof-PV and green roof-PV when examined across an entire year. For the base-case in Pittsburgh seen in Table 4-2, black roof-PV panels outperformed green roof-PV panels by 0.02kW (0.5%) on average across all daytime measurements in the study period. The difference in power output was statistically significant at the 95% confidence interval ($p < 0.05$). The performance difference of 0.02kW was because Pittsburgh has approximately 73% of fifteen minute ambient temperature measurements below 25 °C. During cooler climate conditions, the thermal conductivity and heat storage properties of black roofs allow the air around the back-surface panel temperature to decrease more than green roofs (Gartland 2008; Liu 2003). Figure 4-2 shows the back-surface panel temperature measured at Sunscape. For temperatures below 0°C (32° F), the green roof average back-surface panel temperature was 1-2°C warmer than black. At temperatures above 20°C (32° F), the black roof back-surface panel temperature ranged from at least 1°C to 9°C hotter than green. Since PV panels generate more power when cooler, in Pittsburgh with more cold temperatures, black roof-PV systems slightly outperform green roof-PV assemblies annually.

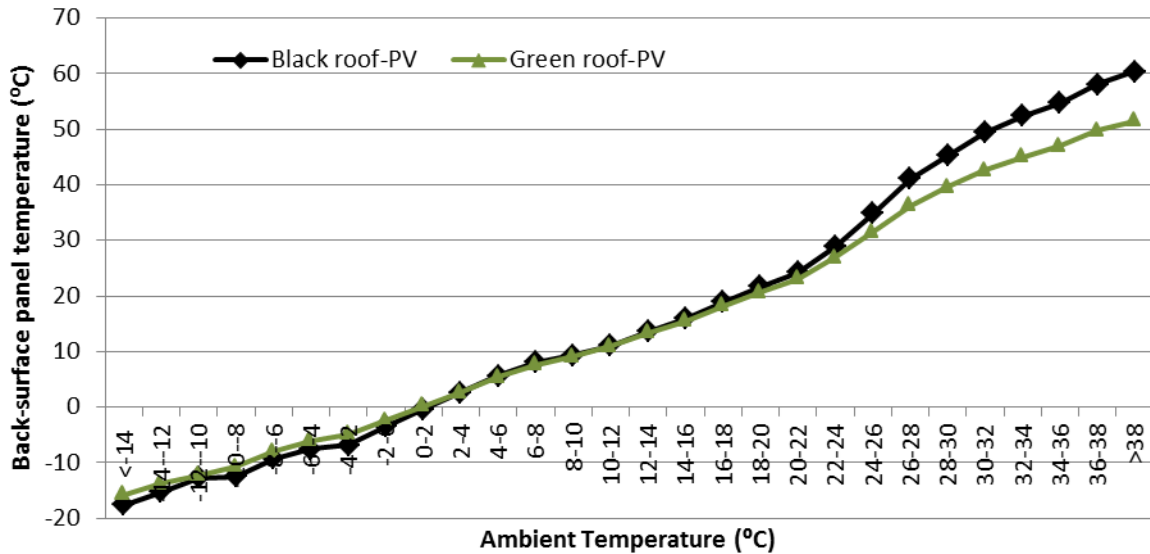


Figure 4-2: Average back-surface panel temperatures for PV panels above the black or green roofs measured on Sunscape separated by ambient temperature (July 1, 2011- June 30, 2012)

Monthly results for Pittsburgh indicate that in July, the green roof under PV panels produced 0.5% more power while in December, black roof under PV panels produced 2% more power (Table 4-1). While the data follows the expected trend of hotter temperatures decreasing power output, the notable result was the small differences in performance (<2%) for either assembly. Current technical specifications for PV panels containing temperature coefficients do not emphasize the relatively small impact of temperature on power output across a range of solar irradiance values.

Table 4-1: Average monthly difference (Green roof-PV minus Black roof-PV) in power output (kW) for panels above green and black roofs on Sunscape. (July 1, 2011- June 30, 2012)

	Month	Average Green-Black (kW)	Average Black PV (kW)	% difference
2012	Jan	-0.04	2.4	-1.5%
	Feb	-0.06	3.6	-1.6%
	Mar	-0.05	4.9	-0.9%
	Apr	-0.04	5.6	-0.8%
	May	0.02	5.7	0.4%
	Jun	0.02	5.7	0.4%
2011	Jul	0.03	5.5	0.5%
	Aug	0.00	5.3	-0.1%
	Sep	-0.02	4.1	-0.4%
	Oct	-0.05	3.7	-1.3%
	Nov	-0.07	3.6	-1.9%
	Dec	-0.06	2.7	-2.3%
	Average	-0.02	4.6	-0.5%

Further trends in the data were seen as developed by Method 2 by grouping the differences in green and black PV power output by ambient temperature and irradiance. The Pittsburgh daytime data in Table 4-2 suggest that for ambient temperatures above 25 °C for all irradiance values, green roofs lower the air temperature surrounding the PV panels in turn producing more power than black roof-PV assemblies. Therefore, all else equal, sites consistently above 25°C will most likely see a positive impact (shaded white in Table 4-2) from a green roof-PV combination. A negative value (shaded red) in Table 4-2 indicates panels above a green roof produce less power than a black roof. Values shaded yellow contain only one or two data points. Figure 4-3 disaggregates the number of hours for each cell⁹. Examining irradiance rows in Table 2, the green roof-PV assembly started to outperform black roof-PV assemblies on average across all ambient temperatures at 800 W/m². Generally, the power production difference between the two roof types increase towards higher values of irradiance and ambient temperature. In other words, the most favorable conditions for green roof-PV assemblies are the lower right of Table 4-2.

⁹ Hours were determined by summing the number of fifteen minute measurements and dividing by four within each solar irradiance and ambient temperature cell in Table 4-2

Table 4-2: Average difference (Green roof-PV minus Black roof-PV) in power output (kW) for panels above green and black roofs partitioned by temperature and solar irradiance. The averages are weighted by the quantity of measurements meeting a certain irradiance and temperature range¹. Cells shaded red indicate black roof-PV produced more power than green roof-PV. Yellow highlighted cells contain only one or two data points.

		Ambient Temperature (° C)											Weighted Average Green-Black PV (kW)	% of daytime data
		<-10	-10--5	-5-0	0-5	5-10	10-15	15-20	20-25	25-30	30-35	>35		
Solar Irradiance (W/m ²)	<100	-0.01	-0.01	-0.02	-0.02	-0.02	-0.02	-0.02	-0.01	0.00	0.01	-0.01	-0.01	31%
	100-200	-0.04	-0.10	-0.08	-0.07	-0.03	-0.07	-0.06	-0.02	0.04	0.06	0.10	-0.04	15%
	200-300		-0.13	-0.11	-0.12	-0.06	-0.10	-0.07	-0.05	0.04	0.08	0.06	-0.05	10%
	300-400		0.01	-0.15	-0.17	-0.11	-0.12	-0.07	-0.05	0.03	0.08	0.11	-0.05	7.8%
	400-500		0.01	-0.09	-0.15	-0.13	-0.11	-0.07	-0.06	0.03	0.11	0.14	-0.04	6.9%
	500-600			-0.15	-0.12	-0.16	-0.15	-0.05	-0.07	0.04	0.10	0.16	-0.04	6.7%
	600-700			-0.11	-0.14	-0.15	-0.16	-0.07	-0.05	0.05	0.11	0.13	-0.03	7.0%
	700-800				-0.13	-0.14	-0.13	-0.07	-0.03	0.03	0.11	0.17	-0.01	6.2%
	800-900				-0.08	-0.15	-0.08	-0.06	0.01	0.07	0.14	0.15	0.05	5.5%
	900-1000				-0.05	-0.06	-0.05	3E-03	0.04	0.11	0.16	0.16	0.09	3.8%
	1000-1100						2E-04	0.06	0.08	0.10	0.17		0.10	0.5%
	>1100							0.06		0.01			0.03	0.02%
Weighted Average Green-Black PV (kW)		-0.01	-0.06	-0.06	-0.07	-0.06	-0.07	-0.05	-0.03	0.04	0.11	0.14	-0.02	
% of daytime data		0.1%	1.1%	3.9%	10%	14%	12%	17%	16%	18%	8.0%	0.8%		
Net Green-Black (kWh)		-0.04	-2.8	-11	-29	-34	-36	-33	-21	34	37	4.7		

¹Due to rounding, % of daytime values do not add perfectly to 100%

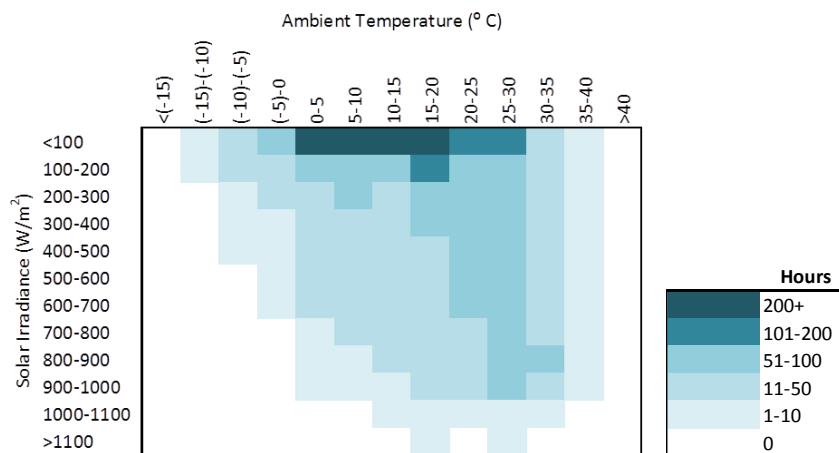


Figure 4-3: Measured hourly values from July 1, 2011 –June 30, 2012 at Sunscape

For additional context, the difference in power output between roof types was converted into energy. From Table 4-2, the “% of daytime data” out of 17,343 fifteen minute measurements was converted into 4,336 hours. For example, 16% of the daytime data in the 20-25°C bin totaled 694 hours (16% x 4,336 hours). Next, hours for each ambient temperature bin were multiplied by the

weighted difference in power from the 60 panels over green and black roofs (Table 4-2) to get annual kWh. Continuing the example, 694 hours multiplied by -0.03kW totals -21kWh. The negative sign means that black roof-PV panels outperformed green roof-PV panels. Total kilowatt hours from adding temperature bins $<25^{\circ}\text{C}$ (black roof-PV dominates) and bins $>25^{\circ}\text{C}$ (green roof-PV dominates) were -165 kWh and 75 kWh respectively annually. If the same methodology is applied to solar irradiance summing bins below and above 800 W/m^2 , the same net 90kWh (1.5 kWh/panel/yr) annual production of black roof-PV over green roof - PV was found.

4.4.2 High temperature scenario

The results above suggest that annual ranges of temperature and irradiance result in PV panels over black roofs generating more power than PV panels over green roofs, which may be counterintuitive given the premise of the study but as described above was an effect of the relatively mild Pittsburgh climate. As a bounding analysis, we considered a scenario where green and black roofs with PV panels were compared only with ambient temperatures higher than 25°C (referring to the columns of Table 4-2). In this bounding case, the benefit of cooler air from green roofs on power performance was the greatest. Of the total 17,343 fifteen minute data points from the daytime dataset, only 27% of them meet the ambient constraint (i.e. $\geq 25^{\circ}\text{C}$). Not surprisingly, 85% of measurements higher than 25°C were recorded in May, June, July and August in Pittsburgh. For this high temperature scenario, the green roof-PV array would be expected to produce 0.07kW (or 0.9%) more power than the average black roof-PV assembly at high temperatures in Pittsburgh. Extrapolating the 0.07kW difference and assuming it was consistent for the 4,336 daylight hours per year identified above, this green roof-PV assembly would generate 300kWh/yr (5kWh/panel/yr) more over the conventional black roof-PV assembly. We explore in Section 4.5 how other regions of the US might fare in approaching such an upper bound scenario for PV over green and black roofs.

4.5 Characteristics of other case study cities

To get a range of climates beyond Pittsburgh, cities in the United States were categorized based on historic averages of Cooling Degree Days (Accu Weather 2012) as a proxy for high temperatures and solar radiation (National Renewable Energy Laboratory 2012). Selected cities were Phoenix, AZ (high temperature and irradiance), San Diego, CA (similar Pittsburgh temperatures, higher solar radiation) and Huntsville, AL (higher temperatures, similar Pittsburgh radiation) seen in Figure 4-4. These three cities as well as Pittsburgh created a bounding analysis most other cities should generally fall within or near. Climates colder than Pittsburgh were excluded because the majority of the year is heating-dominated with cool ambient temperatures.

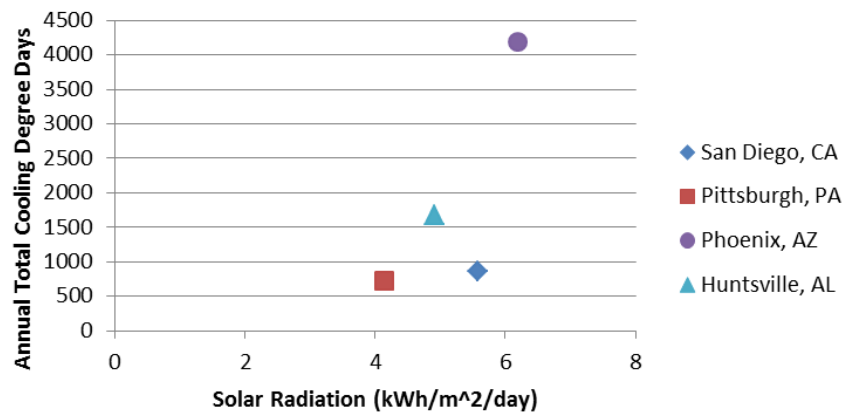


Figure 4-4: Comparison of climate parameters for case study locations.

For the three case studies beyond Pittsburgh, typical annual weather profiles varied. Figure 4-5 contains daylight hours from the three city's datasets separated by solar irradiance and ambient temperature. Solar irradiance rows ranged from 4¹⁰-1200 in 100 W/m² increments while ambient temperature columns had a -20°C to 45 °C range in 5°C increments. The values in parentheses correspond to the number of daylight hours during the year. San Diego's TMY has moderate temperatures (5-30°C) with most solar irradiance values below 1000W/m². Huntsville has a larger spectrum of temperatures compared to San Diego and the majority of the daylight hours

¹⁰ 4W/m² separates daytime and night time values. In this analysis we are only looking at daytime >4W/m² values.

have lower solar irradiance values. Phoenix is hotter than both San Diego and Huntsville. In addition, the quantity of hours within each cell was relatively consistent in 51-100 hours.

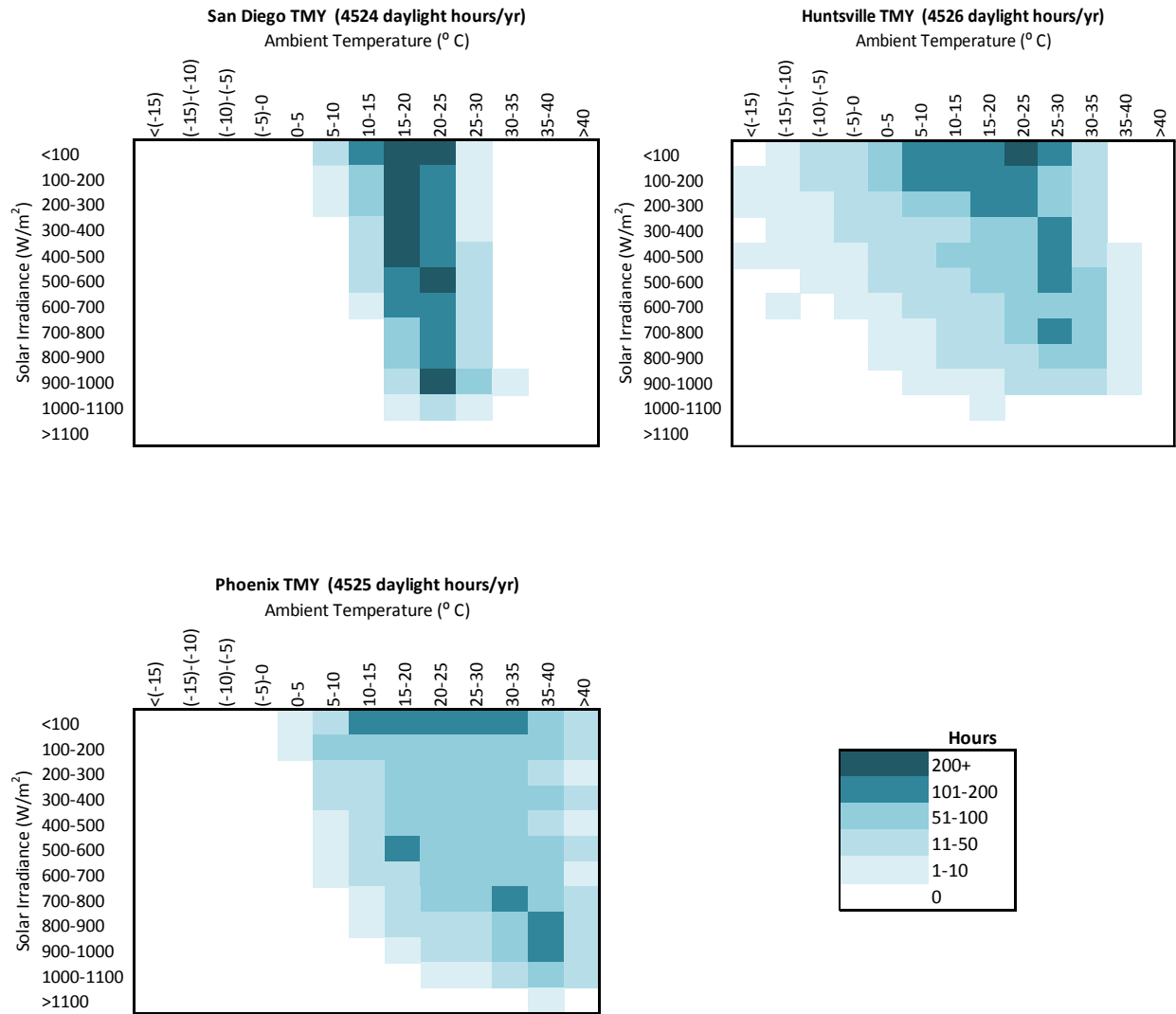


Figure 4-5: Typical Meteorological Year (TMY) daylight profiles based on solar radiation and ambient temperature

4.6 Method 1-Estimated results for other cities

In this bounding analysis, method 1 was used extend the measured Pittsburgh results to Huntsville, San Diego and Phoenix. Method 1 used a regression based approach. The Pittsburgh-based regression functions (Eq. 1, Eq. 3, Table 3-3 and Table 3-4 in Chapter 3) were used to estimate the difference in PV power from green and black roofs if a green roof-PV or black roof-

PV system were located in three case study locations (Huntsville, AL; San Diego, CA; Phoenix, AZ). For all four city's datasets, base-case and high temperature scenarios were analyzed to understand the range of power differences between green roof-PV and black roof-PV systems. The base-case was representative of average weather conditions limited only by day light hours spanning an entire year. The high temperature scenario for the green roof-PV combination was derived from a subset of each city's daytime base data. This scenario represents summer conditions (ambient temperatures above 25⁰C) and was used to provide a hypothetical upper bound to the green roof-PV system impact.

For the three city's base-case model results, the difference between black roof-PV and green roof-PV was small. Both in San Diego and Huntsville, green roof-PV produced slightly more power than black roof-PV (0.04 kW and 0.03kW respectively) when averaged across the entire year of daylight hours (Table 4-3). The relative black roof-PV power difference (5.6kW for San Diego vs. 4.8kW for Huntsville) between these two cities was not unexpected as San Diego was chosen for higher solar radiation while Huntsville was selected for higher temperatures. The net kilowatt hour production estimated for green roof-PV subtracted from black roof-PV was 177kWh in San Diego compared with 150kWh in Huntsville (Table 4-3) annually. Considering Huntsville was chosen for its high temperatures, the expectation was for Huntsville to have a greater net kilowatt hour result over San Diego. This slightly surprising result can be explained by looking at the spread in ambient temperature in Figure 4-5. San Diego is a moderate climate while Huntsville has hot but also quite cold temperatures. Huntsville's large variation in air temperature dampens the net kilowatt hour result. In Phoenix, the green roof-PV combination outproduced black roof-PV by 0.08kW (1.3%) and had a net 85 kWh annually.

The impact of cooling a PV panel using a green roof was examined by selecting regression results for temperatures hotter than 25⁰C as a high temperature scenario. When all locations were constrained to this temperature threshold, a green roof under a PV panel produced 0.8%-1.5% more power compared with a black roof-PV assembly (Table 4-3). The number of hourly daytime data points from the base-case data which met the temperature criteria varied from 5% percent (e.g. 244 data points out of 4524) in San Diego to 59% in Phoenix as listed in Table 4-3.

The number of hours above 25⁰C was an indication of the climate variability between case study locations.

Table 4-3: Base-case and high temperature scenario summary results for all case study locations

	Base-Case Scenario (Solar Irradiance >4W/m2)					High Temperature Scenario (Ambient Temp ≥ 25°C)				Electricity Price (cents/kWh) ¹
	Avg Δ Green-Black PV output (kW)	Average black roof PV output (kW)	% change from Black roof PV	Daylight Hours	Net (Green-Black) kWh/yr	Avg Δ Green-Black PV output (kW)	Average black roof PV output (kW)	% change from Black roof PV	Hours above 25 °C	
Pittsburgh, PA	-0.02	4.6	-0.5%	4336	-90	0.07	6.9	0.9%	1154	10.1
San Diego, CA	0.04	5.6	0.7%	4524	177	0.08	9.6	0.8%	244	13.1
Huntsville, AL	0.03	4.8	0.6%	4526	150	0.08	7.0	1.1%	1407	10.18
Phoenix, AZ	0.08	6.2	1.3%	4525	340	0.11	7.4	1.5%	2677	9.47

¹Data source: average retail commercial electricity price by state (EIA 2010)

With a small PV productivity increase from green roofs in the high temperature scenario, converting to annual electricity revenue showed similar results. Electricity revenue for each city was calculated based on the average kW difference between green roof-PV and black roof-PV, daylight hours in the base-case and average electricity prices found in Table 4-3 (United States Energy Information Administration, 2010b). Converting base-case and high temperature scenario values for each city provided an annual increased revenue estimate range from the installation of a green roof-PV system. In the base-case for Pittsburgh, a black roof under PV panels generated \$9/yr/60 panels (Figure 4-6) more than PV panels under a green roof. In the high temperature scenario for Pittsburgh, the green roof-PV combination generates \$29/yr/60 panels more than a black roof-PV assembly. The remaining three cities had slightly smaller ranges between scenarios, but the values were both positive. Figure 4-6 shows the range of revenue estimates for all four cities from the base-case to the high temperature for Method 1 scenario resulting from a green roof under PV assembly. In addition, Figure 4-6 displays the Method 2 results which are discussed in Section 4.7.

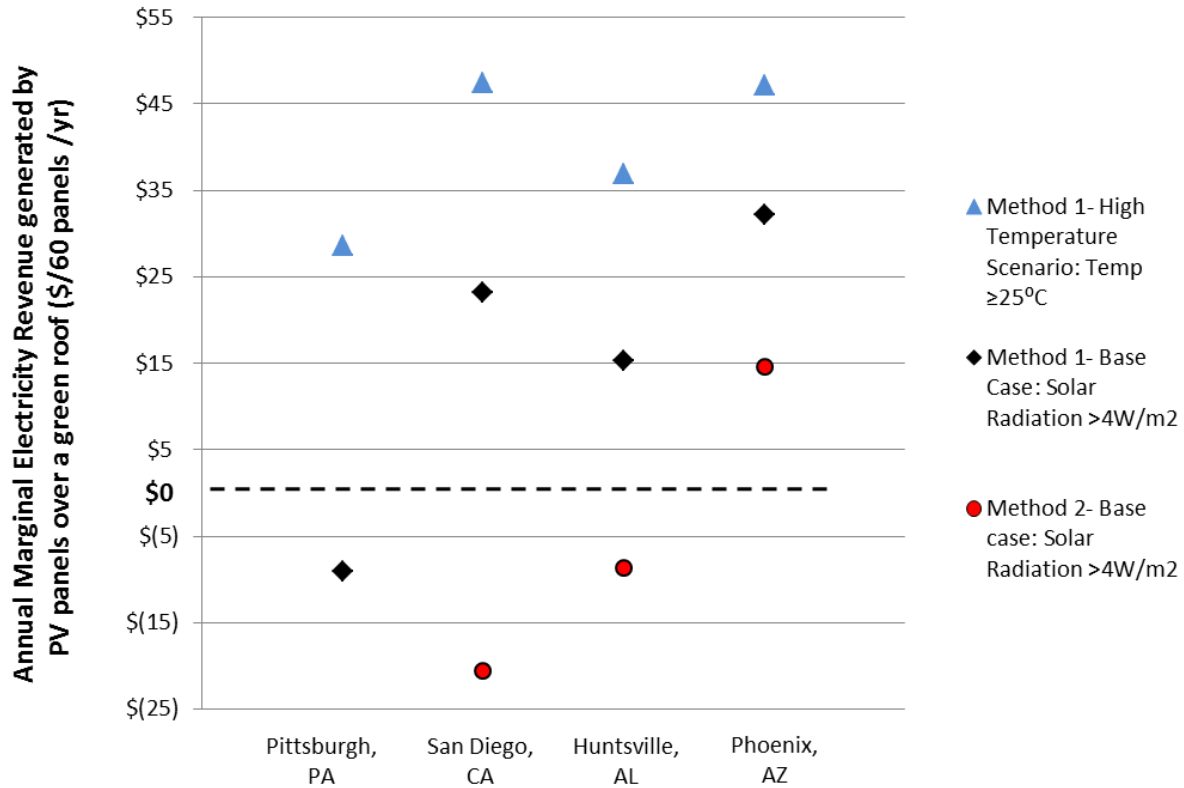


Figure 4-6: Case study ranges for annual net electricity revenue resulting from 60 PV panels over a green roof minus expected revenue over a black roof

4.7 Method 2-Estimated results for other cities

While Method 1 used a regression based approach to extend Pittsburgh values to other cities, method 2 used a matrix methodology. The second method had similar magnitudes of net kilowatt-hours as Method 1, but had opposite signs for San Diego and Huntsville. Table 4-4 compares the net kilowatt hours produced from green roof-PV minus black roof-PV. A positive value indicates the green roof-PV produces more energy than the black roof-PV while a negative value means the black roof-PV produces more. The general trend was that green roof-PV produces more energy in places that are warmer. Method 2 results (Table 4-4) were converted into annual net energy revenue using the same electricity prices in Table 4-3. The comparison of Method 1 and Method 2 in net energy revenue for the three case study cities and Pittsburgh is illustrated in Figure 4-6.

Table 4-4: Comparison of Method 1 and 2 for net kilowatt hours produced from green roof-PV minus black roof-PV for three case studies. Method 1 results are repeated from Table 4-3. A positive value indicates the green roof-PV produces more energy than the black roof PV. The opposite is true for a negative value.

	Base-Case Scenario (Solar Radiation >4W/m ²)	
	Method 1: Net (Green-Black) kWh	Method 2: Net (Green-Black) kWh
San Diego, CA	177	-157
Huntsville, AL	150	-86
Phoenix, AZ	340	154

Possible reasons for the opposite signs and differences in the net kilowatts between method 1 and 2 (Table 4-4) include assumptions within the regression model outlined in Chapter 3. Based on the non-linear analysis in Section 3.3, there exists some non-linearity within the Pittsburgh data that was not included using the linear approach. Furthermore, the explanatory variables such as ambient temperature and solar irradiance may not be statistically independent. Method 2 contains uncertainty and subjectivity in correctly choosing the bin size. In this analysis, 100W/m² and 5°C were chosen as the row and column spacing respectively. Further research needs to be conducted to determine the optimum bin size as well as to verify if the bins should be equally spaced. For example, having larger size bins for solar irradiance and temperature extremes and smaller bins for moderate values could prove more accurate at predicting PV output.

4.8 Conclusions

Green roofs can increase PV power output in high temperatures by lowering the air around the PV panel. On Sunscape, the moss-green roof did lower the air temperature and thus increase the panel efficiency when temperatures were approximately 25°C (77°F) or higher. For Pittsburgh, such high temperatures occurred mainly in summer months. Under these conditions, the green roof-PV combination (60 panels) produced an average of 0.04-0.14 kW more than the equivalent black roof-PV (Table 4-2).

However, the benefit of the green roof-PV combination can only be fully realized when the frequency of temperatures is included in a location across a year. In heating dominated climate

like Pittsburgh, only 27% of the daytime fifteen minute measurements met the greater than 25°C (77°F) ambient temperature condition. Furthermore, temperatures in this study period (July 1, 2011 to June 30, 2012) were even warmer than average which provided more favorable conditions for the green roof-PV assembly (Section 2.7). With the frequency and distribution of Pittsburgh temperatures across the year, black roof-PV panels outperformed the green roof-PV panel. Extending the Sunscape data to three other case study cities showed slightly different results due to the frequency and distribution of the city's temperature and solar irradiance values as well as estimation method. While the bounding analysis in this research was limited to four cities, other locations probably have similar results.

Building managers and designers should consider the interaction between roof type and PV power output a minor economic factor in roof replacement decisions. The relative difference in revenue was small (\$9/60panels/yr or \$0.15/panel/yr in Pittsburgh) in the base-case. Given that each PV panel occupies four square meters (43 sq. ft) of roof space, this value can be normalized \$0.04/sq. m of roof space/yr. Even under the high temperature scenario for green roof-PV where temperatures are always above 25°C (77°F), the green roof-PV assembly would generate \$30 more in revenue from electricity across the 60 panels annually.

This analysis does have limitations which should be considered when extrapolating information to other scenarios or configurations. This research did not look at a variety of PV technologies or green and black roof types. While technologies chosen are represented in the industry, only one of each was modeled. For the PV racking configuration, the height from the roof surface was different across black and green roofs. The bottom edge of the PV panels over the green roof was 51cm (20 inches) from the roof surface compared to 13cm (5 inches) over the black roof. The height difference may alter the impact of wind convection on PV panels as well as the relative effect of cooling from the roofs on the PV panels. The moss on the green roof did not mature in direct sun compared to under the PV panels. The moss grew better in the shade. Therefore, other green roofs could provide more cooling with full coverage of plants. Other factors such as dirt build up, distance to inverter, and equipment losses (Meral 2011) were considered equivalent between black roof-PV and green roof-PV assemblies and therefore not considered. However for other PV configurations, these factors may make an impact.

In addition, designers need to consider the likelihood of roof types in various climates. For example, in Phoenix, green roofs may require additional watering or maintenance expenditures which could possibly counterbalance the modest benefits of a green roof-PV system over a black roof-PV. Furthermore, a green roof in Phoenix would likely have different plant species which could impact the cooling of PV panels.

Manufacturer supplied temperature coefficients could be improved by providing multiple coefficients at solar irradiance ranges less than 1000W/m^2 . Lower solar irradiance temperature coefficients would be particularly useful for places with lower solar irradiance but higher temperatures like San Diego. One possible reason why multiple temperature coefficients is not standard practice could be the small impact temperature has on power output at lower solar irradiance values. Figure 4-1 showed that PV performance declined more with temperature at high solar irradiance values than at low solar irradiance values.

While installing green roofs for the sole purpose of increasing power production of PV panels may not provide significant financial returns, other potential benefits should be included when making a roof replacement decision. Additional factors such as a green roof's ability to mitigate internal building temperature, extend roof membrane longevity, control storm water runoff, and provide recreation areas, to name a few, may have significant environmental and economic benefits that should be included in a roof decision.

Chapter 5: Roof temperatures and heat flow analysis for different roof types

5.1 Introduction

Building roofs are being targeted as opportunities to both reduce energy use and lower the air temperature of surrounding urban areas. Building managers are increasingly examining roof technologies to improve the energy performance of buildings. Huang et al. (1999) found that thirteen percent of heat lost or gained in a building can be attributed to roofs. Furthermore, the roof more than any other single vertical facade receives the largest thermal fluctuation across the year (Eumorfopoulou 1998). With national U.S. commercial roof estimates of 2.6-8.2 billion square meters (28-88 billion square feet) (Levinson & Akbari 2010; CEIR 2012; Chaudhari 2004), total energy transferred through roofs could be significant.

Prior studies have used experimental and/or computational methods to calculate heat flux through roof assemblies into internal spaces. The approaches used to calculate heat flux to date include 1) direct heat flux measurements through transducers (Liu, 2003; Akbari, Levinson & Rainer 2005), 2) equations that quantify conductive heat flux through a temperature gradient (Wong 2003; Akbari, 2003), or 3) simulation models taking into account some or all types of heat flows in the roof energy balance (refer to section 1.4) (Akbari, Levinson & Rainer 2005; Akbari & Konopacki 2005; Rosenfeld, Akbari, Romm & Pomerantz 1998). Simulation models are often used to more accurately determine the energy balance through a green roof (Tabares-Velasco & Srebric 2011; Sailor 2008).

Several field studies have measured the same building pre and post retrofit of a white roof membrane to understand the summertime daily air-conditioning use differences compared to a black roof. Akbari, Levinson and Rainer (2005) monitored a retail store in Sacramento, CA before and after the white roof retrofit during two months in the summer of 2002. From the addition white roof, Akbari (2005) found 33-36°C reduction in maximum surface temperature, a 50% reduction in daily average cooling energy savings (70 Wh/m²/day) and 50% reduction in peak demand savings from 12pm-5pm (10W/m²). During the summer of 2000, the application of white single-ply roofing in Nevada increased the roof reflectivity of two small (15 sq. m each) non-residential buildings by 46% corresponding to a drop of 19-22°C in daytime temperature

from the previously installed black roof (Akbari 2003). Given an R-20 roof assembly, the heat flux was reduced on average 33kWh/day which translated into \$0.67-0.84/m²/yr of air-conditioning savings. Overall, the reduction of heat gain from the roof surmounted to only 1% of the total air-conditioning use (Akbari 2003). For a 9,300m² retail building in Austin, TX, a white roof was retrofitted which reduced the surface temperature by 24°C in the summer. An increase of 78% in roof reflectivity resulted in 39 Wh/m²/day (11%) daily energy reduction with an R-12 roof assembly (Konopacki & Akbari 2001). In addition, the white roof reduced peak demand from 1pm-4pm by 3.8W/m² (14%). Konopacki et al. (1998) measured two medical offices and one retail store in northern California. The white coating resulted in a 28-31°C (50-55°F) lower roof surface temperature. The summertime average daily electricity consumption due to air conditioning was reduced by 13- 18% (36-63 Wh/m²/day). The retail store had 2% (4Wh/m²/day) reduction in electricity use.

A 2008-2009 field experiment in New York City, New York combined white, black and green roof sections on the Con Edison Learning Center to quantify differences in heat transferred into the building and stormwater (Gaffin 2010). In the summer, the white and green roofs peak membrane surface temperatures were 17°C (30°F) and 33°C (60°F) respectively lower than the black roof. In terms of heat loss in the winter, the white roof and green roof had a reduction of 3% and 37% from black roof. For the summer months, the heat gain mitigation of both white and green roofs were significantly larger (55% and 84% respectively) in comparison to the black roof (Gaffin 2010). Two important caveats of this research 1) two models were used to estimate interior temperatures and thus heat flux for white and black roofs instead of empirical measurements 2) the white roof had a double membrane layer while the black had only one. 55% and 84%

The benefits of white roofs are valued less in northern climates with a short cooling season and long heating seasons (Hoff, 2005). In colder U.S. States, white and green roofs incur a heating energy penalty compared to black roofs because they limit external heat from entering a building (Akbari & Konopacki 2005; Gaffin, Rosenzweig, Eichenbaum-Pikser, Khanbilvardi & Susca 2010; Levinson & Akbari, 2010). The heating penalty is the increased use of mechanical heating energy by white or green roofs compared to the conventional black roof during daytime hours in

the winter (Akbari, Konopacki, & Pomerantz 1998). Snyder (2005) found that the “heating energy penalty” offsets the air-conditioning energy savings from white roofs. In other words, the cooling electricity savings in the summer counteracts the heating costs in the winter.

Building energy simulation programs have been used to model energy impacts within the building and to the surrounding community from different roof choices. Rosenfeld et al., (1998) used DOE-2 to determine a 10% reduction in electricity for air-conditioning in a one story office building with the addition of white roofs and shade trees in Los Angeles. Akbari et al. (1998) also used building energy simulation software to determine energy savings from increasing roof albedo of 11 prototype buildings in 11 U.S. metropolitan areas (3 colder climates, 8 warm climates). The cooling energy savings from commercial buildings on average was 3-9% in southern climates. In northern climates (Philadelphia and Chicago), the net energy savings was near zero. The effects of white roofs were mitigated by the level of insulation. In other words, the more insulation the smaller the savings from the white roof. Extrapolating results from U.S. 11 cities (Konopacki 1997; Akbari et al. 1998) to a national scale, Rosenfeld (1998) found a direct electricity (i.e. reduction in cooling) savings in buildings of 3% from cool roofs. Taha et al. (1998) used a mesoscale model of ten regions in the U.S. to estimate energy impacts from a 15% increase in albedo and city's vegetation fraction. Under this scenario, the results suggest up to a 5°C decrease in ambient temperature locally after the implementation of high albedo roofs and vegetation. Lowering the temperature 1-2°C could save 3-11% in peak electricity demand (Taha 1998).

In addition, Oak Ridge National Laboratory (2012) developed an on-line tool to assess the energy differences from increased reflectivity of roofs across climates. The Cool Roof Calculator was developed from DOE 2.1 whole-building energy simulation program and roof specific thermal performance calculations from AtticSim (New et al. 2011). Hoff (2005) used the Department of Energy Cool Roof Calculator to determine the net energy savings across the year from replacing a black roof (0.05 reflectance) with a white roof (0.55 reflectance).

More recent white roof research has relied heavily on various building simulation models with climate models to assess the community benefits (e.g. reduction in smog, greenhouse gas

emissions, urban heat island) from cool roofing technologies (Jacobson 2012; Oleson 2010; Levinson 2010; Akbari 2009). Scherba et al. (2011) explored urban heat island mitigation strategies using building simulation tools to model the sensible heat flux impacts from black, white and green shaded and unshaded roofs on the six U.S. cities.

The field experiment and analysis conducted in this chapter adds to previous literature discussed above by incorporating 1) a colder climate, 2) a side-by-side comparison of alternative roof options, 3) a warehouse building type, and 4) shaded and unshaded roof conditions. In this chapter, the analysis aims to test the hypothesis and subsequently answer the following research questions:

Chapter 5 hypothesis: Green roofs are better building insulators than white or black roofs throughout the year.

Chapter 5 supporting research questions:

5a) What is the reduction in surface temperature and monthly diurnal hourly swing for white, green-moss and green-sedum compared to black roofs on Sunscape?

5b) What quantity of heat gained and lost was measured across black, white and green on Sunscape? How do these values change seasonally?

5c) How does shading of the white or black roof affect the roof heat flux? In terms of reducing heat gain or loss, how do shaded black and white roofs compare with black, white and green unshaded roofs?

5.2 Methods

In this chapter, the Pittsburgh-Sunscape dataset was used to:

- Estimate black surface temperatures used in Studies One, Two and Three,
- Compare membrane and ceiling measurements across roof types,
- Calculate heat flux impacts for Sunscape,

- Estimate heat flux impacts for San Diego, Huntsville and Phoenix based off of the Pittsburgh-Sunscape data, and
- Analyze air temperature differences across roof types in Pittsburgh.

In this section, the methods employed to perform these calculations and develop estimates are described.

5.2.1 Study One and Two: Membrane temperature, ceiling temperature and heat flux

Study One and Two analyzed measured data 1) to understand the impacts of surface temperature on membrane integrity, and 2) to estimate the total heat gained or lost on account of heat flux 3) to quantify the time lag in peak daily flux. Large membrane temperature oscillations reduce the longevity of the roof membrane (Oberndorfer et al., 2007; Desjarlais, Zaltash, Atchley, & Ennis, 2009). While calculating the reduction in roof service life was outside this research scope, Studies One and Two inform roof longevity calculations by measuring surface temperatures and their corresponding fluctuations. Similarly, both studies calculated heat flux across roof types in order to inform more in depth modeling efforts of building heating and cooling loads and associated heating, ventilating and air conditioning (HVAC) needs. This research does not use an energy simulation model to calculate building heating or cooling loads (e.g. DOE-2). Instead, this research used the same approach as Sonne (2006) to calculate the energy and associated cost required by HVAC equipment to counterbalance the net heat gained or lost through the roof. Figure 5-1 shows a schematic of the four step method to calculate the relative energy costs between roof types. Each step is described in more detail below.

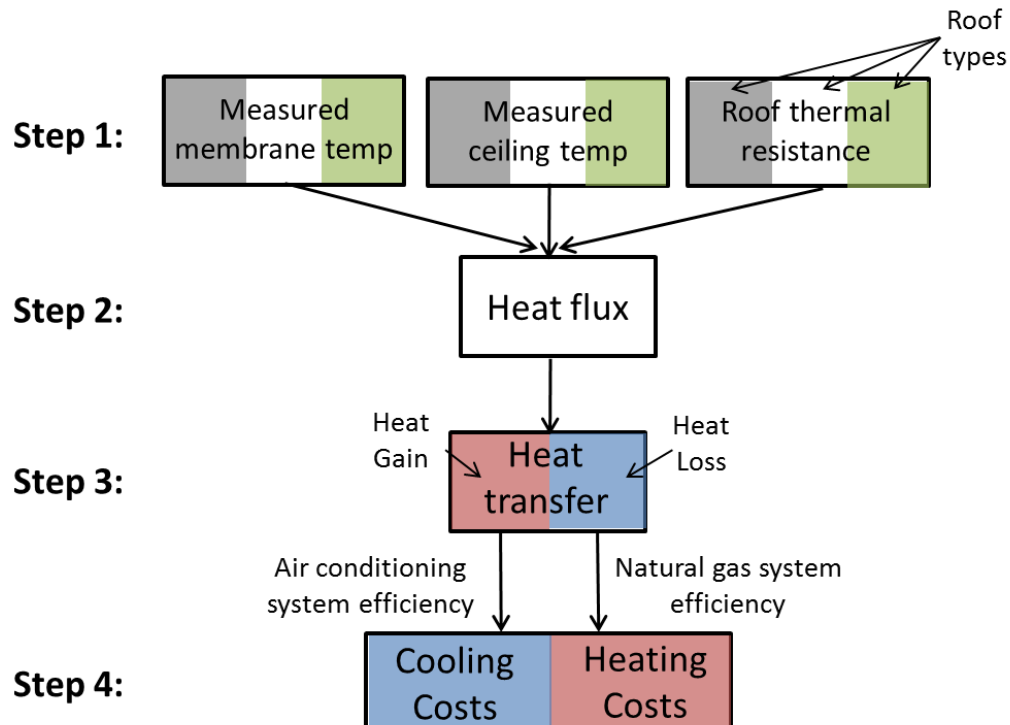


Figure 5-1: Method schematic to calculate heating and cooling costs for each roof type

Before calculating heat flux, the surface membrane temperature and ceiling temperature were compared separately across roof types (Step 1 in Figure 5-1). Examining each of these temperatures separately revealed how the measurements changed on account of ambient temperature, month and warehouse operating condition. More specifically, the average measured membrane and ceiling temperature were normalized by ambient temperature and average monthly hourly profiles. Average monthly hourly profiles were created by averaging four fifteen measurements (0:00, 0:15, 0:30, 0:45) into their respective 0:00-23:00 hours across all days in the month. For example, 1:00, 1:15, 1:30, and 1:45 measurements were averaged into a 1:00 hour.

Ambient temperature and average monthly hourly profiles were chosen as normalizing parameters because they allowed trends to be easily seen for a year worth of data in order to answer the research questions outlined above. Furthermore, ambient temperature was chosen because 1) it was a uniform parameter across roof types, and 2) at the temperatures extremes the thermal properties of the roof material were most apparent. Aggregating the data based on

average monthly hourly profiles allowed time lag and diurnal swings to be easily observed across the year. Other studies use hourly data (Jaffal 2012; Konopacki et al., 1998; Sonne 2008; Jim 2012) but instead of months use a higher resolution (e.g. day or week). By averaging on a monthly level, shorter term trends and global maximum and minimum values could not be seen.

The instantaneous heat flux was calculated (Step 2 in Figure 5-1) for each fifteen minute measurement across the roof types. Similar to other studies (Getter 2011; Gaffin 2010), heat flux was calculated by a simple conductive heat transfer equation (Equation 8) through the roofing assembly. As mentioned above, other studies (Hoff 2005; Suehrcke 2008) use energy models to quantify heat flux from roofs which may produce different results. Equation 8 assumes the transfer of heat is instantaneous (i.e. no time lag).

$$q = \frac{(T_{outside} - T_{inside})}{R} \quad (\text{Eq. 8})$$

where q is the heat flow per unit area (W/m^2), $T_{outside}$ and T_{inside} ($^{\circ}\text{C}$) correspond to the surface temperature on either side of the roof assembly and R ($\text{m}^2\text{K}/\text{W}$) refers to the thermal resistance of the roofing assembly.

The temperature delta was calculated by subtracting the membrane surface temperature measurement i.e. $T_{outside}$, by the inside ceiling temperature under the steel decking, i.e. T_{inside} , for five roofs:

- black,
- white,
- ET Solar 15° + Green (i.e. moss),
- ET Solar 30° + black (i.e. black shaded), and
- ET Solar 30° + White (i.e. white shaded).

This temperature gradient through the roofing assembly was divided by the thermal resistance. As discussed in Section 2.3, the Sunscape roofing profile was the same underneath the

membrane for each of the roofing combinations. The total roofing assembly's R-value was 2.96 K•m²/W (16.8 h•ft²•°F/Btu) according to manufacturer specifications.

The heat flux was calculated for each fifteen minute interval. From Equation 8, a positive heat flux refers to heat entering the building (e.g. T_{outside} equals 30°C and T_{inside} equals 15°C) and is often referred to as heat gain (Figure 5-2). A negative heat flux corresponds to heat leaving the building (e.g. T_{outside} equals 10°C and T_{inside} equals 20°C) or heat loss (Figure 5-2). Since prior studies have varying sign conventions for heat flux (Getter 2011; Gaffin et al. 2005). Figure 5-2 illustrates heat flow nomenclature used in this research.

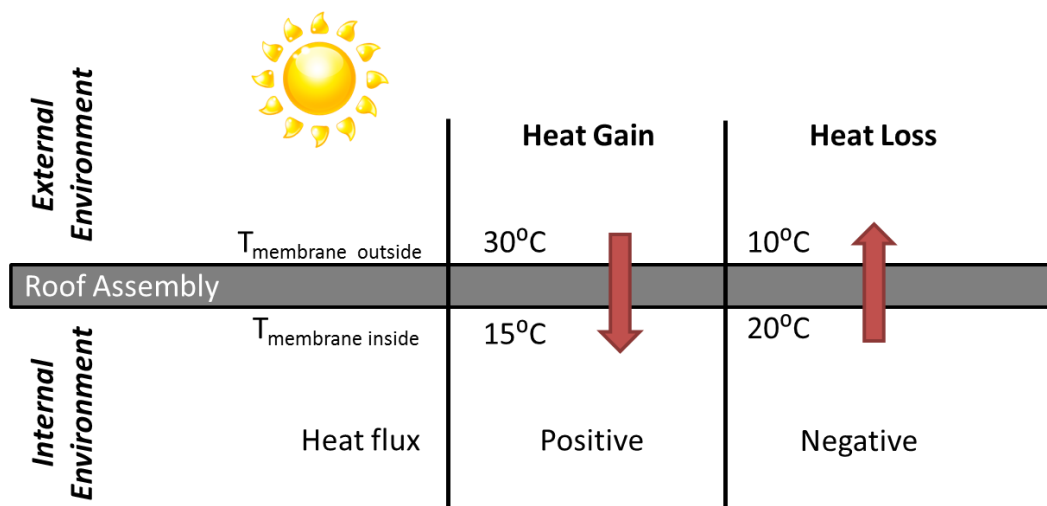


Figure 5-2: Heat Flux (Equation 8) sign convention illustration with example temperatures

Next, the instantaneous heat flux was multiplied by hours (0.25hrs equals fifteen minutes) to obtain a heat transfer quantity¹¹ (Step 3 in Figure 5-1). The quantity of heat gained or lost through the roof was added together by month, season and year. Last, the energy (and corresponding costs) required by heating, ventilation and air-conditioning (HVAC) equipment to counterbalance the net heat gained or lost through the roof was calculated based on typical HVAC equipment efficiency values and thermal comfort ranges (Step 4 in Figure 5-1).

¹¹ Using a physics analogy, heat flux is to power (i.e. rate at which work is performed) as heat (or heat transfer) is to energy (i.e. quantity of work).

Studies One and Two used the same methodology but was applied to different sets of roofs across dissimilar time periods. Study One looked at black, white and ET Solar 15° + Green (referred to as moss) roofs from May 24, 2011 to May 24, 2012. This dataset consists of 34,931 fifteen minute data points. Study Two examined black and white unshaded (referred to as black and white) and ET Solar 30° + black (black shaded), and ET Solar 30° + White (white shaded) roofs from July 5, 2012 to October 13, 2012. The only difference between the unshaded and shaded black membrane is that a portion of the black membrane is shaded by photovoltaic panels tilted at 30° from horizontal. The same is true for the white membrane. Study Two began on July 5 when the white shaded temperature sensors were installed (Refer to Section 2.6). No values collected by the Onset Hobo monitoring system were recorded from August 13, 2012 at 14:45 through August 31, 2012 at 14:00 because the system was accidentally reset. Furthermore, the white shaded ceiling temperature sensor recorded inconsistent measurements sporadically throughout the July 5 to October 13 study period. After removing the irregular values, the dataset contains 3,562 measurements from July 5 to October 13, 2012.

The black roof surface temperature was estimated for part of Study One and all of Study Two. The black surface temperature sensor was faulty after Feb. 10, 2012. Therefore, measurements after February 10, 2012 were discarded because surface temperature values met the data conditions outlined below in Section 5.3. Resulting from these measurement inconsistencies, the black surface temperatures were estimated as a function (Equation 9) of ambient temperature and solar irradiance from Feb 11, 2012- October 13, 2012.

$$y_8 = \beta_{20} + \beta_{21}x_1 + \beta_{22}x_8 \quad (\text{Eq. 9})$$

Where:

y_8 = Black unshaded surface temperature ($^{\circ}\text{C}$)

β_{20} = Y_3 -intercept

β_{21} = ambient temperature coefficient

β_{22} = irradiance coefficient

x_1 = ambient temperature ($^{\circ}\text{C}$)

x_8 = horizontal (0°) solar irradiance (W/m^2)¹²

The second methodology described in Section 4.3 (Equation 7) was used again to extend the Pittsburgh-Sunscape dataset to the same three case study cities used in Chapter 4 (San Diego, Huntsville, and Phoenix). The first matrix categorized average heat flux (W/m^2) from Sunscape by ambient temperature columns and solar irradiance rows. The second matrix used Typical Meteorological Year (TMY) data to bin the number of hours for each case study city by the same row and column delineations in the first matrix. Multiplying elements of matrices together resulted in a third matrix of heat per square meter (Wh/m^2).

5.2.2 Study Three: Comparison of black, white and green roof air temperatures

Study Three investigated the difference in air temperature measurements 15 cm (6 in) above black, white and green roofs to inform research on urban heat island (UHI) effect or HVAC efficiency. Akbari (2001) found that the “peak urban electric demand rises by 2-4% for each 1°C in daily maximum temperature above a threshold of 15 to 20°C .” This thesis only looks at the difference in air normalized by ambient temperature and average monthly profiles. No work was conducted applying the results to UHI effects or HVAC efficiency.

Similar to Study Two, Study Three has the same time period (July 5, 2012 –October 13, 2012). The study period began on July 5, 2012 because the green roof 15 cm (6 in) sensor was installed

¹² The solar irradiance measurements used in this chapter were measured on the horizontal compared with at a 15° angle parallel to the PV panel tilt in Chapter 4.

on that date. Using the same data removal conditions (Section 5.3), the dataset contains 7,810 fifteen minute measurements.

5.3 Data

To examine heat flux and temperature differences for various roof types and height locations, three separate studies were conducted. Due to data availability, each study used a subset of the Sunscape dataset from May 24, 2011- October 13, 2012¹³. The motivation for these studies was to compare how different roof types manage heat. Understanding this energy balance is useful for predicting membrane longevity, heating cooling loads and urban heat island effect to name a few. The first two studies outlined in Table 5-1 focus on membrane and ceiling temperatures as inputs to calculate heat flux. Study Three in Table 5-1 examine air temperature 15 cm (6in) above three roof surfaces.

Table 5-1: Summary of surface temperature, air temperature and heat flux studies. Gray boxes identify data used in each study. EPDM stands for ethylene propylene diene monomer. TPO stands for thermoplastic polyolefin

Study #	Task Description	Data Timeframe (Month, Day, Hour, Year)	ET Solar 15° + Green (Moss) Roof	ET Solar 30° + Black	ET Solar 30° + White	Black (EPDM)	White (TPO)	Green (Sedum)
1	Membrane and Ceiling Temperature, Heat Flux	May 24, 11am 2011 - May 24, 10:45am, 2012						
2	Membrane and Ceiling Temperature, Heat Flux	July 5, 14:00 2012 - August 13, Aug. 31-Oct. 13, 23:45						
3	Moss, black and white air temperature	July 5, 14:00 2012 - August 13, Aug. 31-Oct. 13, 23:45						

Temperature sensor locations used in Studies One, Two and Three for each of the six roof types are illustrated in Figure 5-3 roof cross sections. For a plan view of sensor locations on Sunscape refer to Figure 2-13. The black and white membrane sensors are located on an open, unobstructed portion of the roof (Figure 2-13 location #6 for a plan view of the site). The ET Solar 30° + black and ET Solar 30° + White membrane sensors are located directly underneath the photovoltaic panel tilted at 30° (Figure 2-13 location #4 and #3 respectively). The ET Solar 15° + Green (Moss) membrane sensor is located in between PV panel rows at the sunniest location (Figure 2-13 location #1). However, in the winter when the sun is low, the surface above the ET Solar 15° + Green (Moss) membrane sensor is shaded at some points during the day.

¹³ The complete Sunscape dataset goes from January 26, 2011 to October 13, 2012. However in this chapter, May 24, 2011 was the earliest possible date when the Onset Hobo monitoring system data (which collects measurements for the black roof-PV 15, green (moss) roof-PV and the sedum roof) were available.

Finally, the sedum membrane temperature is installed approximately one foot from the west edge of the ET Solar 15° panels over the moss roof (Figure 2-13 location #8). Therefore during the morning when the sun rises in the east, the sedum surface above the membrane sensor is partially shaded by the PV panel.

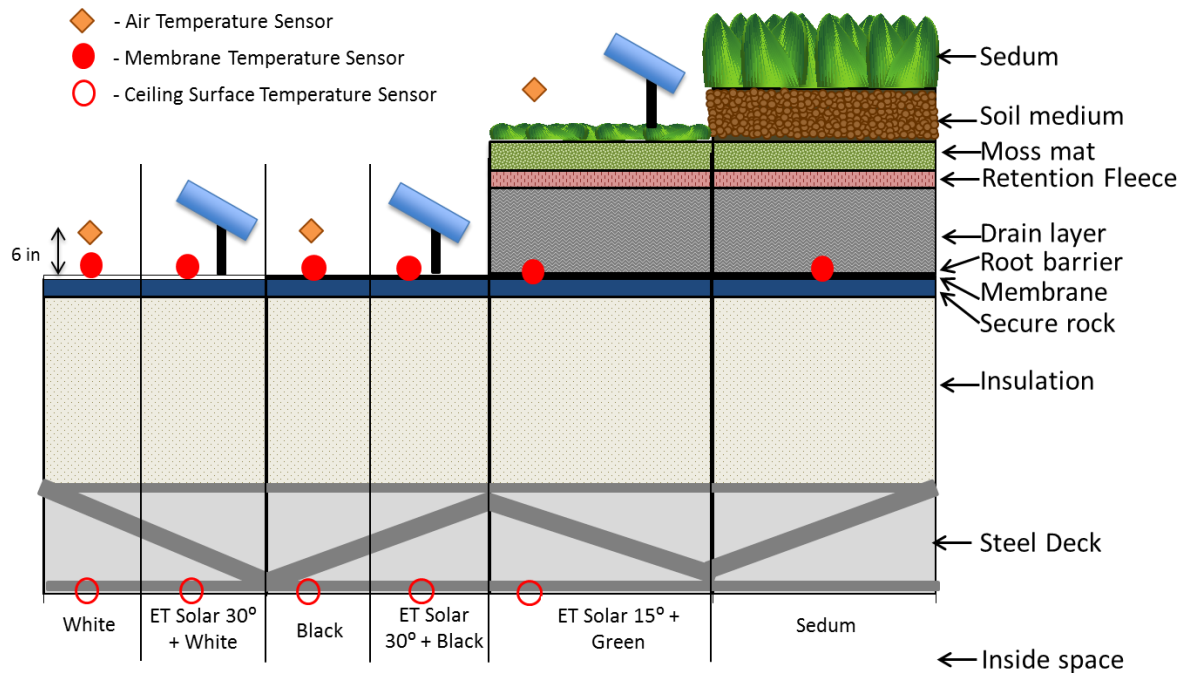


Figure 5-3: Location of temperature sensors installed at Sunspace used for Studies 1-3 in Table 5-1. Figure is not drawn to scale.

Within all three studies, data measurements were discarded because they were inconsistent and/or they had inaccurate readings. Data values were removed if they fell under any one of the following conditions:

- The membrane surface temperatures recorded negative values when ambient temperature was high.
- Sensors recorded “0” for multiple adjacent measurements and/or sporadically for single measurements.
- Data were unrealistically high (e.g. 100°C) for moderate ambient temperatures.
- Large fluctuations (4-10°C) occurred between adjacent fifteen minute measurements.
- The difference in air temperature measurements between roofs were implausibly large (30-80°C).

5.4 Pittsburgh heat flux results

Heat flux results from Studies One and Two outlined in Table 5-1 are examined in the following sections. Before calculating heat flux, the temperature delta ($T_{\text{outside}} - T_{\text{inside}}$) in Equation 8 was decoupled to understand the variation in membrane temperature and ceiling temperature throughout the study period. For the five roof assemblies (black, white, moss, black shaded, white shaded), membrane and ceiling temperature measurements were evaluated by 1) a range of ambient temperatures, and 2) average hourly profiles for each month. The membrane temperature was also separated by seasonal sky conditions which is typical in other studies (Jaffal 2012; Jim & Peng 2012). For the surface membrane temperature comparison only, the sedum green roof measurements were included. The sedum roof membrane temperature provided another reference point for green roof membrane temperatures. Heat flux for the sedum roof cannot be calculated as ceiling temperature was not measured.

5.4.1 Study One: Impact of ambient temperature on surface and ceiling temperature across black, white, moss and sedum roofs

Table 5-2 shows the coefficients results with corresponding statistical parameters from the black membrane temperature as a function of solar irradiance and ambient temperature (Equation 9). Both solar irradiance and ambient temperature explanatory variables were statistically significant (p-value <0.05). Furthermore, the linear regression had a good fit with an adjusted R^2 value of 0.95. Estimated values for the black membrane temperature calculated from the coefficients in Table 5-2 were applied to all fifteen minute intervals after February 11, 2012.

Table 5-2: Linear regression coefficients from Eq. 9 for Black membrane temperature (May 24, 2011 - February 10, 2012)

	Black surface temperature		
	Coefficient	T-statistic	P-Value
Intercept	-5.36	-113	0
Solar Irradiance 0° (W/m^2)	0.05	352	0
Ambient Temperature ($^\circ\text{C}$)	1.13	356	0
Adjusted R-Squared	0.95		
No. of Observations	25,003		

Not surprisingly, the largest differences between membrane temperatures in Study One were found towards higher ambient temperatures (Figure 5-4). With ambient temperatures higher than 22°C (72°F), white roof surface temperatures were 6 to 18°C lower than the conventional black roof membrane averaged across the year (Figure 5-4). Both sedum and moss green roofs had a more pronounced decrease in the membrane surface temperature ranging from 7 to 42°C from the black membrane surface temperature. For all three roof types, 22°C ambient temperature denotes when all surfaces were at least 20% cooler than the black membrane. Gaffin et al. (2010) found similar large temperature differences. The high reflectivity of the white roof curtails the surface temperature. For green roofs, the surface reflectivity and the thermal mass of the assembly both decrease the membrane temperature compared to the black roof. At these high temperatures (above 22°C), the average difference between moss and sedum membrane temperatures was 6°C . The sedum roof reduced the ambient temperature the most which was not surprising considering the sedum has a larger thermal mass.

Two relatively distinct trends resulted for ambient temperatures lower than 22°C across roof types (Figure 5-4). In the 0 - 22°C ambient temperature range, the difference between the four roof types was small (0 - 3°C) on average. One explanation for the small difference could be from the fairly consistent average solar irradiance values between 50 - $150\text{W}/\text{m}^2$ across this temperature band. In other words, the higher solar reflectivity of green and white roofs would have less of an impact at lower solar irradiance values. At cold temperatures ($<0^\circ\text{C}$), both green roof surfaces kept the membrane around 0 - 1°C due to the thermal mass (Figure 5-4). Both white and black

roofs behaved similarly to each other due to the same roof assembly but significantly colder than the green roofs.

For all outside ambient temperatures, the inside ceiling temperature sensors under black, white and moss roofs showed only small deviations from each other. Figure 5-5 shows the average ceiling temperature for each ambient temperature via 2°C bin¹⁴. At higher ambient temperatures, the difference in ceiling temperature ranged from less than 1°C up to 2°C. At lower temperature ranges, relatively small differences were seen between roof types. In addition, the temperature of ceiling temperatures remained fairly constant. One reason for both of these trends was a consequence of winter warehouse operating conditions. In the winter, the warehouse was maintained at a minimum temperature of 15°C (60°F). In contrast, at higher temperatures, the average ceiling temperatures increased and deviated more between roof types. These higher temperatures map to summer months when no temperature set points were used in the warehouse. Therefore, the ceiling temperature was regulated mainly by conductive heat flow through the roof.

¹⁴ A two degree Celsius temperature interval was chosen to provide high data resolution without compromising readability in charts.

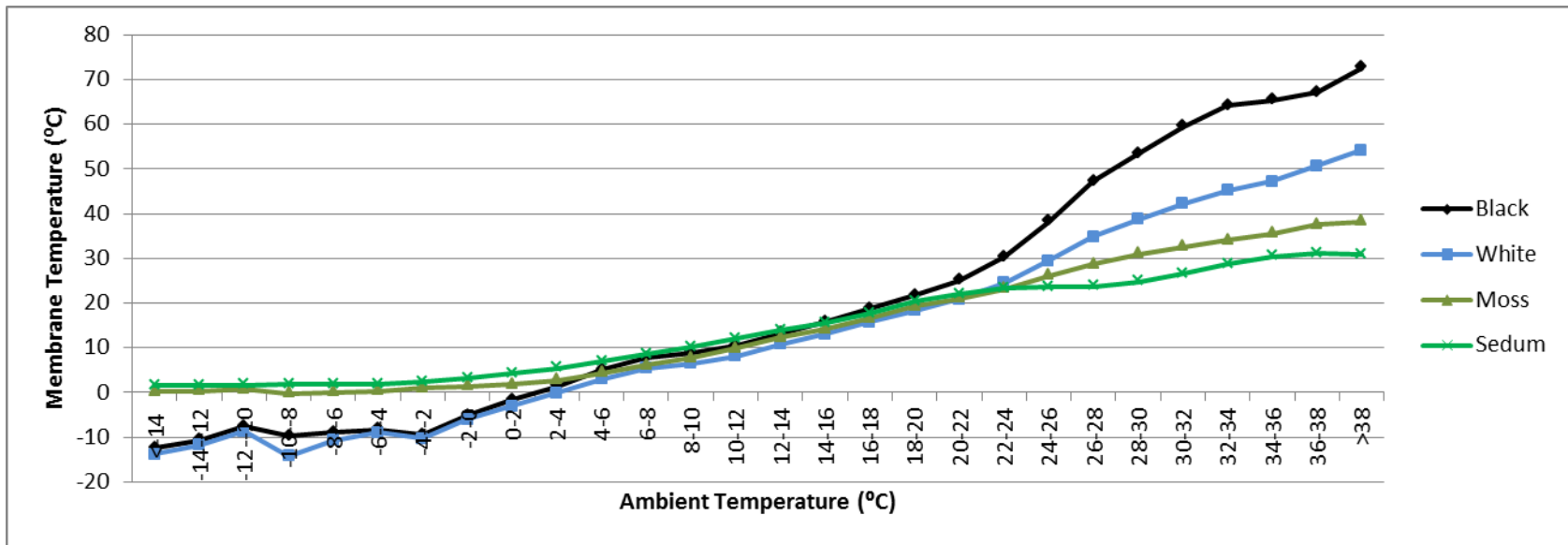


Figure 5-4: Average membrane surface temperatures compared with ambient temperature (May 24, 2011-May 24-2012)

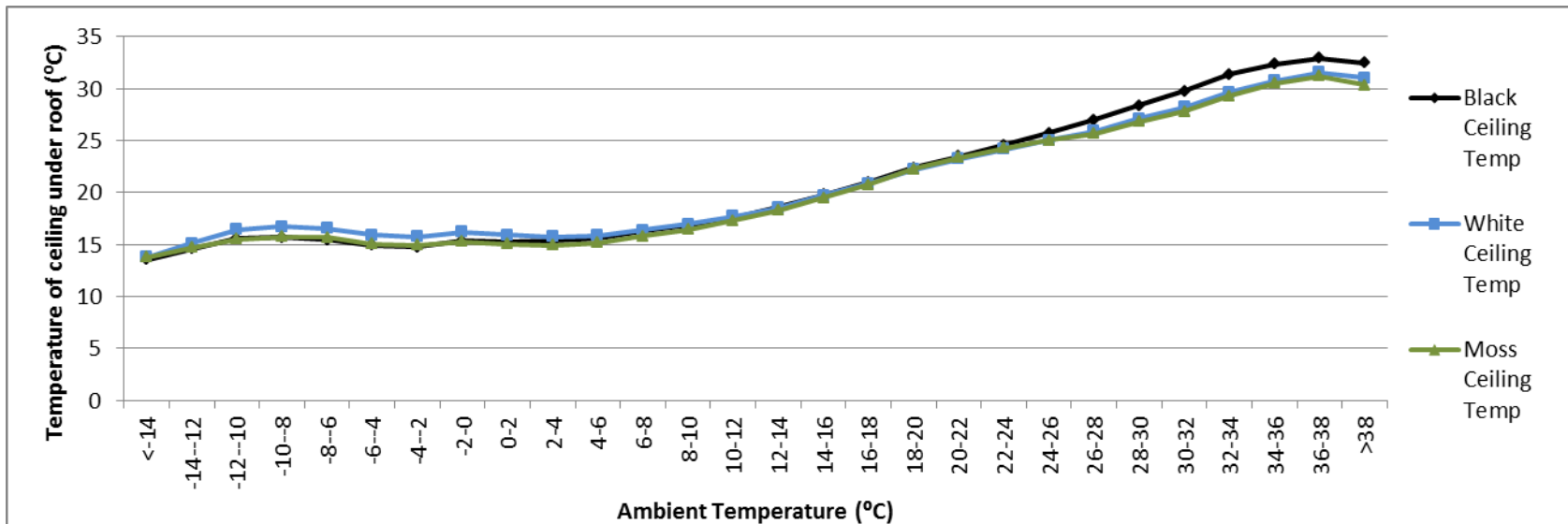


Figure 5-5: Average ceiling temperature under different roof type compared with ambient temperature (May 24, 2011-May 24-2012)

5.4.2 Study Two: Impact of ambient temperature on surface and ceiling temperature across black and white shaded and unshaded roofs

While Study Two had a shorter, three month time duration (July 5-October 13, 2012) and thus a shorter ambient temperature range, shaded black and white membranes significantly lowered the surface temperature at high ambient temperatures (Figure 5-6). For ambient temperatures above 22°C (72°F)¹⁵, a shaded black membrane lowered the temperature by 2-23°C (10-33% reduction) from the unshaded condition. The shade over the white roof membrane reduced membrane temperature by 1-12°C (4-22% reduction) compared to the unshaded white roof. In other words, the shade was more effective over a black roof at reducing the temperature than a white roof. The black shaded roof had a lower temperature than the white unshaded surface. However, the white shaded roof reduced the surface temperature the most from the black unshaded condition as shown in Figure 5-6.

At the colder temperature range, the shaded roofs were approximately the same or slightly warmer than unshaded membranes (Figure 5-6). Except for the white roof, all surface temperatures were within 1°C. A reason for the warmer temperature on the shaded surfaces was due to the PV panel breaking the trajectory of the radiated heat outward to the atmosphere. Because the radiation path was altered, the heat remained closer to the surface.

Direct comparisons between average surface temperatures in Figure 5-4 to the shaded surface conditions in Figure 5-6 should be avoided because of differences in time periods. For example, surface temperatures of 2°C in Figure 5-4 result from both day and night measurements averaged across a year while in Figure 5-6 membrane temperatures of 2°C correspond to night values as the study period was only in the summer and fall. Instead, monthly percent reductions across roof types compared with black roofs were analyzed in the following section.

¹⁵ The 22°C temperature was highlighted here because the difference between black shaded and unshaded and white shaded and unshaded roofs were both at least 1°C.

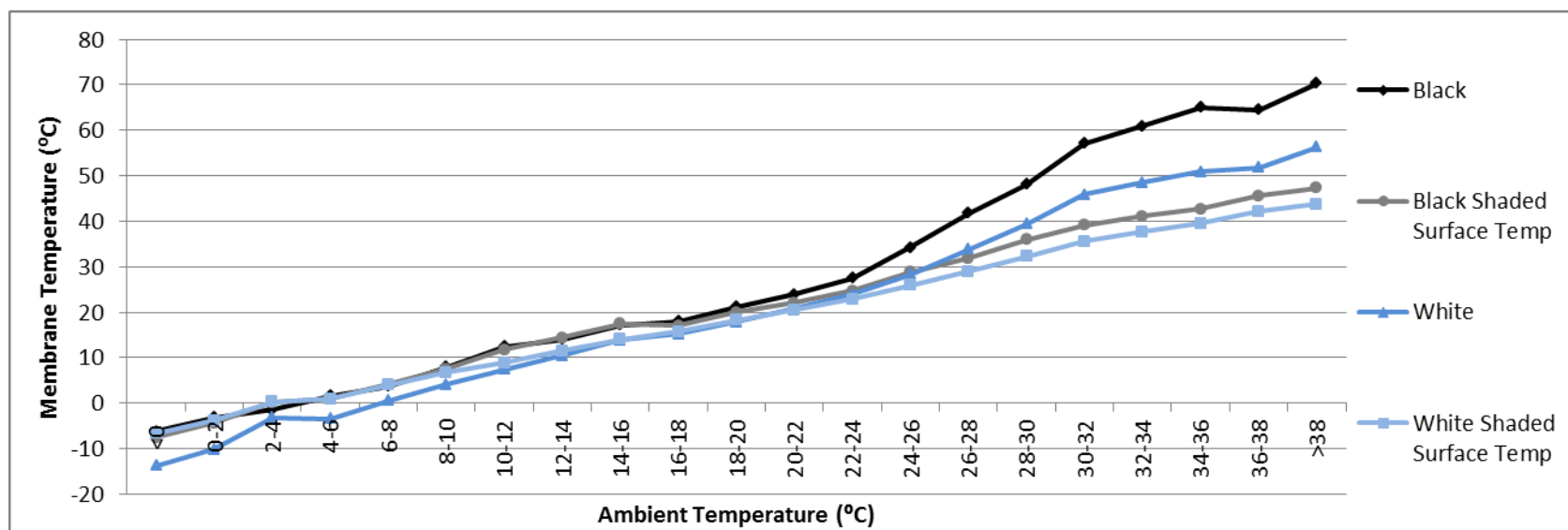


Figure 5-6: Black and white shaded and unshaded average membrane surface temperatures compared with ambient temperature (July 5, 2012-October 13, 2012)

5.4.3 Study One: Average hourly monthly surface and ceiling temperature profiles for black, white, moss and sedum roofs

Another way to see trends in surface and ceiling temperatures across roof types was to develop average monthly hourly temperature profiles. These figures were useful to analyze differences in day and night diurnal temperature swings. Figure 5-7 shows a typical day created by averaging four fifteen measurements into hours across all days in the month.

The diurnal temperature swing in the average hourly membrane surface temperature varied considerably by roof type and by month. In this analysis, diurnal swing refers to the temperature difference between the maximum hourly surface temperatures subtracted from the minimum hourly surface temperature within each month. From May to August, the minimum and maximum range of average hourly surface membrane temperature was the largest. The black roof had a 48-55°C range in hourly temperatures (Figure 5-7). In comparison, the white membrane reduced the fluctuation of the membrane surface temperature by 30-40%, the moss roof by 60-70% and sedum roof by 85-95%. From December to February, the relative temperature swings decreased across all roof types. The ability of white roofs to dampen the fluctuations decreased from 30-40% to 20-30% compared to the black roof in the winter. However, the moss roof increased to almost match the sedum roof at achieving a 90% reduction in the diurnal swing from the black roof in the winter. One possible explanation of why both green roofs had the same performance in temperature reduction could be from similar levels of soil saturation.

While both white and green roofs reduced the difference in monthly diurnal swings in relation to the black roof, these two roof types achieved the reduction in dissimilar ways. The white roof primarily decreased the peak daytime temperature while the green roof moderated both the daytime and evening temperatures. The white roof's high solar reflectance was the most likely reason in the peak membrane temperature reduction. However, the green roof most likely used a combination of material properties (e.g. evapotranspiration, heat storage and reflectivity) to achieve the reductions.

Examining the ceiling temperature separated by average hourly profiles for each month produced little variation across roof types. In the winter months, Figure 5-8 illustrates three roof types having similar ceiling temperatures. The typical daytime bell curve was also dampened as a result of the winter heating temperature set point at 15⁰C. In the summer, the ceiling temperatures resumed the typical daily shape since the warehouse was allowed to fluctuate without set points. Even in the summer months, the ceiling temperature showed at most 2⁰C difference for any average hourly value.

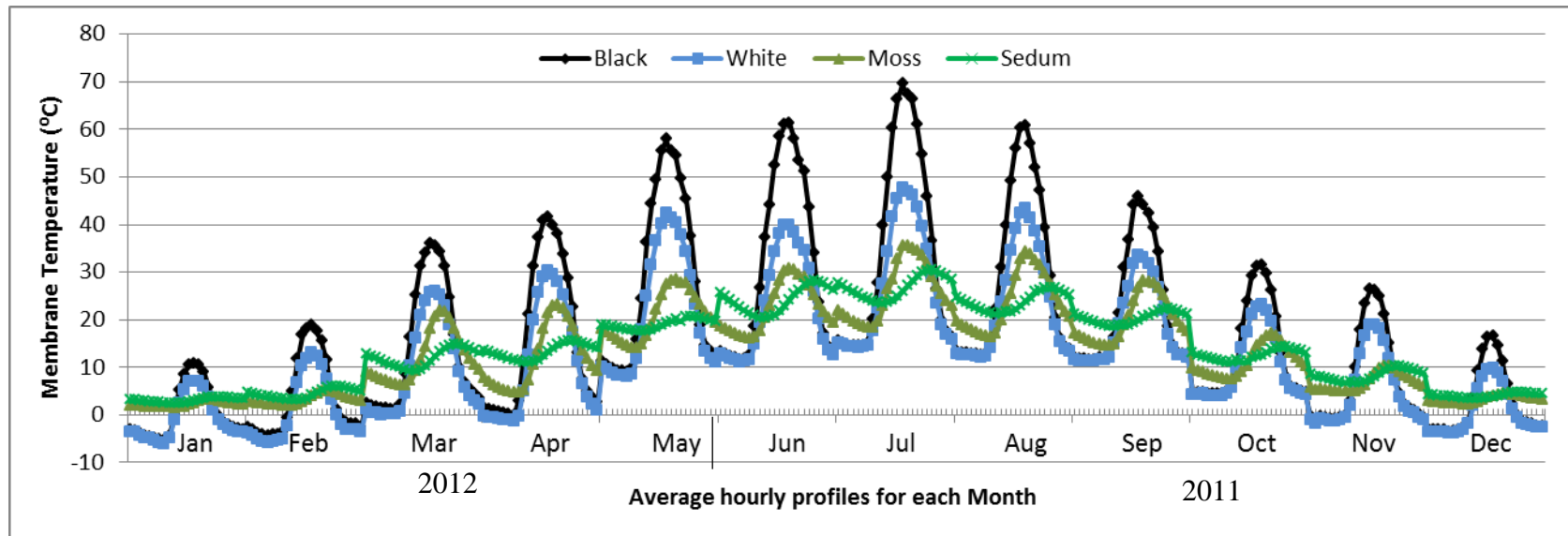


Figure 5-7: Average hourly membrane temperature profiles for each month across black, white, moss and sedum roof types (May 24, 2011-May 24-2012)

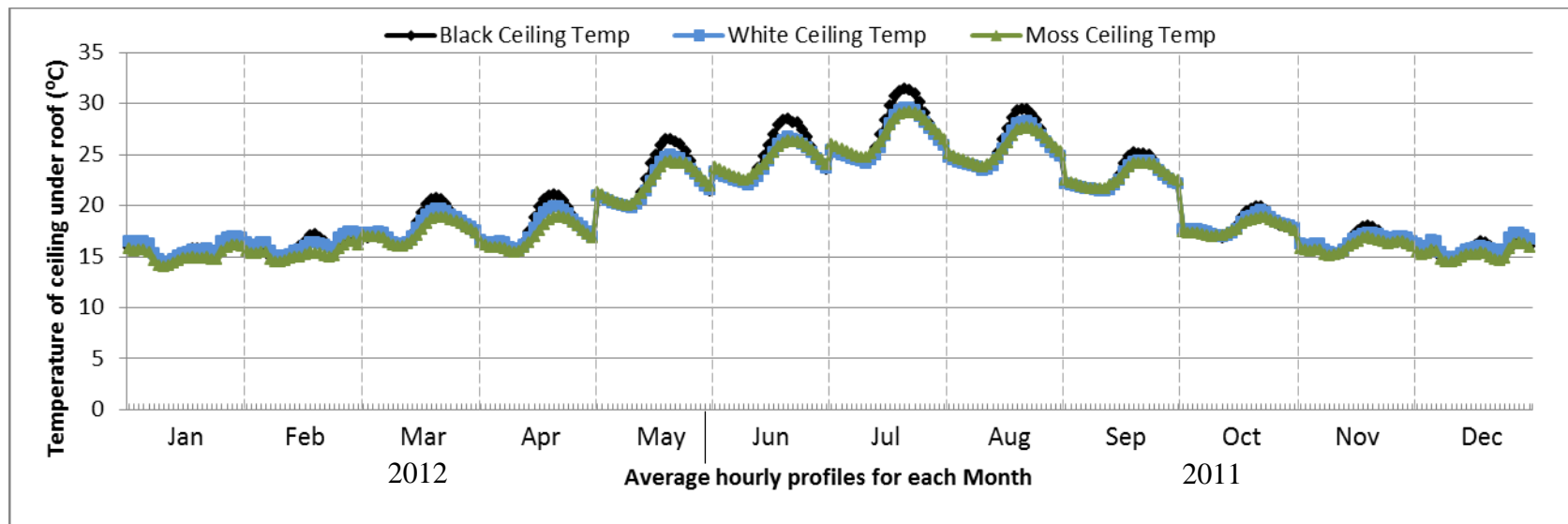


Figure 5-8: Average hourly ceiling temperatures profiles for each month across black, white and moss roof types (May 24, 2011-May 24-2012)

5.4.4 Study Two: Average hourly monthly surface and ceiling temperature profiles for black and white shaded and unshaded roofs

During July 2012-October 2012, the shaded white and black roofs significantly reduced the membrane temperature diurnal swings compared to the black unobstructed membrane (Figure 5-9). The white unshaded roof reduced the maximum and minimum range 20-30% while the black shaded and white shaded roofs achieved a 40-50% and 50-60% reduction respectively compared to the black unshaded roof. However in October 2012, the black shaded roof performed similarly to the black unshaded roof. One possible explanation includes the shaded sensor being exposed to the sun for part of the day in the fall and winter months when the sun angles were lower. Field observations confirmed that the shaded black surface measurement did receive direct sunlight for a portion of the day.

Reduction in diurnal membrane surface temperature fluctuations was compared from July to October in 2011 and 2012 across the five roof types. The monthly temperature range for each roof type (maximum hourly minus minimum hourly value) was compared with the corresponding black 2011 or 2012 unshaded membrane temperature values in Table 5-3. For context, July and August 2011 had higher black and white surface temperatures, and thus, larger ranges, than the same months in 2012. The reverse was true for September and October; the 2012 values had more extreme surface temperatures which resulted in a larger diurnal swing compared to September and October 2011. The percent reduction in Table 5-3 was calculated based off of the black unshaded diurnal swing in the same year. For example, the white 2011 unshaded membrane had a range of 34°C in July which was a 38% reduction from the July Black 2011 fluctuation of 55°C.

The relative percent differences glean insights into the ability of roof types to reduce membrane temperature. Of the five roof types, the sedum green roof reduced the temperature fluctuation the most (87-89%) followed by moss (59-63%), white shaded (53-61%), black shaded (3-50%), and finally white (18-38%).

Table 5-3: Monthly surface temperature diurnal fluctuation (°C) (maximum-minimum hourly surface temperature value) and corresponding percent reduction from Black 2011 and Black 2012 roofs for July through October 2011 and 2012

	Black 2011 (°C)	White 2011 (°C)	Moss 2011 (°C)	Sedum 2011 (°C)	Black 2012 (°C)	White 2012 (°C)	Black Shaded 2012 (°C)	White Shaded 2012 (°C)
July	55	34 -38%	17 -69%	7 -87%	44	31 -30%	22 -50%	17 -61%
August	48	31 -35%	18 -63%	6 -88%	46	36 -22%	24 -48%	19 -59%
September	34	22 -35%	14 -59%	4 -88%	38	30 -21%	23 -39%	18 -53%
October	27	19 -30%	9 -67%	3 -89%	34	28 -18%	33 -3%	16 -53%

The black and white shaded and unshaded roof ceiling temperatures from July to October 2012 illustrated in Figure 5-10 were similar in shape and magnitude for the corresponding months in Figure 5-8. Furthermore, the black and white shaded roofs had similar ceiling temperature reductions (2°C-3°C) during the day as the moss green roof in Figure 5-8 when compared to their respective black roofs.

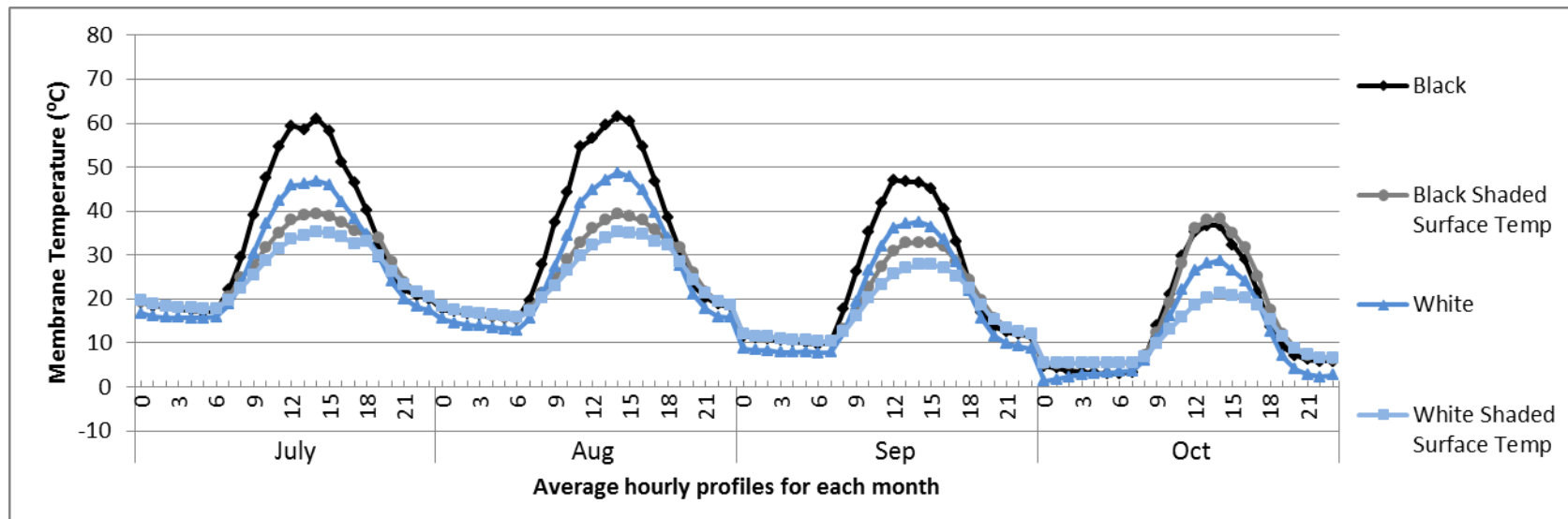


Figure 5-9: Average hourly membrane temperature profiles for each month across black and white shaded and unshaded roof sections (July 5, 2012-October 13, 2012)

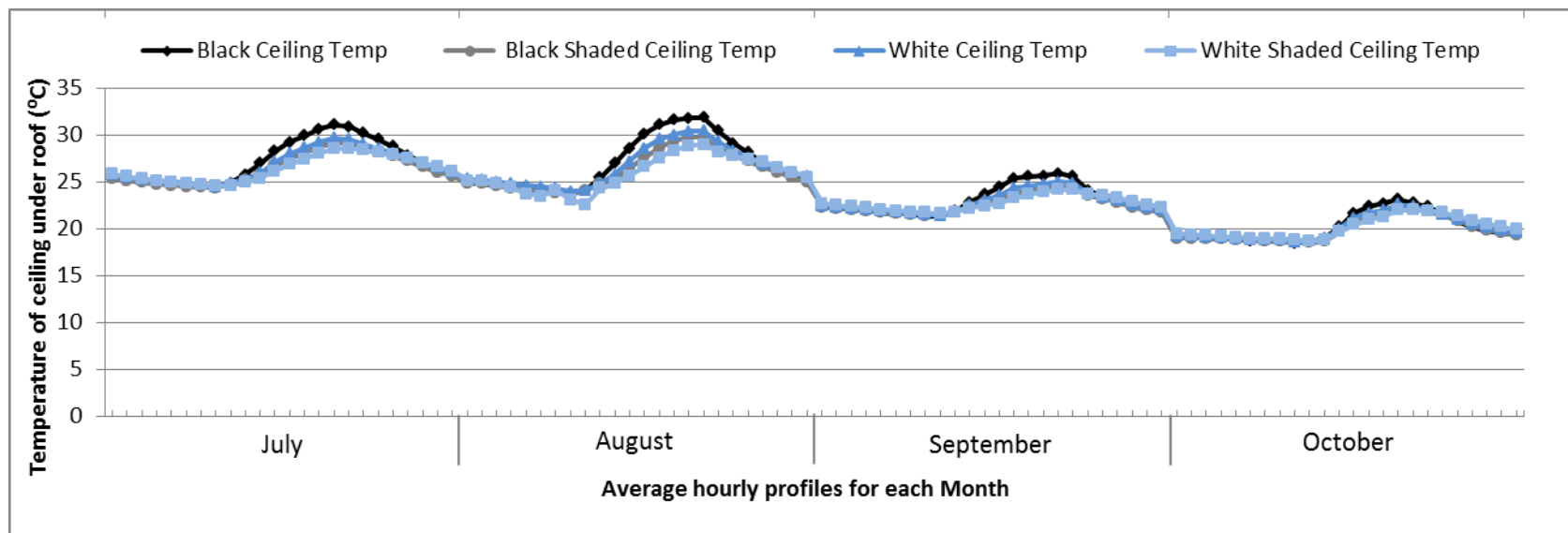


Figure 5-10: Average hourly ceiling temperature profiles for each month across white and black shaded and unshaded roofs (July 5, 2012-October 13, 2012)

5.4.5 Effects of seasonal sky conditions on membrane surface temperatures

To better understand the impact of sky conditions (i.e. sunny, cloudy or rainy) on membrane surface temperature, the May 2011-May 2012 study period was aggregated into seasons. In order to get the data into seasons, the hourly monthly profiles used in Section 5.4.3 were grouped and then averaged. The seasons were divided roughly but not precisely by the spring and fall equinoxes and the winter and summer solstices.

- Spring (April - June 2012)
- Summer (July - September 2011)
- Fall (October – December 2011)
- Winter (January – March 2012)

Sky conditions were assigned by the National Weather Service (NWS) to hourly temperature readings at the Pittsburgh International Airport. No sensors existed on Sunscape which collected sky condition. Therefore, the sky condition for the Pittsburgh International Airport weather station was mapped to Sunscape based on measurement date and time. Appendix C lists all recorded sky condition types by the NWS. Because NWS data were available hourly, the same sky condition was repeated four times for each fifteen minute interval corresponding to the hour observed on Sunscape. For example, if at 2pm the NWS designated the sky condition as sunny, Sunscape's 2:00, 2:15, 2:30 and 2:45pm measurements would be all allocated the same sunny sky condition.

Sunny, cloudy and rainy sky conditions were chosen to show a spectrum of sky conditions and to be consistent with previous studies (Getter et al., 2011; Jim & Peng 2012). For each season, the sunny sky condition was observed for 10-13% of the hours, cloudy 24-35%, and rainy 5-11%. However, these three sky conditions were not the most frequent sky conditions observed in Pittsburgh during May 2011-May 2012. Other common seasonal sky observations included Partly Cloudy/Partly Sunny (15-31%), Mostly Cloudy (8-11%) and Mostly Sunny (7-16%). Appendix C lists all the seasonal sky condition frequencies.

Figure 5-11 illustrates the average hourly profile across roof types for a typical day in fall and winter while spring and summer are represented in Figure 5-12. For all seasons, sunny conditions produced the largest diurnal swing in membrane temperature followed by cloudy conditions. The

smallest differences between the roof types can be seen in rainy conditions. These results were expected because both clouds and rain lower the solar irradiance reaching the roof surface. In Figure 5-11, the sharp decrease in membrane temperatures during sunny conditions at 14:00 (2pm) in the Fall and at 15:00 (3pm) in the Winter were due a small sample size (<8 measurements) for that timeslot. Also, no data values corresponded to summer sunny sky conditions from 13:00-16:00 (1-4pm).

Similar trends for sunny, cloudy or rainy sky conditions were seen for black and white unshaded and shaded roofs in Figure 5-13. Due to the small time period, the shaded and unshaded black and white roofs were averaged only for the Summer (July-September 2012) season. Also, not all hours had data points for the sunny condition in Figure 5-13. The sunny hours without data were from 12:00-18:00 (noon-6pm).

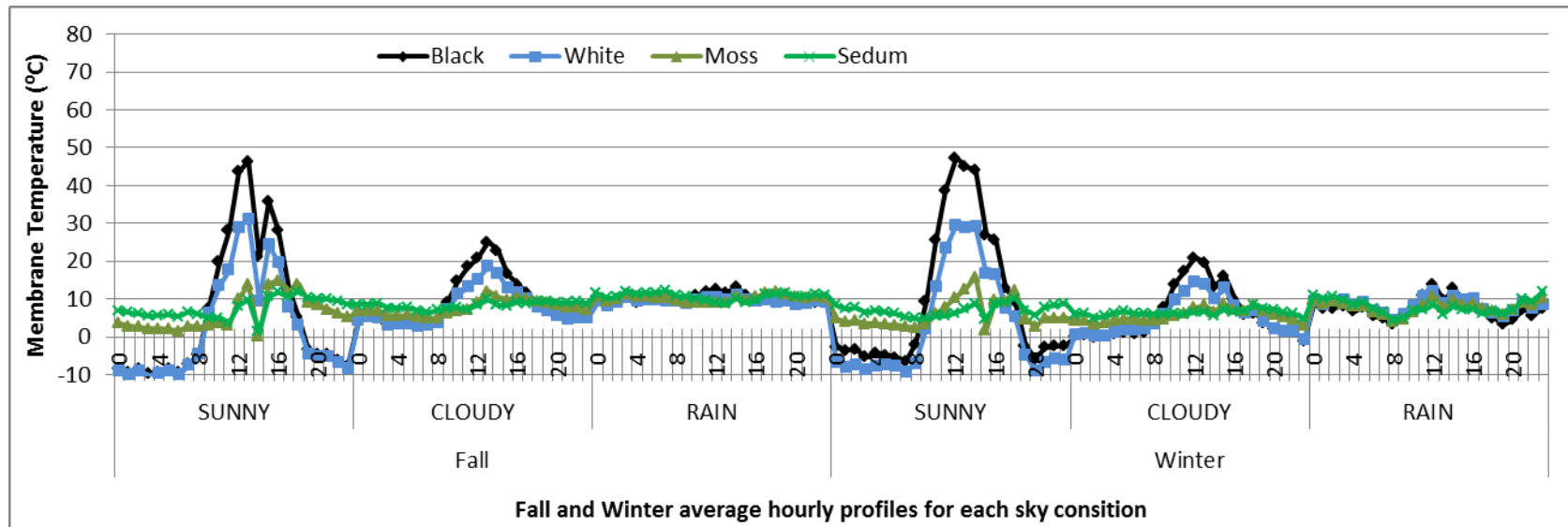


Figure 5-11: Fall and Winter average hourly profiles of membrane temperature across roof surfaces (October 2011 to March 2012)

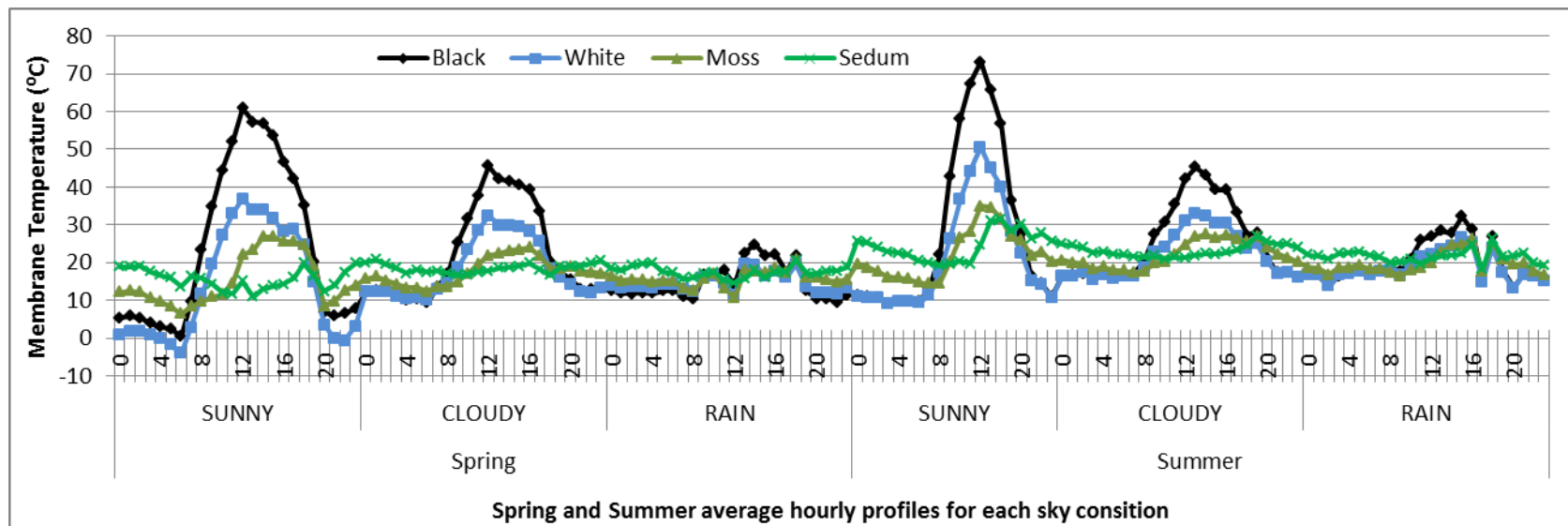


Figure 5-12: Spring and Summer average hourly profiles of membrane temperature across roof surfaces (April 2012- June 2012; July 2011-September 2011)

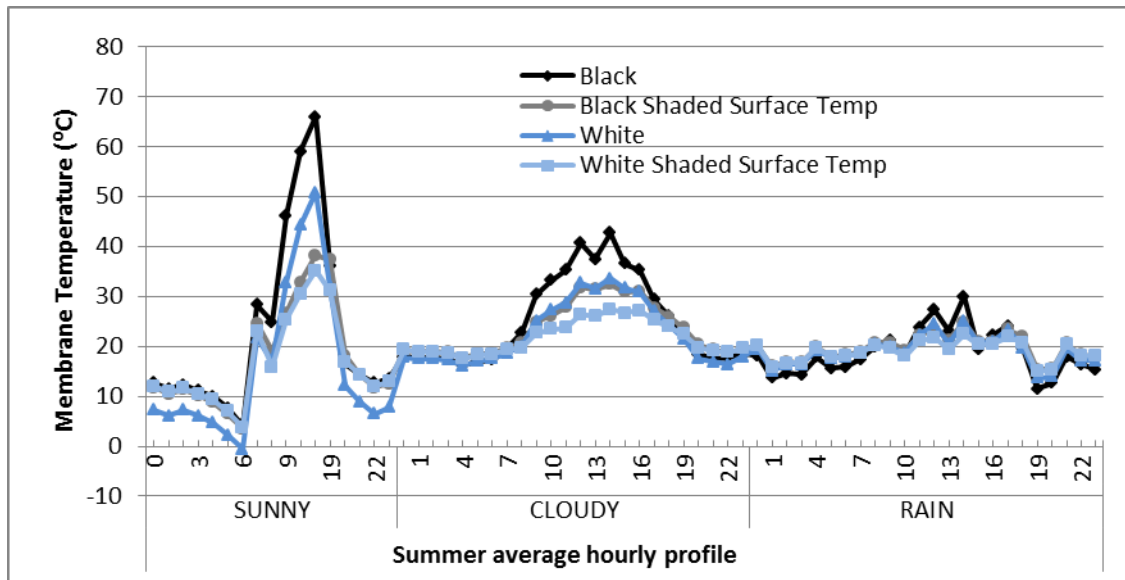


Figure 5-13: Summer average hourly profile for membrane temperature across roof surfaces (July 5, 2012-September 30, 2012)

5.4.6 Study One: Monthly heat flux results

Using Equation 8 and the membrane and ceiling temperatures outlined above, the heat flux for each fifteen minute interval was calculated for black, white and green-moss roofs. Figure 5-14 shows the average hourly heat flux profile for each month based on aggregating fifteen minute measurements. Generally for Pittsburgh, heat gain is advantageous in the winter because it is free heat while heat loss is better in the summer for natural cooling. Not surprisingly, the largest instantaneous heat flux into the building occurred in the summer months while heat loss occurred in the winter months across all roofs. The moss green roof moderated the heat flux for all months compared to the black and white roof.

Another way to analyze roofs was to disaggregate the average hourly values in Figure 5-14 back to fifteen minute intervals in order to sum the positive and negative instantaneous heat flux values. This analysis helps inform building heating and cooling needs. All negative (heat loss) and positive (heat gain) heat flux measurements were totaled together separately. Higher level results were calculated by summing the data by season and year. Table 5-4 lists the summation of heat flux into (heat gain) and out of (heat loss) the building by month, season and year. Note that Table 5-4 shows a summation for the raw fifteen minute measurements prior to averaging. In

other words, positive heat flux values can be found in Table 5-4 for January but not in Figure 5-14 due to averaging hourly values across months.

One interesting monthly result resonated around the winter heating penalty associated with green roofs. Examining the month of January in Figure 5-14, the heating penalty was present. The heating penalty can be seen by the green roof having a larger (-4W/m^2) heat loss during the day than either the black or white roofs (-1 to -3W/m^2). In other words, the thermal mass of the green roof prevents outside natural heat from entering the building during the day compared with a black and white roof. However, at night the green roof maintained the heat flux at -4W/m^2 while the black and white roofs had larger heat loss averaging -7 to -8W/m^2 . Summing the heat gain and loss measurements (Table 5-4), the green roof daytime winter heating penalty was offset by the smaller evening heat flux which resulted in a lower net heat flux value overall compared with black and white roofs.

In the winter, the white roof had the largest net heat flux. The reason was because the white roof had 12% more heat loss (due to colder membrane temperatures) than black roofs and 25% more than green roofs. Depending on internal thermostat set points, this heat loss may need to be supplemented by additional mechanical heating. In terms of heat gain, the black roof allowed 66% and 84% more heat to flow into the space than the white and green roofs respectively. Examining the net heat flux, the green roof would be preferred in the winter to black (only slightly) and white roofs.

For summer months, the black roof had a positive net heat flux while the white and green roofs had a negative net heat flux. The black roof allows 57% more heat to enter the building than the white roof and 85% more than the green roof (Table 5-4). In terms of natural cooling (heat loss), the white roof had the most heat loss followed by black and finally the green roof. Based only on the summer net heat flux, green roofs would be similar to white roofs, but preferred over black roofs.

Across the year, the black roof had over 58% and 87% more heat entering the building compared to white and green roofs respectively. This result was not surprising given the surface reflectivity

of white roofs and both the surface reflectivity and thermal mass of the green roofs. However, white roofs allowed more heat loss compared to a black roof for heat loss. The reason was because the membrane temperature of the white roofs was slightly colder at lower temperatures (Table 5-4).

Adding the absolute value of heat gained and lost across the year, black roofs allow 15% and 47% more heat to flow through the roof assembly (i.e.in or out) compared to the white and green-moss roofs respectively. Both white and green roofs had more sizable reductions of heat gain from the reference black roof than differences in heat loss.

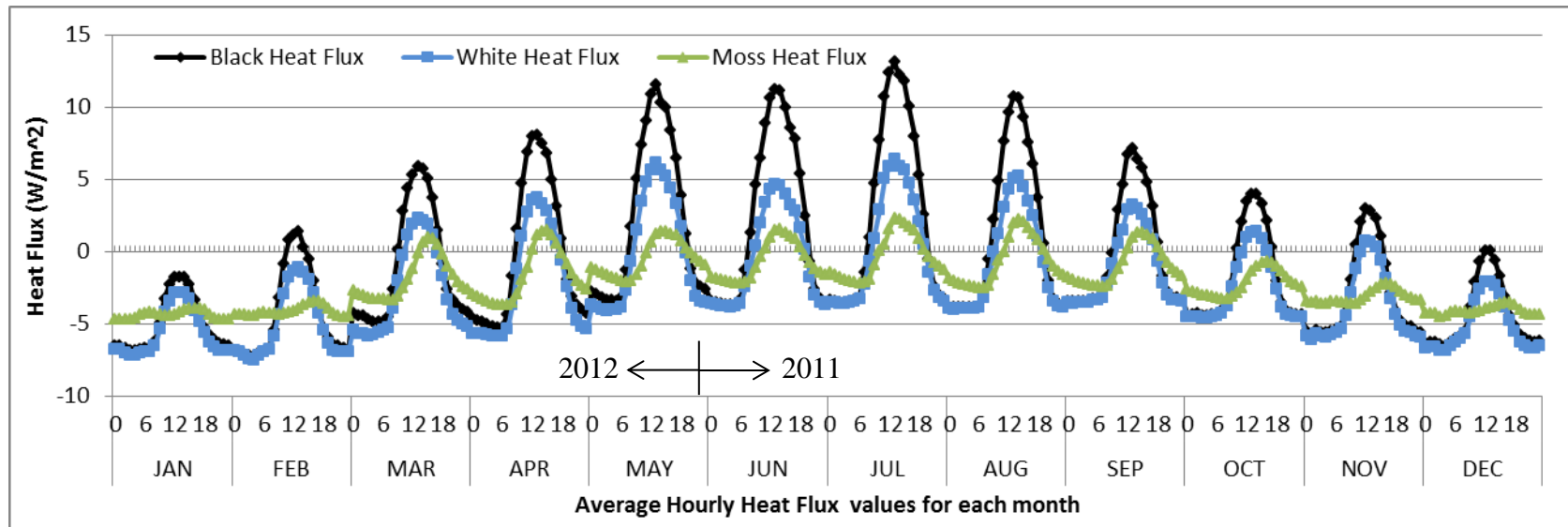


Figure 5-14: Average hourly heat flux profiles for each month for black, white and moss roofs (May 24, 2011 to May 24, 2012)

Table 5-4: Total and percent difference of heat gain and loss by month, season and year for black, white and green-moss roofs (May 24, 2011-May 24, 2012)

	Month	Black Roof			White Roof			Green-Moss Roof			% Difference (White-Black)		% Difference (Green-Black)		# of 15 min data points
		Heat Gain (W/m ²)	Heat Loss (W/m ²)	Net Heat Flux (W/m ²)	Heat Gain (W/m ²)	Heat Loss (W/m ²)	Net Heat Flux (W/m ²)	Heat Gain (W/m ²)	Heat Loss (W/m ²)	Net Heat Flux (W/m ²)	Heat Gain (W/m ²)	Heat Loss (W/m ²)	Heat Gain (W/m ²)	Heat Loss (W/m ²)	
Winter '12	Jan	339	-15,469	-15,130	54	-16,822	-16,769	0	-13,032	-13,032	-84%	9%	-100%	-16%	2,976
	Feb	1,353	-13,702	-12,350	232	-14,623	-14,392	0.7	-11,465	-11,464	-83%	7%	-100%	-16%	2,780
	Mar	5,085	-8,016	-2,930	2,010	-10,027	-8,017	1,077	-6,523	-5,446	-60%	25%	-79%	-19%	2,972
	Total	6,777	-37,187	-30,410	2,295	-41,473	-39,177	1,078	-31,020	-29,942	-66%	12%	-84%	-17%	8,728
Spring '12	Apr	6,944	-7,588	-645	2,946	-9,336	-6,389	1,173	-6,025	-4,852	-58%	23%	-83%	-21%	2,880
	May	10,672	-4,114	6,558	5,251	-5,482	-232	1,114	-2,633	-1,519	-51%	33%	-90%	-36%	2,959
	Jun	10,384	-4,444	5,939	3,737	-5,088	-1,351	1,044	-3,100	-2,056	-64%	14%	-90%	-30%	2,842
	Total	27,999	-16,147	11,852	11,934	-19,906	-7,972	3,331	-11,758	-8,428	-57%	23%	-88%	-27%	8,681
Summer '11	Jul	12,061	-4,391	7,670	5,316	-4,823	493	1,656	-2,759	-1,103	-56%	10%	-86%	-37%	2,936
	Aug	8,873	-5,428	3,445	3,783	-5,952	-2,168	1,415	-3,473	-2,058	-57%	10%	-84%	-36%	2,937
	Sep	5,176	-5,434	-258	2,215	-5,889	-3,674	973	-3,699	-2,726	-57%	8%	-81%	-32%	2,853
	Total	26,110	-15,253	10,857	11,314	-16,664	-5,349	4,044	-9,930	-5,886	-57%	9%	-85%	-35%	8,726
Fall '11	Oct	2,898	-8,390	-5,492	1,226	-9,178	-7,952	185	-6,702	-6,517	-58%	9%	-94%	-20%	2,938
	Nov	1,894	-10,598	-8,704	687	-11,627	-10,941	0.6	-9,034	-9,033	-64%	10%	-100%	-15%	2,882
	Dec	428	-13,744	-13,315	27	-15,495	-15,468	0	-12,173	-12,173	-94%	13%	-100%	-11%	2,976
	Total	5,220	-32,732	-27,512	1,940	-36,301	-34,360	186	-27,909	-27,723	-63%	11%	-96%	-15%	8,796
Annual		66,106	-101,318	-35,212	27,485	-114,343	-86,858	8,639	-80,618	-71,979	-58%	13%	-87%	-20%	34,931

Delays in peak heat flux were observed for white and moss roofs compared to black roofs. Table 5-5 lists the time when the maximum average heat flux was reached in Figure 5-14. When juxtapositioning the white and green-moss roofs to the black roof, the green-moss roof had a noticeable time delay in reaching the maximum heat flux. In the winter months, the time delay was 4-5 hours later than the black roof (Figure 5-5). For the summer, the time delay was smaller (0-2 hours). One possible explanation for the seasonal differences could be the soil heat storage capacity was reached in the summer allowing additional heat to pass through more easily. White roof showed little to no time delay compared to the black roof. This result was expected as the thermal conductivity of the two roofs is the same. From a societal benefit, the delay in heat flux is useful in shifting the need for energy away from the highest energy demand hours. For a building owner, the delay would be beneficial if under a dynamic pricing scenario where energy use during high demand costs more.

Table 5-5: Time delay of maximum heat flux from the monthly hourly profiles in Figure 5-14 (May 24, 2011- May 24, 2012)

Month	Time of peak heat flux			Time delay (hrs) for peak heat flux from black roof	
	Black Roof	White Roof	Green Roof	White Roof	Green Roof
Jan	12:00	14:00	17:00	2	5
Feb	13:00	13:00	17:00	0	4
Mar	13:00	13:00	15:00	0	2
Apr	13:00	13:00	15:00	0	2
May	13:00	13:00	15:00	0	2
Jun	13:00	13:00	14:00	0	1
Jul	13:00	13:00	13:00	0	0
Aug	13:00	14:00	14:00	1	1
Sep	13:00	13:00	15:00	0	2
Oct	14:00	14:00	16:00	0	2
Nov	12:00	12:00	16:00	0	4
Dec	12:00	12:00	17:00	0	5

5.4.7 Study Two: Monthly heat flux results

Figure 5-15 illustrates similar average monthly heat flux profiles for unshaded and shaded black and white roofs compared with the black, white and moss roofs shown in Figure 5-14.

Analogous to the surface temperature analysis above, the heat flux underneath the shaded black and white roof had the largest decrease in July and August from the unshaded condition. For

October, the black shaded sensor almost matches the unshaded condition because the shaded sensor sometimes receives direct sun due to a lower sun angle.

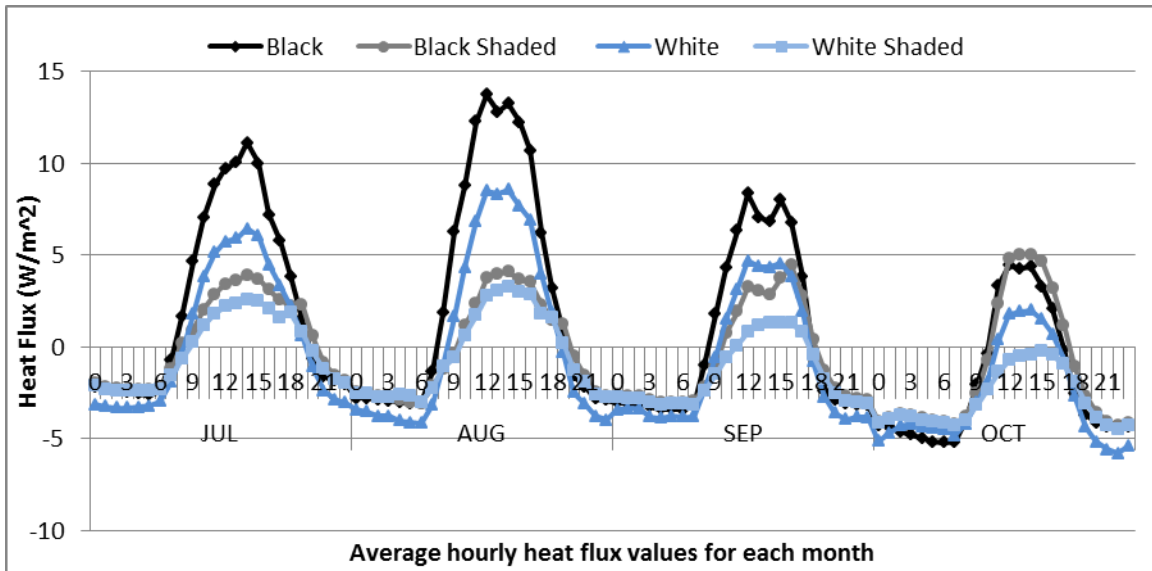


Figure 5-15: Average hourly heat flux profiles for each month for black and white shaded and unshaded roofs (July 5, 2012-October 13, 2012)

Identical to the analysis in Section 5.4.6, the average heat flux profiles (Figure 5-15) for the white and black shaded and unshaded conditions were disaggregated and summed by heat gain and loss. Table 5-6 and Table 5-7 show the summary of the positive and negative heat flux values across months and summer season. Similar to Table 5-4, the black roof had the largest heat gain and net heat flux compared to the other three roof types. However, white roofs had a larger heat loss. These same trends held for the white and black shaded roofs but the heat gain and loss values were lower than the unshaded condition. The shade induced by the PV panels decreased the heat gain compared to the black roof further by 31-38% from the white unobstructed roof. Therefore, the total heat gain reduction of the white shaded roof from the black roof was 75-84%. The shade over the black roofs reduced the heat flux 57-61% compared to the black unobstructed surface (Table 5-7). Therefore, shading the black roof made a larger incremental difference (57-61% for black compared with 31-38% for white). In terms of heat loss, the reverse was true. The incremental difference of the shade decreased heat loss by 20-40% for the white roof compared to the reference black roof while shade over the black roof reduced heat loss by 4-12%. One possible explanation was the PV panel acted as a barrier

maintaining the radiation closer to the surface and thus heating up the surface. Since the white roof membrane was colder, additional heat could make a larger difference.

The shaded white and black roofs fall in between white and green roofs at reducing heat gain or loss. Comparing the percent reduction in heat gain for summer months from black roofs (Table 5-4 and Table 5-7), the green roof was the best at reducing heat gain followed by white shaded, black shaded, and white roofs in order. For percent reduction in heat loss, the ordering was slightly different as the black and white shaded roofs switched. Therefore, the order from best to worst at reducing heat loss was green, black shaded, white shaded, and finally white roofs.

Table 5-6 : Total heat gain and loss by month, season for black and white shaded and unshaded roofs (July 5, 2012 –October 13, 2012)

	Month	Black Roof			White Roof			Black Shaded			White Shaded		
		Heat Gain (W/m ²)	Heat Loss (W/m ²)	Net Heat Flux (W/m ²)	Heat Gain (W/m ²)	Heat Loss (W/m ²)	Net Heat Flux (W/m ²)	Heat Gain (W/m ²)	Heat Loss (W/m ²)	Net Heat Flux (W/m ²)	Heat Gain (W/m ²)	Heat Loss (W/m ²)	Net Heat Flux (W/m ²)
Summer '12	July	7417	-2315	5102	4187	-3230	957	2929	-2033	897	1853	-2311	-458
	Aug	1760	-610	1150	1021	-852	169	489	-587	-98	379	-607	-228
	Sep	1183	-1143	39	634	-1346	-713	507	-1002	-495	192	-1123	-931
	Total	10359	-4068	6291	5842	-5429	413	3925	-3621	304	2424	-4041	-1617
	Oct	400	-1344	-944	183	-1406	-1223	445	-1129	-684	67	-1259	-1192

Table 5-7: Percent difference of heat gain and loss by month and season from Table 5-6 for white, black shaded and white shaded roofs compared to black and white roofs (July 5, 2012 –October 13, 2012)

	Month	% Difference (White-Black)		% Difference (Black shaded-Black)		% Difference (White shaded-Black)		% Difference (White shaded-White)		# of 15 min data points
		Heat Gain (W/m ²)	Heat Loss (W/m ²)	Heat Gain (W/m ²)	Heat Loss (W/m ²)	Heat Gain (W/m ²)	Heat Loss (W/m ²)	Heat Gain (W/m ²)	Heat Loss (W/m ²)	
Summer '12	July	-44%	40%	-61%	-12%	-75%	-0.2%	-56%	-28%	2173
	Aug	-42%	40%	-72%	-4%	-78%	-0.5%	-63%	-29%	425
	Sep	-46%	18%	-57%	-12%	-84%	-2%	-70%	-17%	568
	Total	-44%	33%	-62%	-11%	-77%	-1%	-59%	-26%	3166
	Oct	-54%	5%	11%	-16%	-83%	-6%	-63%	-10%	396

The time delay of heat flux (Table 5-8) was not conclusive between shaded and unshaded black and white roofs during July to October 2012. Because the shaded roofs lower the surface temperature compared to the black roof, the peak heat flux was expected to be shift slightly later in the day. Due to the monthly aggregation level and the short time duration, trends were not easily seen. One reason for the inconsistency could be due a small number of measurements corresponding to hourly heat flux values (Refer to Section 5.2.1). Further investigation could be conducted aggregating the data on daily or weekly basis to determine if shaded roofs do produce a time lag.

Table 5-8: Time delay of maximum heat flux from the monthly hourly profiles in Figure 5-15 (July 5, 2012- October 13, 2012)

Month	Time of peak heat flux				Time delay (hrs) for peak heat flux from a black roof		
	Black	Black Shaded	White	White Shaded	Black Shaded	White	White Shaded
Jul	14:00	14:00	14:00	14:00	0	0	0
Aug	12:00	14:00	14:00	14:00	2	2	2
Sep	12:00	15:00	12:00	15:00	3	0	3
Oct	12:00	13:00	14:00	15:00	1	2	3

5.5 Heat flux separated by ambient temperature and solar irradiance

Two important weather parameters that help determine the membrane surface temperature and, thus heat flux, are solar irradiance and ambient temperature. Table 5-9 to Table 5-11 show 34,391 fifteen minute heat flux measurements from May 24, 2011-May 24, 2012 averaged based on ambient temperature and solar irradiance cells for black (Table 5-9), white (Table 5-10) and green roofs (Table 5-11). The solar irradiance values ranged from -24 W/m^2 to 1153 W/m^2 where values less than 4 W/m^2 were grouped together as night values. The ambient temperature values ranged from -14°C to 39°C separated into 5°C intervals. The rationale for the solar irradiance and ambient temperature intervals were discussed in Section 4.3. The largest heat loss values (shaded white) are seen in the upper left and largest heat gain values (shaded red) are in the lower right in Table 5-9 through Table 5-11. Examining the overall trend of the shaded cells across Table 5-9 to Table 5-11, the black roof has more cells where heat is directed into the

building (shaded red). In contrast, the green roof has more cells where heat is lost from the building. Cells shaded in yellow contain only 1 or 2 measurements.

Table 5-9: Measured BLACK roof instantaneous heat flux values (W/m²) in Pittsburgh separated by solar irradiance and ambient temperature bins (May 24, 2011-May 24, 2012). Red shaded cells identify positive heat flux or heat gain into the building. Cells shaded in yellow are averaged from one or two data points.

		Ambient Temperature (°C)										
		<-10	-10--5	-5-0	0-5	5-10	10-15	15-20	20-25	25-30	30-35	>35
Solar Irradiance (W/m ²)	<4 (Night)	-7.9	-9.7	-7.9	-6.1	-4.4	-3.7	-3.0	-2.2	-1.4	-0.5	
	4-100	-8.9	-7.7	-6.3	-4.3	-3.1	-2.1	-1.3	-0.6	0.6	2.0	3.8
	100-200	-9.0	-6.5	-5.0	-3.1	-1.9	-0.5	0.5	1.4	2.9	4.0	5.0
	200-300		-6.0	-4.4	-1.7	-0.2	0.9	2.1	3.3	4.8	6.1	6.5
	300-400		-5.5	-3.3	-0.7	1.2	2.5	3.6	4.6	6.2	7.7	7.6
	400-500		-7.3	-2.3	0.0	2.6	4.0	5.4	6.1	7.9	9.2	10.7
	500-600			-1.7	1.8	4.8	5.7	7.0	7.6	9.1	10.3	11.1
	600-700			3.1	4.3	6.0	7.8	8.7	9.6	10.6	11.3	12.2
	700-800				6.0	7.8	9.1	10.2	11.0	12.0	13.3	13.0
	800-900					9.1	10.5	11.8	12.6	13.5	14.6	14.5
	900-1000					11.1	12.1	13.1	14.0	14.5	15.7	14.8
	1000-1100						13.3	15.2	14.0	14.2	16.2	
	>1100									14.3		

Table 5-10: Measured WHITE roof instantaneous heat flux values (W/m²) in Pittsburgh separated by solar irradiance and ambient temperature bins (May 24, 2011-May 24, 2012). Red shaded cells identify positive heat flux or heat gain into the building. Cells shaded in yellow are averaged from one or two data points.

		Ambient Temperature (°C)										
		<-10	-10--5	-5-0	0-5	5-10	10-15	15-20	20-25	25-30	30-35	>35
Solar Irradiance (W/m ²)	<4 (Night)	-8.5	-10.3	-8.5	-6.5	-4.8	-4.1	-3.2	-2.4	-1.6	-0.9	
	4-100	-9.6	-7.9	-6.6	-4.8	-3.5	-2.5	-1.8	-1.3	-0.5	0.4	1.7
	100-200	-9.7	-6.7	-5.7	-4.2	-2.9	-1.7	-0.7	0.0	0.9	1.5	2.5
	200-300		-6.2	-5.3	-3.5	-2.2	-1.1	0.0	0.9	1.9	2.6	3.5
	300-400		-5.6	-5.0	-3.1	-1.5	0.0	0.8	1.6	2.6	3.4	4.0
	400-500		-7.4	-4.6	-2.7	-0.6	0.8	1.8	2.2	3.5	4.3	5.6
	500-600			-4.0	-2.4	0.4	1.9	2.8	3.1	4.2	5.0	5.9
	600-700			2.5	-0.3	1.1	2.8	3.7	4.4	5.1	5.6	6.6
	700-800				1.0	1.8	3.6	4.5	5.1	5.8	6.5	7.1
	800-900					2.1	4.6	5.4	5.8	6.5	7.0	7.7
	900-1000					2.9	4.4	6.2	6.3	7.2	7.5	8.0
	1000-1100						4.8	6.3	5.6	7.3	7.8	
	>1100									6.2		

Table 5-11: Measured GREEN-MOSS roof instantaneous heat flux values (W/m²) in Pittsburgh separated by solar irradiance and ambient temperature bins (May 24, 2011-May 24, 2012). Red shaded cells identify positive heat flux or heat gain into the building. Cells shaded in yellow are averaged from one or two data points.

		Ambient Temperature (°C)										
		<-10	-10--5	-5-0	0-5	5-10	10-15	15-20	20-25	25-30	30-35	>35
Solar Irradiance (W/m ²)	<4 (Night)	-5.0	-5.5	-4.8	-4.2	-3.1	-2.1	-1.5	-1.0	-0.6	0.0	
	4-100	-4.6	-4.7	-4.5	-4.0	-3.1	-2.1	-1.3	-0.5	0.1	0.3	1.1
	100-200	-4.2	-4.7	-4.5	-4.1	-3.2	-2.4	-1.5	-0.3	0.6	0.5	1.2
	200-300		-4.7	-4.5	-4.3	-3.5	-2.7	-1.2	-0.2	0.9	0.9	1.3
	300-400		-5.2	-4.5	-4.5	-3.8	-2.7	-1.2	-0.2	1.1	1.2	1.4
	400-500		-5.7	-4.6	-4.6	-4.2	-3.2	-1.2	-0.2	1.3	1.5	2.0
	500-600			-4.9	-4.8	-3.7	-3.0	-0.9	0.0	1.5	1.6	2.1
	600-700			4.7	-4.6	-3.1	-2.1	0.0	0.6	1.4	1.7	2.1
	700-800				-4.4	-2.0	-0.5	0.4	1.0	1.8	1.9	2.1
	800-900					-0.5	0.9	1.9	1.5	1.8	2.1	2.1
	900-1000					2.0	1.6	1.0	1.3	2.2	2.8	2.0
	1000-1100						1.0	0.2	1.7	1.3	2.9	
	>1100									1.9		

Separating the 34,931 annual measurements by positive (heat gain) or negative (heat loss) heat flux, the black roof had the largest number of heat gain measurements while the green roof won for heat loss. The black roof had 7% more positive heat flux measurements than the white roof and 12% more than the green roof. Therefore, the black roof had more measurements where heat entered the building throughout the year than the white or green roof. Table 5-12 outlines the number of fifteen measurements corresponding to a positive (heat gain) or negative (heat loss) heat flux for each roof type.

Table 5-12: Number of fifteen minute measurements itemized by direction of heat flow and roof type during May 24, 2011- May 24, 2011

	Black Roof		White Roof		Green Roof	
	No. of datapoints	Hours	No. of datapoints	Hours	No. of datapoints	Hours
Heat Gain	10,289	2,572	8,065	2,016	5,949	1,487
Heat Gain (%)	29%		23%		17%	
Heat Loss	24,642	6,161	26,866	6,717	28,982	7,246
Heat Loss (%)	71%		77%		83%	

Since the warehouse under Sunscape has two operating conditions (i.e. uncontrolled and heated), the annual average heat flux measurements in Table 5-9 to Table 5-11 above were separated by warehouse condition. From April to October every year, the warehouse has no additional mechanical heating or cooling so the inside temperatures are allowed to fluctuate uncontrolled. From November to March, the inside warehouse temperature is heated in order to maintain a minimum of 15° C (60°F). The exact date when heat is turned on and off is not recorded. Therefore, the uncontrolled and heating warehouse conditions were grouped by months. Table 5-13 to Table 5-15 shows the average heat flux for each black, white and green-moss roof when the warehouse internal temperature was uncontrolled.

Table 5-16 to Table 5-18 depicts the heat flux results for each black, white and green-moss roof when the warehouse interior was heated.

Examining the two sets of tables corresponding to uncontrolled (Table 5-13 to

Table 5-15) and heated (

Table 5-16 to Table 5-18) conditions, the instantaneous heat gain (shaded red) cells decreases in number from black to white and green. In other words, the black roof table has the most cells that are positive (i.e. heat gain and shaded red). Also, the black roof heat gain cell values are the largest compared with the white and green roofs. In terms of heat loss, the green roof has the most cells that are negative (shaded white) followed by the white roof and then the black roof. However, the white roof tables have the largest heat loss values compared to black or green.

Table 5-13: Measured BLACK roof instantaneous heat flux values (W/m^2) for assumed UNCONTROLLED condition in Pittsburgh separated by solar irradiance and ambient temperature bins (May 24, 2011-October 31, 2011 and April 1, 2012-May 24, 2012). Red shaded cells identify positive heat flux or heat gain into the building. Cells shaded in yellow are

averaged from one or two data points.

		Ambient Temperature (°C)										
		<-10	-10- -5	-5	0-5	5-10	10-15	15-20	20-25	25-30	30-35	>35
Solar Irradiance (W/m ²)	<4 (Night)			-7.0	-6.1	-4.8	-4.2	-3.2	-2.3	-1.5	-0.5	
	4-100			-6.7	-5.0	-3.6	-2.6	-1.6	-0.7	0.6	2.0	3.8
	100-200			-4.7	-2.8	-2.2	-0.8	0.2	1.3	2.9	4.0	5.0
	200-300				-0.7	-0.2	0.5	1.8	3.2	4.8	6.1	6.5
	300-400				0.6	1.1	2.2	3.3	4.5	6.2	7.7	7.6
	400-500					3.0	4.1	5.2	6.0	7.9	9.2	10.7
	500-600					5.1	6.1	6.8	7.4	9.1	10.3	11.1
	600-700					6.9	7.7	8.6	9.4	10.5	11.3	12.2
	700-800					8.2	9.2	10.0	10.8	11.9	13.3	13.0
	800-900					10.8	10.7	11.8	12.5	13.5	14.6	14.5
	900-1000					11.1	12.1	13.1	14.0	14.5	15.7	14.8
	1000-1100						13.3	15.2	14.0	14.2	16.2	
	>1100									14.3		

Table 5-14: Measured WHITE roof instantaneous heat flux values (W/m²) for assumed UNCONTROLLED condition in Pittsburgh separated by solar irradiance and ambient temperature bins (May 24, 2011-October 31, 2011 and April 1, 2012-May 24, 2012). Red shaded cells identify positive heat flux or heat gain into the building. Cells shaded in yellow are averaged from one or two data points.

		Ambient Temperature (°C)										
		<-10	-10- -5	-5	0-5	5-10	10-15	15-20	20-25	25-30	30-35	>35
Solar Irradiance (W/m ²)	<4 (Night)			-7.9	-7.0	-5.4	-4.6	-3.4	-2.4	-1.6	-0.9	
	4-100			-8.7	-5.7	-3.8	-3.0	-2.1	-1.3	-0.5	0.4	1.7
	100-200			-7.8	-4.5	-3.0	-2.0	-1.0	-0.05	0.9	1.5	2.5
	200-300				-3.2	-2.3	-1.4	-0.3	0.8	1.9	2.6	3.5
	300-400				-3.1	-2.1	-0.3	0.5	1.4	2.6	3.4	4.0
	400-500					-0.8	0.6	1.6	2.0	3.5	4.3	5.6
	500-600					-0.008	1.8	2.6	2.9	4.1	5.0	5.9
	600-700					1.1	2.8	3.8	4.3	5.0	5.6	6.6
	700-800					2.2	3.6	4.5	5.0	5.6	6.5	7.1
	800-900					0.8	4.6	5.4	5.8	6.5	7.0	7.7
	900-1000					2.9	4.4	6.2	6.3	7.2	7.5	8.0
	1000-1100						4.8	6.3	5.6	7.3	7.8	
	>1100									6.2		

Table 5-15: Measured MOSS-GREEN roof instantaneous heat flux values (W/m²) for assumed UNCONTROLLED condition in Pittsburgh separated by solar irradiance and ambient temperature bins (May 24, 2011-October 31, 2011 and April 1, 2012-May 24, 2012). Red shaded cells identify positive heat flux or heat gain into the building. Cells shaded in

yellow are averaged from one or two data points.

		Ambient Temperature (°C)										
		<-10	-10- -5	-5	0-5	5-10	10-15	15-20	20-25	25-30	30-35	>35
Solar Irradiance (W/m ²)	<4 (Night)			-4.6	-4.0	-3.0	-2.2	-1.6	-1.0	-0.6	0.0	
	4-100			-4.4	-4.1	-2.8	-2.1	-1.4	-0.6	0.1	0.3	1.1
	100-200			-4.5	-3.9	-2.8	-2.3	-1.4	-0.4	0.5	0.5	1.2
	200-300				-3.4	-3.1	-2.3	-1.2	-0.4	0.9	0.9	1.3
	300-400				-3.6	-3.3	-1.9	-1.1	-0.3	1.0	1.2	1.4
	400-500					-3.0	-2.2	-0.7	-0.3	1.2	1.4	2.0
	500-600					-2.5	-2.2	-0.3	-0.1	1.3	1.6	2.1
	600-700					-1.6	-1.4	0.3	0.3	1.3	1.7	2.1
	700-800					-1.8	-0.7	0.8	0.6	1.6	1.8	2.1
	800-900					-0.5	0.7	1.9	1.4	1.8	2.1	2.1
	900-1000					-2.0	1.6	1.0	1.3	2.2	2.8	2.0
	1000-1100						1.0	0.2	1.7	1.3	2.9	
	>1100									1.9		

Table 5-16: Measured **BLACK** roof instantaneous heat flux values (W/m²) for assumed **HEATING** condition in Pittsburgh separated by solar irradiance and ambient temperature bins (November 1, 2011- March 31, 2012). Red shaded cells identify positive heat flux or heat gain into the building. Cells shaded in yellow are averaged from one or two data points.

		Ambient Temperature (°C)										
		<-10	-10- -5	-5	0-5	5-10	10-15	15-20	20-25	25-30	30-35	>35
Solar Irradiance (W/m ²)	<4 (Night)	-7.9	-9.7	-8.0	-6.0	-4.1	-2.6	-1.6	-0.5	0.4		
	4-100	-8.9	-7.7	-6.3	-4.2	-2.9	-1.6	-0.4	0.4	1.2		
	100-200	-9.0	-6.5	-5.0	-3.1	-1.6	-0.04	1.3	2.4	2.7		
	200-300		-6.0	-4.4	-1.9	-0.2	1.2	2.9	3.7	4.8		
	300-400		-5.5	-3.3	-0.7	1.2	2.8	4.3	5.5	6.2		
	400-500		-7.3	-2.3	0.02	2.5	3.9	5.8	7.1	7.5	8.6	
	500-600			-1.7	1.8	4.7	5.5	7.5	8.8	9.3	10.1	
	600-700			3.1	4.3	5.6	7.8	9.4	10.7	11.4	11.8	
	700-800				6.0	7.5	8.7	10.9	12.1	12.7	13.3	
	800-900					9.0	9.7	12.4	13.3			
	900-1000											
	1000-1100											
	>1100											

Table 5-17: Measured **WHITE** roof instantaneous heat flux values (W/m²) for assumed **HEATING** condition in Pittsburgh separated by solar irradiance and ambient temperature bins (November 1, 2011- March 31, 2012). Red shaded

cells identify positive heat flux or heat gain into the building. Cells shaded in yellow are averaged from one or two data points.

		Ambient Temperature (°C)										
		<-10	-10- -5	-5	0-5	5-10	10-15	15-20	20-25	25-30	30-35	>35
Solar Irradiance (W/m ²)	<4 (Night)	-8.5	-10.3	-8.5	-6.4	-4.3	-3.1	-2.1	-1.4	-1.2		
	4-100	-9.6	-7.9	-6.6	-4.6	-3.2	-2.0	-0.8	-0.6	-0.3		
	100-200	-9.7	-6.7	-5.6	-4.2	-2.8	-1.2	0.2	1.0	1.0		
	200-300		-6.2	-5.3	-3.6	-2.1	-0.7	0.7	2.1	2.5		
	300-400		-5.6	-5.0	-3.1	-1.4	0.1	1.6	2.9	3.3		
	400-500		-7.4	-4.6	-2.7	-0.6	0.9	2.1	3.3	4.4	4.2	
	500-600			-4.0	-2.4	0.5	2.0	3.3	4.0	4.9	5.0	
	600-700			-2.5	-0.3	1.1	2.6	3.6	5.0	6.0	6.2	
	700-800				1.0	1.4	3.4	4.5	5.9	6.8	6.8	
	800-900					2.16	4.69	4.92	5.70			
	900-1000											
	1000-1100											
	>1100											

Table 5-18: Measured MOSS-GREEN roof instantaneous heat flux values (W/m²) for assumed HEATING condition in Pittsburgh separated by solar irradiance and ambient temperature bins (November 1, 2011- March 31, 2012). Red shaded cells identify positive heat flux or heat gain into the building. Cells shaded in yellow are averaged from one or two data points.

		Ambient Temperature (°C)										
		<-10	-10- -5	-5	0-5	5-10	10-15	15-20	20-25	25-30	30-35	>35
Solar Irradiance (W/m ²)	<4 (Night)	-5.0	-5.5	-4.8	-4.3	-3.2	-1.9	-1.3	-0.5	0.8		
	4-100	-4.6	-4.7	-4.5	-4.0	-3.2	-2.0	-1.2	0.1	0.9		
	100-200	-4.2	-4.7	-4.5	-4.2	-3.5	-2.5	-1.6	0.8	1.9		
	200-300		-4.7	-4.5	-4.4	-3.8	-3.2	-1.3	1.1	2.5		
	300-400		-5.2	-4.5	-4.5	-3.9	-3.4	-1.4	1.1	3.0		
	400-500		-5.7	-4.6	-4.6	-4.4	-3.9	-2.3	0.9	3.2	3.2	
	500-600			-4.9	-4.8	-4.0	-3.5	-2.4	0.7	3.6	3.5	
	600-700			-4.7	-4.6	-3.8	-3.4	-0.9	2.2	3.3	3.7	
	700-800				-4.4	-2.2	0.2	-0.8	2.8	3.4	4.1	
	800-900					-0.5	1.9	2.7	2.4			
	900-1000											
	1000-1100											
	>1100											

The instantaneous heat flux average values across an entire year (Table 5-9 to Table 5-11) were converted into annual heat gained or lost through the three roof types. From May 24, 2011 to May 24, 2012, the number of fifteen minute measurements for each cell was divided by four to convert into hours (Table 5-19). The number of hours across the year and the average heat flux measurements for each cell were multiplied together to get annual watt-hours per square meter of roof. The annual heat loss results for the black (Table 5-20), white (Table 5-21) and green (Table

5-22) roof are shown by darker shades of blue while heat gain by darker shades of red. The largest quantity of heat lost across the year is seen at night while heat gain during ambient temperatures between 25-35°C and solar irradiance values of 500-900 W/m² (Table 5-20).

Comparing Table 5-20 through Table 5-22, the white roof has the largest quantity of heat loss (darkest blue cells) followed by black and then green roofs. However, the green roof has the largest quantity of blue (heat loss) cells. The important distinction is that the green roof has the highest number of measurements that have a heat loss (Table 5-11), but the magnitude of the heat loss is smaller than the black or white roofs. In contrast to heat loss, black roofs have both the largest number measurements (red cells) and magnitude of heat (darker red cells) followed by white and then green roofs. While reviewing Table 5-20 through Table 5-22, the results include both uncontrolled (April-Oct) and heating (November-Feb) conditions in the warehouse. For the rest of the analysis in this chapter, the uncontrolled and heating warehouse conditions discussed above are combined. In other words, there is no further delineation based on warehouse condition.

Table 5-19: Number of hours from May 24, 2011 to May 24, 2012 corresponding to ambient temperature and solar irradiance ranges measured on Sunscape. The darker gray cells have higher hours.

		Ambient Temperature (°C)												
		<-15	-15--10	-10--5	-5-0	0-5	5-10	10-15	15-20	20-25	25-30	30-35	35-40	>40
Solar Irradiance (W/m ²)	(hours)													
	<4 (Night)													
	4-100													
	100-200													
	200-300													
	300-400													
	400-500													
	500-600													
	600-700													
	700-800													
	800-900													
	900-1000													
1000-1100														
>1100														

Hours

500+

201-500101-20051-10011-501-100

Table 5-20: Annual heat transfer (Wh/m²) for the BLACK roof
separated by solar irradiance and ambient temperature (May 24, 2011- May 24, 2012). Cells shaded blue indicate negative heat transfer (heat loss) while cells shaded red indicate positive heat transfer (heat gain). The darker the color more heat was transferred.

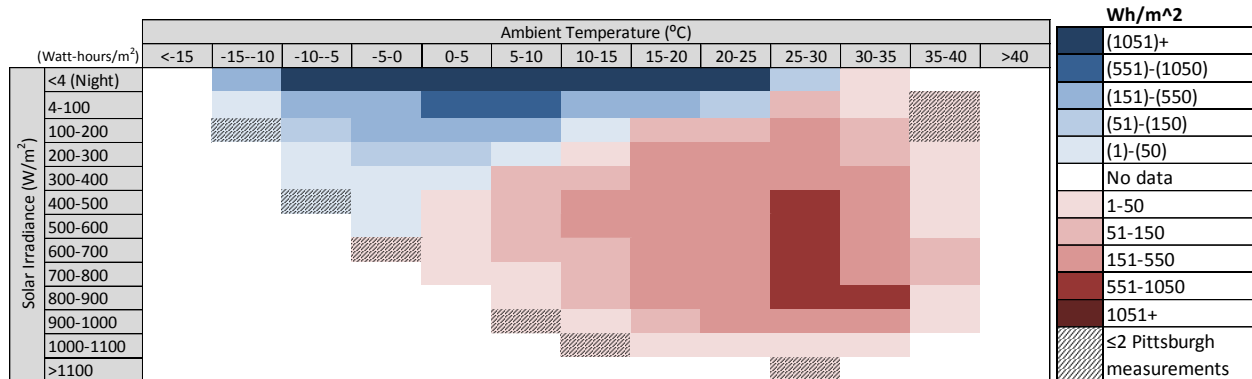


Table 5-21: Annual heat transfer (Wh/m²) for the WHITE roof
separated by solar irradiance and ambient temperature bins (May 24, 2011- May 24, 2012). Cells shaded blue indicate negative heat transfer (heat loss) while cells shaded red indicate positive heat transfer (heat gain). The darker the color more heat was transferred.

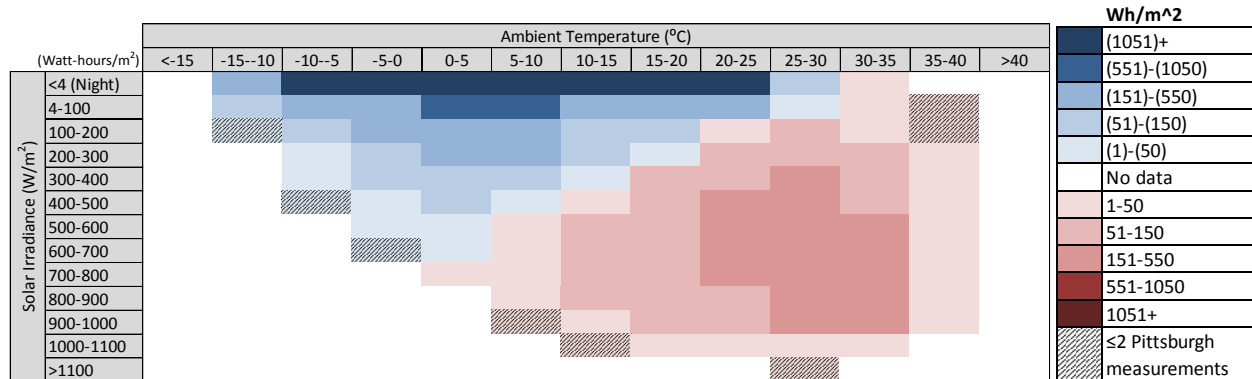
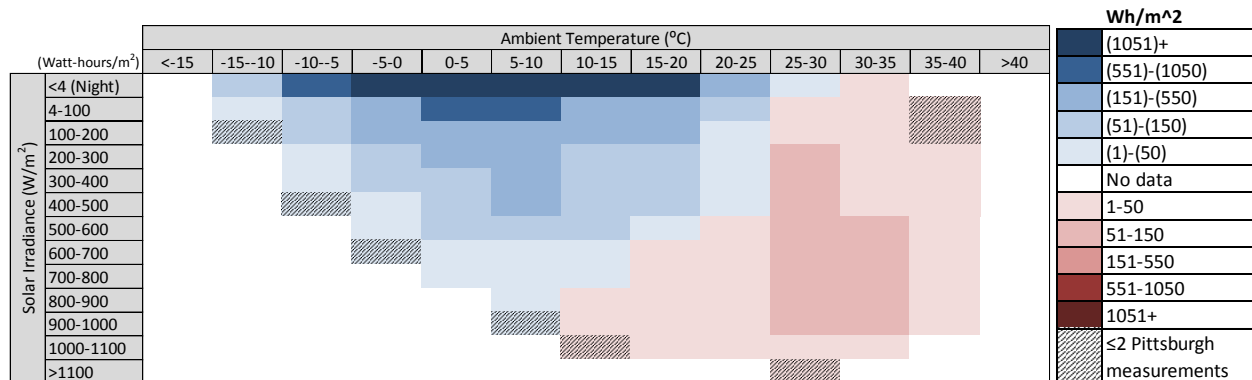


Table 5-22: Annual heat transfer (Wh/m²) for the MOSS-GREEN roof
separated by solar irradiance and ambient temperature (May 24, 2011- May 24, 2012). Cells shaded blue indicate negative heat transfer (heat loss) while cells shaded red indicate positive heat transfer (heat gain). The darker the color more heat was transferred.



To further quantify the differences of heat flux across roof types, the total heat loss or gained was summed based on indoor thermal comfort set points. The American Society of Heating, Refrigerating and Air Conditioning Engineers (ASHRAE) developed a thermal comfort standard (ASHRAE 55) which outlines acceptable thermal conditions for building occupants. Factors affecting a person's thermal comfort include metabolic rate, clothing insulation, air temperature, radiant temperature, air speed and humidity (American Society of Heating Refrigerating and Air-Conditioning Engineers Inc. 2010). Considering Sunscape is a warehouse, occupants typically wear pants with short or long sleeves shirts. The corresponding clothing insulation value is 0.89 (American Society of Heating Refrigerating and Air-Conditioning Engineers Inc., 2010). Furthermore, warehouse workers are typically walking or lifting objects resulting in a metabolic rate of 1.7-4.0. Because of the occupant's clothing and activity, reasonable thermal comfort ranges according to ASHRAE 55 can be 15-25°C (60-77°F). The lower boundary of 15°C (60°F) matches the Scalo Solar winter operating condition. Assuming natural ventilation through windows and doors is the preferred mechanism to condition the warehouse, outside temperatures exceeding the thermal comfort range would need mechanical heating or cooling to maintain thermal comfort for employees. Based on these set points, mechanical heating is needed if the interior ambient temperature falls below 15°C and cooling for temperatures above 25°C. In between 15°C-25°C, occupants would be comfortable with outside air so no mechanical heating, ventilation or air conditioning (HVAC) is needed. To reiterate for clarity, the heating scenario and cooling scenario can exist in both the uncontrolled (April-October) and heated (November-March) warehouse operating condition.

The total annual quantity of heat transferred through a roof which would need to be offset by mechanical heating or cooling was calculated by summing the heat gained or lost above an outside air temperature of 25°C or below 15°C. For simplicity, outside air temperature was used as a proxy for internal temperatures in this analysis. An extension of this research will revise this analysis to use interior temperatures measured under the black, white and green roofs. Figure 5-16 illustrates an example of the positive and negative heat transfer for each heating and cooling scenario measured on the black roof. Within either heating or cooling scenario, all roof types had both heat gain and heat loss. Under the heating scenario, a positive heat flux represented natural

heating from the outside while a negative heat flux was heat lost to the external environment. In the cooling scenario, a negative heat flux was natural cooling while a positive heat flux brought additional heat into the building. Therefore, the overall quantity of mechanical heat needed was the addition of heat gained and heat lost. To be clear, this summation does not infer the total quantity of heat or air conditioning required to bring a space within the thermal comfort range. An energy building model is required for such a calculation. This summation is used to compare the net heat transferred into and out of the building between roof types.

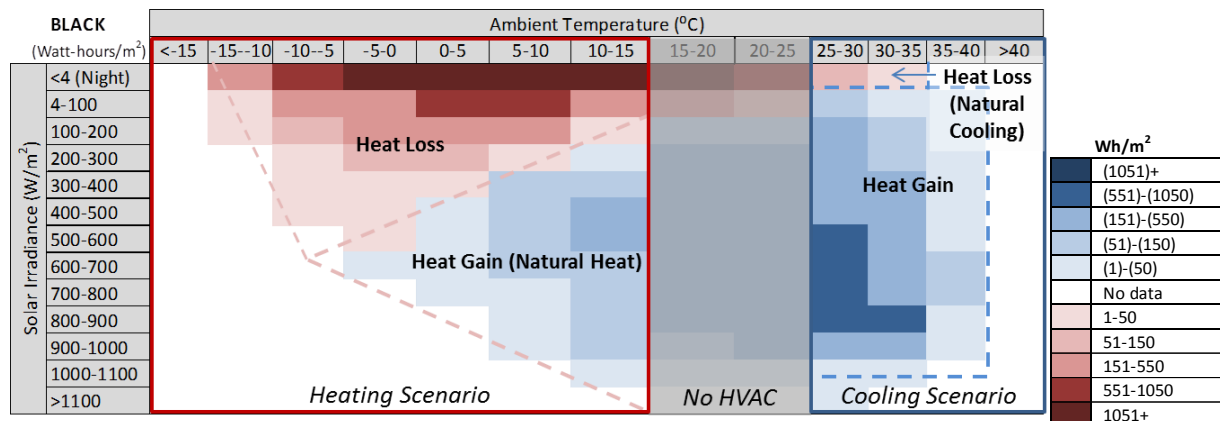


Figure 5-16: Heating and cooling scenario example for the black roof based on 15°C (60°F) and 25°C (77°F) thermal comfort set points (May 24, 2011-May 24, 2012)

The quantity of heat transferred under a heating or cooling scenario was compared across black, white and green roofs Table 5-23 depicts the net quantity of heat gained into the interior space of a building or lost to the external environment under the heating or cooling scenario for each roof type. Not surprisingly, the black roof had the largest quantity of heat gained in either the heating or cooling scenario. For external temperatures under 15°C (60°F), black roofs allowed 77% more heat to penetrate into a building (heat gain) compared with a white roof and 97% more than a green roof. For outside temperatures above 25°C, the black roof permitted 53% and 94% more heat gained into the space than a white or green roof respectively. In terms of heat loss, the white roof allowed more heat to escape from the building under the heating (12% more than black and 39% than green) and cooling scenario (43% more than black and 39% than green) compared to the other roof types.

Table 5-23: Heat gained or lost under heating (outside air temp <15°C) or cooling (outside air temp >25°C) scenarios for black, white and green roofs in Pittsburgh

Scenario	Black Roof		White Roof		Green Roof	
	Heating	Cooling	Heating	Cooling	Heating	Cooling
Gain (Wh/m ²)	1,691	9,407	383	4,374	56	1,515
Loss (Wh/m ²)	-21,119	-136	-23,659	-194	-16,853	-119
Net (Wh/m ²)	-19,428	9,271	-23,276	4,180	-16,797	1,396

These results indicate the quantity of heat transferred into or out of the building independent of Sunscape's winter (interior temperature at a minimum 15 °C) and summer (temperature fluctuates freely) operating conditions. If Sunscape added air conditioning or more heating, then the internal temperature would change so that a greater temperature difference would exist with ambient temperatures. As a result, the roof heat fluxes would similarly increase. Furthermore, including the winter condition heat fluxes averaged with the heat fluxes during summer warehouse operating condition skews the results because in the winter there is mechanical heating. The Figures and Tables in this section only represent the actual experience at Sunscape and the corresponding assumptions assumed in the analysis.

5.6 Heat flux results for other case study cities

The heat flux values for San Diego, Huntsville and Phoenix were estimated from the Sunscape dataset using method two from Section 4.3. The Sunscape heat flux average values for each black, white and green roof (Table 5-9 to Table 5-11) were multiplied by a matrix composed of TMY hourly values corresponding to the same solar irradiance row and ambient temperature column intervals for each case study city. Both the distribution of hours and heat transferred for the three case study cities can be found in the Appendix D.

When no heat flux (W/m²) value existed for Sunscape (e.g. >40°C, also seen by white cells in (Table 5-9 to Table 5-11), the average of the nearest row and/or column data point was used. This extrapolation method was used mainly for hot temperatures in Phoenix and cold temperatures in Huntsville. The specific cells which were extrapolated from Pittsburgh Sunscape data are identified in Appendix D. For comparison, a linear regression approach was used to estimate heat flux for cells within the >40°C column for three solar irradiance bins. Heat flux estimates based on the linear regression were higher. Therefore, extrapolating Pittsburgh-

Sunscape heat flux values based on averaging would be an underestimate. Since this extrapolation was done on cells just outside the perimeter of the Pittsburgh-Sunscape dataset, the corresponding hours for these cells, and thus the overall impact were small.

Similar to Pittsburgh, the net quantity of heat (heat gained + heat lost) were calculated for each case study city under the heating scenario (outside air temp <15°C) or cooling (outside air temp >25°C) scenarios (Table 5-24) across the year. Figure 5-17 illustrates the annual net heat transferred into or away from the building. Pittsburgh has the largest heat loss which was not surprising given Pittsburgh's cold climate. San Diego has the smallest range of heat gained to heat lost (Figure 5-17). Because of San Diego's moderate climate, much of the heat flux values were within the thermal comfort temperature range. Huntsville's results were most similar to Pittsburgh, but shifted slightly towards more heat gain due to a slightly warmer climate. Phoenix had the largest quantity of heat transferred inside the building. For all cities, the black roof allowed approximately 55% to 85% more heat to enter the building than white or green roofs (Table 5-24). However, white roofs let 20-30% more heat flow into the external environment than black roofs. Green roofs reduced the heat transferred both into and out of the building across both the heating and cooling scenario.

Table 5-24: The percent difference between white and green roofs compared with black roofs for heat loss under in the heating scenario and heat gained in the cooling scenario

		Heating Scenario (Temp <15°C)				Cooling Scenario (Temp >25°C)			
		Pittsburgh	San Diego	Huntsville	Phoenix	Pittsburgh	San Diego	Huntsville	Phoenix
Net heat transfer (kWh/m ² /yr)	Black Roof	-19.4	-5.7	-12.7	-5.2	9.3	2.8	12.4	25.4
	White Roof	-23.3	-6.9	-16.4	-6.7	4.2	1.3	5.6	11.5
	Green Roof	-16.8	-4.5	-12.6	-5.0	1.4	0.4	1.9	3.9
% change from black	White Roof	20%	20%	29%	29%	-55%	-52%	-55%	-55%
	Green Roof	-13.5%	-22.3%	-1.4%	-4.6%	-85%	-85%	-85%	-85%

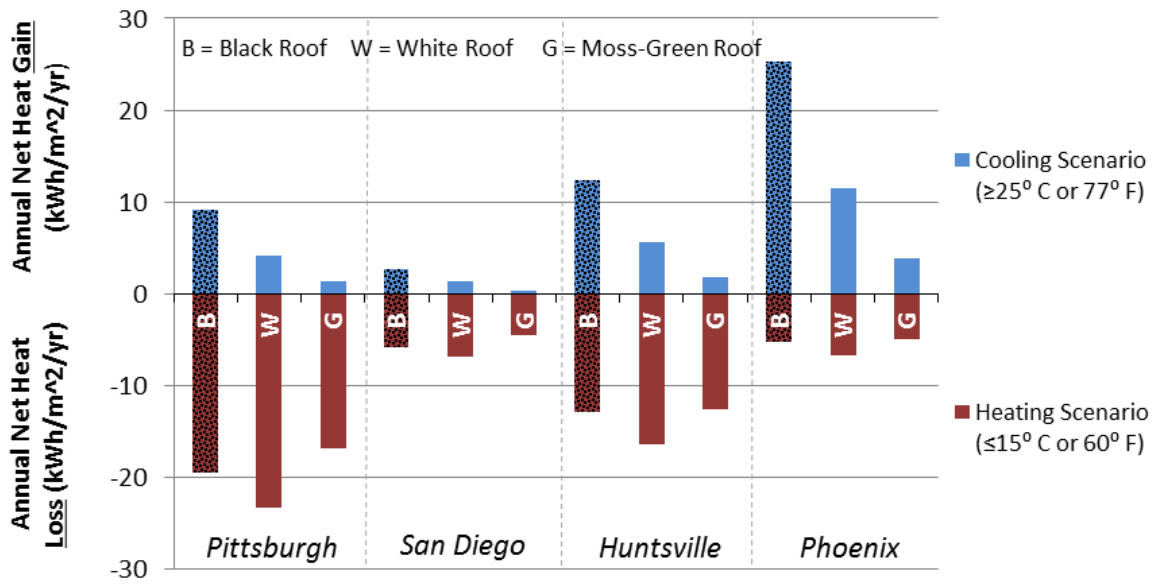


Figure 5-17: Annual net heat gained and loss through black, white and green roof under a heating or cooling scenario

One way to understand the impact of heat transfer was to calculate the energy and corresponding costs required to remove the additional heat gained or lost (Figure 5-17) through the roof for all cities. For this analysis, the HVAC unit size was 100,000BTU/hr with an Energy Efficiency Ratio (EER) of 11BTU/W. The natural gas boiler size was estimated to 100,000BTU/hr with an efficiency of 80%. Both the HVAC and natural gas boiler size were based off of discussions with Trane who manufactured the rooftop units on Sunscape (Nancy Richardson, personal communication November 2012). The corresponding HVAC energy efficiency ratio and natural gas efficiency were from the ASHRAE Standard 90.1-2007.

Under the heating and cooling scenarios, site and source energy required to offset the net heat gain and loss was calculated based on the HVAC and boiler efficiencies above. Site energy refers to energy consumed at the site. Source energy accounts for the energy required to extract, process and deliver natural gas as well as transmission and distribution losses for electricity (Deru 2007). After the heat values in Figure 5-17 were converted into site heating (natural gas) and cooling (electricity) energy, a source energy factor was applied. To convert from site to source natural gas, a 1.092 multiplier was used (Deru 2007). Similarly for electricity, 3.443 was used for the site to source energy ratio (Deru 2007).

To more clearly see the differences in the white and green roofs compared to the black roofs, the site and source natural gas heating and electric cooling were subtracted from each other. For example, the black roof site natural gas was subtracted from the green roof site natural gas. Figure 5-18 shows the difference in natural gas (heating) and electricity (cooling) for all four cities normalized to the black roof. The results illustrate the same trends as discussed in the previous sections above; the white roof required more heating from heat loss compared to black roofs. One important distinction is that cooling by electricity requires significantly more source energy than natural gas heating.

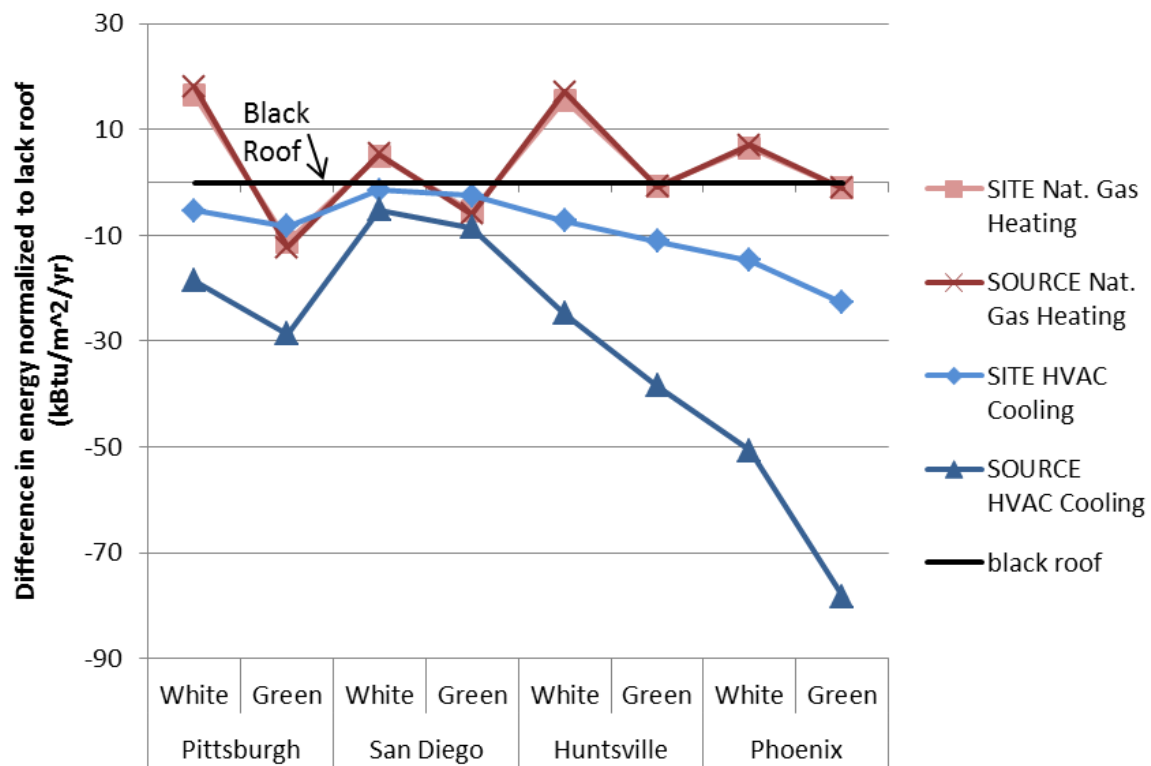


Figure 5-18: Site and source energy required to offset the net heat gain or loss for white and green roofs in Figure 5-17 normalized to the black roof for all cities. For example, the white roof in Pittsburgh requires 16 kBTU/m²/yr more in SITE natural gas than the black roof to replace the annual net heat lost.

Another useful comparison was to convert the normalized site energy in Figure 5-18 to dollars. For each city, Table 5-25 lists the 2010 commercial prices of natural gas and electricity that was used (ref, ref). Figure 5-19 illustrates the marginal heating and cooling costs of the white and green roofs compared to the black roofs. A positive cost value indicates the roof requires additional money for heating (i.e. counteracting heat loss) compared to the black roof. A negative value denotes money saved by the white or green roof compared to the reference black

roof from mitigating heat transfer and thus reducing the supplemental heating and cooling energy.

Table 5-25: 2010 Commercial electricity and natural gas price for Pittsburgh, San Diego, Phoenix and Huntsville

	Electricity Price (\$cents/kWh)	Natural Gas Price \$/MMBTU
Pittsburgh	10.1	10.50
San Diego	13.1	8.23
Phoenix	9.47	10.58
Huntsville	10.18	13.27

The net energy benefit for each roof type was determined by adding both the costs and savings together. Examining Figure 5-19, there is a small energy cost difference for white roofs in Pittsburgh, San Diego and Huntsville. In Pittsburgh, the white roofs cost $\$0.01/\text{m}^2/\text{yr}$ more than the black roof. In San Diego and Huntsville the white roof saved $\$0.01$ - $\$0.02/\text{m}^2/\text{yr}$ compared to the black roof. Based on these findings there is little difference between black and white roofs for these three cities given the 15-25 °C range in thermal comfort. However, for Phoenix a white roof saves $0.34/\text{m}^2/\text{yr}$. Generally, warmer climates had a higher savings from a white roof. For all cities, the green roof resulted in a net $0.14/\text{m}^2/\text{yr}$ savings in San Diego to $\$0.64/\text{m}^2/\text{yr}$ savings in Phoenix compared to the black roof.

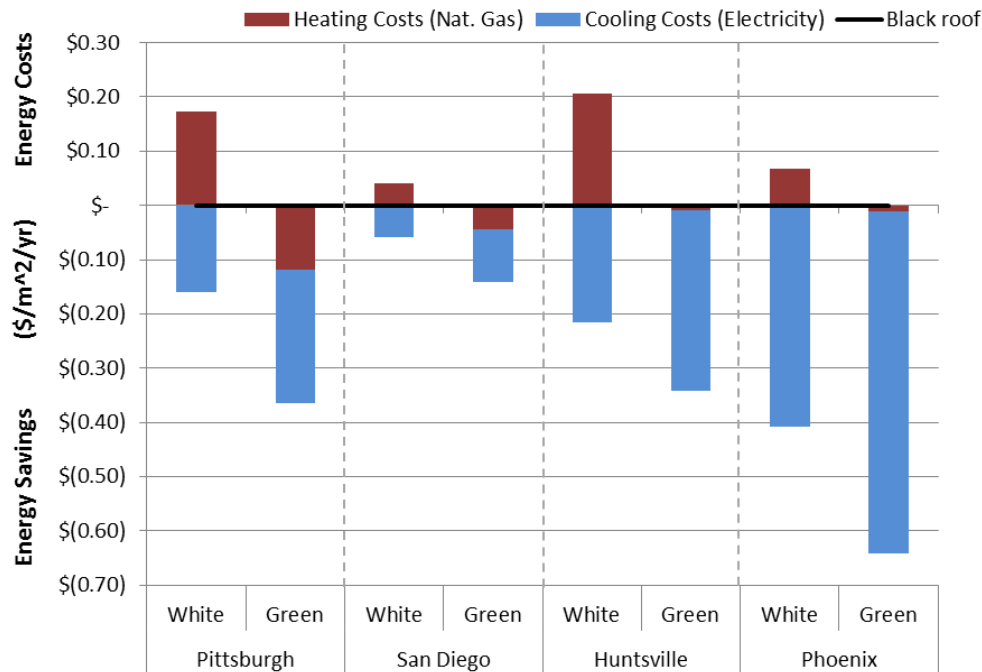


Figure 5-19: Additional net energy savings or costs for the white and green-moss roofs from the heating or cooling scenarios normalized to the black roof for all four cities.

These results show the energy savings based on the quantity of heat transferred into or out of the building across the year. The figures and tables in this section only represent the actual experience at Sunscape and the corresponding assumptions assumed in the analysis. Readers need to keep in mind that there was no delineation in this section based on the two Sunscape operating conditions of winter (minimum interior temperature kept at 15° C) and summer (uncontrolled interior temperature). Results would likely change if the two operating conditions were considered separately. Results may also change if Sunscape added air conditioning or more heating, then the internal temperature would change so that a greater temperature difference would exist with ambient temperatures. As a result, the roof heat fluxes would similarly increase.

5.7 Study Three: Black, white and green roof air temperature comparison

Air temperatures were examined during day and night time hours between July 5, 2012- October 13, 2012 for black, white and green-moss roofs. Similar to Section 5.4, differences in air

temperatures across roof types were grouped by ambient temperature and by average hourly monthly profiles.

White and green roofs lowered air temperature the most at high temperatures (Figure 5-20). For temperatures above 26°C¹⁶, air temperatures measured at 15cm (6in) above the white roof were a 1-3°C lower than the black roof (Table 5-26). The air temperature above a green roof had a slightly larger temperature reduction (1-4°C) compared to the same black roof. Akbari (2001) found that the “peak urban electric demand rises by 2-4% for each 1 °C in daily max temp above a threshold of 15 to 20 °C.” Therefore, these air temperature reductions at high temperatures could have a significant impact on electricity consumption. During moderate temperatures, white and green roofs cooled the air less than 1°C. At cold temperatures which corresponded to night measurements in October, the white roof oscillated between slightly warmer and cooler than the black roof. The green roof however had warmer ambient temperatures which were consistent with surface temperatures described in Section 5.4.1.

Average monthly air temperature hourly profiles in Figure 5-21 illustrate the largest air temperature reductions above white and green roofs compared with black roofs coincide with daytime values. Furthermore comparing across monthly hourly profiles, July and August had larger air temperature reductions for white and green roofs than recorded in September and October. This result was consistent with Figure 5-20 where higher temperatures correspond to a larger difference between white and green roofs compared to the black roof.

¹⁶ 26°C was chosen as a break point because both white and moss air temperatures were cooler than the air over the black roof by at least 1°C.

Table 5-26: Differences in average air temperature measured 15cm (6in) above white and moss roofs compared with a black roof across a range of ambient temperatures (July 5, 2012-October 13, 2012)

Ambient Air Temp (°C)	Black Air Temp (°C)	White-Black Air Temp (°C)	Moss -Black Air Temp (°C)	No. of 15 min data points
<0	-4.8	-0.3	3.3	28
0-2	-2.1	0.3	3.7	45
2-4	1.3	0.0	-0.9	134
4-6	2.4	-0.1	0.9	139
6-8	5.4	-0.1	-0.4	304
8-10	7.7	-0.3	-0.1	276
10-12	9.9	-0.4	0.1	279
12-14	12.3	-0.4	-0.6	331
14-16	14.6	-0.5	-0.5	472
16-18	16.4	-0.2	-0.1	764
18-20	18.5	-0.3	-0.1	826
20-22	20.7	-0.3	-0.2	944
22-24	22.9	-0.4	-0.3	932
24-26	25.6	-0.8	-0.7	570
26-28	28.5	-1.3	-1.0	466
28-30	31.2	-1.8	-1.5	458
30-32	34.0	-2.5	-2.4	465
32-34	35.9	-2.7	-2.5	237
34-36	37.4	-2.3	-2.6	89
36-38	39.8	-2.4	-3.1	41
>38	41.4	-2.8	-3.7	10

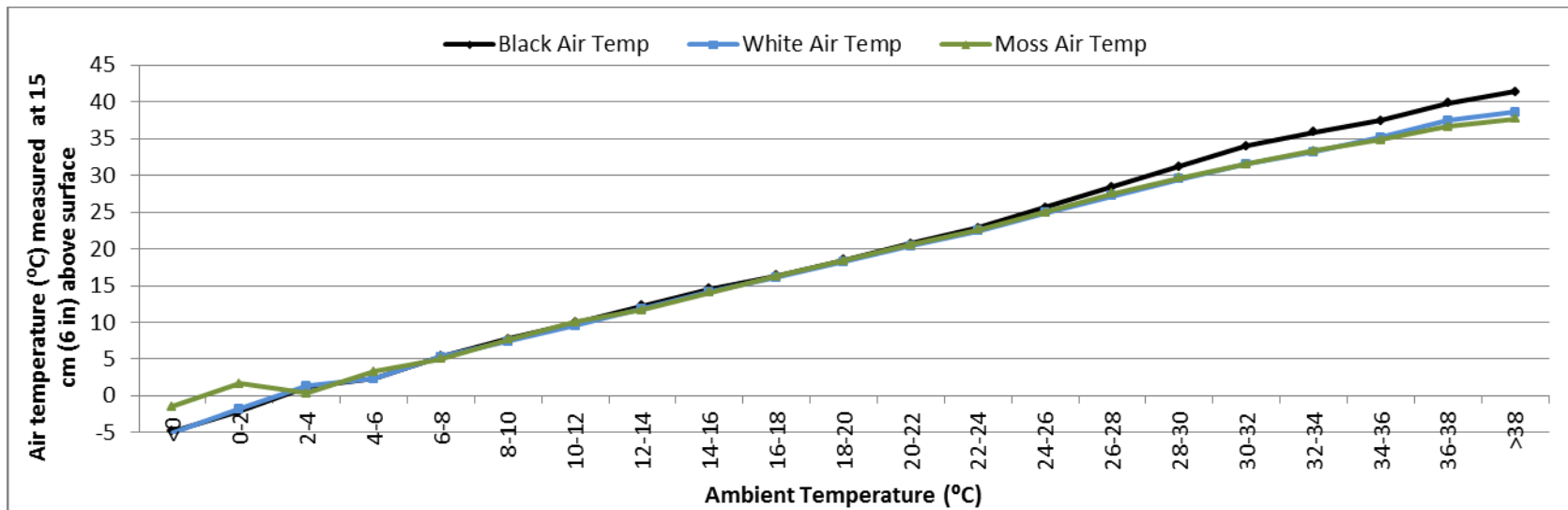


Figure 5-20: Average air temperature 15cm (6in) above surface of black, white and green roofs separated by ambient temperature (July 5, 2012-October 13, 2012)

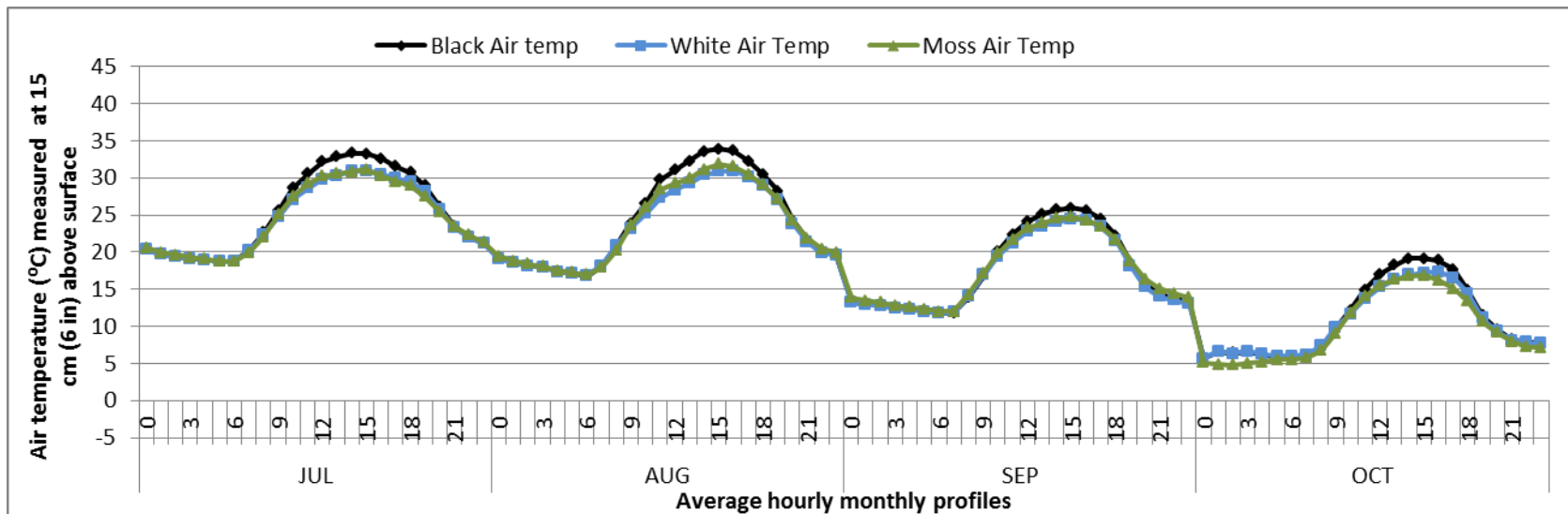


Figure 5-21: Average hourly air temperature 15cm (6in) above surface of black, white and green roofs separated by month (July 5, 2012-October 13, 2012)

5.8 Conclusions

One prominent theme interwoven in this chapter was that the white roof was colder during the night compared to the black and green roofs resulting in greater heat lost to the external environment for white roofs. In a heating dominated climate such as Pittsburgh where temperatures are colder for much of the year, heat loss is unfavorable. While the white roof does curtail the amount of heat gain in the summer, and thus reduce the need for additional air conditioning, the frequency of these occurrences is rather small. In other words, the heat loss penalty of white roofs is more heavily weighted than the reduction in heat gain for Pittsburgh in the summer. Under the research assumptions presented in this chapter, the black roof is preferred only slightly over the white roof. These results are in agreement with past research that white roofs are preferred in areas with a long cooling season and a short heating season (Levinson 2010).


Since the heat flux savings and costs were quite similar for black and white roofs, changes in weather, thermal comfort ranges or energy prices could affect the magnitude of the difference or the overall result. During May 24, 2011- May 24, 2012, the weather conditions favored the white roof as the study period was warmer than the typical meteorological year (TMY) for Pittsburgh (Refer to Section 2.7). Therefore, black roofs could have a higher benefit if the study year was colder than the average TMY. Similarly, the lower bound of 15°C (60°F) for the thermal comfort range used in this study was advantageous to the white roof. Under another work environment where people were moving less, the minimum thermal comfort temperature range would be higher. A higher set point for heating would include colder values in the heating scenario, thus adversely affecting the white roof. Last, the energy costs can change the white versus black decision. If the cost of natural gas declines and electricity prices increase, the value of white roofs to reduce air conditioning costs would make white roofs more beneficial.

Another interesting conclusion from this chapter was the role of shading on the roof surface. Shading had two functions 1) reduce surface temperature and thus heat flux and fluctuations 2) interrupt the solar radiation trajectory away from the building. The shade over the black roof made a larger incremental difference (57-61% for black compared with 31-38% for white) at reducing heat gain compared to the white roof. For heat loss, the shade was more beneficial for

the white roof. Overall, the favorable roof types based on reducing diurnal temperature swing, heat gain or loss can be seen in Table 5-27.

Therefore, shading the black roof made a larger incremental difference (57-61% for black compared with 31-38% for white). In terms of heat loss, the reverse was true. The incremental difference of the shade decreased heat loss by 20-40% for the white roof compared to the reference black roof while shade over the black roof reduced heat loss by 4-12%. One possible explanation was the PV panel acted as a barrier maintaining the radiation closer to the surface and thus heating up the surface. Since the white roof membrane was colder, additional heat could make a larger difference.

Table 5-27: Roof types on Sunscape ranked from best to worst at reducing temperature swings, heat gain and heat loss.

		Reducing diurnal temperature swing	Reducing Heat gain	Reducing Heat loss
Best  Worst	1	Sedum	Moss	Moss
	2	Moss	White shaded	Black shaded
	3	White shaded	Black shaded	White shaded
	4	Black shaded	White	Black
	5	White	Black	White
	6	Black		

Green roofs reduced both heat gain and heat loss. Compared to black roofs, the green roof was more effective at reducing heat gain (87% on average annually) than heat loss (20% on average annually). These reductions translated into significantly more cost savings than the other options. While only the membrane temperature of sedum green roofs was measured, the significant reduction in membrane temperature and the additional thermal mass of the sedum would likely moderate the heat flux more than the moss-green roofs. This research supports that the green-moss roof has a heating penalty during daytime hours in winter months. However, the net heat flux showed that the green roof daytime heating penalty was offset by the nighttime reduction in heat loss compared to the black and white roofs. Furthermore, green roofs had a noticeable time delay in the peak heat flux compared to the white or black roofs.

Extending Pittsburgh-Sunscape results to other cities showed the impact of black, white and green roofs due to a range of temperature and solar irradiance values and frequencies. Emphasis was also placed on heat gain and loss between roof types not only annually but monthly and seasonally. In San Diego, differences in heat flux across roof types were of minimal importance because of the climate profile. San Diego's temperatures were temperate throughout the year and relatively consistent with thermal comfort ranges. Therefore, reducing heat flux through San Diego's roofs does matter somewhat but was less important compared to more extreme climates. One general trend was that colder climates like Pittsburgh (i.e. heating dominated climates) favor roofs that reduce heat gain compared to hot climates like Phoenix (i.e. cooling dominated climates) which would benefit from reduction in heat loss. While green roofs do both moderate heat gain and loss, green roofs may not grow in certain climates without significant amounts of water or a location specific mix of plants. Further design considerations are needed to measure heat flux on account of other plant species in other cities to help inform the feasibility of green roofs elsewhere.

Lastly, there was a noticeable difference in air temperature above the black, white and green roofs. Above 26°C, white roof and green roofs reduced the air temperature 1-3°C and 1-4°C respectively. While these differences were small, reducing the air temperature during high temperatures would help reduce the urban heat island impact.

Chapter 6: Research conclusions and future work


6.1 Discussion

Presented with a roof design or replacement decision, a building owner may be overwhelmed by numerous competing roof options and segmented supporting information. Under such a scenario, the outcome likely results in the installation of a familiar roof or the same type of roof reinstalled. By making a legacy roof choice, the opportunity cost in terms of reducing energy consumption and thus energy savings from a different roof choice may be significant. The central focus of this research was to quantify two energy impacts with field experiments that would be useful from a building owner's perspective in order to help them prioritize and quantify the factors that influence their roof decision. Of course other building stakeholders could also use the research results in this thesis to inform their decision framework as well. On a high level, the hope is that with empirical energy data, building owners as well as other building stakeholders would consider alternative roofs options during initial design or when the roof is ready for replacement.

The two main empirical studies conducted in this thesis quantified the increase in efficiency of PV panels on account of roof choices (Chapter 4) and the corresponding reduction in energy consumption due to heat flux through different roof assemblies (Chapter 5). Green roofs do increase the efficiency of a PV panel at high temperatures, but the increase was quite small. For the range of cities, the difference in power output between green roof-PV and black roof-PV was -0.02kW (green roof-PV produces -0.5% less than black roof-PV) in Pittsburgh to 0.08 kW (green roof-PV produces 1.3% more than black roof-PV) in Phoenix averaged across the year. These power differences were converted into energy and then electricity revenue. In Pittsburgh's base-case, the net kilowatt hours translates into a \$9/60panels/yr or \$0.15/panel/yr loss in revenue for the green roof-PV system compared to the black-roof PV system. Given that each PV panel occupies four square meters (43 sq. ft) of roof space, this value can be normalized to \$0.04/ m² of roof /yr in Pittsburgh. For Phoenix, the green roof-PV generates \$32/60panels/yr (\$0.53/panel/yr or \$0.13/ m² of roof /yr) more compared to the black roof-PV. Based on these empirical results, the financial benefit from the interaction between roof type and the PV panel was small.

The second empirical study examined heat flux across roof types. The white roof reduced the total heat gain into the building by 55% and the green-moss roof by 85% under a cooling scenario (i.e. ambient temperatures greater than 25°C) (Table 5-24). For heat loss under a heating scenario (i.e. ambient temperatures less than 15°C), the white roof allowed 20-29% more heat to escape from the building. In contrast to the white roof, the green roof's thermal mass insulated the building reducing the heat loss by 1-14% depending on the city. Shading from the PV panel reduced the heat gain and loss further from the unobstructed case. Table 5-27 (repeated from Chapter 5) rank orders the five different roof types on Sunscape in terms of reducing heat gain or loss. From the Sunscape field experiment in Pittsburgh, the energy associated with removing the unwanted heat (heat gain) through air conditioning saved $-\$0.16/\text{m}^2$ of roof/yr for the white roof and $\$0.25/\text{m}^2$ roof/yr for the green roof compared to the black roof. In terms of additional heating (heat loss), the white roof cost $\$0.17/\text{m}^2$ of roof/yr more than the black roof while the green roof saved $\$0.12/\text{m}^2$ roof/yr. These results mean that for Pittsburgh, the white roof and black roof are almost equivalent in energy savings. However, the green roof saves $\$0.36/\text{m}^2$ of roof/yr in Pittsburgh and $\$0.64/\text{m}^2$ of roof /yr in Phoenix. These results were specific to Sunscape and did not delineate between the unconditioned and heating warehouse operating condition which if separated would have different results. Decision makers need to keep in mind that changes in weather, thermal comfort ranges or energy prices could affect the magnitude of the difference or the over overall result. Based on these two separate empirical studies, a building owner should spend more time considering the heat flux implications to the building more than the efficiency improvements of PV panels based off roof choices.

Table 5-27 (repeated from Chapter 5): Roof types on Sunscape ranked from best to worst at reducing heat gain or loss

		Reducing Heat gain	Reducing Heat loss
Best  Worst	1	Green-moss	Green-moss
	2	White shaded	Black shaded
	3	Black shaded	White shaded
	4	White	Black
	5	Black	White

Regional impacts were investigated through extrapolating Pittsburgh-Sunscape data to three case study cities: San Diego, Huntsville and Phoenix. One important outcome was assessing the importance of a systems level analysis which incorporated the range of climate parameters and the frequency for when they occurred. For example, Huntsville was chosen for high temperatures also had considerable cold temperatures. This distribution of temperatures lowered the total energy efficiency benefits from a green roof-PV combination and increased the amount of heat transferred into the space. In contrast, San Diego had a narrow range of temperatures near the thermal comfort zone. Therefore, HVAC energy savings from heat flux were minimal. In sum, basing roof replacement decisions only on total annual heating and cooling days or being in a heating-dominated climate or cooling-dominated climate is not sufficient. The energy performance costs and savings depend on where along the temperature continuum the city's temperature range is located across the year.

Other useful studies to building owners from empirical Sunscape data included differences in surface membrane temperature during diurnal swings and the time delay in heat flux across different roof types (Chapter 5). Reducing diurnal swing can prolong the service life of the membrane, thus saving the building owners money. In addition, the time delay of heat flux is especially important under dynamic pricing scenarios where peak demand results in high energy prices. The ability of the roof to delay heat flux into or out of the building offsets the need for supplemental heating or cooling for a time when energy prices are lower. This research quantifies both the diurnal swing and time lag so other researchers or building owners can determine the extension of roof service life and potential cost savings from heat flux time delay.

Considering only private costs and benefits to roof replacement ignores other significant impacts to the surrounding community which should also be incorporated into the roof replacement decision. Several other studies focus on quantifying the public impacts of roof choices (e.g. storm water mitigation or urban heat island abatement) to inform roof replacement decisions. Such city-scale research is important as often public costs and benefits are not able to be quantified down to the impacts incurred by private stakeholders. This thesis research supports work on public impacts associated with roofs by providing empirical building data. The optimal roof replacement decision would factor in both private and public costs and benefits.

The results presented in this thesis were determined from a single roof configuration across 16 months in 2011 and 2012 in Pittsburgh, PA. Because of the peculiarities in PV racking height, green roof plant growth and sensor inconsistencies specific to this experiment, generalizing these results to other cities especially in dissimilar climates is cautioned. Instead, the bounding analysis and higher level insights are helpful across climates in providing direction for future research and prioritizing energy factors in roof decision making.

6.2 Research questions revisited

The research questions discussed in the introduction sections of Chapters 3-5 are all revisited here with brief answers.

Chapter 3 hypothesis: Back-surface panel temperature and PV power output from green or black roofs under PV panels can be sufficiently modeled using a linear function with climate parameters as explanatory variables.

Linear regression equations from the empirical data collected at Sunscape had the same or slightly lower coefficients of determination (R^2 value) than the non-linear functions. Since the non-linear functions do not greatly improve the goodness of fit to the data over linear equations, the linear regression equations were chosen because they would be more straight-forward to understand if incorporated in a decision support tool. The tradeoff is at the ambient temperature extremes (above 35° C or below -10°C in Figure 3-2), the linear equation would result in significantly different results compared with the non-linear equation. In cities like San Diego who have a moderate temperature climate, no values were at the temperature extremes. However, in places like Phoenix, hot temperatures (above 35° C) constituted 25% of the daylight hours.

Chapter 3 supporting research questions:

3a) How well do linear and non-linear regression equations fit the Sunscape dataset for back surface panel temperature and power output?

Both sets of linear and non-linear equations had high coefficient of determination (R^2). The first linear regression related ambient temperature to back-surface panel temperature relatively well with coefficients of determination $R^2=0.75$ for black roof-PV and $R^2=0.80$ for green roof-PV assemblies (Table 3-3). In the second linear regression equation derived from Sunscape (Eq. 3), irradiance and PV cell temperature account for 98% ($R^2 = 0.98$) of the variation in the estimation of power output.

The first non-linear regression equation to predict back-surface panel temperature had slightly higher R^2 values for both black ($R^2 = 0.78$ non-linear vs. 0.75 linear) and green ($R^2 = 0.82$ non-linear vs. 0.80 linear) roof PV assemblies. The second non-linear regression equation for PV output (Eq. 5, Table 3-6) did not improve upon the coefficient of determination when rounded to two significant figures compared to the linear regression equation.

3b) How important are wind speed and direction as explanatory variables in predicting PV power output?

Wind speed and direction added little when included individually or together as explanatory variables to increase the goodness of fit for the regression equations. Wind speed had a larger impact on increasing the R^2 value than wind direction. However for any wind speed, wind direction or a combination of both, the R^2 values increased at most by 0.4% for the green roof-PV and 0.6% for the black roof-PV assemblies.

Chapter 4 hypothesis: The combination of PV panels over a green roof will produce more electricity than PV panels over a black roof.

Based on the Sunscape field experiment from July 1 2011 to June 30, 2012, green roofs underneath PV panels do produce more power than a black roof-PV assembly when the

temperatures are hot ($\sim 25^{\circ}\text{C}$). However when temperatures are cooler, the black roof-PV combination produced slightly more power. Overall, the difference between green roof-PV and black roof-PV is small (0.5%). In Pittsburgh, the black roof-PV produces more power because of the colder climate. However in the other three cities (San Diego, Huntsville and Phoenix), the green roof-PV assembly outperforms the black roof-PV by 0.6-1.3% (Table 4-3).

Chapter 4 supporting research questions:

4a) Under what climate parameters does cooler air above the green roof increase PV output compared to black roofs on Sunscape?

The Pittsburgh daytime data in Table 4-2 suggest that for ambient temperatures above 25°C for all irradiance values, green roofs lower the air temperature surrounding the PV panels in turn producing more power than black roof-PV assemblies. For solar irradiance, at or above 800W/m^2 green roof-PV produces more power than the black roof-PV.

4b) What is the magnitude of the difference in PV output for Sunscape and for other cities? Given the base-case and high-temperature scenario, what are a range of cost savings from the green roof-PV combination?

The measured power difference on Sunscape between the black roof-PV and green roof-PV was small. For Pittsburgh, the black roof-PV outperforms the green roof-PV by an average of 0.02kW or 0.5%. Across the year, this power difference translates into a net $90\text{ kWh}/60\text{ panels/yr}$ (1.5kWh/yr/panel) or $\$9/60\text{panels/yr}$ more for the black roof-PV. Averaging the power difference across only temperatures above $>25^{\circ}\text{C}$ (i.e. the high temperature scenario), the green roof-PV system produces 0.07kW (0.9%) more power than the comparable black roof-PV system. Assuming the same 0.07kW power output for all daylight hours as an upper bound results in $\$29/60\text{panels/yr}$ of additional revenue from the green roof-PV assembly.

For the base-case scenario in San Diego, Huntsville and Phoenix, the green roof-PV had a 0.03-0.08kW or 0.6-1.3% additional power output using Method 1. This power delta translates into \$15-\$32/60 panels/yr of more revenue. Under the high temperature scenario, the difference in power output reaches 0.8-0.11kW (0.8%-1.5%) which corresponds to \$37-\$47/60 panels/yr. Using Method 2 in the base-case, the green roof-PV produces less than the black roof-PV, but the overall magnitude was similar.

Chapter 5 hypothesis: Green roofs are better building insulators than white or black roofs throughout the year.

With ambient temperatures higher than 22°C (72°F), both sedum and moss green roofs had the most pronounced decrease in the membrane surface temperature ranging from 1 to 24°C cooler than white membrane and 7 to 42°C from the black membrane surface temperature.

At cold temperatures (<0°C), both green roof surfaces kept the membrane around 0-1°C due to the thermal mass which is approximately 7 to 13°C warmer than the black and white roofs.

Green roofs reduced the annual quantity of heat transferred through the roof assembly (i.e. heat gain or heat loss) by 32% and 47% compared with the white and black roofs respectively. These percentages also vary seasonally (Refer to Table 5-4). Generally, both white and green roofs had more sizable reductions in heat gain than heat loss compared to the reference black roof.

Chapter 5 supporting research questions:

5a) What is the reduction in surface temperature and monthly diurnal hourly swing for white, green-moss and green-sedum compared to black roofs on Sunscape?

With ambient air temperatures higher than 22°C (72°F), white roof surface temperatures were 6 to 18°C lower than the conventional black roof membrane averaged across the year (Figure 5-4). Both sedum and moss green roofs had a more pronounced decrease in the membrane surface temperature ranging from 7 to 42°C from the black membrane surface temperature.

A higher ambient temperatures, a shaded black membrane lowered the temperature by 2-23°C (10-33% reduction) from the unshaded condition. The shade over the white roof membrane reduced membrane temperature by 1-12°C (4-22% reduction) compared to the unshaded white roof. In other words, the shade was more effective over a black roof at reducing the temperature than a white roof.

Across the entire year, the white membrane reduced the fluctuation of the membrane surface temperature by 30-40%, the moss roof by 60-70% and sedum roof by 85-95% compared to the black roof (Figure 5-7). Comparing only July through October across the five alternative roof types, the sedum green roof reduced the temperature fluctuation the most (87-89%) followed by moss (59-63%), white shaded (53-61%), black shaded (3-50%), and finally white (18-38%) compared to black roof.

5b) What quantity of heat gained and lost was measured across black, white and green on Sunscape? How do these values change seasonally?

In the winter, the white roof had the largest net heat flux. The reason was because the white roof had 12% more heat loss (due to colder membrane temperatures) than black roofs and 25% more than green roofs. For summer months, the black roof had a positive net heat flux (heat gain) while the white and green roofs had a negative net heat flux. The black roof allows 57% more heat to enter the building than the white roof and 85% more than the green roof (Table 5-4).

5c) How does shading the white or black roof affect the roof heat flux? In terms of reducing heat gain or loss, how do shaded black and white roofs compare with black, white and green unshaded roofs?

The white shaded roof decreased the heat gain 31-38% further from the white unobstructed roof when compared to the black roof. The shade over the black roofs reduced the heat flux 57-61% compared to the black unobstructed surface (Table 5-7). Therefore, shading the black roof made a larger incremental difference (57-61% for black compared with 31-38% for white). In terms of

heat loss, the reverse was true. The incremental difference of the shade decreased heat loss by 20-40% for the white roof compared to the reference black roof while shade over the black roof reduced heat loss by 4-12%.

The shaded white and black roofs fall in between white and green roofs at reducing heat gain or loss. Comparing the percent reduction in heat gain for summer months from black roofs (Table 5-4 and Table 5-7), the green roof was the best at reducing heat gain followed by white shaded, black shaded, white and black roofs in order. In terms of heat loss, the order switched slightly from best to worst: green, black shaded, white shaded, black and finally white roofs.

In summary, the main take away points from this research are as follows:

- When considering energy performance, roof choices need to include a systems level analysis across an entire year for the specific region. For example, this research verified that Sunscape's green roof cooled the PV panel at high ambient temperatures. However in Pittsburgh, high temperatures are infrequent minimizing the green roof-PV benefit. Similarly for Pittsburgh, white roofs did lower the heat gain in the summer reducing air-conditioning costs. Because Pittsburgh is a heating-dominated climate, the white roof cooling benefit was marginalized. Yet another example, the green roof winter heating penalty was observed on Sunscape, but the total heat flux across an average day offset the penalty. Last, Huntsville was chosen in this research for its hot temperatures and similar solar radiation as Pittsburgh. Separating cities based on heating or cooling climate ignores the full spectrum of annual temperatures which influence energy consumption.
- Based on the specific Sunscape configuration, the roof choice of green-moss or black-EPDM under the PV panels had little impact on the PV performance.
- When prioritizing factors that influence a roof decision, more time and effort should be spent quantifying the heat flux impact rather than the interaction between roof and PV. Under the specific conditions modeled on Sunscape, the cost difference between these two energy impacts was significant.

- The method developed in this thesis (outlined in Section 4.3) to categorize the data measured on Sunscape into bins is valuable for decision makers to visually understand total heat flux impacts (e.g. Table 5-20 to Table 5-22). Furthermore, this methodology is easy to use and suitable as a rough estimate to extend Sunscape's measured data to other climates (e.g. Sections 4.7 and 5.6).
- This thesis work was based off of an extensive roof dataset composed of over 35 sensors each recorded values at fifteen minute intervals beginning in January 2011. The sensors are placed across different roof types and PV panels. More specifics on the dataset are described in Chapter 2. The Pittsburgh Sunscape dataset is available to other interested individuals and organizations for future research by contacting Scalo Solar Solutions (www.scalosolar.com). Currently, T.J. Willetts is the contact person managing the dataset at Scalo Solar.

6.3 Future work

As is common in research, insights gained while working on this thesis uncovered additional research questions and topics. The list below is by no means exhaustive, but highlights a few topics of interest for future work.

1. Alternative roof research configuration

As discussed above, this research was conducted on an imperfect testbed because the heights of the PV were different between green and black roofs. Therefore, reconfiguring Sunscape to include the same PV racking systems at the same heights would enhance the research as would a comparison with a white roof underneath PV panels. In addition, these identical systems across roof types could vary in height. For example, one set of white roof-PV, green-PV and black roof-PV assemblies could be installed at 1ft, 2 ft and 3ft from the ground which would inform potential efficiencies of PV panels and urban heat island effects. Furthermore, incorporating different types of green roofs would increase the robustness of the results.

2. Building simulation model and sensitivity analysis

To fully understand the differences in heating and cooling loads imposed through differences in roof heat flux, a building energy model would be needed. Within a building energy model, a

sensitivity analysis could be conducted on thermal comfort thresholds and energy prices to get a further range of results.

3. Carbon emissions for energy use

Natural gas has a lower carbon intensity than electricity in most areas. Therefore, more carbon emissions will likely be released using electricity for air conditioning than when using natural gas for heating a building. Viewing the energy results in terms of carbon emissions would add another comparison between roofing choices.

4. Quantifying private and public costs and benefits for roof alternative technologies

Two reasons why making a roof replacement decision is complex: the cost and benefits are born by different stake holders and the data quantifying the cost and benefits are not consolidated. Numerous studies have compared different benefits of white or green roofs to conventional roofs. However, no study to date quantifies private and public impacts separately for a larger range of roofs types. Incorporating more progressive roof types such as “PV-ready” or a Building Integrate Photovoltaic (BIPV) roofs with more traditional white, black and green roofs into a consolidated model would be useful. The model could be built using peer-reviewed literature, technology cost and performance information, and applicable case studies already in existence. The results from such a model could be used by building owners to understand trade-offs with roof types. In addition, policy makers could use such a model to design programs that make public benefits (e.g. Urban Heat Island reduction) a tangible line item (e.g. credit or tax break) in return on investment calculations for a private building owner.

5. Categorizing roofs within the energy efficiency and conservation strategies

Since roofs are often overlooked in the scope of energy efficiency or conservation, ranking alternative roof options among more common efficiency or conservation strategies would provide a more straight-forward way for decision makers to categorize roofs. One strategy would be to relate a roof efficiency or conservation measure to typical rebate catalog options. For example, how does a green roof compare to programmable thermostats at reducing energy? How does installing skylights to reduce lighting costs compare with switching to LED lights? Another rank list could be normalized based on return on investment for technologies.

References

- Accu Weather. (2012). Weather data depot- degree day reports- year 2009 base 65degree HDD/CDD. Retrieved from <http://www.weatherdatadepot.com/#>
- Akbari, H. (2003). Measured energy savings from the application of reflective roofs in two small non-residential buildings. *Energy*, 28(9), 953–967. doi:10.1016/S0360-5442(03)00032-X
- Akbari, H. (2005). Energy saving potentials and air quality benefits of urban heat island mitigation: updated. *Solar Energy*, 1–19. Retrieved from <http://escholarship.org/uc/item/4qs5f42s.pdf>
- Akbari, H., Berhe, A. A., Levinson, R., Graveline, S., Foley, K., Delgado, A. H., & Paroli, R. M. (2005). Aging and weathering of cool roofing membranes. *Proceedings of the Cool Roofing-Cutting Through the Glare* (pp. 1–11). Atlanta, GA.
- Akbari, H., Davis, S., Dorsano, S., Huang, J. & Winnett, S. (1992). *Cooling our communities: a guidebook on tree planting and light-colored surfacing* (LBNL-31587). Lawrence Berkeley National Laboratory. Berkeley, CA. Retrieved from <http://escholarship.org/uc/item/98z8p10x>
- Akbari, H., & Konopacki, S. (2005). Calculating energy-saving potentials of heat-island reduction strategies. *Energy Policy*, 33(6), 721–756. doi:10.1016/j.enpol.2003.10.001
- Akbari, H, Konopacki, S, & Pomerantz, M. (1998). Cooling energy savings potential of reflective roofs for residential and commercial building in the United States. *Energy*, 24(5), 391–407.
- Akbari, H., & Levinson, R. (2008). Evolution of cool-roof standards in the US. *Advances in Building Energy Research*, 2(1), 1–32. doi:10.3763/aber.2008.0201
- Akbari, H, Levinson, R., & Rainer, L. (2005). Monitoring the energy-use effects of cool roofs on California commercial buildings. *Energy and Buildings*, 37(10), 1007–1016. doi:10.1016/j.enbuild.2004.11.013
- Akbari, H., Menon, S., & Rosenfeld, A. (2009). Global cooling: increasing world-wide urban albedos to offset CO₂. *Climatic Change*, 95(3-4), 275–286. doi:10.1007/s10584-008-9515-9
- Akbari, H., Pomerantz, M., & Taha, H. (2001). Cool surfaces and shade trees to reduce energy use and improve air quality in urban areas. *Solar Energy*, 70(3), 295–310. doi:10.1016/S0038-092X(00)00089-X
- Akbari, H., Rose, L.S., & Taha, H. (2003). Analyzing the land cover of an urban environment using high-resolution orthophotos. *Landscape and Urban Planning*, 63(1), 1–14.

- Alchemie Limited Inc. (2012). Solar panel temperature affects output. Retrieved from <http://www.solar-facts-and-advice.com/solar-panel-temperature>
- American Society of Heating Refrigerating and Air-Conditioning Engineers Inc [ASHRAE].(2010). ANSI/ASHRAE Standard 55-2010: thermal environmental conditions for human occupancy
- Ayata, T., Tabares-Velasco, P. C., & Srebric, J. (2011). An investigation of sensible heat fluxes at a green roof in a laboratory setup. *Building and Environment*, 46(9), 1851–1861. doi:10.1016/j.buildenv.2011.03.006
- Banting, D., Doshi, H., Li, J., Missios, P., Au, A., Currie, B. A., & Verrati, M. (2005). *Report on the environmental benefits and costs of green roof technology for the City of Toronto*. City of Toronto, Canada. Retrieved from <http://www.toronto.ca/greenroofs/pdf/fullreport103105.pdf>
- Bass, B., Krayenhoff, S., Martilli, A., & Stull, R. (2002). Mitigating the urban heat island with green roof infrastructure. *Urban Heat Island Summit: Toronto*.
- Blackhurst, M., Hendrickson, C., & Matthews, H. S. (2010). Cost-effectiveness of green roofs. *Journal of Architectural Engineering*, 16(4), 136. doi:10.1061/(ASCE)AE.1943-5568.0000022
- Carlisle Syntec Systems. (2012a). Sure-weld reinforced TPO membrane product data sheet. Retrieved from <http://www.carlislesyntec.com>
- Carlisle Syntec Systems. (2012b). Sure-seal dusted non-reinforced EPDM membranes product data sheet. Retrieved from <http://www.carlislesyntec.com>
- Carter, T., & Keeler, A. (2008). Life-cycle cost-benefit analysis of extensive vegetated roof systems. *Journal of Environmental Management*, 87(3), 350–63. doi:10.1016/j.jenvman.2007.01.024
- Castleton, H. F., Stovin, V., Beck, S. B. M., & Davison, J. B. (2010). Green roofs; building energy savings and the potential for retrofit. *Energy and Buildings*, 42(10), 1582–1591. doi:10.1016/j.enbuild.2010.05.004
- Center for Environmental Innovation in Roofing (CEIR). (2012). Successful rooftop photovoltaics: how to achieve a high-quality, well-maintained, compatible rooftop PV system. Washington, DC. Retrieved from http://www.roofingcenter.org/syncshow/uploaded_media/SUCCESSFUL ROOFTOP PHOTOVOLTAICS.pdf
- Center for Neighborhood Technology & American Rivers. (2010). *The value of green infrastructure- a guide to recognizing its economic, environmental and social benefit*. Chicago, IL & Washington, DC. Retrieved May 2012 from

<http://www.infrastructureusa.org/the-value-of-green-infrastructure-a-guide-to-recognizing-its-economic-environmental-and-social-benefits/>

- Cess, R.D.; Zhang, M.H.; Minnis, P.; Corsetti, L.; Dutton, E.G.; Forgan B.W.; Garber, D.P.; Gates, W.L.; Hack, J.J.; Harrison, E.F.; Jing, X.; Kiehl, J.T.; Long, C.N.; Morcrette, J.J.; Potter, G.T.; Ramanathan, V.; Subasilar, B.; Whitlock, C.H.; Young, D.F.; Zhou, Y. (1995). Absorption of solar radiation by clouds: observations versus models. *Science*. 267(5197). 496-499. doi: 10.1016/j.enbuild.2011.09.018
- Chaudhari, M., Frantzis, L., Hoff, T. (2004). *PV grid connected market potential under a cost breakthrough scenario*. Retrieved from <http://www.ef.org/documents/EF-Final-Final2.pdf>
- Coffelt, D., & Hendrickson, C. (2012). Case study of occupant costs in roof management. *Journal of Architectural Engineering*, 18(4), 341–348. doi:10.1061/(ASCE)AE.1943-5568.0000080.
- Curtright, A., Morgan, M. G., & Keith, D. W. (2008). Expert assessments of future photovoltaic technologies. *Environmental Science & Technology*, 42(24), 9031–9038.
- Denholm, P., & Margolis, R. M. (2008). Land-use requirements and the per-capita solar footprint for photovoltaic generation in the United States. *Energy Policy*, 36(9), 3531–3543. doi:10.1016/j.enpol.2008.05.035
- Denardo, J.C., Jarrett, A.R., Manbeck, H.B., Beattie, D.J., & Berghage, R.D. (2005). Stormwater mitigation and surface temperature reduction by green roofs. *Transactions of the American Society of Agricultural Engineers [ASAE]*, 46(4), 1491-1496
- Deru, M., & Torcellini, P. (2007). *Source energy and emission factors for energy use in buildings(NREL/TP-550-38617)*. National Renewable Energy Laboratory. Golden, Colorado. Retrieved from <http://www.nrel.gov/docs/fy07osti/38617.pdf>
- Desjarlais, A. O., Zaltash, A., Atchley, J. A., & Ennis, M. (2009). *Thermal performance of vegetated roof systems*. Oak Ridge, Tennessee. Oak Ridge National Laboratory. Retrieved from <http://www.spri.org/publications/policy.htm?submit=1>
- Dunnett, N. & Kingsbury, N. (2008). *Planting Green Roofs and Living Walls* (2nd Edition). Timber Press.
- Duro-Last Roofing. (2011). Why photovoltaic? why now? Retrieved from <http://duro-last.com/blog/?cat=7>
- Earth Pledge Foundation (2004). *Green roofs: Ecological design and construction*. (pp. 108–112). Schiffer Publishing
- Ehrlich, B. (2011). Crystalline technology still dominates PV landscape. *Environmental Building News*, 20(7). Retrieved from

<http://www.buildinggreen.com/auth/article.cfm/2011/6/29/Crystalline-Technology-Still-Dominates-PV-Landscape/>

- Eilert, P. (2000). *AB 970 nonresidential standards proposals: codes and standards enhancement (CASE) study-high albedo roofs*. San Francisco, CA. Retrieved from http://www.energy.ca.gov/title24/archive/2001standards/associated_documents/2000-11-17_PGE_CASE.PDF
- Emery, K. (1999). The rating of photovoltaic performance. *IEEE Transactions on Electron Devices*, 46(10), 1928–1931.
- ET Solar. (2012). ET Solar polycrystalline module (ET-P672WB) 275W technical specifications. Retrieved from www.etsolar.com
- Eumorfopoulou, E., & Aravantinos, D. (1998). The contribution of a planted roof to the thermal protection of buildings in Greece. *Energy and Buildings*, 27(1), 29–36. doi:10.1016/S0378-7788(97)00023-6
- Feng, C., Meng, Q., & Zhang, Y. (2010). Theoretical and experimental analysis of the energy balance of extensive green roofs. *Energy and Buildings*, 42(6), 959–965. doi:10.1016/j.enbuild.2009.12.014
- Foster, Josh, Lowe, Ashley, Winkelman, S. (2011). *The value of green infrastructure for urban climate adaptation*. New York. Washington, DC. Retrieved from <http://www.cakex.org/virtual-library/value-green-infrastructure-urban-climate-adaptation>
- Gaffin, S. R., Rosenzweig, C., Eichenbaum-Pikser, J., Khanbilvardi, R. and Susca, T. (2010). *A Temperature and Seasonal Energy Analysis of Green , White , and Black Roofs* (pp. 1–19). New York. Retrieved from <http://ccsr.columbia.edu/cig/greenroofs>
- Gaffin, S., Rosenzweig, C., Parshall, L., Beattie, D., Berghage, R., O’Keeffe, G., & Braman, D. (2005). Energy Balance Modeling Applied to a Comparison of White and Green Roof Cooling Efficiency. In *Proc. of 3rd North American Green Roof Conference: Greening rooftops for sustainable communities* (pp. p. 583–597). Washington, DC.
- Gartland, L. (2008). *Heat Islands: Understanding and Mitigating Heat in Urban Islands* (1st Edition., p. 208). Sterling, VA: Earthscan.
- Getter, K. L., Rowe, D. B., Andresen, J. a., & Wichman, I. S. (2011). Seasonal heat flux properties of an extensive green roof in a Midwestern U.S. climate. *Energy and Buildings*, 3548–3557. doi:10.1016/j.enbuild.2011.09.018
- Good, C. (2005, April). Surveying the roofing market. *Professional Roofing Magazine*. Retrieved from <http://www.professionalroofing.net/article.aspx?id=623>
- Google Maps (2012). Google Maps for Pittsburgh, PA. Retrieved from <https://maps.google.com/>

- Grant, G. (2006). *Green Roofs and facades*. IHS BRE Press.
- Greenroofs.com. (2011). International Greenroof & Greenwall Projects Database. Retrieved from <http://www.greenroofs.com/projects/plist.php>
- Griffith, J. S., Rathod, M.S., & Paslaski, J. (1981). Some tests of flat plate photovoltaic module cell temperatures in simulated field conditions. *IEEE* (pp. 822–830).
- Gwandu, B.A.L., & Creasey, D.J. (1995). Humidity: a factor in the appropriate positioning of photovoltaic power station. *Renewable Energy*, 6(3), 313-316
- Hoff, J. L. (2005). The economics of cool roofing: A local and regional approach. *Cool Roofing...Cutting through the Glare*. Atlanta, GA.
- Huang, J., & Franconi, E. (1999). *Commercial heating and cooling loads component analysis. System* (LBNL-37208). Lawrence Berkeley National Laboratory. Retrieved from <http://simulationresearch.lbl.gov/dirpubs/37208.pdf>
- Hui, S. C. M., & Chan, S. C. (2011). Integration of green roof and solar photovoltaic systems. *Joint Symposium 2011: Integrated Building Design in the New Era of Sustainability* (pp. 1–12). Hong Kong.
- International Energy Agency. (2010). *Technology roadmap- solar photovoltaic energy. current*. Retrieved from http://www.iea.org/publications/freepublications/publication/pv_roadmap.pdf
- Jacobson, M. Z., & Hoeve, J. E. T. (2012). Effects of urban surfaces and white roofs on Global and regional climate. *Journal of Climate*, 25(3), 1028–1044. doi:10.1175/JCLI-D-11-00032.1
- Jaffal, I., Ouldboukhite, S.-E., & Belarbi, R. (2012). A comprehensive study of the impact of green roofs on building energy performance. *Renewable Energy*, 43, 157–164. doi:10.1016/j.renene.2011.12.004
- Jim, C.Y., & Peng, L.L.H., (2012) Weather effect on thermal and energy performance of an extensive tropical green roof. *Urban Forestry & Urban Greening*, 11(1), 73-85. doi: 10.1016/j.enbuild.2011.09.018
- Kern, J., & Harris, I. (1975). On the optimum tilt of a solar collector. *Solar Energy*, 17, 97–102.
- King, D L, Boyson, W. E., & Kratochvil, J. A. (2004). *Photovoltaic array performance model* (SAND2004-3535). Albuquerque, NM. Sandia National Laboratories
- King, D.L., Kratochvil, J. A., & Boyson, W. E. (1997). Temperature coefficients for PV modules and arrays: measurement methods, difficulties, and results. *Conference Record of the*

Twenty Sixth IEEE Photovoltaic Specialists Conference - 1997, 1183–1186.
doi:10.1109/PVSC.1997.654300

Kirby, J. R. (2011). Low slope roofs as platforms for PV systems. *SolarPro*, 32–46. Retrieved from http://www.nrca.net/rp/news/0311_solarpro_kirby.pdf

Konopacki, S. & Akbari, H. (2001) *Measured energy savings and demand reduction from a reflective roof membrane on a large retail store in Austin, TX* (LBNL-47149). Lawrence Berkeley National Labs. Berkeley, CA. Retrieved October 2012 from <http://escholarship.org/uc/item/7gw9f9sc>

Konopacki, S., Akbari, H., Pomerantz, M., Gabersek, S., & Gartland, L. (1997). *Cooling energy savings potential of light-colored roofs for residential and commercial buildings in 11 U.S. metropolitan areas* (LBNL-39433). Lawrence Berkeley National Laboratory. Berkeley, CA. Retrieved from http://www.epa.gov/hiri/resources/pdf/11_cities_main.pdf

Konopacki, S., Gartland, L., Akbari, H., & Rainer, L. (1998). *Demonstration of energy savings of cool roofs* (LBNL-40673). Lawrence Berkeley National Labs. Berkeley, CA.

Köhler, M. Schmidt, M., Laar, M., Wachsmann, U., & Krauter, S. (2002). Photovoltaic-panels on green roofs: positive interaction between two elements of sustainable architecture. *Proceedings of the RIO 02 - World Climate - 11 - & Energy Event, January 6-11* (pp. 151–158). Rio de Janeiro, Brazil. Retrieved from www.rio02.com/proceedings/

Köhler, M., Wiartalla, W., & Feige, R. (2007). Interaction between PV-Systems and extensive green roofs. *Greening Rooftops for Sustainable Communities*. Minneapolis, MN

Lazzarin, R., Castellotti, F., & Busato, F. (2005). Experimental measurements and numerical modeling of a green roof. *Energy and Buildings*, 37(12), 1260–1267.
doi:10.1016/j.enbuild.2005.02.001

Levinson, R., & Akbari, H. (2010). Potential benefits of cool roofs on commercial buildings: conserving energy, saving money, and reducing emission of greenhouse gases and air pollutants. *Energy Efficiency*, 3(1), 53–109. doi:10.1007/s12053-008-9038-2

Levinson, R., Akbari, H., Konopacki, S., Bretz, S. (2005). Inclusion of cool roofs in nonresidential Title 24 prescriptive requirements. *Energy Policy*, 33(2), 151–170.
doi:10.1016/S0301-4215(03)00206-4

Lewis, G. (1987). Optimum tilt of a solar collector. *Solar and Wind Technology*, 4(3), 1–4.

Liu, K. (2003). Engineering performance of rooftop gardens through field evaluation. *RCI 18th International Convention and Trade Show* (pp. 1–15). Tampa, Florida.

Liu, K. (2006). *Green , reflective , and photovoltaic roofs* (NRCC-48692). National Research Council Canada

- Marion, B. (2008). Comparison of predictive models for photovoltaic module performance. *Photovoltaic Specialists Conference, 2008 PVSC' 08 33rd IEEE* (p. 6).
- Meneses-Rodrigues, D., Horley, P. P., Gonzalez-Hernandez, J., Vorobiev, Y. V., & Gorley, P. N. (2005). Photovoltaic solar cells performance at elevated temperatures. *Solar Energy*, 78(2), 243–250.
- Meral, M.E. & Dincer, F. (2011). A review of the factors affecting operation and efficiency of photovoltaic based electricity generation systems. *Renewable and Sustainable Energy Reviews*, 15, 2176–2184. doi:10.1016/j.rser.2011.01.010
- Miller, W. A., Cheng, M.-D., Pfiffner, S., & Byars, N. (2002). *The field performance of high-reflectance single-ply membranes exposed to three years of weathering in various U.S. climates*. Oak Ridge, Tennessee. Retrieved from <http://www.spri.org/publications/policy.htm?submit=1>
- National Oceanic and Atmospheric Administration [NOAA] National Climatic Data Center. (2012). Quality controlled local climatological data-Pittsburgh International Airport (#94823). Retrieved from <http://www.ncdc.noaa.gov/oa/mpp/#MR>
- National Oceanic and Atmospheric Administration [NOAA] National Weather Service Forecast Office-Pittsburgh. (2012). Hourly climate data archive for Pittsburgh. Retrieved from http://www.nws.noaa.gov/climate/local_data.php?wfo=pbz
- National Renewable Energy Laboratory [NREL]. (2005). National solar radiation data base: 1991-2005 update: typical meteorological year 3. Retrieved from http://rredc.nrel.gov/solar/old_data/nsrdb/1991-2005/tmy3/
- National Renewable Energy Laboratory [NREL]. (2012). PV Watts. Retrieved from <http://www.nrel.gov/rredc/pvwatts/>
- National Weather Service. (2012). National Weather Service glossary. Retrieved from <http://w1.weather.gov/glossary/>
- New, J., Miller W., Desjarlais, A., Huang Y.J., & Erdem, E., (2011). Development of a roof savings calculator. *Proceedings of the RCI 26th International convention and trade show*. Reno, NV. Retrieved from http://web.eecs.utk.edu/~new/publications/2011_RCI.pdf
- Niachou, A., Papakonstantinou, K., Sanamouris, M., Tsangrassoulis, A., & Mihalakakou, G. (2001). Analysis of the green roof thermal properties and investigation of its energy performance. *Energy and Buildings*, 33(7), 719–729. doi:10.1016/S0378-7788(01)00062-7
- Nordman, T., & Clavadetscher, L. (2003). Understanding temperature effects on PV system performance. *3rd World Conference on Photovoltaic Energy Conversion May* (pp. 2243–2246).

- Oak Ridge National Laboratory & Lawrence Berkeley National Laboratory (2012). DOE cool roof calculator. Retrieved from <http://www.ornl.gov/sci/roofs+walls/facts/CoolCalcEnergy.htm>
- Oberndorfer, E., Lundholm, J., Bass, B., Coffman, R. R., Doshi, H., Dunnett, N., Gaffin, S., Köhler, M., Liu, K.K.Y., & Rowe, B. (2007). Green roofs as urban ecosystems: ecological structures, functions, and services. *BioScience*, 57(10), 823. doi:10.1641/B571005
- Oleson, K. W., Bonan, G. B., & Feddema, J. (2010). Effects of white roofs on urban temperature in a global climate model. *Geophysical Research Letters*, 37(3). doi:10.1029/2009GL042194
- Peck, S. (2011). *Annual Green Roof Industry Survey April 2011*. Retrieved from http://greenroofs.org/resources/2011_GRHC_Survey_Report.pdf
- Peck, S., Callaghan, C., Kuhn, M., & Bass, B. (1999). *Greenback from greenroofs: forging a new industry in Canada*. Toronto, Canada. Retrieved from <http://commons.bcit.ca/greenroof/files/2012/01/Greenbacks.pdf>
- Peck, S., & Kuhn, M. (2003). *Design guidelines for green roofs*. Retrieved from <http://www.cmhc.ca/en/inpr/bude/himu/coedar/loader.cfm?url=/commonspot/security/getfile.cfm&PageID=70146>
- Rosell, J. I., & Ibáñez, M. (2006). Modeling power output in photovoltaic modules for outdoor operating conditions. *Energy Conversion and Management*, 47(15-16), 2424–2430. doi:10.1016/j.enconman.2005.11.004
- Rosenfeld, A. H., Akbari, H., Romm, J. J., & Pomerantz, M. (1998). Cool communities: strategies for heat island mitigation and smog reduction. *Energy and Buildings*, 28(1), 51–62. doi:10.1016/S0378-7788(97)00063-7
- Rosenzweig, C., Gaffin, S., & Parshall, L. (2003). *Green roofs in the New York metropolitan region research report*. New York City, New York. Retrieved from <http://www.statisticstutors.com/articles/debrat-green-roofs.pdf>
- Rowlands, I. H., & Kemery, B. P., & Beausoleil-Morrison, I. (2011). Optimal solar-PV tilt angle and azimuth: an Ontario (Canada) case-study. *Energy Policy*, 39(3), 1397–1409. doi:10.1016/j.enpol.2010.12.012
- Sailor, D. (2008). A green roof model for building energy simulation programs. *Energy and Buildings*, 40(8), 1466–1478. doi:10.1016/j.enbuild.2008.02.001
- Sailor, D., Hutchinson, D., & Bokovoy, L. (2008). Thermal property measurements for ecoroof soils common in the western U.S. *Energy and Buildings*, 40, 1246–1251. doi:10.1016/j.enbuild.2007.11.004

- Scalo Solar. (2012). Scalo Solar solutions. Retrieved from <http://www.scalosolar.com/>
- Scherba, A., Sailor, D. J., Rosenstiel, T. N., & Wamser, C. C. (2011). Modeling impacts of roof reflectivity, integrated photovoltaic panels and green roof systems on sensible heat flux into the urban environment. *Building and Environment*, 46(12), 2542–2551. doi:10.1016/j.buildenv.2011.06.012
- Shaari, S., Sopian, K., Amin, N., & Kassim, M. N. (2009). The temperature dependence coefficients of amorphous silicon and crystalline photovoltaic modules using Malaysian field test investigation. *American Journal of Applied Sciences*, 6(4), 586–593.
- Simmons, M. T., Gardiner, B., Windhager, S., & Tinsley, J. (2008). Green roofs are not created equal: the hydrologic and thermal performance of six different extensive green roofs and reflective and non-reflective roofs in a sub-tropical climate. *Urban Ecosystems*, 11(4), 339–348. doi:10.1007/s11252-008-0069-4
- Skoplaki, E., & Palyvos, J. A. (2009a). On the temperature dependence of photovoltaic module electrical performance: a review of efficiency/power correlations. *Solar Energy*, 83(5), 614–624. doi:10.1016/j.solener.2008.10.008
- Skoplaki, E., & Palyvos, J. A. (2009b). Operating temperature of photovoltaic modules: a survey of pertinent correlations. *Renewable Energy*, 34, 23–29.
- Smith, T. (2009). *Whole building design guide-roofing systems*. Retrieved April 25, 2011 from http://www.wbdg.org/design/env_roofing.php#emerg
- Snyder, R. A., & Roodvoets, D. L. (2005). Economic feasibility of cleaning roofs to maintain their “Solar reflectance” ratings. *RCI Cool Roofing...Cutting through the Glare*. Atlanta, GA
- Solar Buzz. (2011). Solar technologies. Retrieved from <http://www.solarbuzz.com/going-solar/understanding/technologies>
- Solar Energy Industries Association [SEIA] & GTM Research. (2011). *U.S. solar market insight 1st quarter 2011 executive summary*. Retrieved June 2011 from <http://www.seia.org/research-resources/>
- Sonne, J. (2006). Evaluating green roof energy performance. *American Society of Heating, Refrigerating and Air-Conditioning Engineers, Inc. [ASHRAE] Journal*, 48, 59-61
- Sonne, J., & Parker, D., (2008) *Energy performance aspects of a Florida green roof part 2* (FSEC-PF-442-08). Dallas, TX. Retrieved from <http://www.fsec.ucf.edu/en/publications/pdf/FSEC-PF-442-08.pdf>

- St. John, A. (2011). A sustainability laboratory-Scalo Solar solutions completes a sustainability demonstration project. *Professional Roofing*, 27–29. Retrieved from www.professionalroofing.net
- Stafford, B., Robichaud, R., & Mosey, G. (2011). *Feasibility study of economics and performance of solar photovoltaics at Massachusetts Military Reservation* (NREL/TP 6A20-49417) National Renewable Energy Laboratory. Retrieved from <http://www.nrel.gov/docs/fy11osti/49417.pdf>
- Suehrcke, H., Peterson, E. L., & Selby, N. (2008). Effect of roof solar reflectance on the building heat gain in a hot climate. *Energy and Buildings*, 40(12), 2224–2235. doi:10.1016/j.enbuild.2008.06.015
- Sulaiman, S. A., Hussain, H. H., Siti, N., Leh, H. N., & Razali, M. S. I. (2011). Effects of dust on the performance of PV panels. *Engineering and Technology*, 588–593.
- Susca, T., Gaffin, S.R., & Dell’Osso, G.R. (2011). Positive effects of vegetation: urban heat island and green roofs. *Environmental Pollution*, 159(8-9), 2119–26. doi:10.1016/j.envpol.2011.03.007
- Tabares-Velasco, P. C., & Srebric, J. (2011). Experimental quantification of heat and mass transfer process through vegetated roof samples in a new laboratory setup. *International Journal of Heat and Mass Transfer*, 54(25-26), 5149–5162. doi:10.1016/j.ijheatmasstransfer.2011.08.034
- Taha, H., Konopacki, S., Gabersek, S. (1998). Impacts of large-scale surface modifications on meteorological conditions and energy use: a 10 region modeling study. *Theoretical and Applied Climatology*, 1–11.
- Tamizhmani, G., Ji, L., Tang, Y., Petacci, L., & Osterwald, C. (2003). Photovoltaic module thermal/wind performance: Long -Term Monitoring and Model Development For Energy Rating. *NCPV and Solar Program Review Meeting* (pp. 936–939).
- Teemusk, A. & Mander, U. (2007). Rainwater runoff quantity and quality performance from a greenroof: The effects of short-term events. *Ecological Engineering*, 30, 271–277.
- Thakkar, N., Cormode, D., Lonij, V.P.A., Pulver, S. & Cronin, A.D. (2010). A simple non-linear model for the effect of partial shade on PV systems. *Proceedings from Photovoltaic Specialists Conference (PVSC), 2010 35th IEEE*. (pp. 2321-2326). Tucson, AZ
- Theodosiou, T. (2009). Green roofs in buildings: thermal and environmental behaviour. *Advances in Building Energy Research Volume 3* (pp. 271–288).
- United States Department of Energy-Energy Efficiency and Renewable Energy [US DOE-EERE]. (2004). *Federal technology alert-green roofs*. Retrieved from http://www1.eere.energy.gov/femp/pdfs/fta_green_roofs.pdf

- United States Department of Energy-Energy Efficiency and Renewable Energy [US DOE-EERE]. (2011a). *2010 solar technologies market report*. Retrieved from <http://www.nrel.gov/docs/fy12osti/51847.pdf>
- United States Department of Energy-Energy Efficiency and Renewable Energy [US DOE-EERE]. (2011b). Photovoltaics. Retrieved from http://www.eere.energy.gov/basics/renewable_energy/photovoltaics.html
- United States Energy Information Administration [US EIA]. (2010a). Table 3.8 average energy conservation efficiency of photovoltaic cells and modules shipped. Retrieved from <http://205.254.135.24/cneaf/solar.renewables/page/solarphotv/solarpv.html>
- United States Energy Information Administration [US EIA]. (2010b). Table 4. average retail price for bundled and unbundled consumers by sector, Census Division, and State 2011. Retrieved from http://www.eia.gov/electricity/sales_revenue_price/pdf/table4.pdf
- United States Energy Information Administration [US EIA]. (2011). Electricity in the United States. Retrieved from http://www.eia.gov/energyexplained/index.cfm?page=electricity_in_the_united_states
- United States Energy Information Administration [US EIA]. (2012). Frequently asked questions: how much electricity is lost in transmission and distribution in the United States? Retrieved from <http://www.eia.gov/tools/faqs/faq.cfm?id=105&t=3>
- United States Environmental Protection Agency [US EPA]. (2008a). *Reducing urban heat islands: compendium of strategies cool roofs*. Retrieved from <http://www.epa.gov/heatisd/resources/compendium.htm>
- United States Environmental Protection Agency [US EPA]. (2008b). *Reducing urban heat islands: compendium of strategies green roofs*. Retrieved from <http://www.epa.gov/heatisd/resources/compendium.htm>
- United States Environmental Protection Agency [US EPA]. (2008c). *Reducing urban heat islands: compendium of strategies urban heat island basics*. Retrieved from <http://www.epa.gov/hiri/resources/compendium.htm>
- United States Environmental Protection Agency [US EPA]. (2009). Heat island effect basic information. Retrieved from <http://www.epa.gov/heatisland/about/index.htm>
- Urban, B., & Roth, K. (2010). *Guidelines for selecting cool roofs v1.2*. Department of Energy-Energy Efficiency and Renewable Energy. Retrieved from http://www1.eere.energy.gov/femp/features/cool_roof_resources.html
- Vanwoert, N. D., Rowe, D. B., Andresen, J. A., Rugh, C. L., Fernandez, R. T., & Xiao, L. (2005). Green roof stormwater retention: effects of roof surface, slope, and media depth. *Journal of Environmental Quality*, 34, 1036–1044. doi:10.2134/jeq2004.0364

- Villalva, M. G., Gazoli, J. R., & Filho, E. R. (2009). Comprehensive Approach to Modeling and Simulation of Photovoltaic Arrays. *IEEE Transactions on Power Electronics*, 24(5), 1198–1208. doi:10.1109/TPEL.2009.2013862
- Weiler, S. & Scholz-Barth, K. (2009). *Green roof systems: A guide to the planning, design and construction of landscape over structure* (1st edition). Hoboken, New Jersey: John Wiley & Sons.
- Whitaker, C. M.; Townsend, T.U.; Wenger, H.J.; Iliceto, A.; Chimento, G.; Paletta, F. (1991). Effects of irradiance and other factors on PV temperature coefficients. *The Conference Record of the Twenty-Second IEEE Photovoltaic Specialists Conference*. 608-613
- Wilcox, S., & Marion, W. (2008). *User's manual for TMY3 data sets- technical report* (NREL/TP-581-43156). Retrieved from http://rredc.nrel.gov/solar/old_data/nsrdb/1991-2005/tmy3/
- Wong, N.H., Cheong, D.K.W., Yan, H., Soh, J., Ong, C.L., & Sia, A. (2003). The effects of rooftop garden on energy consumption of a commercial building in Singapore. *Energy and Buildings*, 35(4), 353-364. doi: 10.1016/S0378-7788(02)00108-1
- Wong, N. H., & Tan, P. (2007). Study of thermal performance of extensive rooftop greenery systems in the tropical climate. *Building and Environment*, 42(1), 25–54. doi:10.1016/j.buildenv.2005.07.030
- Xero Flor (2012). Xero Flor XF301 pre-vegetated blanket. Retrieved from <http://www.xeroflora.com/specs-tech/technical-documents/>
- Xiao, W., Dunford, W.G., Capel, A. (2004). A novel modeling method for photovoltaic cells. *Proceedings of 35th Annual IEEE Power Electronics Specialists Conference*. (pp. 1950-1956) Aachen, Germany
- Young, R. (1998). Cool roof light-colored coverings reflect energy savings and environmental benefits. *Building Design & Construction*, 39(2), 62–64.

Appendix A: Complete list of data collected at Sunscape

Table A1 lists all the data collected on Sunscape. Table A1 is arranged in sections starting at the site level and then disaggregated by temperature measurements and roof-PV combinations.

Further organization is given by row subcategories. The column corresponding to “Date of data used” refers to the date when the data were used in this research (broadly, not counting discrepancies or gaps filtered out of the final analytic dataset). Many of the electricity parameters were not used and so left blank but were included for completeness here.

Table A1: Complete list of data collected (and used) on Sunscape

Site Parameters						
Subcategories	#	Data Name	Units	Beginning date of data collection	Date of data used	Monitoring System
System Group	1	Aggregate PV Index (100.0% Derate Factor)	%	26-Jan-11	--	Draker Laboratories
	2	Aggregate PV Index (Base)	%	26-Jan-11	--	Draker Laboratories
	3	Weighted Avg POA Irradiance	W/m²	26-Jan-11	--	Draker Laboratories
	4	AC Power Consumption	kW	26-Jan-11	--	Draker Laboratories
	5	Aggregate AC Power	kW	26-Jan-11	--	Draker Laboratories
	6	Aggregate AC Energy Record	kWh	26-Jan-11	--	Draker Laboratories
	7	Aggregate AC Energy Total	kWh	26-Jan-11	--	Draker Laboratories
	8	Aggregate Modeled AC Power (100.0% Derate Factor)	kW	26-Jan-11	--	Draker Laboratories
	9	Aggregate Modeled AC Power (Base)	kW	26-Jan-11	--	Draker Laboratories
Aggregate Generation Meter	10	AC Energy Import Record		26-Jan-11	--	Draker Laboratories
	11	AC Power Factor		26-Jan-11	--	Draker Laboratories
	12	COMM Status		26-Jan-11	--	Draker Laboratories
	13	AC Current Neutral	Amps (A)	26-Jan-11	--	Draker Laboratories
	14	AC Current Phase A	Amps (A)	26-Jan-11	--	Draker Laboratories
	15	AC Current Phase B	Amps (A)	26-Jan-11	--	Draker Laboratories
	16	AC Current Phase C	Amps (A)	26-Jan-11	--	Draker Laboratories
	17	AC Frequency	Hertz (Hz)	26-Jan-11	--	Draker Laboratories
	18	AC Voltage AN	Volts (V)	26-Jan-11	--	Draker Laboratories
	19	AC Voltage BN	Volts (V)	26-Jan-11	--	Draker Laboratories
	20	AC Voltage CN	Volts (V)	26-Jan-11	--	Draker Laboratories
	21	AC Apparent Power	Volt-Amps (VA)	26-Jan-11	--	Draker Laboratories
	22	AC Aggregate Energy Total	kWh	26-Jan-11	--	Draker Laboratories
	23	AC Aggregate Power	kW	26-Jan-11	--	Draker Laboratories
Datalogger	24	Datalogger Temperature	°C	26-Jan-11	--	Draker Laboratories
	25	Datalogger Voltage	Volts (V)	26-Jan-11	--	Draker Laboratories

Weather	26	Ambient Temperature	°C	26-Jan-11	24-May-11	Draker Laboratories
	27	Wind Direction	Deg	26-Jan-11	1-Jan-12	Draker Laboratories
	28	Wind Speed	(m/s)	26-Jan-11	1-Jan-12	Draker Laboratories
	29	Wind Speed Max	(m/s)	26-Jan-11	1-Jan-12	Draker Laboratories
	30	Rain Accumulation Record	(mm)	26-Jan-11	--	Draker Laboratories
	31	TC Temp #1 - Sunscape Ambient Air Temp.	°C	26-Jan-11	--	Draker Laboratories
	32	0 Degree POA Irradiance	W/m ²	26-Jan-11	24-May-11	Draker Laboratories
Air Temperature, Surface Temperature and Moisture Measurements						
Subcategories	#	Data Name	Units	Beginning date of data collection	Date of data used	Monitoring System
Skylights	33	TC Temp #2 - Surface Temp Inside Skylight Dome	°C	26-Jan-11	--	Draker Laboratories
	34	TC Temp #13 - Surface Temp Outside Skylight Dome	°C	26-Jan-11	--	Draker Laboratories
Black Roof	35	TC Temp #3 - Air Temp 6" over EPDM	°C	26-Jan-11	5-Jul-12	Draker Laboratories
	36	TC Temp #4 - EPDM Surface Temp	°C	26-Jan-11	24-May-11	Draker Laboratories
	37	TC Temp #5 - Inside Deck Surface Temp under EPDM	°C	26-Jan-11	24-May-11	Draker Laboratories
	38	TC Temp #9 - Surface Temp of EPDM Under 30° Array	°C	26-Jan-11	5-Jul-12	Draker Laboratories
	39	TC Temp #12 - Inside Deck Temp Under 30° Array	°C	26-Jan-11	5-Jul-12	Draker Laboratories
	40	TC Temp #10 - Back of panel of 30 deg. Array	°C	26-Jan-11	--	Draker Laboratories
	41	Indoor Air Temperature 6" below ceiling	°C	24-May-11	--	Onset Hobo
	42	Ceiling Surface Temperature	°C	24-May-11	24-May-11	Onset Hobo
	43	Roof Surface Temperature	°C	24-May-11	24-May-11	Onset Hobo
	44	Back Surface Panel Temperature	°C	24-May-11	1-Jul-11	Onset Hobo
	45	Air Temperature 9" above membrane	°C	24-May-11	--	Onset Hobo
White Roof	46	TC Temp #6 - Air Temp 6" over TPO	°C	26-Jan-11	5-Jul-12	Draker Laboratories
	47	TC Temp #7 - TPO Surface Temp	°C	26-Jan-11	24-May-11	Draker Laboratories
	48	TC Temp #8 - Inside Deck Temp under TPO	°C	26-Jan-11	24-May-11	Draker Laboratories
	49	TC 16-Inside Deck Surface Temp Under 30° TPO	°C	5-Jul-12	5-Jul-12	Draker Laboratories
	50	TC 17-Surface Temp Under 30° Array TPO	°C	5-Jul-12	5-Jul-12	Draker Laboratories
	51	TC 18- Back of Panel 30° Array TPO	°C	5-Jul-12	--	Draker Laboratories
	52	TC Temp #11 - Air Temp 6" over TPO under Solyndra	°C	26-Jan-11	--	Draker Laboratories

Moss Roof	53	TC 14-Air Temp 6" Over Moss	°C	5-Jul-12	5-Jul-12	Draker Laboratories
	54	TC 15- Air Temp 13" Over Moss	°C	5-Jul-12	--	Draker Laboratories
	55	Indoor Air Temp Under Moss 6" below ceiling	°C	24-May-11	--	Onset Hobo
	56	Ceiling Temp Under Moss	°C	24-May-11	24-May-11	Onset Hobo
	57	Roof Surface Temperature Under Moss	°C	24-May-11	24-May-11	Onset Hobo
	58	Moss Surface Temperature	°C	24-May-11	--	Onset Hobo
	59	Air Temperature 30" over Moss	°C	24-May-11	--	Onset Hobo
	60	Back Surface Panel Temperature	°C	24-May-11	1-Jul-11	Onset Hobo
	61	Moss Soil Moisture - Green Roof PV	°C	24-May-11	--	Onset Hobo
Sedum Roof	62	Roof Surface Temperature Under Sedum	°C	24-May-11	24-May-11	Onset Hobo
	63	Sedum Surface Temperature	°C	24-May-11	--	Onset Hobo
	64	Sedum Soil Moisture - Green Roof PV	°C	24-May-11	--	Onset Hobo
Photovoltaics-Uni Solar						
Subcategories	#	Data Name	Units	Beginning date of data collection	Date of data used	Monitoring System
System Group	65	PV Index (Base)	%	26-Jan-11	--	Draker Laboratories
	66	PV Index (100.0% Derate Factor)	%	26-Jan-11	--	Draker Laboratories
	67	Modeled AC Power (Base)	kW	26-Jan-11	--	Draker Laboratories
	68	Modeled AC Power (100.0% Derate Factor)	kW	26-Jan-11	--	Draker Laboratories
	69	Normalized AC Power	kW/kWrated	26-Jan-11	--	Draker Laboratories
Inverter A	70	Draker Modeled Inverter AC Power	kW	26-Jan-11	--	Draker Laboratories
	71	Draker Modeled Inverter AC Power Derated	kW	26-Jan-11	--	Draker Laboratories

Generation Meter	72	AC Power Factor		26-Jan-11	--	Draker Laboratories
	73	COMM Status		26-Jan-11	--	Draker Laboratories
	74	AC Current Neutral	Amps (A)	26-Jan-11	--	Draker Laboratories
	75	AC Current Phase A	Amps (A)	26-Jan-11	--	Draker Laboratories
	76	AC Current Phase B	Amps (A)	26-Jan-11	--	Draker Laboratories
	77	AC Current Phase C	Amps (A)	26-Jan-11	--	Draker Laboratories
	78	AC Frequency	Hertz (Hz)	26-Jan-11	--	Draker Laboratories
	79	AC Voltage AN	Volts (V)	26-Jan-11	--	Draker Laboratories
	80	AC Voltage BN	Volts (V)	26-Jan-11	--	Draker Laboratories
	81	AC Voltage CN	Volts (V)	26-Jan-11	--	Draker Laboratories
	82	AC Apparent Power	Volt-Amps (VA)	26-Jan-11	--	Draker Laboratories
	83	AC Power	kW	26-Jan-11	--	Draker Laboratories
	84	AC Energy Record	kWh	26-Jan-11	--	Draker Laboratories
	85	AC Energy Total	kWh	26-Jan-11	--	Draker Laboratories
Photovoltaics-ET Solar 15 Degree Black Roof						
Subcategories	#	Data Name	Units	Beginning date of data collection	Date of data used	Monitoring System
System Group	86	PV Index (Base)	%	26-Jan-11	--	Draker Laboratories
	87	PV Index (100.0% Derate Factor)	%	26-Jan-11	--	Draker Laboratories
	88	Modeled AC Power (Base)	kW	26-Jan-11	--	Draker Laboratories
	89	Modeled AC Power (100.0% Derate Factor)	kW	26-Jan-11	--	Draker Laboratories
	90	Normalized AC Power	kW/kWrated	26-Jan-11	--	Draker Laboratories
Inverter B-1	91	Draker Modeled Inverter AC Power	kW	26-Jan-11	--	Draker Laboratories
	92	Draker Modeled Inverter AC Power Derated	kW	26-Jan-11	--	Draker Laboratories
Inverter B-2	93	Draker Modeled Inverter AC Power	kW	26-Jan-11	--	Draker Laboratories
	94	Draker Modeled Inverter AC Power Derated	kW	26-Jan-11	--	Draker Laboratories
Inverter B-3	95	Draker Modeled Inverter AC Power	kW	26-Jan-11	--	Draker Laboratories
	96	Draker Modeled Inverter AC Power Derated	kW	26-Jan-11	--	Draker Laboratories

Generation Meter	97	AC Power Factor		26-Jan-11	--	Draker Laboratories
	98	COMM Status		26-Jan-11	--	Draker Laboratories
	99	AC Current Neutral	Amps (A)	26-Jan-11	--	Draker Laboratories
	100	AC Current Phase A	Amps (A)	26-Jan-11	--	Draker Laboratories
	101	AC Current Phase B	Amps (A)	26-Jan-11	--	Draker Laboratories
	102	AC Current Phase C	Amps (A)	26-Jan-11	--	Draker Laboratories
	103	AC Frequency	Hertz (Hz)	26-Jan-11	--	Draker Laboratories
	104	AC Voltage AN	Volts (V)	26-Jan-11	--	Draker Laboratories
	105	AC Voltage BN	Volts (V)	26-Jan-11	--	Draker Laboratories
	106	AC Voltage CN	Volts (V)	26-Jan-11	--	Draker Laboratories
	107	AC Apparent Power	Volt-Amps (VA)	26-Jan-11	--	Draker Laboratories
	108	AC Power	kW	26-Jan-11	--	Draker Laboratories
	109	AC Energy Record	kWh	26-Jan-11	--	Draker Laboratories
	110	AC Energy Total	kWh	26-Jan-11	--	Draker Laboratories
Photovoltaics-ET Solar 15 Degree Green Roof						
Subcategories	#	Data Name	Units	Beginning date of data collection	Date of data used	Monitoring System
System Group	111	PV Index (Base)	%	26-Jan-11	--	Draker Laboratories
	112	PV Index (100.0% Derate Factor)	%	26-Jan-11	--	Draker Laboratories
	113	Modeled AC Power (Base)	kW	26-Jan-11	--	Draker Laboratories
	114	Modeled AC Power (100.0% Derate Factor)	kW	26-Jan-11	--	Draker Laboratories
	115	Normalized AC Power	kW/kWrated	26-Jan-11	--	Draker Laboratories
Inverter B-5	116	Draker Modeled Inverter AC Power	kW	26-Jan-11	--	Draker Laboratories
	117	Draker Modeled Inverter AC Power Derated	kW	26-Jan-11	--	Draker Laboratories
Inverter B-6	118	Draker Modeled Inverter AC Power	kW	26-Jan-11	--	Draker Laboratories
	119	Draker Modeled Inverter AC Power Derated	kW	26-Jan-11	--	Draker Laboratories

Generation Meter	120	AC Power Factor		26-Jan-11	--	Draker Laboratories
	121	COMM Status		26-Jan-11	--	Draker Laboratories
	122	AC Current Neutral	Amps (A)	26-Jan-11	--	Draker Laboratories
	123	AC Current Phase A	Amps (A)	26-Jan-11	--	Draker Laboratories
	124	AC Current Phase B	Amps (A)	26-Jan-11	--	Draker Laboratories
	125	AC Current Phase C	Amps (A)	26-Jan-11	--	Draker Laboratories
	126	AC Frequency	Hertz (Hz)	26-Jan-11	--	Draker Laboratories
	127	AC Voltage AN	Volts (V)	26-Jan-11	--	Draker Laboratories
	128	AC Voltage BN	Volts (V)	26-Jan-11	--	Draker Laboratories
	129	AC Voltage CN	Volts (V)	26-Jan-11	--	Draker Laboratories
	130	AC Apparent Power	Volt-Amps (VA)	26-Jan-11	--	Draker Laboratories
	131	AC Power	kW	26-Jan-11	--	Draker Laboratories
	132	AC Energy Record	kWh	26-Jan-11	--	Draker Laboratories
	133	AC Energy Total	kWh	26-Jan-11	--	Draker Laboratories
Photovoltaics-ET Solar 30 Degree Black and White Roof						
Subcategories	#	Data Name	Units	Beginning date of data collection	Date of data used	Monitoring System
System Group	134	PV Index (Base)	%	26-Jan-11	--	Draker Laboratories
	135	PV Index (100.0% Derate Factor)	%	26-Jan-11	--	Draker Laboratories
	136	Modeled AC Power (Base)	kW	26-Jan-11	--	Draker Laboratories
	137	Modeled AC Power (100.0% Derate Factor)	kW	26-Jan-11	--	Draker Laboratories
	138	Normalized AC Power	kW/kWrated	26-Jan-11	--	Draker Laboratories
Inverter B-4	139	Draker Modeled Inverter AC Power	kW	26-Jan-11	--	Draker Laboratories
	140	Draker Modeled Inverter AC Power Derated	kW	26-Jan-11	--	Draker Laboratories

Generation Meter	141	AC Power Factor		26-Jan-11	--	Draker Laboratories
	142	COMM Status		26-Jan-11	--	Draker Laboratories
	143	AC Current Neutral	Amps (A)	26-Jan-11	--	Draker Laboratories
	144	AC Current Phase A	Amps (A)	26-Jan-11	--	Draker Laboratories
	145	AC Current Phase B	Amps (A)	26-Jan-11	--	Draker Laboratories
	146	AC Current Phase C	Amps (A)	26-Jan-11	--	Draker Laboratories
	147	AC Frequency	Hertz (Hz)	26-Jan-11	--	Draker Laboratories
	148	AC Voltage AN	Volts (V)	26-Jan-11	--	Draker Laboratories
	149	AC Voltage BN	Volts (V)	26-Jan-11	--	Draker Laboratories
	150	AC Voltage CN	Volts (V)	26-Jan-11	--	Draker Laboratories
	151	AC Apparent Power	Volt-Amps (VA)	26-Jan-11	--	Draker Laboratories
	152	AC Power	kW	26-Jan-11	--	Draker Laboratories
	153	AC Energy Record	kWh	26-Jan-11	--	Draker Laboratories
	154	AC Energy Total	kWh	26-Jan-11	--	Draker Laboratories
Photovoltaics-Solyndra						
Subcategories	#	Data Name	Units	Beginning date of data collection	Date of data used	Monitoring System
System Group	155	PV Index (Base)	%	26-Jan-11	--	Draker Laboratories
	156	PV Index (100.0% Derate Factor)	%	26-Jan-11	--	Draker Laboratories
	157	Modeled AC Power (Base)	kW	26-Jan-11	--	Draker Laboratories
	158	Modeled AC Power (100.0% Derate Factor)	kW	26-Jan-11	--	Draker Laboratories
	159	Normalized AC Power	kW/kWrated	26-Jan-11	--	Draker Laboratories
Inverter C-1	160	Draker Modeled Inverter AC Power	kW	26-Jan-11	--	Draker Laboratories
	161	Draker Modeled Inverter AC Power Derated	kW	26-Jan-11	--	Draker Laboratories
Inverter C-2	162	Draker Modeled Inverter AC Power	kW	26-Jan-11	--	Draker Laboratories
	163	Draker Modeled Inverter AC Power Derated	kW	26-Jan-11	--	Draker Laboratories
Inverter C-3	164	Draker Modeled Inverter AC Power	kW	26-Jan-11	--	Draker Laboratories
	165	Draker Modeled Inverter AC Power Derated	kW	26-Jan-11	--	Draker Laboratories

Inverter C-4	166 Draker Modeled Inverter AC Power	kW	26-Jan-11	--	Draker Laboratories
	167 Draker Modeled Inverter AC Power Derated	kW	26-Jan-11	--	Draker Laboratories
Inverter C-5	168 Draker Modeled Inverter AC Power	kW	26-Jan-11	--	Draker Laboratories
	169 Draker Modeled Inverter AC Power Derated	kW	26-Jan-11	--	Draker Laboratories
Inverter C-6	170 Draker Modeled Inverter AC Power	kW	26-Jan-11	--	Draker Laboratories
	171 Draker Modeled Inverter AC Power Derated	kW	26-Jan-11	--	Draker Laboratories
Generation Meter	172 AC Power Factor		26-Jan-11	--	Draker Laboratories
	173 COMM Status		26-Jan-11	--	Draker Laboratories
	174 AC Current Neutral	Amps (A)	26-Jan-11	--	Draker Laboratories
	175 AC Current Phase A	Amps (A)	26-Jan-11	--	Draker Laboratories
	176 AC Current Phase B	Amps (A)	26-Jan-11	--	Draker Laboratories
	177 AC Current Phase C	Amps (A)	26-Jan-11	--	Draker Laboratories
	178 AC Frequency	Hertz (Hz)	26-Jan-11	--	Draker Laboratories
	179 AC Voltage AN	Volts (V)	26-Jan-11	--	Draker Laboratories
	180 AC Voltage BN	Volts (V)	26-Jan-11	--	Draker Laboratories
	181 AC Voltage CN	Volts (V)	26-Jan-11	--	Draker Laboratories
	182 AC Apparent Power	Volt-Amps (VA)	26-Jan-11	--	Draker Laboratories
	183 AC Power	kW	26-Jan-11	--	Draker Laboratories
	184 AC Energy Record	kWh	26-Jan-11	--	Draker Laboratories
	185 AC Energy Total	kWh	26-Jan-11	--	Draker Laboratories

Appendix B: Wind speed and wind direction statistical results

Important statistical parameters from the ten iterations of Equation 6 presented in Section 3.5 (Figure 3-4) are listed below. These regression functions were based on 8,862 daytime values from January 1, 2012-June 30, 2012. Values highlighted in yellow are not statistically significant ($p < 0.05$).

1. Ambient Temperature Only

Table B1: Linear regression coefficient values (Eq. 6) for green (top) and black (bottom) roof-PV for predicting back-surface panel temperature using ambient temperature only as an explanatory variable (July 1, 2011- June 30, 2012)

Green Roof-PV					
	<i>Coefficients</i>	<i>Standard Error</i>	<i>t Stat</i>	<i>P-value</i>	Adjusted R Square
Intercept	0	NA	NA	NA	0.9374
Ambient Temperature (°C)	1.29	0.01	230	0	

Black Roof-PV					
	<i>Coefficients</i>	<i>Standard Error</i>	<i>t Stat</i>	<i>P-value</i>	Adjusted R Square
Intercept	0	NA	NA	NA	0.9188
Ambient Temperature (°C)	1.46	0.01	197	0	

2. Ambient Temperature & Wind Speed

Table B2: Linear regression coefficient values (Eq. 6) for green (top) and black (bottom) roof-PV for predicting back-surface panel temperature using ambient temperature and wind speed as explanatory variables (July 1, 2011- June 30, 2012)

Green Roof-PV					
	<i>Coefficients</i>	<i>Standard Error</i>	<i>t Stat</i>	<i>P-value</i>	Adjusted R Square
Intercept	0	NA	NA	NA	0.9374
Site-Wind Speed (m/s)	0.93	0.04	23	2.2E-116	
Ambient Temperature (°C)	1.29	0.01	230	0	

Black Roof-PV					
	<i>Coefficients</i>	<i>Standard Error</i>	<i>t Stat</i>	<i>P-value</i>	Adjusted R Square
Intercept	0	NA	NA	NA	0.9188
Site-Wind Speed (m/s)	1.26	0.05	24	3.5E-123	
Ambient Temperature (°C)	1.46	0.01	197	0	

3. Ambient Temperature & Wind Direction

The following charts use ambient temperature and wind direction as explanatory variables in Equation 6. Wind direction was a binary variable (0 or 1). Measurements that have values within the North, East, South and West wind direction bins (e.g. North 350^0-10^0) are given a 1 and all other values are 0. The number of measurements with a “1” pertaining to each wind direction category is indicated in the table headers. For example, there are 337 measurements within 350^0-10^0 (North) grouping.

Table B3: Linear regression coefficient values (Eq. 6) for green (top) and black (bottom) roof-PV for predicting back-surface panel temperature using ambient temperature and wind direction from the NORTH as explanatory variables (July 1, 2011- June 30, 2012)

		North (350^0-10^0) N=337				
		<i>Coefficients</i>	<i>Standard Error</i>	<i>t Stat</i>	<i>P-value</i>	Adjusted R Square
GREEN-PV	Intercept	0	NA	NA	NA	0.9336
	Ambient Temperature (°C)	1.38	4.0E-03	348	0	
	Wind Direction	1.52	0.37	4	4.7E-05	
BLACK-PV	Intercept	0	NA	NA	NA	0.9137
	Ambient Temperature (°C)	1.59	5.3E-03	302	0	
	Wind Direction	1.74	0.49	4	4.1E-04	

Table B4: Linear regression coefficient values (Eq. 6) for green (top) and black (bottom) roof-PV for predicting back-surface panel temperature using ambient temperature and wind direction from the EAST as explanatory variables (July 1, 2011- June 30, 2012)

		EAST(80^0-100^0) N=136				
		<i>Coefficients</i>	<i>Standard Error</i>	<i>t Stat</i>	<i>P-value</i>	Adjusted R Square
GREEN-PV	Intercept	0	NA	NA	NA	0.9336
	Ambient Temperature (°C)	1.39	4.0E-03	350	0	
	Wind Direction	2.47	5.8E-01	4	2.3E-05	
BLACK-PV	Intercept	0	NA	NA	NA	0.9137
	Ambient Temperature (°C)	1.59	5.2E-03	303	0	
	Wind Direction	3.19	7.7E-01	4	3.5E-05	

Table B5: Linear regression coefficient values (Eq. 6) for green (top) and black (bottom) roof-PV for predicting back-surface panel temperature using ambient temperature and wind direction from the SOUTH as explanatory variables (July 1, 2011- June 30, 2012)

		SOUTH (170°-190°) N=923				
		<i>Coefficients</i>	<i>Standard Error</i>	<i>t Stat</i>	<i>P-value</i>	Adjusted R Square
GREEN-PV	Intercept	0	NA	NA	NA	0.9335
	Ambient Temperature (°C)	1.39	4.1E-03	337	0	
	Wind Direction	0.17	0.23	1	0.47	
BLACK-PV	Intercept	0	NA	NA	NA	0.9135
	Ambient Temperature (°C)	1.59	5.4E-03	293	0	
	Wind Direction	0.27	0.31	1	0.39	

Table B6: Linear regression coefficient values (Eq. 6) for green (top) and black (bottom) roof-PV for predicting back-surface panel temperature using ambient temperature and wind direction from the WEST as explanatory variables (July 1, 2011- June 30, 2012)

		WEST (260°-280°) N=201				
		<i>Coefficients</i>	<i>Standard Error</i>	<i>t Stat</i>	<i>P-value</i>	Adjusted R Square
GREEN-PV	Intercept	0	NA	NA	NA	0.9335
	Ambient Temperature (°C)	1.39	4.0E-03	350	0	
	Wind Direction	0.33	0.48	1	0.49	
BLACK-PV	Intercept	0	NA	NA	NA	0.9136
	Ambient Temperature (°C)	1.59	5.2E-03	303	0	
	Wind Direction	0.92	0.63	1	0.15	

4. Ambient Temperature & Wind Direction & Wind Speed

Table B7: Linear regression coefficient values (Eq. 6) for green (top) and black (bottom) roof-PV for predicting back-surface panel temperature using ambient temperature, wind speed and wind direction from the NORTH as explanatory variables (July 1, 2011- June 30, 2012)

		North (350°-10°) N=337				
		<i>Coefficients</i>	<i>Standard Error</i>	<i>t Stat</i>	<i>P-value</i>	Adjusted R Square
GREEN-PV	Intercept	0	NA	NA	NA	0.9374
	Site Wind Speed (m/s)	0.92	0.04	23	2.9E-115	
	Ambient Temperature (°C)	1.29	0.01	229	0	
	Wind Direction	1.23	0.36	3	6.9E-04	
BLACK-PV	Intercept	0.00	NA	NA	NA	0.9189
	Site Wind Speed (m/s)	1.25	0.05	24	3.4E-122	
	Ambient Temperature (°C)	1.46	0.01	197	0	
	Wind Direction	1.35	0.48	3	4.8E-03	

Table B8: Linear regression coefficient values (Eq. 6) for green (top) and black (bottom) roof-PV for predicting back-surface panel temperature using ambient temperature, wind speed and wind direction from the EAST as explanatory variables (July 1, 2011- June 30, 2012)

		EAST(80°-100°) N=136				
		<i>Coefficients</i>	<i>Standard Error</i>	<i>t Stat</i>	<i>P-value</i>	Adjusted R Square
GREEN-PV	Intercept	0	NA	NA	NA	0.9375
	Site Wind Speed (m/s)	0.93	0.04	24	1.4E-118	
	Ambient Temperature (°C)	1.29	0.01	228	0	
	Wind Direction	3.01	0.57	5	1.1E-07	
BLACK-PV	Intercept	0.00	NA	NA	NA	0.9190
	Site Wind Speed (m/s)	1.27	0.05	24	2.0E-125	
	Ambient Temperature (°C)	1.45	0.01	196	0	
	Wind Direction	3.92	0.75	5	1.6E-07	

Table B9: Linear regression coefficient values (Eq. 6) for green (top) and black (bottom) roof-PV for predicting back-surface panel temperature using ambient temperature, wind speed and wind direction from the SOUTH as explanatory variables (July 1, 2011- June 30, 2012)

		SOUTH (170°-190°) N=923				
		<i>Coefficients</i>	<i>Standard Error</i>	<i>t Stat</i>	<i>P-value</i>	Adjusted R Square
GREEN-PV	Intercept	0	NA	NA	NA	0.9374
	Site Wind Speed (m/s)	0.96	0.04	24	1.1E-119	
	Ambient Temperature (°C)	1.29	0.01	230	0	
	Wind Direction	-0.92	0.23	-4	7.0E-05	
BLACK-PV	Intercept	0.00	NA	NA	NA	0.9189
	Site Wind Speed (m/s)	1.30	0.05	24	1.9E-126	
	Ambient Temperature (°C)	1.46	0.01	197	0	
	Wind Direction	-1.21	0.30	-4	7.2E-05	

Table B10: Linear regression coefficient values (Eq. 6) for green (top) and black (bottom) roof-PV for predicting back-surface panel temperature using ambient temperature, wind speed and wind direction from the WEST as explanatory variables (July 1, 2011- June 30, 2012)

		WEST (260°-280°) N=201				
		<i>Coefficients</i>	<i>Standard Error</i>	<i>t Stat</i>	<i>P-value</i>	Adjusted R Square
GREEN-PV	Intercept	0	NA	NA	NA	0.9373
	Site Wind Speed (m/s)	0.93	0.04	23	2.8E-116	
	Ambient Temperature (°C)	1.29	0.01	230	0	
	Wind Direction	-0.15	0.47	0	0.75	
BLACK-PV	Intercept	0	NA	NA	NA	0.9188
	Site Wind Speed (m/s)	1.26	0.05	24	9.3E-123	
	Ambient Temperature (°C)	1.46	0.01	197	0	
	Wind Direction	0.27	0.62	0	0.66	

Appendix C: National Weather Service summary of sky conditions at the Pittsburgh International Airport

Definitions for cloud cover by the National Weather Service are in Table C1 (National Weather Service, 2012). Table C2 lists the sky conditions and the corresponding frequency of hours recorded at the Pittsburgh International Weather Station during May 24, 2011-May 24, 2012 (National Oceanic and Atmospheric Administration National Weather Service Forecast Office-Pittsburgh, 2012)

Table C1- National Weather Service definitions for cloud cover

Sky Condition	Cloud Coverage
Clear / Sunny	0/8
Mostly Clear / Mostly Sunny	1/8 to 2/8
Partly Cloudy / Partly Sunny	3/8 to 4/8
Mostly Cloudy / Considerable Cloudiness	5/8 to 7/8
Cloudy	8/8
Fair (mainly for night)	Less than 4/10 opaque clouds, no precipitation, no extremes of visibility/temperature/wind

**Figure C-2: Frequency of seasonal sky conditions at the Pittsburgh International Airport Weather Station
(May 24, 2011- May 24, 2012)**

	Winter	Winter	Spring	Spring	Summer	Summer	Fall	Fall
Sunny	164	2%	210	2%	113	1%	180	2%
Clear	840	10%	664	8%	628	7%	948	11%
Mostly Sunny	644	7%	1242	14%	1276	15%	539	6%
Partly Cloudy	1056	12%	1232	14%	1324	15%	828	9%
Partly Sunny	708	8%	1395	16%	1359	16%	496	6%
Fair	24	0%	32	0%	87	1%	65	1%
Mostly Cloudy	820	9%	744	9%	948	11%	724	8%
Cloudy	2616	30%	2282	26%	2067	24%	3060	35%
Drizzle	92	1%	64	1%	36	0%	272	3%
Drizzle/fog	20	0%		0%		0%	12	0%
Light Rain	464	5%	476	5%	468	5%	1008	11%
Heavy Rain	4	0%	8	0%	4	0%	4	0%
Light Sleet	8	0%		0%		0%		0%
Flurries	432	5%	36	0%		0%	228	3%
Light Snow	520	6%	24	0%		0%	136	2%
Heavy Snow	8	0%		0%		0%		0%
Snow	16	0%		0%		0%		0%
Fog	16	0%	68	1%	88	1%	144	2%
Freezeing	8	0%		0%		0%		0%
Rain	32	0%	20	0%	8	0%	16	0%
Thunderstorm	24	0%	44	1%	88	1%	8	0%
Not Available	212	2%	140	2%	232	3%	128	1%
Total	8728	100%	8681	100%	8726	100%	8796	100%

Appendix D: Total heat flux quantities for black, white and green-moss roofs

For each case study city, typical meteorological data were used to separate the quantity of hours into a matrix with solar irradiance and ambient temperature intervals as the row and column (Tables D1, D3, D5). The annual city's heat transferred within each solar irradiance and ambient temperature cell for black, white and green roof is presented in the Tables D2, D4 and D6 below.

Tables D2, D4, and D6 have two types of patterns in addition to the color gradient outlined in the legend. The diagonal lines show cells that were calculated based on two or less fifteen minute data points from Pittsburgh-Sunscape. In other words, these values are less robust because the average heat flux values were based on a small number of data points. The second type of pattern (dots) identify cells in Phoenix and Huntsville which were not able to be multiplied element by element with the Pittsburgh-Sunscape data because no Sunscape data values existed for those cells. Instead, those dotted cells in Phoenix and Huntsville were calculated based on averaging the nearest row and/or column from Sunscape data.

Table D1: Number of hours corresponding to ambient temperature and solar irradiance ranges from PITTSBURGH, PA dataset (May 24, 2011- May 24, 2012)

		Ambient Temperature (°C)												
(Hours)		<-15	-15--10	-10--5	-5-0	0-5	5-10	10-15	15-20	20-25	25-30	30-35	35-40	>40
Solar Irradiance (W/m ²)	<4 (Night)	28.5	132.75	570	782	753	782	825.75	495.25	78	0.5			
	4-100	2.75	22	81.5	200.0	253.5	210.25	235.75	175.25	94	13	0.25		
	100-200	0.5	16.25	44.75	91	115.75	84.5	134.75	100	69.75	20.25	0.25		
	200-300		6.5	25.5	51.5	77.25	45.75	95.5	105.5	68	23.25	2		
	300-400		1	11.5	31.5	53	37.75	67.5	81.25	75.75	29.5	1.5		
	400-500		0.5	4.5	30	47.5	44	54	71.5	78.25	31.75	2.75		
	500-600			2	14	25.75	35.25	44	67.25	85.5	34.25	2.5		
	600-700			0.25	9.5	12.75	16.5	29.75	53.25	89	32.75	4.75		
	700-800				3.25	5	15	24.25	42.75	80.5	36	4.25		
	800-900					5.25	14	17.25	25.25	73.25	49.25	3		
	900-1000					0.25	3.5	9.75	16.5	37.5	30.5	1.25		
	1000-1100						0.5	1.25	1	2.25	1.25			
>1100									0.5					

Hours	
	500+
	201-500
	101-200
	51-100
	11-50
	1-10
	0

Hours	
	500+
	201-500
	101-200
	51-100
	11-50
	1-10
	0

Table D2: Estimated heat transfer (Wh/m²) through black (top), white (middle), and green (bottom) roof separated by solar irradiance and ambient temperature for PITTSBURGH, PA (May 24, 2011- May 24, 2012)

BLACK		Ambient Temperature (°C)												Wh/m²	
(Watt-hours/m ²)		<-15	-15--10	-10--5	-5-0	0-5	5-10	10-15	15-20	20-25	25-30	30-35	35-40	>40	
Solar Irradiance (W/m ²)	<4 (Night)		-224	-1289	-4527	-4732	-3318	-2860	-2455	-1086	-113	0			(1051)+
	4-100		-24	-169	-515	-867	-792	-445	-316	-104	57	26			(551)-(1050)
	100-200		-5	-105	-222	-278	-216	-42	67	138	203	81	1		(151)-(550)
	200-300			-39	-112	-88	-15	39	200	346	323	142	13		(51)-(150)
	300-400			-6	-38	-21	62	95	244	372	471	227	11		(1)-(50)
	400-500			-4	-10	1	124	176	292	434	619	291	29		No data
	500-600				-3	26	123	202	307	514	780	353	28		1-50
	600-700				1	41	76	128	260	511	943	372	58		51-150
	700-800					19	39	136	247	471	967	479	55		151-550
	800-900						48	147	204	318	988	719	44		551-1050
	900-1000						3	42	128	231	545	480	18		1051+
	1000-1100							7	19	14	32	20			≤2 PA data
	>1100										7				Extrapolated from PA data

WHITE		Ambient Temperature (°C)												Wh/m²	
(Watt-hours/m ²)		<-15	-15--10	-10--5	-5-0	0-5	5-10	10-15	15-20	20-25	25-30	30-35	35-40	>40	
Solar Irradiance (W/m ²)	<4 (Night)		-242	-1362	-4834	-5065	-3604	-3171	-2655	-1184	-126	0			(1051)+
	4-100		-26	-175	-541	-960	-875	-528	-420	-220	-46	6	0		(551)-(1050)
	100-200		-5	-109	-253	-386	-334	-143	-95	2	62	31	1		(151)-(550)
	200-300			-40	-134	-182	-167	-49	-3	99	129	61	7		(51)-(150)
	300-400			-6	-57	-99	-80	-2	57	130	200	101	6		(1)-(50)
	400-500			-4	-21	-82	-28	34	95	155	277	136	15		No data
	500-600				-8	-34	10	67	124	206	357	170	15		1-50
	600-700				1	-3	14	46	111	236	452	183	32		51-150
	700-800					3	9	54	108	220	464	234	30		151-550
	800-900						11	64	94	146	479	345	23		551-1050
	900-1000						1	15	61	104	269	229	10		1051+
	1000-1100							2	8	6	16	10			≤2 PA data
	>1100										3				Extrapolated from PA data

GREEN		Ambient Temperature (°C)												Wh/m²	
(Watt-hours/m ²)		<-15	-15--10	-10--5	-5-0	0-5	5-10	10-15	15-20	20-25	25-30	30-35	35-40	>40	
Solar Irradiance (W/m ²)	<4 (Night)		-142	-724	-2726	-3285	-2332	-1676	-1278	-509	-47	0			(1051)+
	4-100		-13	-104	-365	-803	-779	-433	-317	-95	8	4	0		(551)-(1050)
	100-200		-2	-77	-201	-377	-373	-203	-196	-35	40	11	0		(151)-(550)
	200-300			-31	-115	-219	-273	-124	-117	-21	64	20	3		(51)-(150)
	300-400			-5	-52	-140	-203	-103	-80	-14	83	35	2		(1)-(50)
	400-500			-3	-21	-139	-197	-143	-64	-16	99	47	5		No data
	500-600				-10	-67	-95	-107	-39	2	124	54	5		1-50
	600-700				1	-43	-40	-34	1	30	125	57	10		51-150
	700-800					-14	-10	-8	11	42	145	68	9		151-550
	800-900						-2	13	33	37	135	104	6		551-1050
	900-1000						-1	5	10	21	83	85	2		1051+
	1000-1100							0	0	2	3	4			≤2 PA data
	>1100										1				Extrapolated from PA data

**Table D3: Number of hours corresponding to ambient temperature and solar irradiance ranges from
SAN DIEGO, CA TMY**

		Ambient Temperature (°C)													
(Hours)		<-15	-15--10	-10--5	-5-0	0-5	5-10	10-15	15-20	20-25	25-30	30-35	35-40	>40	
Solar Irradiance (W/m ²)	<4 (Night)						175	1323	2266	453					
	4-100						19	201	493	206	8				
	100-200						1	74	310	147	3				
	200-300						2	51	238	133	10				
	300-400							41	237	175	9				
	400-500							31	216	163	13				
	500-600							20	192	201	29				
	600-700							2	124	195	27				
	700-800								93	196	31				
	800-900								61	194	45				
	900-1000								40	201	59	1			
	1000-1100								7	35	9				
	>1100														

Hours
500+
201-500
101-200
51-100
11-50
1-10
0

Hours	
	500+
	201-500
	101-200
	51-100
	11-50
	1-10
	0

Table D4: Estimated heat transfer (Wh/m²) through black (top), white (middle), and green (bottom) roof separated by solar irradiance and ambient temperature for SAN DIEGO, CA

BLACK		Ambient Temperature (°C)												Wh/m²	
(Watt-hours/m ²)		<-15	-15--10	-10--5	-5-0	0-5	5-10	10-15	15-20	20-25	25-30	30-35	35-40	>40	
Solar Irradiance (W/m ²)	<4 (Night)						-771	-4839	-6738	-994					(1051)+
	4-100						-59	-425	-661	-122	5				(551)-(1050)
	100-200						-2	-37	154	204	9				(151)-(550)
	200-300							43	498	436	48				(51)-(150)
	300-400							103	856	802	56				(1)-(50)
	400-500							124	1167	990	103				No data
	500-600							115	1339	1537	265				1-50
	600-700							16	1083	1872	286				51-150
	700-800								949	2159	373				151-550
	800-900								720	2444	607				551-1050
	900-1000								524	2811	857	16			1051+
	1000-1100								106	490	128				≤2 PA data
	>1100														Extrapolated from PA data

WHITE		Ambient Temperature (°C)												Wh/m²	
(Watt-hours/m ²)		<-15	-15--10	-10--5	-5-0	0-5	5-10	10-15	15-20	20-25	25-30	30-35	35-40	>40	
Solar Irradiance (W/m ²)	<4 (Night)						-838	-5364	-7286	-1083					(1051)+
	4-100						-66	-505	-878	-258	-4				(551)-(1050)
	100-200						-3	-125	-217	2	3				(151)-(550)
	200-300						-4	-54	-7	125	19				(51)-(150)
	300-400							-2	200	280	24				(1)-(50)
	400-500							24	378	354	46				No data
	500-600							38	542	617	121				1-50
	600-700							6	462	863	137				51-150
	700-800								416	1007	179				151-550
	800-900								331	1119	294				551-1050
	900-1000								249	1261	423	8			1051+
	1000-1100								44	197	65				≤2 PA data
	>1100														Extrapolated from PA data

GREEN		Ambient Temperature (°C)												Wh/m²	
(Watt-hours/m ²)		<-15	-15--10	-10--5	-5-0	0-5	5-10	10-15	15-20	20-25	25-30	30-35	35-40	>40	
Solar Irradiance (W/m ²)	<4 (Night)						-542	-2835	-3508	-466					(1051)+
	4-100						-58	-414	-663	-112	1				(551)-(1050)
	100-200						-3	-178	-452	-51	2				(151)-(550)
	200-300						-7	-138	-291	-26	9				(51)-(150)
	300-400							-111	-281	-30	10				(1)-(50)
	400-500							-100	-255	-35	16				No data
	500-600							-61	-170	5	42				1-50
	600-700							-4	5	109	38				51-150
	700-800								41	193	56				151-550
	800-900								115	286	83				551-1050
	900-1000								40	255	130	3			1051+
	1000-1100								1	60	12				≤2 PA data
	>1100														Extrapolated from PA data

**Table D5: Number of hours corresponding to ambient temperature and solar irradiance ranges from
HUNTSVILLE, AL TMY**

		Ambient Temperature (°C)												
(Hours)		<-15	-15--10	-10--5	-5-0	0-5	5-10	10-15	15-20	20-25	25-30	30-35	35-40	>40
Solar Irradiance (W/m ²)	<4 (Night)	6	37	103	279	516	664	675	772	1013	134	2		
	4-100		3	25	48	75	144	146	189	281	105	11		
	100-200	1	3	12	23	54	101	111	120	174	93	21		
	200-300	1	2	6	22	33	76	77	105	134	86	17		
	300-400		3	3	13	27	38	49	71	93	109	45		
	400-500	1	2	3	9	20	40	65	68	81	113	24	3	
	500-600			3	9	14	39	48	53	63	112	58	1	
	600-700		4		3	5	14	30	39	74	96	66	1	
	700-800					2	10	21	24	64	108	90	2	
	800-900					1	8	15	13	20	83	81	3	
	900-1000						1	4	5	13	33	43	3	
	1000-1100								1					
>1100														

Hours	
	500+
	201-500
	101-200
	51-100
	11-50
	1-10
	0

Hours	
	500+
	201-500
	101-200
	51-100
	11-50
	1-10
	0

Table D6: Estimated heat transfer (Wh/m²) through black (top), white (middle), and green (bottom) roof separated by solar irradiance and ambient temperature for HUNTSVILLE, AL

BLACK		Ambient Temperature (°C)													Wh/m²	
(Watt-hours/m ²)		<-15	-15--10	-10--5	-5-0	0-5	5-10	10-15	15-20	20-25	25-30	30-35	35-40	>40		
Solar Irradiance (W/m ²)	<4 (Night)	-47	-291	-1000	-2216	-3122	-2926	-2469	-2296	-2222	-194	-1			(1051)+	
	4-100		-27	-192	-303	-325	-450	-309	-253	-167	63	22			(551)-(1050)	
	100-200	-9	-27	-78	-114	-165	-188	-55	60	241	271	84			(151)-(550)	
	200-300	-7	-15	-36	-96	-57	-15	66	220	439	409	104			(51)-(150)	
	300-400		-22	-17	-43	-18	45	123	256	426	678	347			No data	
	400-500	-7	-16	-22	-20	0	105	260	367	492	894	220	32		1-50	
	500-600			-14	-16	26	186	275	370	482	1022	598	11		51-150	
	600-700		-12		9	22	84	233	341	711	1017	749	12		151-550	
	700-800					12	78	191	245	705	1298	1197	26		551-1050	
	800-900					8	73	158	153	252	1119	1183	44		1051+	
	900-1000						11	48	66	182	480	676	44		≤2 PA data	
	1000-1100								15						Extrapolated from PA data	
	>1100															

WHITE		Ambient Temperature (°C)													Wh/m²	
(Watt-hours/m ²)		<-15	-15--10	-10--5	-5-0	0-5	5-10	10-15	15-20	20-25	25-30	30-35	35-40	>40		
Solar Irradiance (W/m ²)	<4 (Night)	-51	-314	-1056	-2366	-3342	-3178	-2737	-2482	-2422	-217	-2			(1051)+	
	4-100		-29	-199	-319	-360	-497	-367	-337	-352	-51	5			(551)-(1050)	
	100-200	-10	-29	-80	-130	-229	-292	-187	-84	3	82	32			(151)-(550)	
	200-300	-8	-16	-37	-116	-117	-164	-82	-3	126	163	45			(51)-(150)	
	300-400		-23	-17	-65	-84	-57	-2	60	149	287	154			No data	
	400-500	-7	-17	-22	-42	-55	-24	51	119	176	399	103	17		1-50	
	500-600			-17	-36	-34	15	91	150	193	468	288	6		51-150	
	600-700		-24		-7	-1	15	83	145	328	488	368	7		151-550	
	700-800					2	18	75	107	329	622	584	14		551-1050	
	800-900					2	17	69	70	115	543	568	23		1051+	
	900-1000						3	18	31	82	236	323	24		≤2 PA data	
	1000-1100								6						Extrapolated from PA data	
	>1100															

GREEN		Ambient Temperature (°C)													Wh/m²	
(Watt-hours/m ²)		<-15	-15--10	-10--5	-5-0	0-5	5-10	10-15	15-20	20-25	25-30	30-35	35-40	>40		
Solar Irradiance (W/m ²)	<4 (Night)	-30	-185	-562	-1334	-2168	-2056	-1446	-1195	-1041	-81				(1051)+	
	4-100		-14	-118	-215	-301	-443	-301	-254	-153	9	3			(551)-(1050)	
	100-200	-4	-12	-57	-104	-224	-325	-267	-175	-60	53	11			(151)-(550)	
	200-300	-4	-9	-28	-99	-140	-269	-209	-129	-27	81	15			(51)-(150)	
	300-400		-14	-16	-59	-120	-145	-133	-84	-16	120	54			No data	
	400-500	-6	-10	-17	-41	-92	-166	-211	-80	-18	142	35	6		1-50	
	500-600			-16	-44	-67	-144	-146	-47	2	163	91	2		51-150	
	600-700		-18		-14	-23	-44	-62	1	41	135	115	2		151-550	
	700-800					-9	-20	-11	11	63	194	169	4		551-1050	
	800-900					-2	-4	13	25	30	153	171	6		1051+	
	900-1000						-2	6	5	16	73	120	6		≤2 PA data	
	1000-1100								0						Extrapolated from PA data	
	>1100															

**Table D7: Number of hours corresponding to ambient temperature and solar irradiance ranges from
PHOENIX, AZ TMY**

		Ambient Temperature (°C)												
(Hours)		<-15	-15--10	-10--5	-5-0	0-5	5-10	10-15	15-20	20-25	25-30	30-35	35-40	>40
Solar Irradiance (W/m ²)	<4 (Night)					66	463	864	749	603	683	582	207	4
	4-100					4	37	105	113	142	111	132	87	19
	100-200					1	52	66	80	93	68	73	51	19
	200-300						14	48	91	60	65	59	41	9
	300-400						17	45	72	79	65	68	51	30
	400-500						8	44	88	74	71	51	42	10
	500-600						4	41	101	93	78	71	71	46
	600-700						2	21	42	75	62	80	60	9
	700-800							6	16	57	67	118	96	49
	800-900							2	14	28	41	82	115	27
	900-1000								6	15	40	76	155	43
	1000-1100									1	7	44	76	45
	>1100												2	

Hours
500+
201-500
101-200
51-100
11-50
1-10
0

Hours	
	500+
	201-500
	101-200
	51-100
	11-50
	1-10
	0

Table D8: Estimated heat transfer (Wh/m²) through black (top), white (middle), and green (bottom) roof separated by solar irradiance and ambient temperature for PHOENIX, AZ

BLACK		Ambient Temperature (°C)													Wh/m²	
(Watt-hours/m ²)		<-15	-15--10	-10--5	-5-0	0-5	5-10	10-15	15-20	20-25	25-30	30-35	35-40	>40		
Solar Irradiance (W/m ²)	<4 (Night)					-399	-2040	-3160	-2227	-1323	-990	-306	335	15	(1051)+	
	4-100					-17	-116	-222	-151	-84	67	260	327	71	(551)-(1050)	
	100-200					-3	-97	-33	40	129	198	292	257	96	(151)-(550)	
	200-300						-3	41	190	197	309	361	266	58	(51)-(150)	
	300-400						20	113	260	362	405	524	385	227	(1)-(50)	
	400-500						21	176	476	450	562	467	450	107	No data	
	500-600						19	235	705	711	711	732	791	513	1-50	
	600-700						12	163	367	720	657	908	733	110	51-150	
	700-800							55	163	628	805	1569	1250	638	151-550	
	800-900							21	165	353	553	1198	1669	392	551-1050	
	900-1000								79	210	581	1196	2293	636	1051+	
	1000-1100									14	99	715	1180	666	≤2 PA data	
	>1100												31		Extrapolated from PA data	

WHITE		Ambient Temperature (°C)													Wh/m²	
(Watt-hours/m ²)		<-15	-15--10	-10--5	-5-0	0-5	5-10	10-15	15-20	20-25	25-30	30-35	35-40	>40		
Solar Irradiance (W/m ²)	<4 (Night)					-428	-2216	-3503	-2408	-1442	-1105	-525	85	7	(1051)+	
	4-100					-19	-128	-264	-201	-178	-54	58	150	33	(551)-(1050)	
	100-200					-4	-150	-111	-56	1	60	111	126	47	(151)-(550)	
	200-300						-30	-51	-3	56	123	156	145	32	(51)-(150)	
	300-400						-26	-2	61	126	171	233	205	121	(1)-(50)	
	400-500						-5	34	154	161	251	219	234	56	No data	
	500-600						2	78	285	285	326	352	416	270	1-50	
	600-700						2	58	156	332	315	447	398	60	51-150	
	700-800							21	71	293	386	766	681	348	151-550	
	800-900							9	76	162	268	575	883	207	551-1050	
	900-1000								37	94	287	571	1245	345	1051+	
	1000-1100									6	51	343	602	361	≤2 PA data	
	>1100												16		Extrapolated from PA data	

GREEN		Ambient Temperature (°C)													Wh/m²	
(Watt-hours/m ²)		<-15	-15--10	-10--5	-5-0	0-5	5-10	10-15	15-20	20-25	25-30	30-35	35-40	>40		
Solar Irradiance (W/m ²)	<4 (Night)					-277	-1434	-1851	-1160	-620	-414	11	113	4	(1051)+	
	4-100					-16	-114	-216	-152	-77	10	39	94	20	(551)-(1050)	
	100-200					-4	-167	-159	-117	-32	39	38	61	23	(151)-(550)	
	200-300						-50	-130	-111	-12	61	52	53	12	(51)-(150)	
	300-400						-65	-122	-85	-14	72	82	70	41	(1)-(50)	
	400-500						-33	-143	-104	-16	89	75	83	20	No data	
	500-600						-15	-125	-89	2	113	111	149	96	1-50	
	600-700						-6	-43	2	42	87	140	129	19	51-150	
	700-800							-3	7	56	120	222	197	101	151-550	
	800-900							2	26	41	76	173	237	56	551-1050	
	900-1000								6	19	88	213	309	86	1051+	
	1000-1100									2	9	129	187	90	≤2 PA data	
	>1100												5		Extrapolated from PA data	